Contracts for field projects
and supporting research on . . .

81

Enhanced Oil Recovery

Reporting Period October–December 1994

DOE/BC--95/1
(DE96001203)
PROGRESS REVIEW
Quarter Ending December 31, 1994

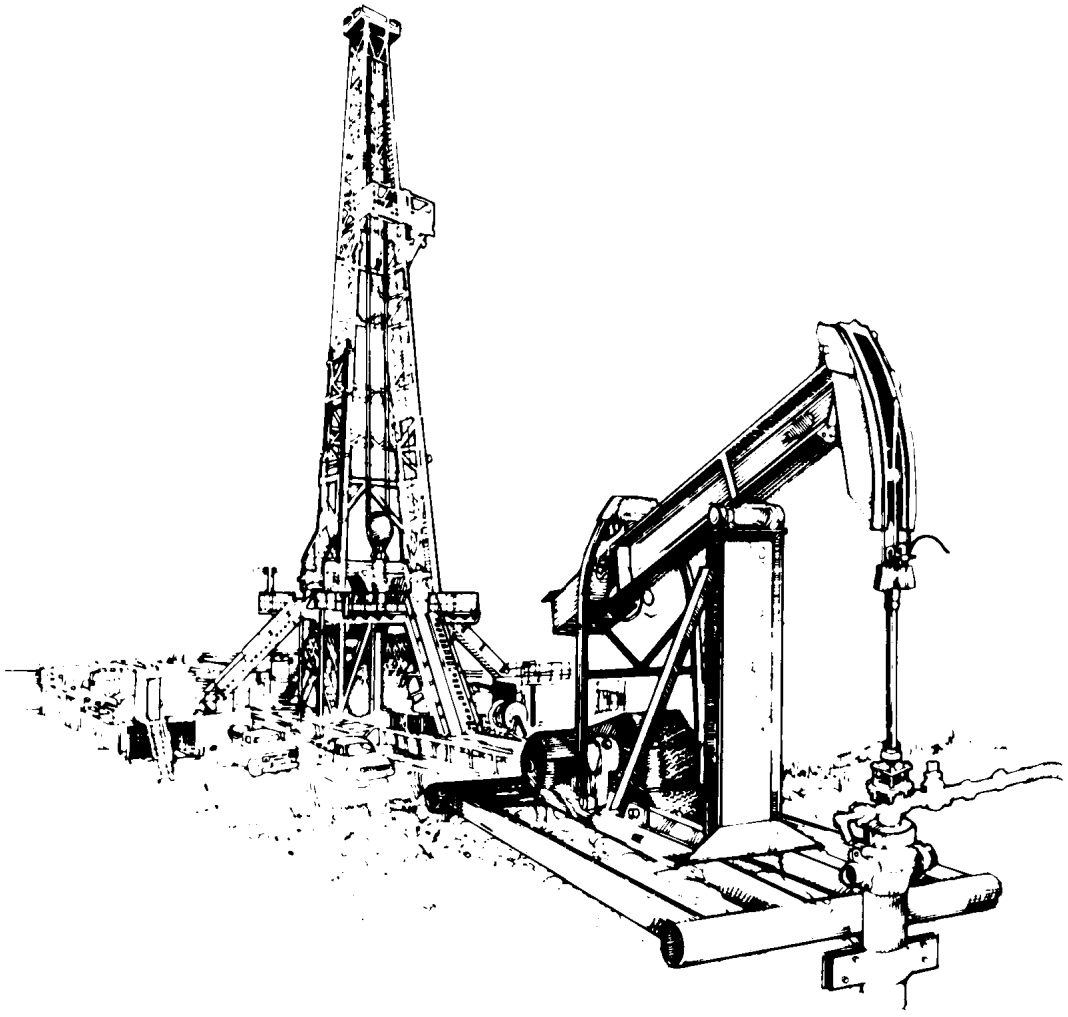

United States Department of Energy
Office of Gas and Petroleum Technology
and Bartlesville Project Office

DISCLAIMER

Available to DOE and DOE contractors from the Office of Scientific and Technical Information, P.O. Box 62, Oak Ridge, Tennessee 37831; prices available from (423) 576-8401.

Available to the public from the U.S. Department of Commerce, Technology Administration, National Technical Information Service, Springfield, Virginia 22161; prices available from (703) 487-4650.

Printed in the United States of America

U.S. Department of Energy
Washington, D.C. 20545

PATRICIA GODLEY
Assistant Secretary for Fossil Energy
Room 4G-084 Forrestal Building
Telephone Number 202-586-4695

REGINAL SPILLER
Deputy Assistant Secretary for Gas and Petroleum Technologies

SANDRA WAISLEY
Director for Oil and Gas Exploration and Production

Bartlesville Project Office
P.O. Box 1398
Bartlesville, Oklahoma 74005

Telephone No. 918-337-4401

THOMAS C. WESSON
Director

R. M. RAY
Deputy Director

BETTY J. FELBER
Program Coordinator, Enhanced Oil Recovery

HERBERT A. TIEDEMANN
Project Manager for Technology Transfer

DOE/BC--95/1
(DE96001203)
Distribution Category UC-122

PROGRESS REVIEW NO. 81

CONTRACTS FOR FIELD PROJECTS AND SUPPORTING RESEARCH ON ENHANCED OIL RECOVERY

Date Published - March 1996

UNITED STATES DEPARTMENT OF ENERGY

PUBLICATIONS LIST

Bartlesville Project Office

Thomas C. Wesson, *Director*

AVAILABILITY OF PUBLICATIONS

The Department of Energy makes the results of all DOE-funded research and development efforts available to DOE and DOE contractors from the **Office of Scientific and Technical Information, P.O. Box 62, Oak Ridge, TN 37831; prices available from (615) 576-8401.**

Available to the public from the **National Technical Information Service, U.S. Department of Commerce, 5285 Port Royal Road, Springfield, VA 22161; prices available from (703) 487-4650.**

Give the full title of the report and the report number.

Sometimes there are slight delays between the time reports are shipped to NTIS and the time it takes for NTIS to process the reports and make them available. Accordingly, we will provide one copy of any individual report as long as our limited supply lasts. Please help us in our effort to eliminate wasteful spending on government publications by requesting only those publications needed. Order the report number listed at the beginning of each citation and enclose a self-addressed mailing label. Available from **DOE Bartlesville Project Office, ATTN: Herbert A. Tiedemann, P.O. Box 1398, Bartlesville, OK 74005; (918) 337-4293.**

Quarterly Reports

DOE/BC-94/3 **Contracts for Field Projects and Supporting Research on Enhanced Oil Recovery. Progress Review No. 79. Quarter ending June 30, 1994. August 1995. 117 pp. Order No. DE94000200.** Status reports are given for various enhanced oil recovery and gas recovery projects sponsored by the Department of Energy. The field tests and supporting research on enhanced oil recovery include chemical flooding, gas displacement, thermal/heavy oil, resource assessment, geoscience technology, microbial technology, field demonstrations in high-priority reservoir classes, novel technology, and environmental technology.

DOE/BC-94/4 **Contracts for Field Projects and Supporting Research on Enhanced Oil Recovery. Progress Review No. 80. Quarter Ending September 30, 1994. November 1995. 156 pp. Order No. DE96001206.** Status reports are given for various enhanced oil recovery and gas recovery projects sponsored by the Department of Energy. The field tests and supporting research on enhanced oil recovery include chemical flooding, gas displacement, thermal/heavy oil, resource assessment, geoscience technology, microbial technology, field demonstrations in high-priority reservoir classes, novel technology, and environmental technology.

Chemical Flooding

DOE/BC/14881-12 **Improving Reservoir Conformance Using Gelled Polymer Systems. Annual Report for September 25, 1993 to September 24, 1994. The University of Kansas. July 1995. 96 pp. Order No. DE95000158.** The objectives of the research program are to identify and develop polymer systems which have potential to improve reservoir conformance of fluid displacement processes; to determine the performance of these systems in bulk and in porous media; and to develop methods to predict their performance in field applications. The research focuses on three types of aqueous gel systems - a polysaccharide (KUSP1) that gels as a function of pH, a polyacrylamide-chromium(III) system and a polyacrylamide-aluminum citrate system. This report describes work conducted during the second year of a three-year program. Progress was made in the utilization of KUSP1 as a gelling agent. It was shown that gels can be formed in situ in porous media using CO_2 or ester hydrolysis to lower pH. An ester was identified that could be used in field-scale operations. It was determined that KUSP1 will form strong gels when ortho boric acid is added to the system. It was also determined, in cooperation with Abbott Laboratories, that KUSP1 can be produced on a commercial scale. Rheological studies showed that shear rate significantly affects gelation time and gel strength. The effect of rock-fluid interactions at alkaline conditions was examined experimentally and through mathematical modeling.

DOE/BC/14884-12 **Surfactant Loss Control in Chemical Flooding Spectroscopic and Calorimetric Study of Adsorption and Precipitation on Reservoir Minerals. Annual Report for September 30, 1993 to September 30, 1994. Columbia University. June 1995. 60 pp. Order No. DE95000157.** The aim of this project is to elucidate the mechanisms underlying adsorption and surface precipitation of flooding surfactants on reservoir minerals. Effect of surfactant structure, surfactant combinations, other inorganic and polymeric species is being studied. A multi-pronged approach consisting of micro and nano spectroscopy, microcalorimetry, electrokinetics, surface tension and wettability is used to achieve the goals. The results of this study should help in controlling surfactant loss in chemical flooding and also in developing optimum structures and conditions for efficient chemical flooding processes.

DOE/BC/14885-10 **Development of Cost-Effective Surfactant Flooding Technology. Annual Report for September 30, 1993 to September 29, 1994. University of Texas. August 1995. 104 pp. Order No. DE95000180.** This research consists of the parallel development of a new chemical flooding simulator and the application of our existing UTCHEM simulation code to model surfactant flooding. The new code is based upon a completely new numerical method that combines for the first time higher-order finite-difference methods, flux limiters, and implicit algorithms. Results indicate that this approach has significant advantages in some problems and will likely enable us to simulate much larger and more realistic chemical floods once it is fully developed. Additional improvements have also been made to the UTCHEM code, and it has been applied to the study of stochastic reservoirs with and without horizontal wells to evaluate methods to reduce the cost and risk of surfactant flooding. During the second year of this contract, significant progress has already been made on both of these tasks.

DOE/BC/14886-14 **Investigation of Oil Recovery Improvement by Coupling an Interfacial Tension Agent and a Mobility Control Agent in Light Oil Reservoirs. Final Report. Surtek, Inc. December 1995. 72 pp. Order No. DE96001204.** This report studied the oil recovery potential of flooding light oil reservoirs by combining interfacial tension reducing agent(s) with a mobility control agent. The first objective was to define the mechanisms and limitations of co-injecting interfacial tension reduction agent(s) and a mobility control agent to recover incremental oil. Specifically, the study focused on the fluid-fluid and fluid-rock interactions. The fluid-fluid evaluations defined how the various alkalis and surfactants interact to develop low interfacial tension values and how physical parameters affect these interactions. The fluid-rock studies evaluated the effect of rock type on the oil recovery efficiency. The second objective was to evaluate the economics of the combination technology and investigate methods to make the process more profitable. Specific areas of study were to evaluate different chemical concentration tapers and the volume of chemical injection required to give optimal oil recovery.

NIPER/BDM-0074 **Chemical Systems for Improved Oil Recovery: Phase Behavior, Oil Recovery, and Mobility Control Studies. Topical Report. BDM-Oklahoma, Inc. September 1995. 76 pp. Order No. DE95000183.** Selected surfactant systems containing a series of ethoxylated nonionic surfactants in combination with an anionic surfactant system have been studied to evaluate phase behavior as well as oil recovery potential. These experiments were conducted to evaluate possible improved phase behavior and overall oil recovery potential of mixed surfactant systems over a broad range of conditions. The importance of maximizing the production of oil initially mobilized by surfactant chemical systems resulted in an evaluation of mobility control polymers for selected experimental conditions. Both polyacrylamide polymers and Xanthan biopolymers were evaluated. In addition, studies were initiated to use a chemical flooding simulation program, UTCHEM, to simulate oil recovery for laboratory and field applications and evaluate its use to simulate oil saturation distributions obtained in CT-monitoring of oil recovery experiments.

Thermal Recovery

CONF-9502114 **Fueling for a Clean and Safe Environment. Volume 1. Proceedings for the 6th UNITAR International Conference on Heavy Crude and Tar Sands on February 12-17, 1995. 811 pp. Order No. DE95000188.** The theme for the conference was "Fueling for a Clean and Safe Environment." The program included 167 technical papers and poster presentations by authors representing 20 countries. Sessions subjects included Production, Field Projects, Processing and Refining, Environment, laboratory Studies, Upgrading, Numerical Simulation, Equipment, Reservoir Characterization, Handling and Transportation, Analytical Properties, Resource Development, and other Worldwide Activities.

CONF-9502114 **Fueling for a Clean and Safe Environment. Volume 2. Proceedings for the 6th UNITAR International Conference on Heavy Crude and Tar Sands on February 12-17, 1995. 733 pp. Order No. DE95000189.** The theme for the conference was "Fueling for a Clean and Safe Environment." The program included 167 technical papers and poster presentations by authors representing 20 countries. Sessions subjects included Production, Field Projects, Processing and Refining, Environment, laboratory Studies, Upgrading, Numerical Simulation, Equipment, Reservoir Characterization, Handling and Transportation, Analytical Properties, Resource Development, and other Worldwide Activities.

DOE/BC/14864-14 **Study of Hydrocarbon Miscible Solvent Slug Injection Process for Improved Recovery of Heavy Oil from Schrader Bluff Pool, Milne Point Unit, Alaska. Annual Report for January 1, 1994 to December 31, 1994. University of Alaska Fairbanks. July 1995. 120 pp. Order No. DE95000162.** The oil production in Alaska has started to decline in the early 1990's which is attributed to decline in the production from supergiant Prodhoe Bay field. In the 1990's, the National Energy Strategy Plan developed by U.S. Department of Energy called for 900,000 barrels/day production of heavy oil in the mid 1990's to meet the national demand. To meet this goal, it is imperative that Alaskan heavy oil fields be brought into production. Schrader Bluff reservoir, located in the Milne Point Unit, which is part of the heavy oil field known as West Sak, is estimated to contain 1.5 billion barrels of (14 to 21 degree API) oil-in-place. The field is currently under production by primary depletion. However, the primary recovery was expected to be much less than expected value of 12% because of complex reservoir structure. Hence, waterflood has been implemented earlier than anticipated. The eventual implementation of enhanced oil recovery (EOR) techniques will be vital for the recovery of additional oil from this reservoir.

DOE/BC/14899-24 **Flow and Displacement of Bingham Plastics in Porous Media. Topical Report. University of Southern California. July 1995. 32 pp. Order No. DE95000165.** Bingham plastics, which exhibit a finite yield stress at zero shear rate, have been used to model the flow behavior of certain heavy oils at reservoir conditions (Barenblatt et al., 1990). In such fluids, the onset of flow and displacement occurs only after the applied pressure gradient exceeds a minimum value. Understanding the flow behavior of such fluids has been limited to phenomenological approaches (Barenblatt et al., 1990, Wu et al. 1992). Numerical simulations and experimental visualization of flow and immiscible displacement of Bingham plastics in porous media using micromodels are presented. First, a novel pore network simulation approach to determine the onset of flow is described. The dependence of the critical yield stress on the pore-size distribution is discussed. Visualization experiments of the constant-rate immiscible displacement of Bingham plastics in glass micromodels and Hele-Shaw cells are next presented. The process is subsequently simulated in a pore network. Experiments are successfully simulated with the pore network model. The effect of the yield stress and injection rate on the displacement patterns is discussed. A classification of the displacement patterns, similar to that for Newtonian displacement is proposed (Lenormand, 1989).

DOE/BC/14899-25 **Visualization and Simulation of Immiscible Displacement in Fractured Systems Using Micromodels: Steam Injection. University of Southern California. July 1995. 36 pp. Order No. DE95000150.** A study of steam and hot water injection processes in micromodel geometries that mimic a matrix-fracture system was undertaken. The following was observed: light components existing in the crude oil generated a very high efficient gas-drive at elevated temperatures. This gas generation in conjunction with natural surfactant existing in the crude oil lead to the formation of a foam in the fracture and to improved displacement in the matrix. It was observed that the steam enters the fracture and the matrix depending on whether the steam rate exceeds or not the critical values. The resulting condensed water also moves preferentially into the matrix or the fracture depending on the corresponding capillary number. Since steam is a non-wetting phase as a vapor, but becomes a wetting phase when condensed in a water-wet system, steam injection involves both drainage and imbibition. It was found that all of the oil trapped by the condensed water can be mobilized and recovered when in contact with steam.

DOE/BC/14899-26 **Visualization and Simulation of Immiscible Displacement in Fractured Systems Using Micromodels: Imbibition. University of Southern California. July 1995. 52 pp. Order No. DE95000149.** A study of imbibition processes in micromodel geometries that mimic a matrix-fracture system was undertaken. Experiments in glass micromodels and pore network simulation were conducted. It was observed that, at low capillary number values the wetting fluid preferentially invaded the matrix. Two critical capillary numbers were identified, one for the start of penetration in the fracture when the viscosity ratio was much less than one, and another for which the rate of propagation of the front in the fracture is the same with that in the matrix, when the viscosity ratio was greater than one. These critical capillary numbers were well matched with the results of a pore network simulation. A simplified theory for both critical numbers was developed. Free imbibition in fractured system was investigated and compared favorably with pore network simulation. This process first involves the rapid invasion of the matrix, followed by the subsequent penetration of the fracture.

DOE/BC/14899-27 **Scaling of Bubble Growth in a Porous Medium. Topical Report. University of Southern California. July 1995. 16 pp. Order No. DE95000166.** Processes involving liquid-to-gas phase change in porous media are routinely encountered, for example in the recovery of oil, geothermal processes, nuclear waste disposal or enhanced heat transfer. They involve diffusion (and convection) in the pore space, driven by an imposed supersaturation in pressure or temperature. Phase change proceeds by nucleation and phase growth. Depending on pore surface roughness, a number of nucleation centers exist, thus phase growth occurs from a multitude of clusters. Contrary to growth in the bulk or in a Hele-Shaw cell, however, growth patterns in porous media are disordered and not compact. As in immiscible displacements, they reflect the underlying pore microstructure. The competition between multiple clusters is also different from the bulk. For example, cluster growth may be controlled by a combination of diffusion with percolation. Novel growth patterns are expected from this competition.

DOE/BC/14899-28 **SUPRI Heavy Oil Research Program. Annual Report for February 8, 1994 to February 7, 1995. Stanford University. July 1995. 184 pp. Order No. DE95000167.** The goals of this project are to 1) assess the influence of different reservoir conditions (temperature and pressure) on the absolute and relative permeability to oil and water and on capillary pressure; 2) evaluate the effect of different reservoir parameters on the in-situ combustion process. This project includes the study of the kinetics of the reactions; 3) develop and understand the mechanisms of the process using commercially available surfactants for reduction of gravity override and channeling of steam; 4) develop and improve techniques of formation evaluation such as tracer tests and pressure transient tests; and 5) provide technical support for design and monitoring of DOE-sponsored or industry-initiated field projects.

DOE/BC/95000151 **Multifrequency Crosshole EM Imaging for Reservoir Characterization. FY 1994 Annual Report. Lawrence Berkeley Laboratory. June 1995. 12 pp. Order No. DE95000151.** Electrical conductivity of sedimentary rock is controlled by the porosity, hydraulic permeability, temperature, saturation, and the pore fluid conductivity. These rock parameters play important roles in the development and production of hydrocarbon (petroleum and natural gas) resources. For these reasons, resistivity well logs have long been used by geologists and reservoir engineers in petroleum industries to map variations in pore fluid, to distinguish between rock types, and to determine completion intervals in wells. It is therefore a natural extension to use the electrical conductivity structure to provide additional information about the reservoir. Reservoir simulation and process monitoring rely heavily on the physical characteristics of the reservoir model. At present, numerical codes use point measurements of porosity, permeability, and fluid saturation and extrapolate these data throughout a three-dimensional (3-D) grid. The knowledge of a high-resolution geophysical parameter such as electrical conductivity would aid this extrapolation and improve the reservoir simulation effort. In addition, since conductivity is sensitive to changes in the composition and state of fluids in pores and fractures it becomes an ideal method for monitoring a reservoir process.

DOE/BC/95000152 **Electrical and Electromagnetic Methods for Reservoir Description and Process Monitoring. Annual Report for October 1, 1992 to September 30, 1993. Lawrence Berkeley Laboratory. July 1995. 20 pp. Order No. DE95000152.** At the beginning of FY 91 a coordinated electrical and electromagnetic (EM) geophysical research program for petroleum reservoir characterization and process monitoring was initiated. The overall objectives of the program were to: integrate research funded by DOE for hydrocarbon recovery into a focused effort to demonstrate the technology in the shortest time with the least cost; assure industry acceptance of the technology developed by having industry involvement in the planning, implementation, and funding of the research; and focus the research on real world problems that have the potential for solution in the near term with significant energy payoff. Specific research activities conducted through this integrated effort have been in the following five general areas: EM modeling development, data interpretation methods development, hardware and instrumentation development, EOR and reservoir characterization, and controlled field experiments.

DOE/BC/95000153 **Electrical and Electromagnetic Methods for Reservoir Description and Process Monitoring. Annual Report for October 1, 1991 to September 30, 1992. Lawrence Berkeley Laboratory. July 1995. 28 pp. Order No. DE95000153.** One of the important geophysical parameters that can be used to help monitor and characterize a petroleum reservoir is the electrical conductivity. The electrical conductivity of rock is dominantly a function of fluid type, its saturation, the porosity, and hydraulic permeability of the rock. For these reasons, resistivity well logs have long been used by geologists and reservoir engineers in petroleum industries to map variations in pore fluid, to distinguish between rock types, and to determine completion intervals in wells. It is therefore a natural extension to use the electrical conductivity structure to provide additional information about the reservoir. Reservoir simulation and process monitoring rely heavily on the physical characteristics of the reservoir model. At present, numerical codes use point measurements of porosity, permeability, and fluid saturation and extrapolate these data throughout a three-dimensional (3-D) grid. The knowledge of a high-resolution geophysical parameter such as electrical conductivity would aid this extrapolation and improve the reservoir simulation effort. In addition, since conductivity is sensitive to changes in the composition and state of fluids in pores and fractures it becomes an ideal method for monitoring a reservoir process.

DOE/BC/95000168 **Foam Flow Through a Transparent Rough-Walled Rock Fracture. Lawrence Berkeley Laboratory. July 1995. 36 pp. Order No. DE95000168.** This paper presents an experimental study of nitrogen, water, and aqueous foam flow through a transparent replica of a natural rough-walled rock fracture with a hydraulic aperture of roughly 30μm. It is established that single-phase flow of both nitrogen and water is well described by analogy to flow between parallel plates. Inertial effects caused by fracture roughness become important in single-phase flow as the Reynolds number approaches 1. Foam exhibits effective control of gas mobility. Foam flow resistances are approximately 10 to 20 times

greater than those of nitrogen over foam qualities spanning from 0.60 to 0.99, indicating effective gas-mobility control. Because previous studies of foam flow have focused mainly upon unfractured porous media, little information is available about foam flow mechanisms in fractured media. The transparency of the fracture allowed flow visualization and demonstrated that foam rheology in fractured media depends upon bubble shape and size. Changes in flow behavior are directly tied to transitions in bubble morphology.

DOE/BC/95000169 **Population Balance Model for Transient and Steady-State Foam Flow in Boise Sandstone. Lawrence Berkeley Laboratory. July 1995. 60 pp. Order No. DE95000169.** An experimental and mechanistic-modeling study is reported for the transient flow of aqueous foam through 1.3-μm2 (1.3-D) Boise sandstone at backpressures in excess of 5 Mpa (700 psi) over a quality range from 0.80 to 0.99. Total superficial velocities range from as little as 0.42 to 2.20 m/day (1.4 ft/day to 7 ft/day). Sequential pressure taps and gamma-ray densitometry measure flow resistance and in-situ liquid saturations, respectively. Experimental pressure and saturation profiles in both the transient and steady states are garnered. Adoption of a mean-size foam-bubble conservation equation along with the traditional reservoir simulation equations allows mechanistic foam simulation.

Geoscience

DOE/BC/14477-18 **An Experimental and Theoretical Study to Relate Uncommon Rock/Fluid Properties to Oil Recovery. Final Report. Pennsylvania State University. July 1995. 340 pp. Order No.DE95000164.** The most commonly used secondary oil recovery technique is waterflooding. Macroscopic (or common) rock-pore characteristics such as porosity, permeability, and irreducible water saturation and fluid properties such as viscosity have been shown by previous investigators to influence the results of waterflooding and consequently ultimate oil recovery. The objectives of this study are to consider the influence of microscopic (or uncommon) rock-pore characteristics such as wettability, tortuosity, mercury intrusion volume, pore surface area, specific surface area, average pore diameter, median pore-throat diameter, pore length, apparent (skeletal) density and mercury recovery efficiency on residual oil saturation and oil recovery realized in linear-core waterfloods. The results were statistically analyzed to determine the quantitative relations between the various properties, and empirical equations were developed for predicting waterflood performance. The characteristics were analyzed and modeled at both breakthrough and floodout.

Resource Assessment Technology

DOE/BC/14831-14 **Assist in the Recovery of Bypassed Oil from Reservoirs in the Gulf of Mexico. Annual Report for February 18, 1994 to February 18, 1995. Louisiana State University. September 1995. 244 pp. Order No. DE95000185.** During the past year, a report on the simulation work performed on the U-8 reservoir was completed. Also, modifications to handle steeply dipping reservoirs have been successfully implemented in the MASTER simulator and critical process parameter laboratory experiments and computer simulations of the experiments have been completed. In addition, development of predictive models for undeveloped oil and immiscible/miscible processes began. The methodology for determination of undeveloped potential has been completed. The design of the miscible and updip displacement models as well as the design of the economic and timing models is under way. The coding and calibration of the models began. Data validation, map measurements, model development and supporting cost data collection was in progress.

Gas Displacement

DOE/BC/14862-10 **Productivity and Injectivity of Horizontal Wells. Annual Report for March 10, 1994 to March 9, 1995. Stanford University. July 1995. 172 pp. Order No. DE95000163.** This project has eight principal goals to be studied and developed over a five-year period. These goals are as follows: Task 1 is to develop special gridding techniques and associated averaging algorithms for accurate simulation of HW-performance. Task 2 is to study impacts of various types of heterogeneity and develop methods for incorporating their effects in both fine-grid and coarse-grid models. Task 3 is to plan, execute, and interpret two-phase flow experiments at an oil company research facility, and use results to analyze/validate a new two-phase model. Task 4 is to define improved methods for computing two-phase pseudo-functions for effective relative permeabilities for coarse grid blocks near an HW - determine sensitivities to heterogeneities, flow conditions, skin factors, etc. Task 5 is to develop numerical techniques and software in a parallel computing architecture capable of interactively coupling multiple detailed HW - models to a large scale reservoir simulator. Task 6 is to work with affiliate's member companies to establish HW-modeling capabilities from field measurements, particularly for pathological problem cases. Task 7 is to provide and implement practical HW aspects into modeling of EOR processes - miscible gas, steam displacement, in-situ combustion. Task 8 is to seek field opportunities for HW's and study their best implementation in various reservoir scenarios e.g., multiple laterals, hydraulic fracture variants, etc.

DOE/BC/14977-6 **Improved Efficiency of Miscible CO_2 Floods and Enhanced Prospects for CO_2 Flooding Heterogeneous Reservoirs. Annual Report for April 14, 1994 to April 13, 1995. New Mexico Institute of Mining and Technology. September 1995. 80 pp. Order No. DE95000187.** The overall goal of this project is to improve the efficiency of miscible CO_2 floods and enhance the prospects for flooding heterogeneous reservoirs. This objective is being accomplished by extending experimental research in three task areas: 1) foams for selective mobility control in heterogeneous reservoirs, 2) reduction of the amount of CO_2 required in CO_2 floods, and 3) miscible CO_2 flooding in fractured reservoirs. In the first task, a desirable characteristic of CO_2-foam called Selective Mobility Reduction (SMR) that promises an improvement in displacement efficiency by reducing the effects of reservoir heterogeneity is investigated. In the second task, preliminary results on the phase behavior tests of a West Texas crude with CO_2 are reported. In the third task, the results of prediction of multicomponent, reservoir condition interfacial tension (IFT) are reported.

Reservoir Characterization

DOE/BC/14894-5 **Application of Artificial Intelligence to Reservoir Characterization. Annual Report for October 1993 to October 1994. The University of Tulsa. July 1995. 72 pp. Order No. DE95000145.** The basis of this research is to apply novel techniques from Artificial Intelligence and Expert Systems in capturing, integrating and articulating key knowledge from geology, geostatistics, and petroleum engineering to develop accurate descriptions of petroleum reservoirs. The ultimate goal is to design and implement a single powerful expert system for use by small producers and independents to efficiently exploit reservoirs.

DOE/BC/14896-6 **Geological and Petrophysical Characterization of the Ferron Sandstone for 3-D Simulation of a Fluvial-Deltaic Reservoir. Annual Report for September 29, 1993 to September 29, 1994. Utah Geological**

Survey. July 1995. 52 pp. Order No. DE95000172. The objective of the Ferron Sandstone project is to develop a comprehensive, interdisciplinary, quantitative characterization of a fluvial-deltaic reservoir to allow realistic inter-well and reservoir-scale models to be developed for improved oil-field development in similar reservoirs worldwide. Quantitative geological and petrophysical information on the Cretaceous Ferron Sandstone in east-central Utah will be collected. Both new and existing data will be integrated into a three-dimensional model of spatial variations in porosity, storativity, and tensorial rock permeability at a scale appropriate for inter-well to regional-scale reservoir simulation. Simulation results could improve reservoir management through proper infill and extension drilling strategies, reduction of economic risks, increased recovery from existing oil fields, and more reliable reserve calculations. Transfer of the project results to the petroleum industry is an integral component of the project. This report covers research activities for fiscal year 1993-94, the first year of the project. Most work consisted of developing field methods and collecting large quantities of existing and new data.

DOE/BC/14897-6 **Anisotropy and Spatial Variation of Relative Permeability and Lithologic Character of Tensleep Sandstone Reservoirs in the Bighorn and Wind River Basins, Wyoming. Annual Report for September 15, 1993 to September 30, 1994. University of Wyoming. July 1995. 80 pp. Order No. DE95000156.** This research will associate spatial distributions and anisotropy of relative permeability with the depositional subfacies and zones of diagenetic alteration found within the Tensleep Sandstone. The associations between depositional lithofacies diagenetic alteration, and pore geometry will link relative permeability with the distinct and measurable dimensions of lithofacies, and authigenic mineral facies. Effects of the depositional processes and burial diagenesis will be investigated. The primary goal of this task is to establish the regional trends and variations in lithologic character of the eolian and marine subfacies of the upper Tensleep Sandstone in the Bighorn and Wind River basins.

Field Demonstrations

DOE/BC/14953-10 **Increased Oil Production and Reserves from Improved Completion Techniques in the Bluebell Field, Uinta Basin, Utah. Annual Report for September 30, 1993 to September 30, 1994. Utah Geological Survey. July 1995. 132 pp. Order No. DE95000171.** The Bluebell field produces from the Tertiary lower Green River and Wasatch Formations of the Uinta Basin, Utah. The productive interval consists of thousands of feet of interbedded fractured clastic and carbonate beds deposited in a fluvial-dominated deltaic lacustrine environment. Although some wells have produced over 1 million barrels (159,000 m3) of oil, many have produced only 100,000 to 250,000 barrels (15,000-31,000 m3), or less, of oil. The lower portion of the productive interval is overpressured, requiring that approximately 10,000 feet (3,050 m) of intermediate casing be set. The final 2,000 to 4,000 feet (610-1,220 m) of drilling is slow and difficult requiring weighted mud. Wells are typically completed by perforating 40 or more beds over 1,000 to 3,000 vertical feet (305-915 m), then applying an acid-frac treatment to the entire interval. This completion technique is believed to leave many potentially productive beds damaged and/or untreated, while opening up some water and thief zones.

DOE/BC/14954-5 **Advanced Secondary Recovery Demonstration for the Sooner Unit. Annual Report for October 1992 to May 1993. Diversified Operating Corporation. July 1995. 160 pp. Order No. DE95000170.** The objective of this project is to demonstrate the effectiveness of a multi-disciplinary approach to targeted infill drilling and improved reservoir management. The first phase of the project involves geophysical, geological and engineering data acquisition and analysis to identify optimum well sites and to develop a reservoir operations plan, maximizing secondary recovery using water injection and gas recycling. The second phase will involve drilling of up to three geologically targeted infill wells and establishing production/injection schedules. Reservoir simulation, transient well tests and careful production monitoring will be used to evaluate the results. The third phase will involve technology transfer through a series of technical papers and presentations of a short course. Emphasis will be on the economics of the project and the implemented technologies. This report summarizes the activities, results and conclusions from Phase I activities of the Sooner Unit Project. The Sooner Unit is located in Weld County, Colorado and produces from the "d" sandstone member of the Upper Cretaceous Graneros formation at a depth of about 6,300 ft.

DOE/BC/14955-8 **Applications of Advanced Petroleum Production Technology and Water Alternating Gas Injection for Enhanced Oil Recovery - Mattoon Oil Field, Illinois. Final Report. American Oil Recovery, Inc. September 1995. 80 pp. Order No. DE95000184.** Phase I results of a CO_2-assisted oil recovery demonstration project in selected Cypress Sandstone reservoirs at Mattoon Field, Illinois are reported. The design and scope of this project included CO_2 injectivity testing in the Pinnell and Sawyer units, well stimulation treatments with CO_2 in the Strong unit, and infill well drilling, completion and oil production. The field activities were supported by extensive CO_2-oil-water coreflood experiments, CO_2-oil phase interaction experiments, and integrated geologic modeling and reservoir simulations. Five Cypress Sandstone layers ("A", "B", "C", "D", "E") were identified within the study area in Mattoon Field. Three-dimensional geologic models, created from well data, were used to interpret the location, size and continuity of the productive intervals. The CO_2 injectivity tests were performed in the "A" interval in the Pinnell unit, "E" interval in the Sawyer unit and "D" interval in the Strong unit.

DOE/BC/14957-7 **Improved Oil Recovery in Fluvial Dominated Deltaic Reservoirs of Kansas - Near-Term. Annual Report for June 18, 1993 to June 18, 1994. The University of Kansas. October 1995. 204 pp. Order No. DE95000161.** Common oil field problems exist in fluvial dominated deltaic reservoirs in Kansas. The problems are poor waterflood sweep and lack of reservoir management. The poor waterflood sweep efficiency is the result of 1) reservoir heterogeneity, 2) channeling of injected water through high permeability zones or fractures, and 3) clogging of water injection wells with solids as a result of poor water quality. In many instances the lack of reservoir management results from failure to 1) collect and organize data, 2) integrate analyses of existing data by geological and engineering personnel, and 3) identify optimum recovery techniques.

DOE/BC/14958-11 **Green River Formation Water Flood Demonstration Project. Annual Report for April 1, 1994 to March 31, 1995. Lomax Exploration Company. September 1995. 72 pp. Order No. DE95000182.** The successful water flood of the Green River Formation in the Monument Butte unit was analyzed in detail in the last yearly report. It was shown that primary recovery and the water flood in the unit were typical of oil production from an undersaturated oil reservoir close to its bubble point. The reservoir performance of the smaller Travis unit was also analyzed. The Monument Butte unit is currently producing at around 300 barrels per day of oil. Two of the new wells drilled in the unit had zones pressurized by the water flood. The third well produced from pressurized as well as from zones which were unaffected by the water flood. The water flood response of the Travis unit is slow, possibly because of problems

with reservoir continuity. Water injection continues in the unit and the reservoir pressure is increasing steadily. The new well that was drilled in Travis did not intersect the Lower Douglas Creek Sand into which most of the water has been injected. Plans for water flooding the Boundary unit were drawn.

DOE/BC/14959-13 **Revitalizing a Mature Oil Play: Strategies for Finding and Producing Unrecovered Oil in Frio Fluvial-Deltaic Sandstone Reservoirs of South Texas. Annual Report for October 1993 to October 1994. The University of Texas at Austin. July 1995. 168 pp. Order No. DE95000160.** The objectives of this project are to develop interwell-scale geological facies models of Frio fluvial-deltaic reservoirs from selected fields in South Texas and combine them with engineering assessments to characterize reservoir architecture and flow-unit boundaries and to try to determine the controls that these characteristics exert on the location and volume of unrecovered mobile and residual oil. Results of these studies should lead directly to the identification of specific near-term opportunities to exploit these heterogeneous reservoirs for incremental recovery by recompletion and strategic infill drilling.

DOE/BC/14959-15 **Strategies for Reservoir Characterization and Identification of Incremental Recovery Opportunities in Mature Reservoirs in Frio Fluvial-Deltaic Sandstones, South Texas: An Example from Rincon Field, Starr County. Topical Report. The University of Texas at Austin. November 1995. 120 pp. Order No. DE95000190.** Fluvial-deltaic sandstone reservoirs in the United States are being abandoned at high rates, yet they still contain more than 34 billion barrels of unrecovered oil. The mature Oligocene-age fluvial-deltaic reservoirs of the Frio Formation along the Vicksburg Fault Zone in South Texas are typical of this class in that, after more than three decades of production, they still contain 61 percent of the original mobile oil in place, or 1.6 billion barrels. This resource represents a tremendous target for advanced reservoir characterization studies that integrate geological and engineering analysis to locate untapped and incompletely drained reservoir compartments isolated by stratigraphic heterogeneities.

DOE/BC/14960-8 **Post Waterflood CO_2 Miscible Flood in Light Oil, Fluvial-Dominated Deltaic Reservoir. Annual Report for October 1, 1993 to September 30, 1994. Texaco Exploration and Production. July 1995. 52 pp. Order No. DE95000173.** Texaco Exploration and Production Inc. (TEPI) and the U. S. Department of Energy (DOE) entered into a cost sharing cooperative agreement to conduct an Enhanced Oil Recovery demonstration project at Port Neches. The field is located in Orange County near Beaumont, Texas. The project will demonstrate the effectiveness of the CO_2 miscible process in Fluvial Dominated Deltaic reservoirs. It will also evaluate the use of horizontal CO_2 injection wells to improve the overall sweep efficiency. A database of FDD reservoirs for the gulf coast region will be developed by Louisiana State University, using a screening model developed by Texaco Research Center in Houston. Finally, the results and the information gained from this project will be disseminated throughout the oil industry via a series of Society of Petroleum Engineers papers and industry open forums.

DOE/BC/14962-7 **The Utilization of the Microflora Indigenous to and Present in Oil-Bearing Formations to Selectively Plug the More Porous Zones Thereby Increasing Oil Recovery During Waterflooding. Annual Report for January 1, 1994 to December 31, 1994. Hughes Eastern Corporation. August 1995. 60 pp. Order No. DE95000177.** This project is a field demonstration of the ability of in-situ indigenous microorganisms in the North Blowhorn Creek Oil Field to reduce the flow of injection water in the more permeable zones thereby diverting flow to other areas of the reservoir and thus increasing the efficiency of the waterflooding operation. This effect is to be accomplished by adding inorganic nutrients in the form of potassium nitrate and orthophosphate to the injection water. Work on the project is divided into three phases, Planning and Analysis (9 months), Implementation (45 months), and Technology Transfer (12 months).

DOE/BC/14983-5 **Recovery of Bypassed Oil in the Dundee Formation Using Horizontal Drains. Annual Report for April 1994 to June 1995. Michigan Technological University. August 1995. 260 pp. Order No. DE95000181.** Devonian rocks have been the most prolific hydrocarbon producers in the Michigan Basin. The Traverse, Dundee, and Lucas Formations have produced more than half of Michigan's oil since the late 1920's. The Dundee Formation is Michigan's all-time leader with 352 million barrels of oil and 42 billion cubic feet of gas. About 30% of the original oil in place and 80% of the original gas in place is usually recovered from hydrocarbon reservoirs during the initial production phase. This project will demonstrate through a field trial that horizontal wells can substantially increase oil production in older reservoirs that are at or near their economic limit. To maximize the potential of the horizontal well and to ensure that a comprehensive evaluation can be made, extensive reservoir characterization will be performed. In addition to the proposed field trial at Crystal Field, 29 additional Dundee fields in a seven-county area have been selected for study in the reservoir characterization portion of this project.

DOE/BC/14984-5 **Improved Recovery Demonstration for Williston Basin Carbonates. Annual Report for June 10, 1994 to June 9, 1995. Luff Exploration Company. September 1995. 88 pp. Order No. DE95000186.** The purpose of this project is to demonstrate targeted infill and extension drilling opportunities, better determinations of oil-in-place, methods for improved completion efficiency and the suitability of waterflooding in Red River and Ratcliffe shallow-shelf carbonate reservoirs in the Williston Basin, Montana, North Dakota and South Dakota. Improved reservoir characterization utilizing three-dimensional and multi-component seismic are being investigated for identification of structural and stratigraphic reservoir compartments. These seismic characterization tools are integrated with geological and engineering studies. Improved completion efficiency is being tested with extended-reach jetting lance and other ultra-short-radius lateral technologies. Improved completion efficiency, additional wells at closer spacing and better estimates of oil in place will result in additional oil recovery by primary and enhanced recovery processes.

Environmental

DOE/MT/92006-9 **The Cost of Wetland Creation and Restoration. Final Report. University of Maryland. August 1995. 120 pp. Order No. DE95000174.** This report examines the economics of wetland creation, restoration, and enhancement projects, especially as they are used within the context of mitigation for unavoidable wetland losses. Complete engineering-cost-accounting profiles of over 90 wetland projects were developed in collaboration with leading wetland restoration and creation practitioners around the country to develop a primary source database. Data on the costs of over 1,000 wetland projects were gathered from published sources and other available databases to develop a secondary source database. Cases in both databases were carefully analyzed and a set of baseline cost per acre estimates were developed for wetland creation, restoration, and enhancement.

DOE/MT/92007-9 **Characterization of Oil and Gas Waste Disposal Practices and Assessment of Treatment Costs. Final Report. Rice University. August 1995. 220 pp. Order No. DE95000175.** This study examines wastes associated with the onshore exploration and production of crude oil and natural gas in the United States. The objective of this study was to update and enhance the current state of knowledge with regard to oil and gas waste quantities, the potential environmental impact of these wastes, potential methods of treatment, and the costs associated with meeting various degrees of treatment. To meet this objective, the study consisted of three tasks: 1) the development of a Production Environmental Database (PED) for the purpose of assessing current oil and gas waste volumes by state and for investigating the potential environmental impacts associated with current waste disposal practices on a local scale; 2) the evaluation of available and developing technologies for treating produced water waste streams and the identification of unit process configurations; and 3) the evaluation of the costs associated with various degrees of treatment achievable by different treatment configurations.

DOE/MT/92008-10 **Oil Production Enhancement Through a Standardized Brine Treatment. Final Report. Pennsylvania State University. August 1995. 272 pp. Order No. DE95000179.** The Pennsylvania Oil and Gas Association (POGA) approached the Pennsylvania State University to develop a program designed to demonstrate that a treatment process to meet acceptable discharge conditions and effluent limitations can be standardized for all potential stripper well brine discharge. This project has been under way since 1987. A bench-scale prototype model was developed for conducting experiments in laboratory conditions. The experiments in the laboratory conditions were focused on the removal of ferrous iron from synthetically made brine. The results of a number of experiments in the lab were indicative of the capability of the proposed brine treatment process in the removal of iron. In the second phase of this project, a field-based prototype was developed to evaluate and demonstrate the treatment process effectiveness. These experiments were conducted under various conditions and included the testing on five brines from different locations with dissolved constituents.

DOE/MT/92010-10 **Wetland Treatment of Oil and Gas Well Waste Waters. Final Report. University of Michigan. August 1995. 64 pp. Order No. DE95000176.** Constructed wetlands are small, on-site systems that possess three of the most desirable components of an industrial waste water treatment scheme: low cost, low maintenance and upset resistance. The main objectives of the present study is to extend the knowledge base of wetland treatment systems to include processes and substances of particular importance to small, on-site systems receiving oil and gas well wastewaters. A list of the most relevant and comprehensive publications on the design of wetlands for water quality improvement was compiled and critically reviewed. Based on our literature search and conversations with researchers in the private sector, toxic organics such as phenolics and b-naphthoic acid, (NA), and metals such as Cu(II) and Cr(VI) were selected as target adsorbates. A total of 90 lysimeteres equivalent to a laboratory-scale wetland were designed and built to monitor the uptake and transformation of toxic organics and the immobilization of metal ions.

DOE/MT/92011-12 **Geologic, Geochemical, and Geographic Controls on NORM in Produced Water from Texas Oil, Gas, and Geothermal Reservoirs. Final Report. The University of Texas at Austin. August 1995. 76 pp. Order No. DE95000178.** Water from Texas oil, gas, and geothermal wells contains natural radioactivity that ranges from several hundred to several thousand picocuries per liter (pCi/L). This natural radioactivity in produced fluids and the scale that forms in producing and processing equipment can lead to increased concerns for worker safety and additional costs for handling and disposing of water and scale. Naturally occurring radioactive materials (NORM) in oil and gas operations are mainly caused by concentrations of radium-226 and radium-228, daughter products of uranium-238 and thorium-232, respectively, in barite scale. The following areas are examined (1) the geographic distribution of high NORM levels in oil-producing and gas-processing equipment, (2) geologic controls on uranium, thorium, and radium in sedimentary basins and reservoirs, (3) mineralogy of NORM scale, (4) chemical variability and potential to form barite scale in Texas formation waters, (5) radium activity in Texas formation waters, and (6) geochemical controls on radium isotopes in formation water and barite scale to explore natural controls on radioactivity. The approach combined extensive compilations of published data, collection and analyses of new water samples and scale material, and geochemical modeling of scale precipitation and radium incorporation in barite.

Microbial Technology

BNL 60119 **Effects of Selected Thermophilic Microorganisms on Crude Oils at Elevated Temperatures and Pressures. Final Report. Brookhaven National Laboratory. July 1995. 184 pp. Order No. DE95000159.** During the past several years, a considerable amount of work has been carried out showing that microbially enhanced oil recovery (MEOR) is promising and the resulting biotechnology may be deliverable. At the Brookhaven National Laboratory (BNL), systematic studies have been conducted which dealt with the effects of thermophilic and thermoadapted bacteria on the chemical and physical properties of selected types of crude oils at elevated temperatures and pressures. Current studies indicate that during the biotreatment several chemical and physical properties of crude oils are affected.

INDEX

COMPANIES AND INSTITUTIONS

CONTENTS BY EOR PROCESS

DOE Technical Project Officers for Enhanced Oil Recovery

DIRECTORY

Name	Phone number	Name of contractor
U. S. Department of Energy Gas and Petroleum Technology Oil and Gas Exploration and Production 3E-028/FORS Washington, D.C. 20585		
Bartlesville Project Office P. O. Box 1398 Bartlesville, Oklahoma 74005		
Edith Allison	918-337-4390	Columbia University Lomax Exploration Company Louisiana State University University of Texas Utah Geological Survey
Jerry Casteel	918-337-4412	Columbia University Illinois Institute of Technology New Mexico Institute of Mining and Technology Surtek, Inc. Texaco Exploration and Production, Inc. University of Kansas University of Southern Mississippi University of Texas
Robert Lemmon	918-337-4405	Colorado School of Mines Lawrence Berkeley Laboratory Michigan Technological University New Mexico Institute of Mining and Technology ParaMagnetic Logging, Inc. Reservoir Engineering Research Institute University of Texas University of Tulsa University of Wyoming Utah Geological Survey
Rhonda Lindsey	918-337-4407	Hughes Eastern Corporation Oklahoma Geological Survery
Chandra Nautiyal	918-337-4409	Luff Exploration Company Michigan Technological University Oxy USA, Inc. University of Kansas
R. Michael Ray	918-337-4403	Oklahoma Geological Survey
Thomas Reid	918-337-4233	Lawrence Livermore National Laboratory Stanford University University of Alaska University of Southern California
Morgantown Energy Technology Center P.O. Box 880 Morgantown, West Virginia 26505		
Royal Watts	304-285-4218	New Mexico Institute of Mining and Technology

CHEMICAL FLOODING—
SUPPORTING RESEARCH

INVESTIGATION OF OIL RECOVERY IMPROVEMENT BY COUPLING AN INTERFACIAL TENSION AGENT AND A MOBILITY CONTROL AGENT IN LIGHT OIL RESERVOIRS

Contract No. DE-AC22-92BC14886

Surtek, Inc.
Golden, Colo.

Contract Date: Sept. 28, 1992
Anticipated Completion: Sept. 30, 1995
Government Award: $219,925

Principal Investigator:
Malcolm J. Pitts

Project Manager:
Jerry Casteel
Bartlesville Project Office

Reporting Period: Oct. 1–Dec. 31, 1994

Objective

The objective of this study is to investigate two major areas concerning the coinjection of an interfacial tension (IFT) reduction agent(s) and a mobility control agent into petroleum reservoirs. The first task will consist of defining the mechanisms of interaction of an alkaline agent, a surfactant, and a polymer on a fluid–fluid and a fluid–rock basis. The second task is the improvement of the economics of the combined technology.

Summary of Technical Progress

This report examines the effect of rock type on oil recovery by alkaline–surfactant–polymer (ASP) solutions. This report also begins a series of evaluations to improve the economics of ASP oil recovery.

A 1000-mg/L sodium chloride (NaCl) solution was used for coreflooding and chemical make-up. Crude oil was from the Adena field, Morgan County, Colo., a fluvial-deltaic reservoir. The crude oil has an API gravity of 42°. The crude oil with a dead oil viscosity is 3.8 cP at 72 °F and 1.3 cP at the 180 °F reservoir temperature. All studies performed for this research were performed at 150 °F. Dead crude oil viscosity was 1.4 cP at 150 °F.

A series of corefloods conducted previously indicated polymer addition to the alkaline–surfactant solution prevented mobility ratio increases and improved oil recovery.[1–2] Injection of sodium carbonate (Na_2CO_3)–surfactant–polymer recovered up to 30% of the waterflood residual oil.[2]

The rock matrix effect on ASP oil recovery was evaluated with a series of corefloods using Berea, J Sand, and Muddy Sand cores. Each core was waterflooded to residual oil

saturation (S_{or}), which varied with rock type, but all corefloods used the same crude oil, waters, and chemicals. Waterflood S_{or} for Berea averaged 0.318 pore volume (PV), J Sand averaged 0.377 PV, and Muddy Sand averaged 0.256 PV. In each coreflood, 0.300 PV of either 1.0 wt % Na_2CO_3 plus 0.2 wt % Petrostep B-100 plus 500 mg/L Flopaam 3330S or 0.5 wt % Na_2CO_3 plus 0.1 wt % LXS 420 plus 500 mg/L Flopaam 3330S was injected followed by 0.300 PV of 500 mg/L Flopaam 3330S. A water flush of 1.5 PV followed chemical injection. Radial cores were used in Berea and Muddy Sand corefloods and linear cores were used in the J Sand corefloods.

Figures 1 and 2 show the normalized cumulative oil recovery vs. normalized cumulative produced fluid for the two chemical systems. Each coreflood was normalized so that the waterflood oil recovery is 1 and the total fluid injected at the end of the waterflood is 1. Oil recovery with the same oil, water, and ASP solution varied with rock type. The ASP oil recovery variance with rock type is dependent on the chemical solution. No difference between Berea and J Sand is seen with the LXS 420–Na_2CO_3–polymer solution, but a difference is observed when Petrostep B-100–Na_2CO_3–polymer is used. Tertiary oil recoveries as high as 58% of the waterflood oil recovery were observed.

The ASP flood economics can be improved either by decreasing chemical use or by increasing oil recovery efficiency. Table l lists the cost of the ASP injectants used in a previous coreflood.

Polymer and surfactant are the most costly injectants and are therefore the key components to affect economics.

The initial series of corefloods to evaluate different injection methods to improve the ASP economics were ones in which the volume of ASP solution injected was

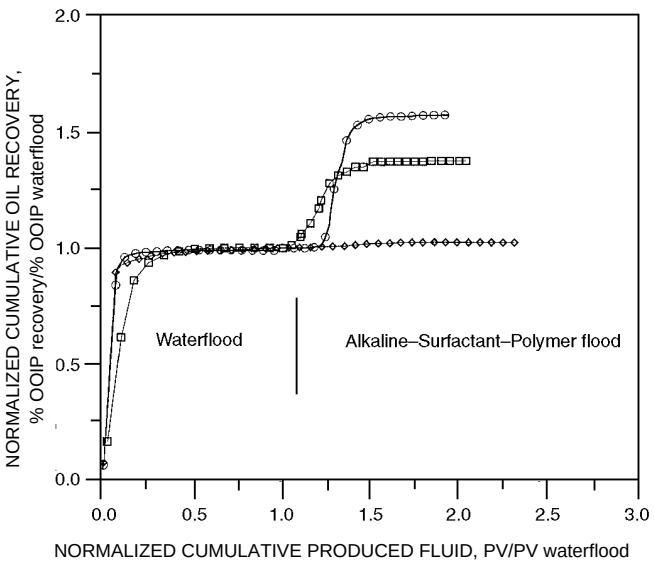

Fig. 1 Sand type effect on oil recovery by alkaline–surfactant–polymer solutions, Petrostep B-100 + Na_2CO_3 + polymer. ○, Berea sandstone. ♦, Muddy Sand sandstone. □, J Sand sandstone.

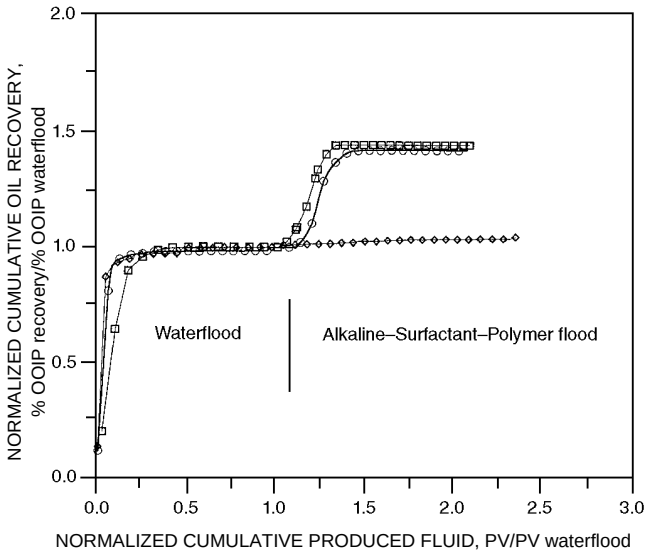

Fig. 2 Sand type effect on oil recovery by alkaline–surfactant–polymer solutions, LXS 420 + Na_2CO_3 + polymer. ○, Berea sandstone. ♦, Muddy Sand sandstone. □, J Sand sandstone.

TABLE 1

Cost of Injected Alkaline–Surfactant–Polymer Solution

Chemical	$/injected bbl	Pore volume injected	$/bbl PV
1.0 wt % Na_2CO_3	0.228	0.30	0.068
0.2 wt % Petrostep B-100	0.665	0.30	0.200
500 mg/L Flopaam 3330S	0.262	0.60	0.157

reduced from 30% PV while maintaining total mobility control fluid volume at 60% PV. Radial corefloods with Berea core were performed in which 0, 10, 20, and 30% PV of 1.0 wt % Na_2CO_3 plus 0.2 wt % Petrostep B-100 plus 500 mg/L Flopaam 3330S was injected, followed by 60, 50, 40, and 30% PV of 500 mg/L Flopaam 3330S. A water flush of 1.5 to 2 PV followed chemical injection. The incremental oil recovery for each of the corefloods is shown as percent of initial oil saturation (S_{oi}) and percent of waterflood S_{or} in Fig. 3. The oil recovery is approaching an asymptote between 20 and 30% PV ASP solution injected. Table 2 shows the cost per incremental barrel of oil. In this case, the most economic injection scenario would be to inject 0.20 PV ASP solution followed by 0.40 PV polymer solution.

Because surfactant is the most expensive component in the Na_2CO_3–Petrostep B-100–Flopaam 3330S injection scheme, a series of corefloods were performed to evaluate a surfactant taper within the ASP slug. The total volume of 1.0 wt % Na_2CO_3 plus Petrostep B-100 plus 500 mg/L Flopaam 3330S injected was 0.3 PV, followed by 0.3 PV of 500 mg/L Flopaam 3330S in each case. Initial surfactant

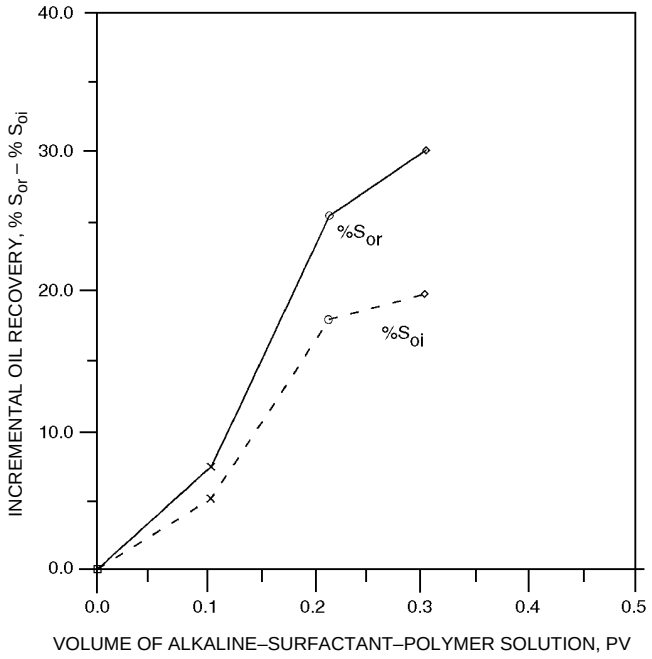

Fig. 3 Volume of alkaline–surfactant–polymer solution, Petrostep B-100 + Na_2CO_3 + polymer, injection vs. oil recovery. ◇, 30% injected. ○, 20% injected. ×, 10% injected. □, 0% injected. S_{or}, residual oil saturation. S_{oi}, initial oil saturation.

TABLE 2

Cost per Incremental Barrel of Oil

Volume injected ASP:polymer drive % PV:% PV	Injectant cost, $/bbl PV	Incremental oil recovery, PV	Cost per incremental bbl, $/bbl
0:60	0.157	0.009	17.44
10:50	0.246	0.027	9.12
20:40	0.335	0.101	3.32
30:30	0.425	0.106	4.01

concentration was 0.2 wt %. Surfactant concentration was tapered to 0.0 wt % over the 30% PV injected in a linear fashion such that the total mass of surfactant injected was 80 and 68% of the base coreflood. The 30% PV:30% PV (1.0 wt % Na_2CO_3 plus 0.2 wt % Petrostep B-100 plus 500 mg/L Flopaam 3330S:500 mg/L Flopaam 3330) coreflood discussed previously is the base coreflood. Alkali and polymer concentrations were maintained at design values as the surfactant concentration was reduced. The normalized cumulative oil recovery vs. normalized cumulative produced fluid is compared in Fig. 4. Again, the oil recoveries and volume injected are normalized to the ending waterflood values for each coreflood. Oil recovery declines as the surfactant is tapered proportional to the mass of surfactant injected. Economic changes are listed in Table 3. Tapering surfactant concentration did not improve ASP economics.

Continued evaluations will study methods to improve ASP economics. Alteration of polymer and alkali concentrations will be investigated.

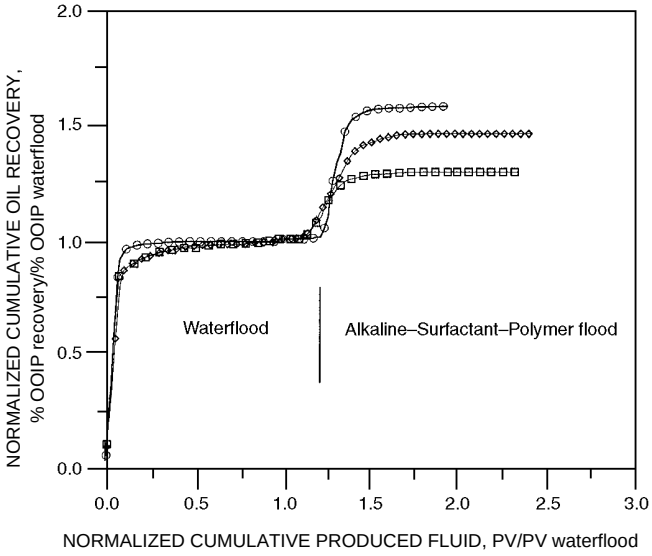

Fig. 4 Effect of tapering the surfactant component of the alkaline–surfactant–polymer (ASP) solution, Petrostep B-100 + Na_2CO_3 + polymer, on oil recovery. ○, 30% PV ASP—surfactant base, no taper. ◇, 30% PV ASP—80% of surfactant base, tapered. □, 30% PV ASP—68% of surfactant base, tapered.

TABLE 3

Surfactant Taper Cost per Incremental Barrel of Oil

Mass of surfactant injected, % of base	Injectant cost, $/bbl PV	Incremental oil recovery, PV	Cost per incremental bbl, $/bbl
100	0.425	0.106	4.01
80	0.406	0.075	5.41
68	0.365	0.048	7.60

References

1. M. J. Pitts, *Investigation of Oil Recovery Improvement by Coupling an Interfacial Tension Agent and a Mobility Control Agent in Light Oil Reservoirs*, DOE Contract No. DE-AC22-92BC14886, Quarterly Report, April 1–June 30, 1994.
2. M. J. Pitts, *Investigation of Oil Recovery Improvement by Coupling an Interfacial Tension Agent and a Mobility Control Agent in Light Oil Reservoirs*, DOE Contract No. DE-AC22-92BC14886, Quarterly Report, July 1–September 30, 1994.

IMPROVING RESERVOIR CONFORMANCE USING GELLED POLYMER SYSTEMS

Contract No. DE-AC22-92BC14881

University of Kansas
Center for Research
Lawrence, Kans.

Contract Date: Sept. 25, 1992
Anticipated Completion: Sept. 24, 1995
Government Award: $707,123

Principal Investigators:
Don W. Green
G. Paul Willhite

Project Manager:
Jerry Casteel
Bartlesville Project Office

Reporting Period: Oct. 1–Dec. 31, 1994

Objectives

The general objectives are to (1) identify and develop gelled polymer systems that have potential to improve reservoir conformance of fluid displacement processes, (2) determine the performance of these systems in bulk and in porous media, and (3) to develop methods to predict the capability of these systems to recover oil from petroleum reservoirs.

This work focuses on three types of gel systems—an aqueous polysaccharide (KUSP1) system that gels as a function of pH, the chromium(III)–polyacrylamide system, and the aluminum citrate–polyacrylamide system. Laboratory research is directed at the fundamental understanding of the physics and chemistry of the gelation process in bulk form and in porous media. This knowledge will be used to develop conceptual and mathematical models of the gelation process. Mathematical models will then be extended to predict the performance of gelled polymer treatments in oil reservoirs.

Summary of Technical Progress

Physical and Chemical Characterization of Gel Systems

Work has continued on a procedure to determine the size of polymer–gel aggregates that form during the gelation of the polyacrylamide–aluminum citrate gel system. One step in this procedure that had been problematic is the determination of polymer concentration. A technique to measure the concentration of the HiVis 350 polymer was identified and tested. The size of gel aggregates will be measured by applying membrane dialysis in different experiments in which membranes of various pore sizes will be used. Experiments were conducted to determine the length of time required for the dialysis process to approach equilibrium.

Mechanisms of In Situ Gelation

Gel treatments using the KUSP1 polysaccharide were conducted in sandpacks and carbonate core plugs. These tests consisted of determining initial permeability, injecting several pore volumes of gelant through the porous medium, shutting in the plugs for sufficient time to allow for gelation, and injecting brine to determine posttreatment permeability. The long-term stability of the treatment is also being assessed.

Two methods were used to gel the KUSP1 polymer in situ. In one method, gelation was promoted by the addition of an ester. The ester reacts slowly with water to produce acid, which reduces pH and causes the KUSP1 polymer to gel. The KUSP1–ester system was tested in a 6.5-cm-long carbonate core plug with an initial permeability of 18 mD. The gel treatment reduced the permeability to 0.093 mD, a reduction by a factor of 600. The KUSP1–ester system was also tested in a 1-ft-long sandpack that had an initial permeability of 7300 mD. The treatment reduced the permeability by a factor of 1700 to 4.3 mD.

A second method to gel KUSP1 is by cross-linking with borate. Borate is introduced to the system as orthoboric acid. Gels formed from the KUSP1–boric acid system are transparent and much firmer than those formed by reducing the pH of KUSP1 solutions. A gel treatment using the KUSP1–boric acid system was conducted in a 1-ft-long sandpack. The treatment reduced the permeability from 7000 to 0.3 mD, a reduction by a factor of greater than 20,000. Testing of the long-term stability of the permeability reduction treatments is under way.

Mathematical Modeling of Gel Systems

A numerical model for in situ gelation of cross-linking polymer solutions is being developed. Preliminary simulations were performed to study crossflow in layered reservoirs. The following points summarize the physical description and key assumptions in the simulations:

- Two-dimensional flow in the axial and vertical directions from a single well is considered with symmetry around the well bore. In order to simplify the numerical calculations, Cartesian geometry is assumed. The model will be extended to radial coordinates, but the results are expected to be qualitatively similar to the results presented.
- Single-phase flow is assumed. The oil in the region surrounding the well bore is assumed to be completely immobile.
- The displacement of an initial solution with another solution of equal viscosity (1 cP) in a two-layered reservoir is considered. The layers are assumed to be of equal height (H) of 500 cm (16.40 ft) and are characterized by an axial permeability (k_x) and a vertical permeability (k_v). A constant bottomhole

pressure of 200 psi is applied at time equal to zero, and the concentration profile of the injected solution is examined within an axial distance (L) of 300 cm (9.84 ft) from the well bore.

The degree of crossflow in a given layer is a function of the ratio of its vertical permeability and its axial permeability (k_v/k_x). Depending on the value of this parameter, the flow behavior in the layered reservoir lies between two limiting cases.

The first limit consists of the case when the ratio k_v/k_x is zero for both layers. This limit physically represents a reservoir with each layer separated by an impermeable shale layer. Figure 1 shows the concentration profiles of the injected solution in the two layers after 10 h of injection. The dark region indicates the injected value of concentration, and the light region indicates the initial concentration. The intermediate shaded band represents the front of the concentration profile as the injected solution traverses the reservoir. Pressure is transmitted in each layer independently of the other, with no crossflow between layers. The concentration fronts of the injected solution are closest to each other under these conditions, and the vertical velocity is identically zero for all times.

The second limit represents the case with complete vertical communication between the layers as the value of k_v/k_x approaches infinity. For the given parameters, this limit is effectively realized when the ratio of k_v/k_x of each layer is unity. The corresponding concentration profiles are shown in Fig. 2. Pressure is instantaneously equalized across the height of the reservoir, with the axial velocities in each layer being proportional to axial permeability. Thus the concentration fronts are farthest apart under these conditions, and the injected solution in layer 1 travels twice the distance as that of the solution in layer 2. Vertical velocities are identically zero for all times.

For intermediate values of k_v/k_x for the two layers, finite vertical velocities exist for varying periods of time, but the concentration profiles always lie between the bounds defined by the two limiting cases. This conclusion is not restricted only to two-layered systems but may also be extended to multilayered reservoirs for Cartesian and radial geometries.

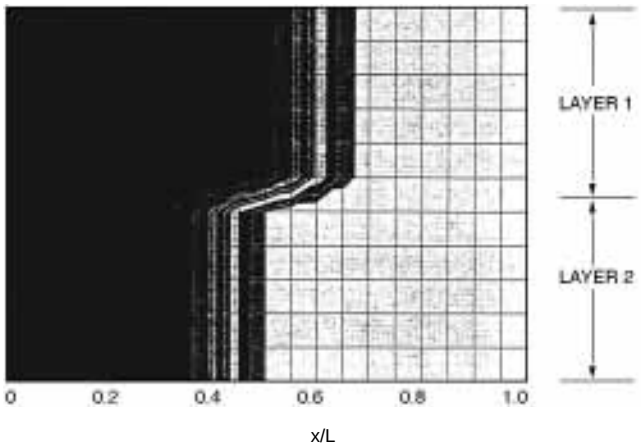

Fig. 1 Concentration profile in a two-layered reservoir after 10 h of injection for $k_v/k_x = 0$ in each layer ($k_x = 1.0$ D, $k_v = 0$ D in layer 1, and $k_x = 0.5$ D, $k_v = 0$ D in layer 2).

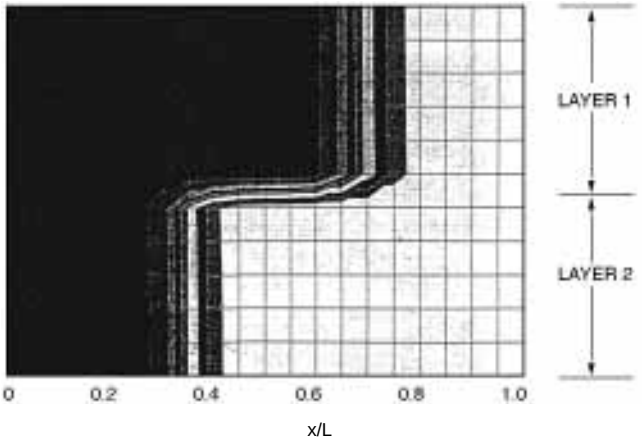

Fig. 2 Concentration profile in a two-layered reservoir after 10 h of injection for $k_v/k_x = 1$ in each layer ($k_x = 1.0$ D, $k_v = 1.0$ D in layer 1, and $k_x = 0.5$ D, $k_v = 0.5$ D in layer 2).

RESPONSIVE COPOLYMERS FOR ENHANCED PETROLEUM RECOVERY

Contract No. DE-AC22-92BC14882

University of Southern Mississippi
Hattiesburg, Miss.

Contract Date: Sept. 22, 1992
Anticipated Completion: Sept. 21, 1995
Government Award: $276,650
(Current year)

Principal Investigators:
Charles McCormick
Roger Hester

Project Manager:
Jerry Casteel
Bartlesville Project Office

Reporting Period: Oct. 1–Dec. 31, 1994

Objective

The overall objective of this research is the development of advanced water-soluble copolymers for use in enhanced oil

recovery (EOR) that rely on reversible microheterogeneous associations for mobility control and reservoir conformance.

Summary of Technical Progress

Quaternary Ammonium Cyclopolymer Synthesis

Cationic quaternary ammonium polyelectrolytes have been the subject of increased research efforts in recent years because of their diverse commercial applications.[1] Among the most prominent technological water-soluble cationic ammonium polymers is poly(diallyldimethylammonium chloride) (PDADMAC). The synthesis of the hydrophobic comonomer N,N-diallyl-N-(4-hexyloxybenzyl)-N-methyl-ammonium chloride is depicted in Scheme 1. The synthesis of the cyclocopolymer from N,N-diallyl-N,N-dimethylammonium chloride (DADMAC) and N,N-diallyl-N-methyl-N-(4-alkoxybenzyl)ammonium chloride is illustrated in Scheme 2.

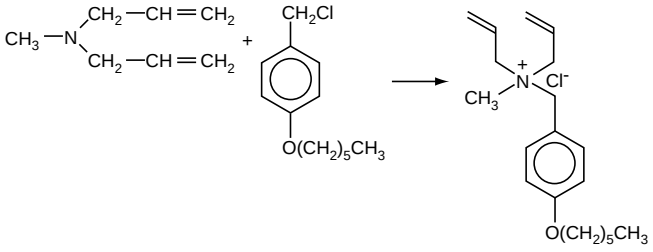

Scheme 1 Synthesis of N,N-diallyl-N-(4-hexyloxybenzyl)-N-methyl-ammonium chloride.

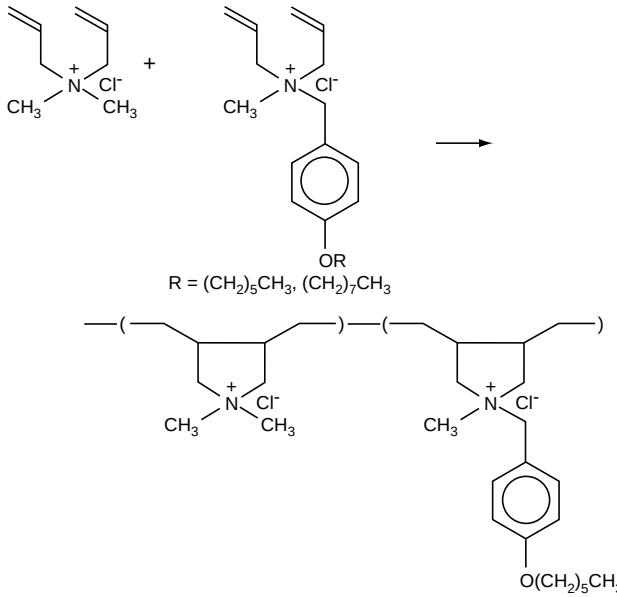

Scheme 2 Copolymerization of diallyl monomers to give hydrophobically modified cyclopolymers.

Characterization of Molecular Structure and Solution Behavior

^{1}H and ^{13}C nuclear magnetic resonance (NMR) spectra were recorded with a Bruker AC-200. A Mattson 2020 Galaxy Series Fourier transform infrared radiation spectroscope (FTIR) was used to obtain infrared spectra. A Hewlett Packard 5890 Series II gas chromatograph equipped with an Alltech AT-5 capillary column was used to determine the purity of liquid samples. A Hewlett Packard Model 1050 high-pressure liquid chromatograph (HPLC) was used to determine the purity of solid samples. A Waters Bondapak C18 column was used with methanol as the mobile phase. Classical light-scattering studies were performed with a Chromatix KMX-6 low-angle laser light-scattering spectrophotometer with a 2-mW helium–neon laser operating at 633 nm. Refractive index increments (dn/dc) were obtained with a Chromatix KMX-16 differential refractometer. The molecular weight of PDADMAC was measured in 0.5*M* sodium chloride (NaCl) solution. For hydrophobically modified copolymers, methanol was used as a solvent in the light-scattering studies to disrupt hydrophobic associations and to keep the copolymers from interacting with the filter. Steady-state fluorescence measurements were made with a Spex Fluorolog-2 fluorescence spectrometer and corrected for the wavelength dependence of the detector with the use of an internal correction function provided by the manufacturer. Viscosity measurements were conducted with a Contraves LS-30 low shear rheometer at a constant shear rate of 1.28 s^{-1} at 25 °C unless otherwise noted.

The viscometric studies were performed at low shear rate (1.28 s^{-1}) to minimize shear-dependent conformational changes. Figure 1 shows the change of intrinsic viscosity as a

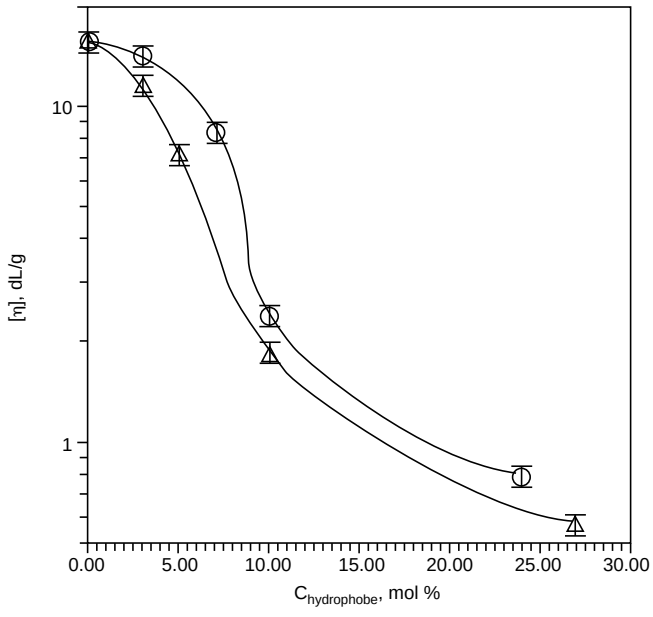

Fig. 1 Effect of hexyl and octyl group content on the intrinsic viscosity [η] of hydrophobically modified cyclopolymers in deionized water at 25 °C. Φ, 17-C6. Δ, 17-C8.

function of hydrophobic group content for the hexylbenzyl and octylbenzyl copolymer series. Intrinsic viscosities decrease continuously with increasing hydrophobe concentration for both hexyl and octyl copolymers.

^{23}Na NMR Studies of Ion-Binding to Anionic Polyelectrolytes

Copolymers of acrylamide with sodium 2-acrylamido-2-propanesulfonate (NaAMPS) and 3-acrylamido-3-methylbutanoic acid (NaAMB) maintain viscosity in high concentrations of divalent salts and do not phase separate in the presence of Ca^{2+} at temperatures up to 100 °C [polymer structures (poly(sodium acrylate) (NaAA), poly(sodium galacturonate) (NaGAL), NaAMB, and NaAMPS are shown in Fig. 2]. Unlike NaAMPS, however, the NaAMB homopolymer will phase separate at temperatures above 70 °C in high concentrations of calcium chloride ($CaCl_2$). The amount of Ca^{2+} necessary to precipitate NaAMB far exceeds the stoichiometric concentration required to bind to all the anionic sites.

The ^{23}Na relaxation rates for the polyion systems studied in this work have been used to yield correlation times, τ_c; a theoretical estimate was used for the fraction of bound monovalent ions, P_b, in the presence of excess divalent ions. Correlation times were then used to obtain values for the quadrupolar coupling constant, χ. The Manning two-variable theory,[2] which has been demonstrated to be qualitatively descriptive of the fraction of ions bound in the presence of divalent ions, was used to determine the values for P_b for Na^+ in the presence of excess divalent ions.

^{23}Na nuclei are well suited for the study of cation binding behavior to electrolytes because of a 100% natural abundance and a high magnetogyric ratio that allow observation by NMR. The sodium ion has a spin 3/2 nucleus in which relaxation is dominated by quadrupolar effects in

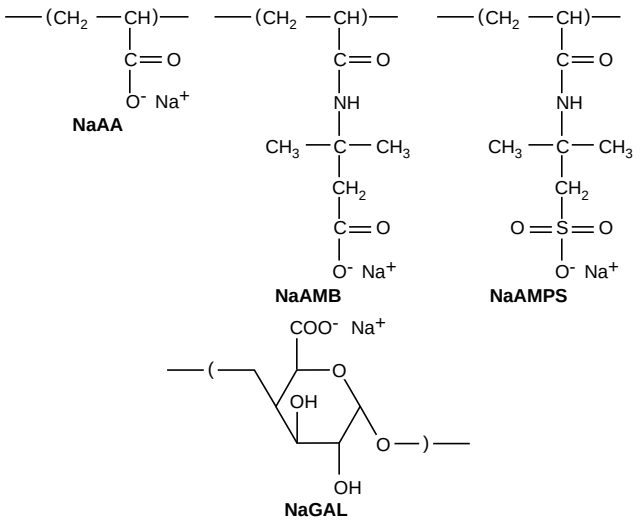

Fig. 2 Structure of copolymers used in NMR study.

solution. The relaxation rates, R_1 and R_2, are sensitive to changes that affect the overall motion in solution and to electric field gradients (efg) about the nuclei. ^{23}Na relaxation rate measurements and chemical shift values thus provide a meansfor investigation of cation binding to polyelectrolytes and for observation of conformational changes that may occur as the degree of ionization along the polymer backbone increases.

The results for ^{23}Na NMR relaxation studies have generally been interpreted with the use of a two-site model for the observed line widths or relaxation rates. The two-site model is justified when the exchange rate for the Na^+ nuclei between the polyanion and bulk solution is faster than the NMR observation time, which is usually the case for the sodium salts of polyanions. The observed relaxation rates are therefore an average of the relaxation rates for the unbound fraction (P_F) or free sodium nuclei and the fraction of ions bound (P_b) to the polymer

$$R_{1,obs} = P_F R_{1,F} + P_b R_{1,b} \quad (1)$$

$$R_{2,obs} = P_F R_{2,F} + P_b R_{2,b} \quad (2)$$

The magnitude of the relaxation rate depends on the strength of the efg experienced by the sodium nuclei at the polyion surface, the lifetime of the Na^+ at the site, and the number of the sodium nuclei that are bound. The longitudinal and transverse relaxation rates generally display single exponential behavior of the intensity of the NMR signal (M_{obs}) as a function of t, the relaxation delay.

$$M_{L,obs}(t) - M_{L,0} = [M_L(0) - M_{L,0}]\, e^{-R_1 t} \quad (3)$$

$$M_{T,obs}(t) = M_T(0)\, e^{-R_2 t} \quad (4)$$

This is a result of the rapid motion and reorientation of the sodium nuclei such that $\omega\tau_c < 0.25$ and consequently $R_1 = R_2$. Under conditions of fast exchange and $\omega\tau_c > 1.5$, R_1 is no longer equal to R_2, and the relaxation rates become biexponential decays of the intensity of the NMR transition and the relaxation delay, t.

$$M_{L,obs}(t) = M_L(0)\ 0.6\ e^{-R_{2f} t} + M_{L,0}(0)\ 0.4\ e^{-R_{2s} t} \quad (5)$$

Here R_{2f} and R_{2s} refer to the fast and slow components of the relaxation decay, respectively. In practice, only the transverse relaxation has been observed to display significant biexponential decay with the longitudinal relaxation having single exponential behavior. When $0.25 < \omega\tau_c < 1.5$, the biexponential behavior is diminished, but the relaxation rates are approximately exponential with $R_1 \neq R_2$. Under these conditions, τ_c can be obtained from the ratio of R_1 to R_2.[3–4]

NMR, Viscosity, and Phase Separation Measurements

Sodium NMR measurements were conducted at 25 °C with a Bruker MSL-400 operating at 105.6 MHz for ^{23}Na nuclei. Interpretation of the ^{23}Na NMR measurements requires the condition of fast exchange such that the observed relaxation rates are an average of the bound and unbound Na^+ ions (two-site model). This was verified as an increase in R_{2s} with reciprocal of temperature (Fig. 3), as described by Grasdalen and Kvam,[3] and has been reported for a number of polyelectrolytes.[3–6] The relaxation data vs. the ratio of the number of equivalents of added salt to the number of charged polymer sites are plotted.

Biexponential relaxation rates were observed to be time dependent in solutions of NaAA, NaAMB, and NaAMPS with R_{2f} decreasing slightly to a constant value over the course of approximately 1 month. This behavior is reminiscent of the time dependency in the viscosity of NaAMB[2] and is consistent with initial clustering of polymer chains that slowly deaggregate upon dissolution. Polymer solutions stored in polypropylene containers to eliminate the possibility of Na^+ ions diffusing into the solutions from glass behaved the same as those stored in glass containers. The increase in biexponential relaxation ($\Delta R_2 = R_{2f} - R_{2s}$) with decreasing polymer concentration for NaAA correlated with that predicted by Halle et al.[5] For the polymer concentration (0.011*M*) used in this work, ΔR_2 with no added salt is approximately 140 Hz.[5]

The behavior of R_2 for sodium counterions with NaAA in the presence of added Na^+ and K^+ is shown in Fig. 4. The effect of added Na^+ on R_1 is also shown. The R_1 data for K^+ and the single exponential fits to the transverse relaxation are not presented to avoid further confusion on the plots. The R_1 data for K^+ are nearly identical to those for Na^+. The experiments by Leyte and coworkers[6] demonstrated that the biexponential behavior of sodium (polystyrenesulfonate), NaPSS, diminished as the concentration of added NaCl increased to approximately twice the polymer concentration. In Fig. 4, R_{2f} and R_{2s} reach similar values at $C_{salt}/C_p \approx 3$. Biexponential relaxation of NaAA with added Na^+ and K^+ is nearly identical, which indicates similar binding of the ions to NaAA.

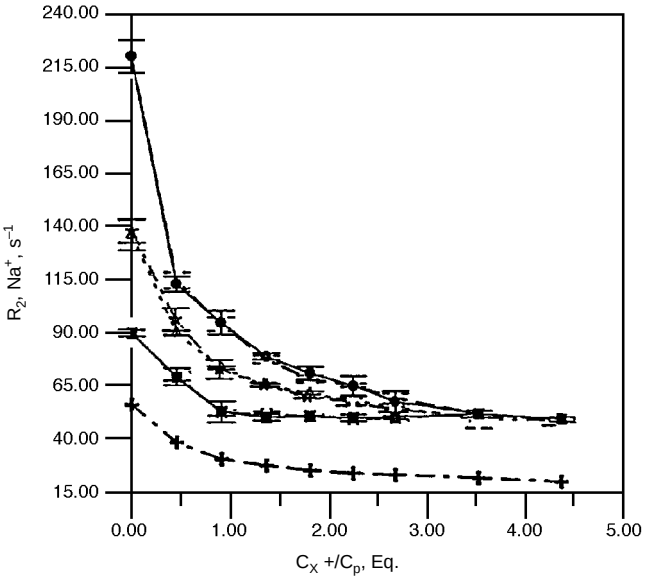

Fig. 4 Longitudinal (R_1) and transverse (R_{2s} and R_{2f}) relaxation rates of NaAA with increasing Na^+ and K^+ concentration. The polymer concentration is 0.1 g/dL. —■—, R_{2s}, Na^+. —●—, R_{2f}, Na^+. —□—, R_{2s}, K^+. —○—, R_{2f}, K^+. — + --, R_1, Na^+. -- Δ --, R_2, Na^+. —*--, R_2, K^+.

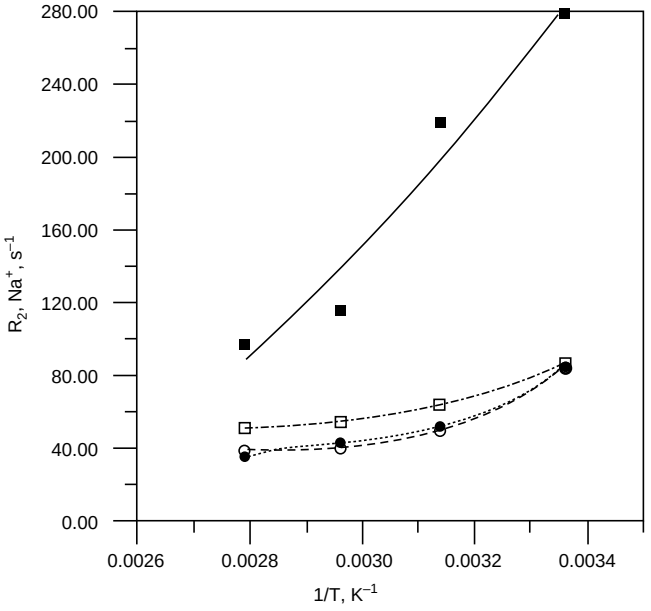

Fig. 3 Slow component of the relaxation rate, R_{2s}, of NaAA (□), NaGAL (■), NaAMB (○), and NaAMPS (●) as a function of temperature (T) at a polymer concentration of 0.1 g/dL.

^{23}Na NMR Studies of Hydrophobically Modified Polyacids

The major objective of this work was to investigate, via ^{23}Na NMR, the behavior of sodium hydroxide-neutralized acrylic and methacrylic acid copolymers that have been prepared with 1 and 10 mol % 2-(1-naphthylacetamido)ethylacrylamide (NAEAM) comonomer (Fig. 5). The NAEAM comonomer serves a dual purpose of acting as a hydrophobe and a fluorescence label. A further objective of this work was to ascertain whether or not the ^{23}Na NMR method might be useful in probing the pH-responsive domain organization deduced from previous photophysical and viscometric studies.

The longitudinal and transverse relaxation rates of poly(acrylic acid) (PAA), poly(methacrylic acid) (PMA), and the labeled, hydrophobically modified NAA and NMA series (Fig. 5) will be presented. The slow and fast transverse relaxation rates, R_{2s} and R_{2f}, respectively, are included when the relaxation

decays displayed biexponential character at low degree of ionization, α. At α values above 0.8, biexponential rate behavior was observed; however, these data are not presented because the region of interest for this study is α values less than approximately 0.8. Correlation times, τ_c, are calculated from $\Delta(R_1 / R_2)$ because $\omega\tau_c > 0.25$ over the range of all α values. For the NMA series, the biexponential relaxation rates observed at low α were also used to calculate $P_b\chi^2$.

In Fig. 6 the transverse and longitudinal relaxation rates for NAA-1 are plotted as a function of the degree of ionization. R_1 and R_2 values are nearly identical for NAA-1 and PAA. Also, the values for the latter are consistent with those from previous studies.[7] In Ref. 7, R_2 has slightly higher values than R_1, which indicates that $\omega\tau_c > 0.25$.[8] The data presented in this work also demonstrate that $\omega\tau_c > 0.25$, as evidenced by the inequality of R_1 and R_2 over the range of pH values studied. Both relaxation rates increase smoothly toward $\alpha = 1$. The similarity in the relaxation rates for PAA and NAA-1 demonstrates that incorporation of 1% NAEAM has no observable effect on the ^{23}Na NMR behavior.

Figure 7 illustrates the dependence of R_1 and R_2 on α for NAA-10. The behavior is quite different from that observed in PAA and NAA-1. Below $\alpha = 0.5$, R_2 can be resolved into slow and fast (R_{2s} and R_{2f}, respectively) components. Note that a substantial decrease in R_2 and R_{2f} is matched by a marked increase in I_E/I_M (the fluorescence intensity ratio of excimer to monomer designated by the stars in Fig. 7) as α approaches 0.5. These superimposed data are from previous studies[9] on this polymer by this group. This behavior is consistent with the adoption of a pseudomicellar conformation with high values of I_E/I_M.[9] The micelle-like or hypercoil structure persists at still higher values of α up to 0.7, beyond which R_2 increases dramatically and I_E/I_M decreases slightly. The number of ions bound and the strength of the binding in the hypercoil play roles in the observed changes.

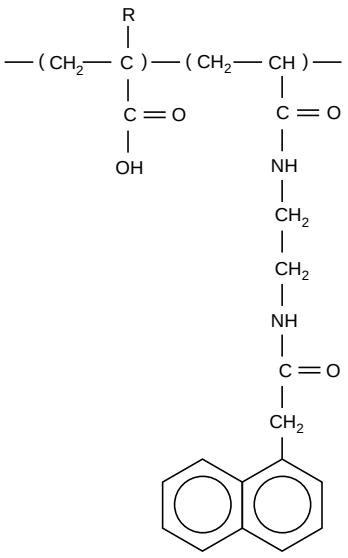

Fig. 5 Structures of the NAA and NMA copolymers. R = –H: NAA-1, 10. R = –CH_3: NMA-1, 10.

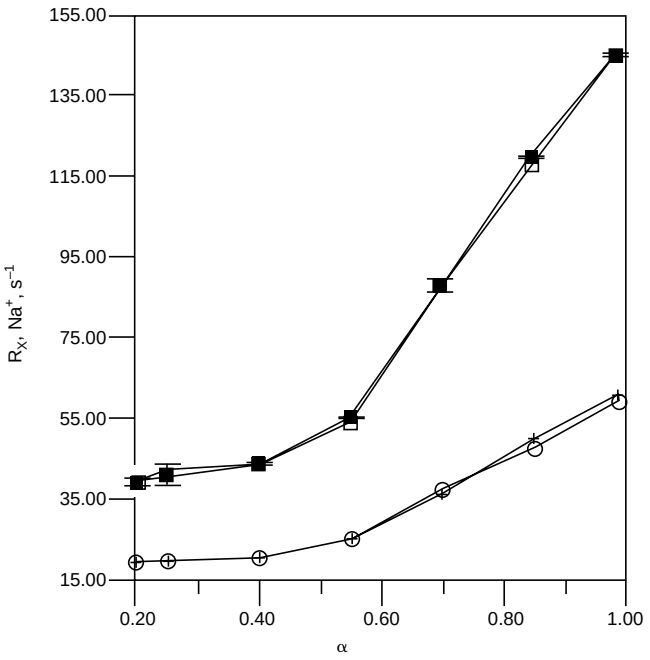

Fig. 6 Transverse (R_2) and longitudinal (R_1) relaxation rates of PAA and NAA-1 with increasing α. The polymer concentration is 0.1 g/dL. —□—, PAA R_2. —○—, PAA R_1. —■—, NAA-1 R_2. — + —, NAA-1 R_1.

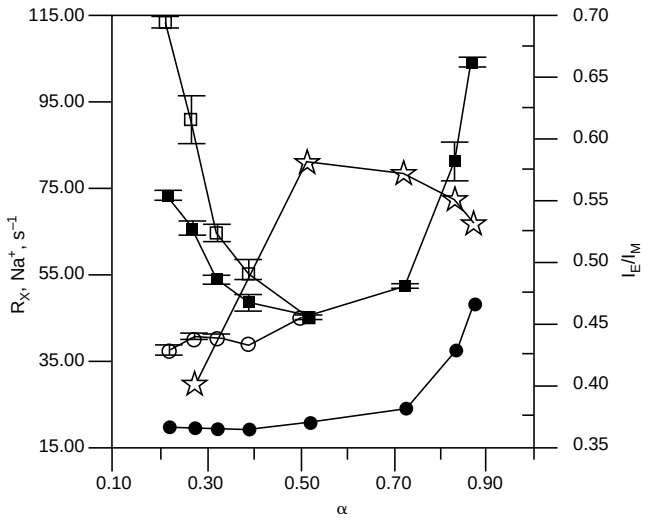

Fig. 7 Transverse (R_2) and longitudinal (R_1) relaxation rates of NAA-10 with increasing α along with the biexponential transverse relaxation rates (R_{2s} and R_{2f}). The ratio of excimer to monomer, fluorescence emission (I_E/I_M) is also depicted. The polymer concentration is 0.1 g/dL. —●—, R_1. —■—, R_2. —○—, R_{2s}. —□—, R_{2f}. —*—, $I_E I_M$.

Solution Rheology

NaAMB/AM Copolymer Solution Flow Behavior in Porous Media

When using a dilute polymer solution to flood an oil reservoir, the displacing fluid should have a high resistance to flow within the porous medium. High flow resistance increases movement of residual oil to a producing well and thus enhances oil recovery. Fluid resistance results from polymer coil molecular distortions during flow through the small and tortuous channels of the porous medium. Polymer solution behavior in complex porous media can be modeled with the use of packed beds of uniform solid spheres.

As polymer coils in solution pass through a bed of packed spheres of diameter d, they travel through a continuous and interconnected series of converging and diverging cavities. The fluid in this geometry will continually accelerate and decelerate as it passes from cavity to cavity. Fluid acceleration and deceleration forces will compel the polymer coils to extend and then contract or recover after each extension. The number of coil extensions and recovery cycles is equal to the number of cavities passed through by the polymer in a given time.

Each coil extension recovery cycle will convert some fluid kinetic energy into heat. This energy conversion will be sensed as a higher solution pressure drop across the bed, ΔP, as compared to the pressure drop of a solvent flowing through the bed at the same flow conditions. This fluid pressure increase is expressed as a normalized flow resistance, Ψ.

The normalized flow resistance, Ψ, is directly related to the amount of energy converted to heat by the polymer coils as they travel through the packed bed and are continually extended and contracted. Thus Durst plots, which show the normalized flow resistance vs. Deborah number (D_e), show the efficiency that polymer coils convert kinetic energy to heat as a function of flow conditions, porous media geometry, and polymer properties and concentration.

The normalized flow resistance, Ψ, measures solution flow resistance in a porous media under conditions specified by the Reynolds and Deborah numbers. It is calculated from the friction factor of the solution, f, and the friction factor of the solvent, f_s, measured at the same bed Reynolds number. The D_e is the product of the polymer coil response time, τ, and the average fluid extension rate, $\in$, which depend upon average fluid velocity and the pore geometry. These dimensionless parameters are defined by the following relationships:

$$D_e = \in \lambda \qquad \Psi = \frac{f - f_s}{f_s [\eta] C} \tag{6}$$

$$\in = \frac{(2)^{1/2}\, v}{d\phi} \qquad Re \equiv \frac{vd\rho}{\eta_s (1-\phi)} \tag{7}$$

$$\tau = \frac{\eta_s [\eta] M}{RT} \qquad f \equiv \frac{d\phi^3}{v^2 (1-\phi)\rho} \quad \frac{\Delta P}{\Delta l} \tag{8}$$

As shown in the preceding equations, the nature of the porous medium is specified by the diameter of the spherical particles, d, forming a bed with porosity, ϕ. The fluid flow resistance through the bed is measured by the pressure drop per unit length of bed, $\Delta P / \Delta l$. Flow conditions through the bed are defined by the average fluid velocity, v. This velocity is based on the cross-sectional area of an empty bed. The fluid velocity within the pore channels within the bed would be the empty bed velocity divided by the bed porosity. Solution properties of shear viscosity, η_s, and density, ρ, are also used in the dimensionless groups. The coil response time, τ, can be estimated from the intrinsic viscosity of the polymer, $[\eta]$, its molecular weight, *M*, and the temperature, T.

Past experimental work has shown that, as the D_e approaches unity, a maximum solution flow resistance develops and is maintained at higher D_e's.[10] The maximum in the normalized flow resistance is expected to be a function of polymer molecular weight, macromolecular structure, and the concentration of polymer coils in solution.

The high-molecular-weight random copolymers used in this study were synthesized from acrylamide (AM) and 3-acrylamido-3-methylbutanoic acid (AMBA) monomers in the ratio as described in previous publications.[11–12] Four copolymers in the solid form were synthesized and had AM/NaAMB monomer ratios of 5/95, 10/90 (two samples of different molecular weights), and 20/80. The aqueous solvent used to make all polymer solutions contained 0.514*M* NaCl and had a viscosity of 0.934 cP at 25 °C.

Solutions of these copolymers were analyzed with the use of static and dynamic light-scattering characterization techniques to find coil sizes, molecular weights, and viral coefficients. A low shear Contraves rheometer was used to estimate each solution intrinsic viscosity in the limit of zero shear rates. Table 1 lists polymer properties and the calculated dilute solution coil response times for each polymer.

The porous media rheometer[13] used for this study is shown in Fig. 8. As shown by the Durst plots of Figs. 9 and 10, all polymer solutions show the same generally expected Ψ vs. D_e relationship.

As shown by both figures, at D_e's less than 0.1, Ψ values are usually less than 4. As the D_e increases above 0.1, the Ψ values increase to a maximum at a D_e of about 0.5. In contrast to previous observations,[10] however, the Ψ parameter decreases as the D_e increases to values greater than 0.5. This reduction in the normalized flow resistance at higher D_e's is probably due to the diminished ability of polymer coils to convert kinetic energy to heat as they are extended and compressed at faster rates. At faster fluid flow conditions, the polymer coils are unable to follow in concert with the rapidly changing local fluid flow fields because insufficient time is available for coil deformation during fluid acceleration and coil recovery during fluid deceleration. As a consequence, less total coil extension and compression is experienced each cycle, and thus less energy is converted into heat by the macromolecules. Therefore the solution will have less resistance to flow through the porous medium at higher D_e's.

TABLE 1

NaAMB/AM Copolymer Solution Properties at 25 °C Using 0.514*M* NaCl Aqueous Solvent

Copolymer monomer molar ratio	Intrinsic viscosity	Diffusional coefficient	Hydrodynamic radius	Radius of gyration	Weight average molecular weight	Second viral coefficient	Polymer coil response time
NaAMB:AM	[η]	$D_{true} \times 10^8$	R_h	R_g	$M \times 10^6$	$A_2 \times 10^4$	τ
Dimensionless	dL/g	cm^2/s	Å	Å	g/mol	mL mol/g^2	$s \times 10^3$
0:100	7.2	–	–	–	3.3	–	1
5:95	17	1.3	1800	2950	12	2.8	8.3
10:90	4.8	–	–	–	1.9	–	0.4
10:90	18	5	460	–	11	–	7.8
20:80	46	0.68	3400	3700	14	3.1	26.2

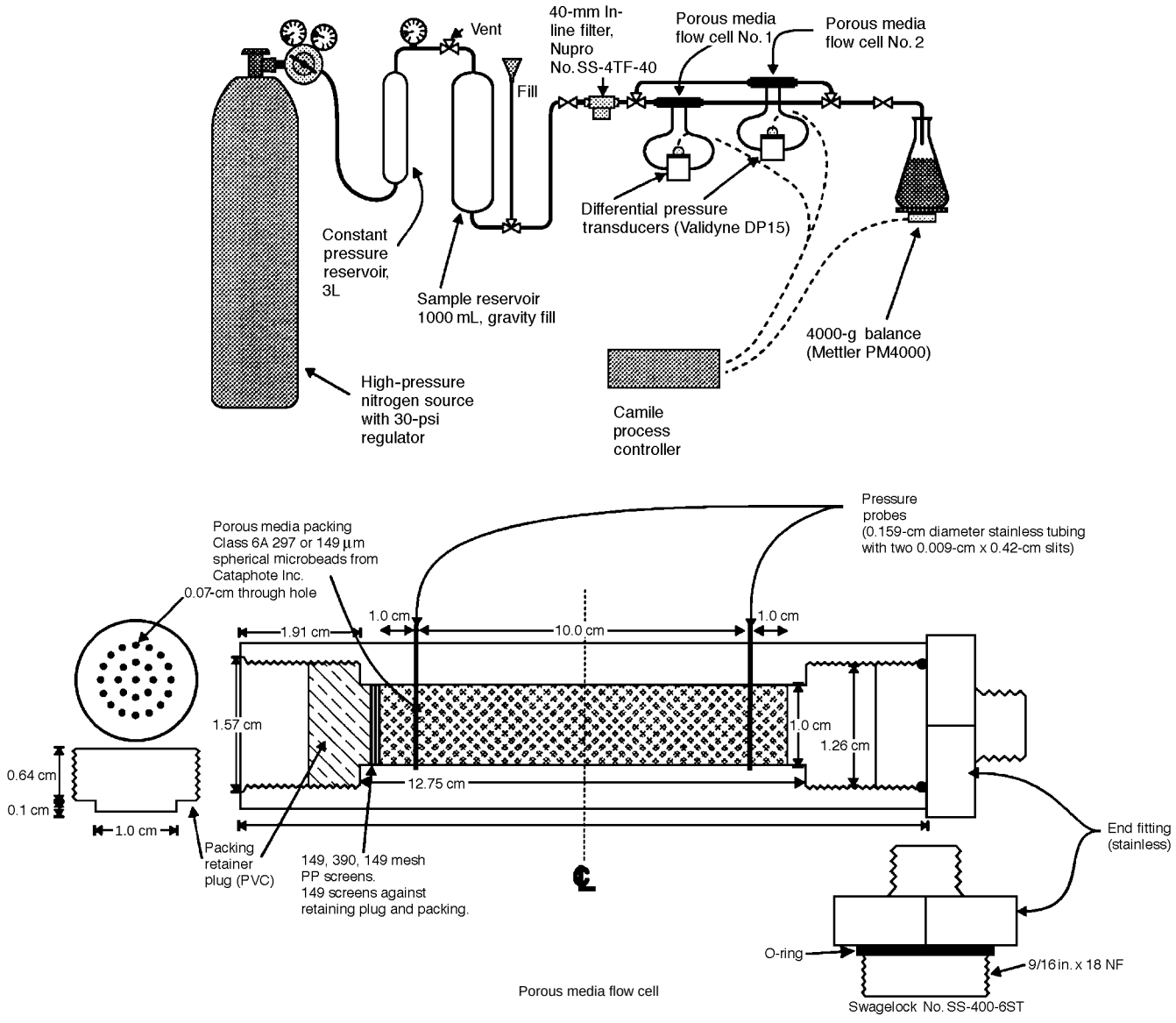

Fig. 8 Porous media elongational flow rheometer system.

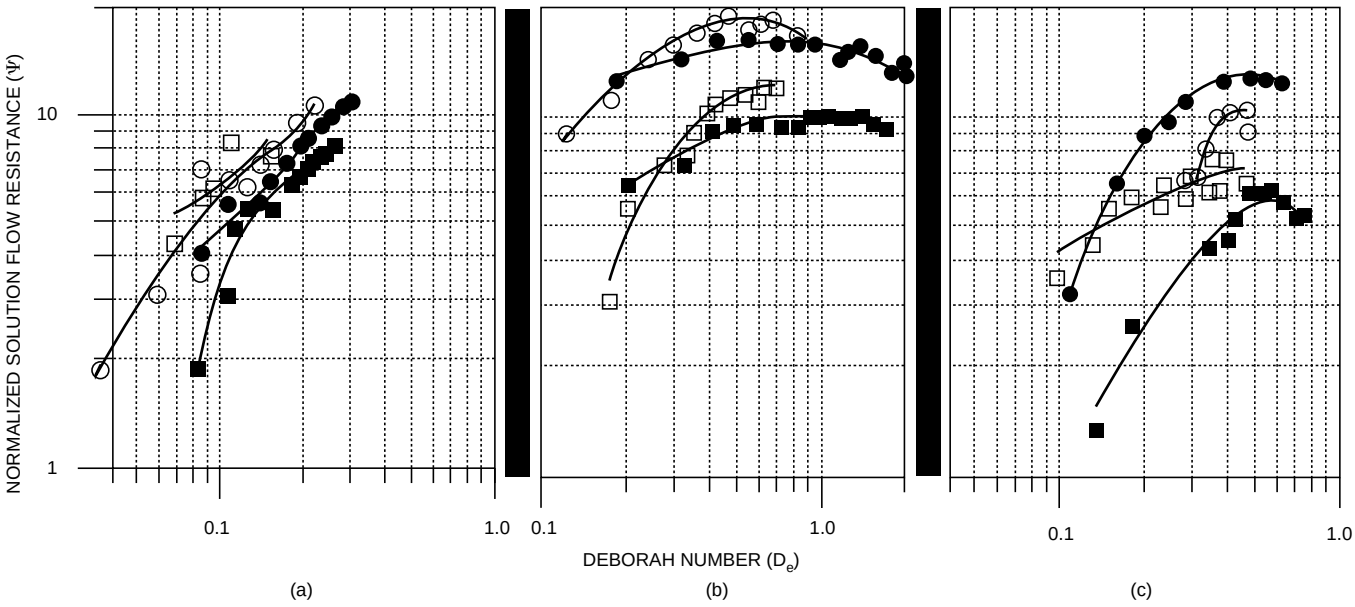

Fig. 9 Flow resistance of 3-acrylamido-3-methylbutanoic acid–acrylamide (mole ratio of 1:9) copolymers and polyacrylamide homopolymer solutions. ● and ■, bed 1 (d = 283 μm). ○ and □, bed 2 (d = 150 μm). Note: d = diameter of spherical beads forming the packed bed.

When the polymer has a low molecular weight, very large fluid velocities are needed in a porous medium to achieve a D_e greater than 0.1. This can be shown by using parts a and b of Fig. 9 to compare the flow performance of low and high molecular weight NaAMB/AM copolymers. For these two copolymers to have the same D_e flow conditions, the fluid velocity of the low-molecular-weight copolymer must be about 20 times as large as the high-molecular-weight copolymer because, for equal D_e's, the fluid velocities must scale to the ratio of the inverse of each copolymer response time (7.8 ms/0.4 ms ≅ 20).

These results show that low-molecular-weight polymers would not have significant extensional flow resistance in reservoirs because the fluid velocities at typical flooding conditions away from the injection well are too low to cause coil extension. In contrast, a high-molecular-weight copolymer coil can be extended in the porous media at much lower fluid velocity, and therefore high-molecular-weight polymers are better candidates for reservoir flooding.

The normalized flow resistance, Ψ, is directly proportional to the difference between solution and solvent friction factors, $f - f_s$, and is also inversely proportional to the product of the dimensionless concentration of polymer coils in solution and solvent friction factor. The dimensionless concentration of polymer coils is the product of the polymer's mass concentration and its intrinsic viscosity, $C[\eta]$; thus Ψ is a measure of the increase in solution flow resistance as compared to solvent per dimensionless concentration of polymer coils in solution. Because higher molecular-weight polymers have larger intrinsic viscosities than lower molecular-weight polymers (coils occupy more volume per unit mass polymer), less high-molecular-weight polymer mass is needed for the same dimensionless concentration; thus less mass of a high-molecular-weight polymer is needed to achieve the same normalized flow resistance, Ψ, when compared with lower molecular-weight polymer.

Polymer molecular structure is also an important factor influencing solution flow resistance. Parts a and b of Fig. 10 show Durst plots of three different NaAMB/AM copolymers. The molecular weights of all three copolymers are about the same; however, the difference in copolymer monomer composition has greatly affected the expansion of the polymer coils. The NaAMB/AM 20/80 copolymer with 20% NaAMB monomer has an intrinsic viscosity of 46 dL/g. This intrinsic viscosity is 2.5 times as great as the other two copolymers. Also, as shown by Table 1, the macromolecular coils of the 20/80 copolymer are much larger in diameter than those of the other two copolymers. The 20/80 monomer composition has greatly expanded the polymer coils in solution.

When compared with the 3.3 million molecular-weight AM homopolymer shown in part c of Fig. 9, the 14 million molecular-weight 20/80 copolymer shown in part c of Fig. 10 has a coil response time that is 26 times as great (26 ms vs. 1 ms). Thus, even at very low porous media fluid velocities,

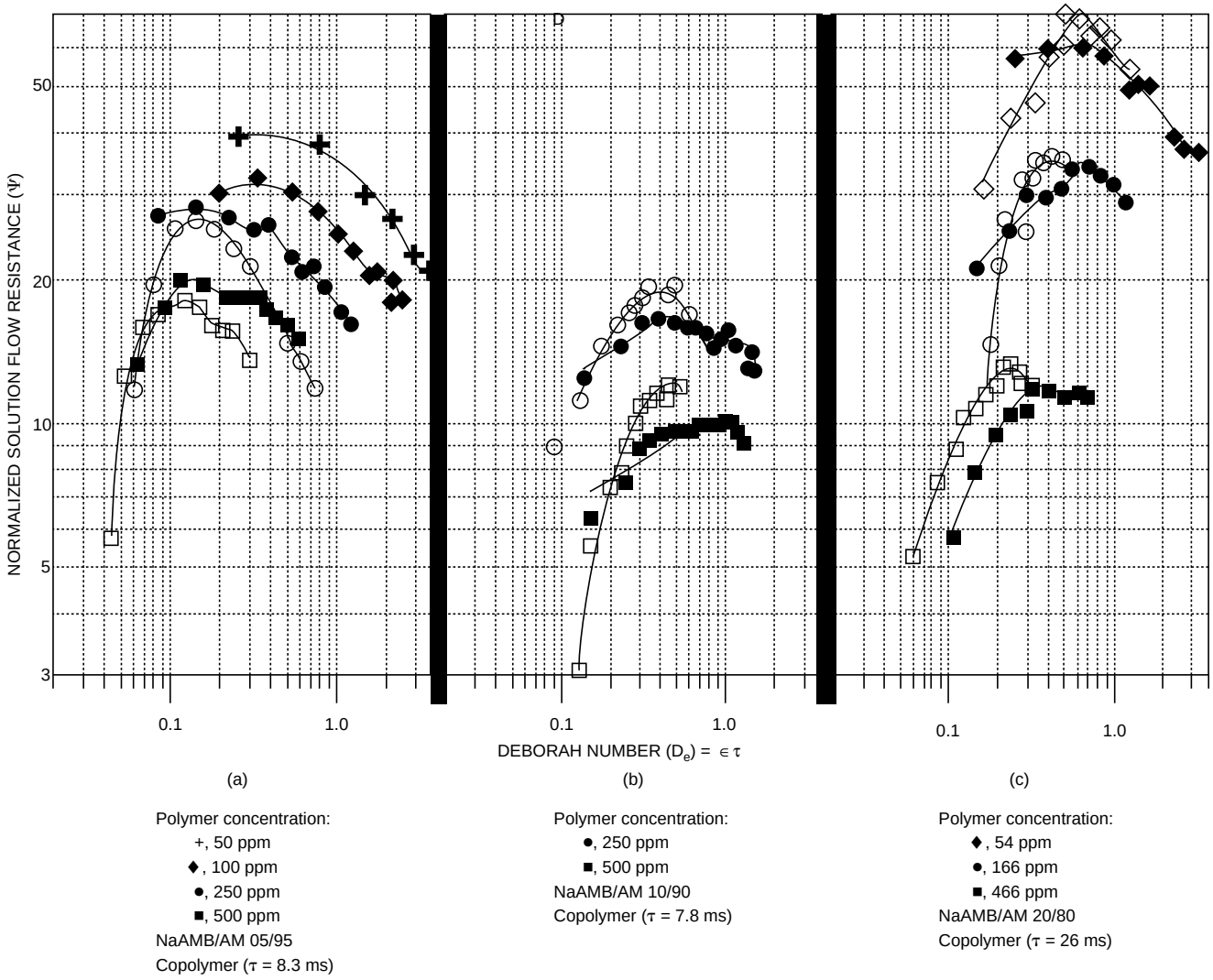

Fig. 10 Durst plots showing flow resistance of 3-acrylamido-3-methylbutanoic acid–acrylamide copolymer solutions through packed beds at 25 °C. ● and ■, bed 1 (d = 297 μm). ○ and □, bed 2 (d = 149 μm).

the 20/80 polymer coils will experience elongation and therefore have a large resistance to flow.

All of the Durst plots show the same general behavior regardless of polymer type. At D_e numbers less than about 0.1, the normalized flow resistance is very low, which indicates that almost no polymer coil extension and recovery are occurring under these conditions. At D_e's between 0.1 and 0.8, the normalized flow resistance increases to a maximum but then decreases as the D_e increases to higher values. This suggests that the degree of polymer coil expansion and recovery is at first accelerating under these conditions and then reaches a limit at a D_e of about 0.6. Above this D_e, the polymer coils are probably not able to completely recover all the large extensional strains developed during previous extension recovery cycles. Thus they have less potential to extend in subsequent extension recovery cycles. Therefore, at higher D_e's, the coils travel through the bed in a more extended state. They will have less and less recoverable extension as they travel from cavity to cavity. At very high D_e's, the polymers travel through the bed in a highly extended state, and less fluid kinetic energy is converted to heat. Thus the normalized flow resistance should decrease to zero in the limit of high D_e's.

Conclusions

Of all the polymers examined, the NaAMB/AM 20/80 copolymer solutions had the greatest porous media flow resistance because the polymer coils of these macromolecular structures are greatly expanded and can elongate and recover in extensional flow fields with low average fluid velocities.

The use of high-molecular-weight, highly expanded copolymers (such as the NaAMB/AM 20/80 shown in part c of Fig. 10) vs. lower molecular-weight polymers that are not greatly expanded (such as the AM homopolymer shown in part c of Fig. 9) has a dual advantage in reservoir flooding. Solutions of larger molecular-weight macromolecules with expanded polymer coils not only require less polymer mass for a given fluid flow resistance but also this resistance is

experienced at lower flow rates through the porous media. Thus they are effective flooding agents even at low concentrations and have a significant economic advantage.

References

1. *Chemical Economics Handbook*, pp. 581–1011I, 581–2022L, and 581–1012D, Stanford Research Institute, Menlo Park, Calif., 1983.
2. G. S. Manning, *Q. Rev. Biophys.*, II(2): 179 (1978).
3. H. Grasdalen and B. J. Kvam, *Macromolecules*, 19: 1913 (1986).
4. H. Gustavvson and B. Lindman, *J. Am. Chem. Soc.*, 100(15): 4647 (1978).
5. B. Halle, H. Wennerstrom, and L. Picullel, *J. Phys. Chem.*, 88: 2482 (1984).
6. M. Levij, J. De Bleijser, and J. Leyte, *Chem. Phys. Lett.*, 83(1): 183 (1981).
7. G. Gunnarsson and H. Gustavvson, *J. Chem. Soc. Faraday. Trans. I*, 78: 2901 (1982).
8. H. Gustavvson and B. Lindman, *J. Am. Chem. Soc.*, 100(15): 4647 (1978).
9. C. L. McCormick, C. E. Hoyle, and M. D. Clark, *Macromolecules*, 24: 2397 (1991).
10. F. Durst and R. Haas, *Rheol. Acta*, 20: 179 (1981).
11. C. L. McCormick and K. P. Blackmon, *J. Polym. Sci., Polym. Chem.*, A24: 2635 (1986).
12. C. L. McCormick, K. P. Blackmon, and D. L. Elliott, *J. Polym. Sci. Polym. Chem.*, A24: 2619 (1986).
13. C. L. McCormick and R. D. Hester, *Responsive Copolymers for Enhanced Petroleum Recovery*, Quarterly Technical Progress Report, June 22, 1993.

SURFACTANT LOSS CONTROL IN CHEMICAL FLOODING: SPECTROSCOPIC AND CALORIMETRIC STUDY OF ADSORPTION AND PRECIPITATION ON RESERVOIR MINERALS

Contract No. DE-AC22-92BC14884

Columbia University
New York, N.Y.

Contract Date: Sept. 30, 1992
Anticipated Completion: Sept. 29, 1995
Government Award: $602,232
(Current year)

Principal Investigator:
P. Somasundaran

Project Manager:
Jerry Casteel
Bartlesville Project Office

Reporting Period: Oct. 1–Dec. 31, 1994

Objectives

The objective of this research is to elucidate the mechanisms of adsorption and surface precipitation of flooding surfactants on reservoir minerals. The effect of surfactant structure, surfactant combinations, and other inorganic and polymeric species and solids of relevant mineralogy will also be determined. A multipronged approach consisting of microspectroscopy and nanospectroscopy, microcalorimetry, electrokinetics, surface tension, and wettability will be used to achieve the objectives. The results of this study should help in controlling surfactant loss in chemical flooding and also in developing optimum structures and conditions for efficient chemical flooding processes.

Summary of Technical Progress

The adsorption and desorption behaviors of tetradecyltrimethyl ammonium chloride (TTAC) and pentadecylethoxylated nonylphenol (NP-5) mixtures as reported earlier were rather complex. To better elucidate the interactions involved, fluorescence spectroscopy and ultrafiltration were used during this report period to probe the microstructure of the adsorbed layer and to determine individual surfactant monomer concentration, respectively. It was observed that pyrene was solubilized in mixed aggregates (hemimicelles) of a 1:1 TTAC:NP-15 mixture at the alumina–water interface over a wider concentration range than for TTAC alone. It was also observed that the adsorbed aggregate of a 1:1 TTAC:NP-15 mixture is as hydrophobic as the mixed micelle in solution. This is contrary to what was observed for the adsorption of TTAC alone: pyrene was preferentially solubilized in the TTAC micelles rather than the adsorbed aggregate. The preference of pyrene for the mixed adsorbed aggregates over individual aggregates is relevant to the application of surfactant mixtures in enhanced oil recovery (EOR) and solubilization.

The adsorption/desorption behavior of surfactants is directly related to the monomer concentration of the surfactant, hence it is important to monitor changes in monomer concentration during the adsorption and desorption processes. Ultrafiltration can be used to monitor the monomer concentration in solution and at the interface to determine the partitioning of the surfactants to the solid–liquid interface. During this report period, ultrafiltration techniques were first adopted to determine the monomer concentrations of the individual surfactants, which were then compared to those obtained from theory. The results show that ultrafiltration is a reliable method for the TTAC and NP-15 system, and the phase separation model is suitable for these two single surfactants.

Fluorescence Probing of Mixed Surfactant Adsorbed Layers

Pyrene monomer fluorescence is known to be sensitive to the medium in which pyrene resides. In a hydrophobic

environment, the ratio of the intensities of the third to the first peak (I_3/I_1) on a pyrene emission spectrum is higher than that when the pyrene is in a hydrophilic environment. Because this ratio can be used to characterize the polarity of environments, it is termed the polarity parameter.

The changes in the polarity parameter of pyrene adsorbed at the alumina–water interface in the presence of a 1:1 mixture of TTAC and NP-15 are shown in Fig. 1a. In addition, emission of pyrene in the supernatant after adsorption is also indicated in Fig. 1b. It is observed that pyrene goes to the alumina–water interface when the total residual concentration reaches about 1.5×10^{-4} M. The value of the I_3/I_1 ratio (polarity parameter) increases with increase in adsorption density, suggesting an increase in the number of hydrophobic aggregates at the interface. In the supernatant there are also hydrophobic aggregates as indicated by the increase in the value of the polarity parameter. It is interesting to note that the critical micelle concentration (CMC) of the mixture is 1.7×10^{-4} mol/L (total surfactant concentration), but the adsorption continues to increase even above this concentration. This is attributed to partitioning of the surfactants to the interface, which results in different mixture compositions in the bulk and in the adsorbed layer. Rise in the adsorption density, which usually is indicative of strong lateral surfactant chain–chain interactions at the solid–liquid interface, is less sharp in this case. This is attributed to the poor ability of the surfactant species to pack at the interface.

It is interesting to compare the behavior of the 1:1 TTAC:NP-15 mixtures to that of TTAC alone at the alumina–water interface. The adsorption of TTAC alone on alumina along with the emission of pyrene from the adsorbed layer is shown in Fig. 2.

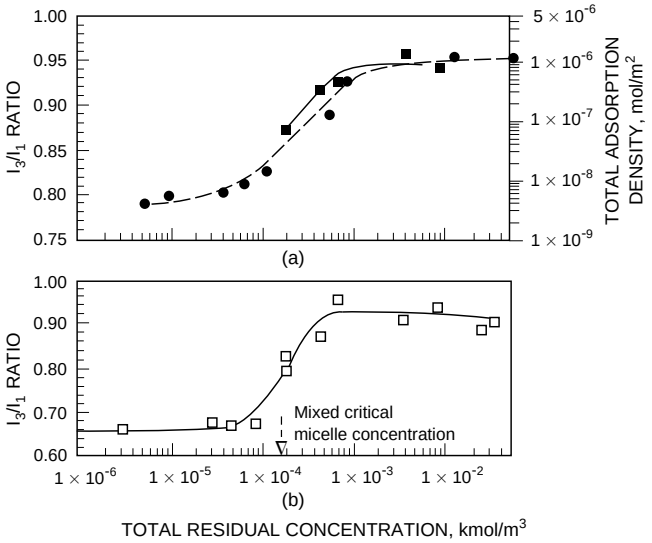

Fig. 1 Changes in pyrene polarity parameter at the alumina–water interface in the presence of a 1:1 mixture of tetradecyltrimethyl ammonium chloride (TTAC) and pentadecylethoxylated nonyl phenol (NP-15) (a) and emission of pyrene in the supernatant after adsorption (b). ■, at interface. ●, adsorption. □, in supernatant.

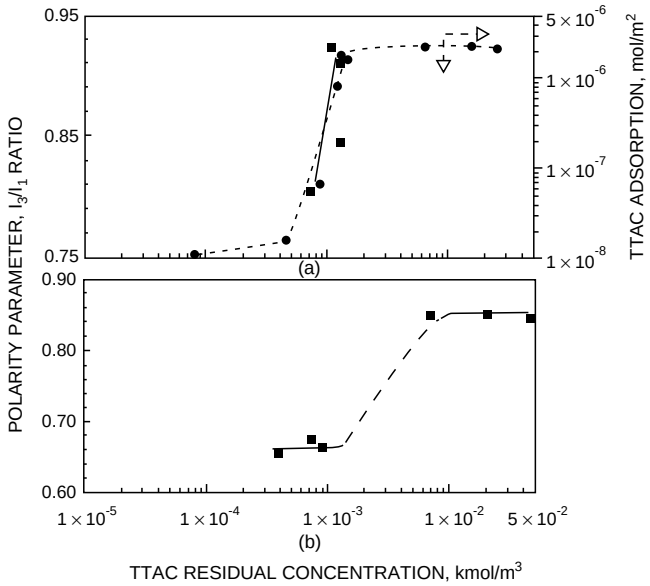

Fig. 2 Adsorption isotherm of tetradecyltrimethyl ammonium chloride (TTAC) on alumina (a) and corresponding changes in pyrene monomer fluorescence from the interface and in supernatant (b). ●, adsorption of TTAC. ■, emission of pyrene.

It is seen that pyrene dissolves in 1:1 TTAC:NP-15 mixture aggregates once they form at the interface and remains in the mixed aggregates even after the formation of mixed micelles in the supernatant. In contrast, in the case of TTAC alone, pyrene goes to the alumina–water interface over a narrow concentration range. Once TTAC micelles appear in the supernatant, pyrene is preferentially solubilized into these micelles and does not go to the alumina–water interface despite the presence of TTAC aggregates. This indicates that for TTAC alone the hydrophobicity of micelles of TTAC is higher than that of adsorbed TTAC. This is most interesting and different from earlier observations with linear alkyl surfactants, such as sodium dodecyl sulfate (SDS). Also, in the 1:1 TTAC:NP-15 mixture system, the hydrophobicity of adsorbed aggregates and micelles is almost the same over the concentration range studied. Presence of the nonionic surfactant in the mixed aggregate will reduce the repulsion between the cationic heads of the adsorbed surfactant and assist the packing (and hydrophobicity). It may also be geometrically easier to pack the two together than TTAC alone, which has a bulky head group. It will be useful to determine the composition of the adsorbed aggregates to ascertain the partitioning of the component surfactants to the interface. Note that partitioning of organic compounds in EOR processes will be dictated by the relative hydrophobicity of the adsorbed aggregates and micelles in the system, and hence it is important to understand the nature of hydrophobicity changes in mixed surfactant systems.

Measurement of Monomer Concentration by Ultrafiltration

Information on changes in the monomer concentration of individual surfactants in mixtures during the adsorption is vital

because the adsorption behaviors are directly related to the monomer concentration of each component in the mixtures. Ultrafiltration is a method that can be used to separate the monomer and micelles directly. During this report period ultrafiltration was used for determining TTAC and NP-15 monomer concentrations.

The cell and membrane used in this study were obtained from Amicon Co. (model 8050 and YM-3 membrane). The membrane chosen was specified to exclude molecules with molecular weight greater than 3000. Because the micelles of both TTAC and NP-15 will be considerably larger than this molecular-weight cutoff, this membrane was considered satisfactory for separating monomers from micelles. A constant pressure of 910 mm mercury was exerted on the mother liquor using compressed nitrogen, and the effluent was collected at atmospheric pressure. All experiments were performed at an ionic strength of 0.2*M* sodium chloride (NaCl) so that the effects of diffusion potential on the transport of dispersed surfactant through membrane was negligible.

The results obtained from ultrafiltration experiments are shown in Figs. 3 and 4. It is observed that when the mother liquor concentrations are lower than the CMC of the surfactants, monomer concentrations (or filtrate concentrations) are the same as the mother liquor concentrations and increase linearly with concentration. Above the CMC, the monomer concentrations obtained by ultrafiltration are relatively constant.

These results show that the ultrafiltration method is suitable for separating monomers from micelles in this system. The monomer concentrations predicted by the phase separation model are also plotted in Figs. 3 and 4 so that the results from ultrafiltration can be compared with the results with the phase separation model. It can be found that experimental results and the phase separation model are almost the same except around the CMC. In this concentration range, the monomer concentrations obtained from ultrafiltration are lower than the concentrations predicted by the phase separation model. This may indicate formation of some pre-micellar aggregates in solution, and this aspect merits further investigation. The monomer concentrations for the mixed surfactant systems will be measured in future work.

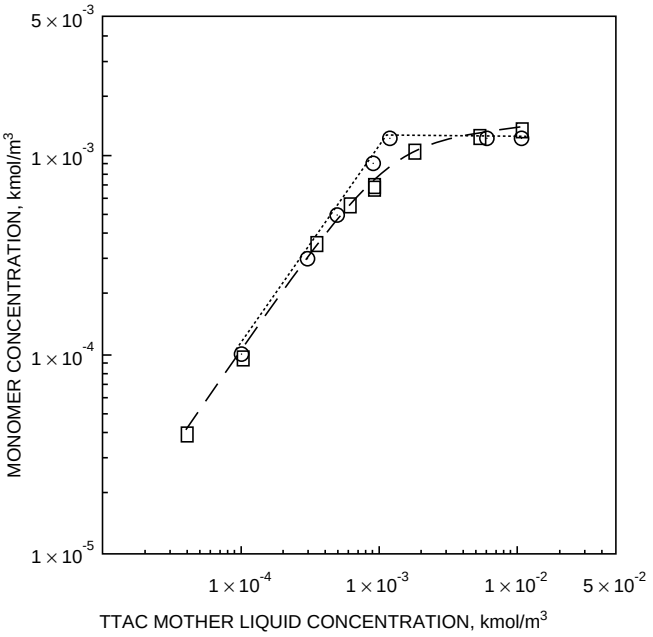

Fig. 3 Monomer concentration of tetradecyltrimethylammonium chloride (TTAC) as the function of total concentration. □, experimental. ○, phase separation model.

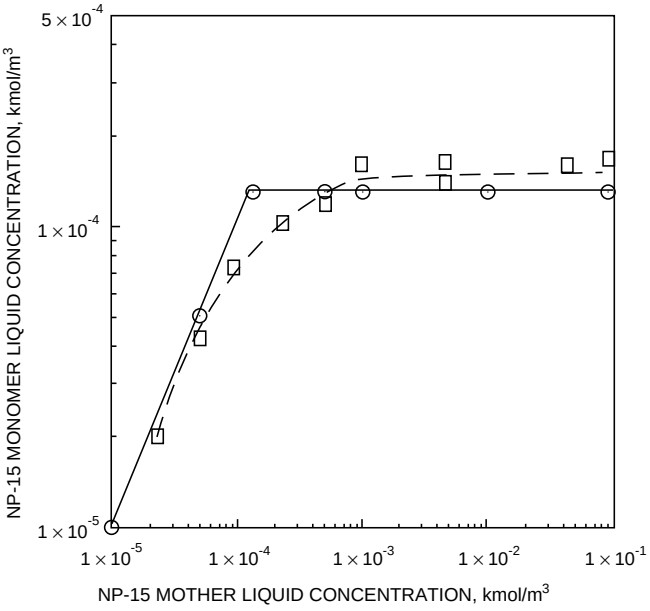

Fig. 4 Monomer concentration of pentadecylethoxylated nonylphenol (NP-15) as the function of total concentration. □, experimental. ○, phase separation model.

SURFACTANT-ENHANCED ALKALINE FLOODING FOR LIGHT OIL RECOVERY

Contract No. DE-AC22-92BC14883

Illinois Institute of Technology
Chicago, Ill.

Contract Date: Sept. 21, 1992
Anticipated Completion: Sept. 20, 1995
Government Award: $150,000
(Current year)

Principal Investigator:
Darsh T. Wasan

Project Manager:
Jerry Casteel
Bartlesville Project Office

Reporting Period: Oct. 1–Dec. 31, 1994

Objective

The overall objective of this project is to develop a cost-effective method for formulating a successful surfactant-enhanced alkaline flood by appropriately choosing mixed alkalis that form inexpensive buffers to obtain the desired pH (between 8.5 and 12.0) for ultimate spontaneous emulsification and ultralow tension. In addition, the novel concept of pH gradient design to optimize floodwater conditions will be tested.

Summary of Technical Progress

The characterization of emulsions in porous media is important in enhanced oil recovery (EOR) applications. This is usually accomplished by the addition of external or in situ generated surfactants to sweep the oil out of the reservoir. Emulsification of the trapped oil is one of the mechanisms of recovery. The ability to detect emulsions in the porous medium is therefore crucial to the design of profitable flood systems. The capability of microwave dielectric techniques to detect emulsions in porous media is demonstrated by mathematical modeling and by experiments.

During this quarter the dielectric properties of porous media were predicted adequately by treating the media as an oil-in-water (O/W)-type dispersion of sand grains in water. Dielectric measurements of emulsion flow in porous media show that dielectric techniques can be used to determine emulsion characteristics in porous media. The experimental observations were confirmed by theoretical analysis.

Theory

For a spherical dispersion of sand grains, the dielectric behavior of the porous medium can be described by Hanai's model as

$$\frac{(\varepsilon_1-\varepsilon_2)^3}{(\varepsilon_1-\varepsilon_m)^3}\left(\frac{\varepsilon_m}{\varepsilon_2}\right)=\frac{1}{(1-\phi)^3} \quad (1)$$

In the modeling of a bicontinuous structure such as a porous medium, the first question is whether a water-saturated core should be treated as an O/W emulsion or a water-in-oil (W/O)-type dispersion. The experimental data of Sen[1] suggest that the answer to this question is to treat the rock grains as if they were dispersed in water. Therefore the ternary system of emulsions in porous media can be modeled by successive iteration of two binary systems. The effective dielectric constant of the emulsions could be determined from Hanai's model for two-phase dispersions. The rock grains could then be treated as being dispersed in a fluid of dielectric constant that is equal to the effective dielectric constant of the emulsions. The dielectric constant of this binary mixture could again be computed by Hanai's model. For rock formations with little or no clay content, however, the dielectric constant of the rock grains will be comparable to that of oil. Therefore an O/W emulsion system in porous media can in effect be modeled as a dual dispersion of sand grains and oil in water. Similarly, a W/O emulsion in porous media can be regarded as a dual dispersion of water and sand grains in oil. This approach implies that a 50% emulsion of O/W in a porous medium with a 20% porosity will be similar to a 90% O/W-type dispersion. A 50% W/O emulsion, on the other hand, will be similar to a 10% W/O-type dispersion. Differences in the dielectric behavior of the two systems are to be expected. The computed results for the two emulsion systems with dispersed phase volume fractions of up to 60% in a Berea sandstone core with a 20% porosity shown in Figs. 1 to 3 clearly demonstrate the differences. Figure 4 compares the computed loss tangent values of the two emulsions with a system containing equivalent proportions of unemulsified constituents. The differences in emulsified and unemulsified systems indicated that dielectric properties may be used not only to determine the emulsion type and composition but also to ascertain whether emulsification occurs at all.

Emulsion Coreflood Experiments

Two-inch-square Berea sandstone pieces were prepared by coating them with resin. The ends were covered with Plexiglas pieces with holes drilled to allow for inflow and outflow. W/O emulsions of varying concentrations were first prepared and characterized dielectrically. Water was pumped into the core at a flow rate of 1 ft/d, and the dielectric constant was monitored. After breakthrough, 5 pore volumes

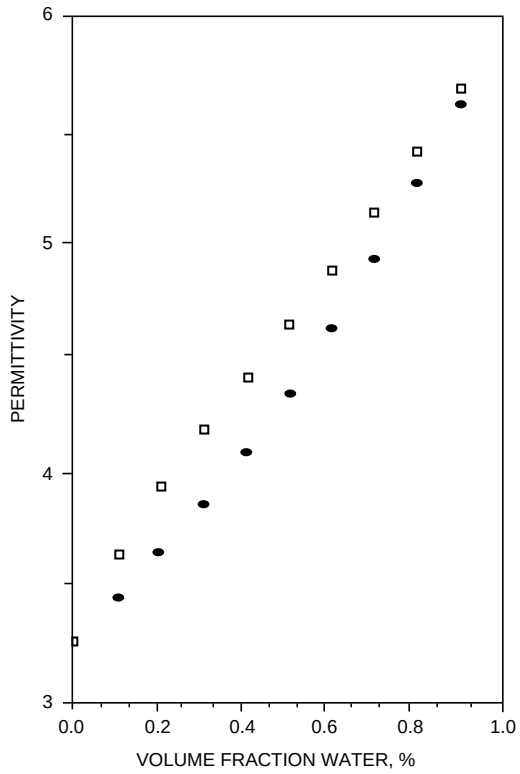

Fig. 1 Computed permittivity values at 23.45 GHz for oil-in-water and water-in-oil emulsions inside Berea sandstone core with a 20% porosity. □, oil in water. ●, water in oil.

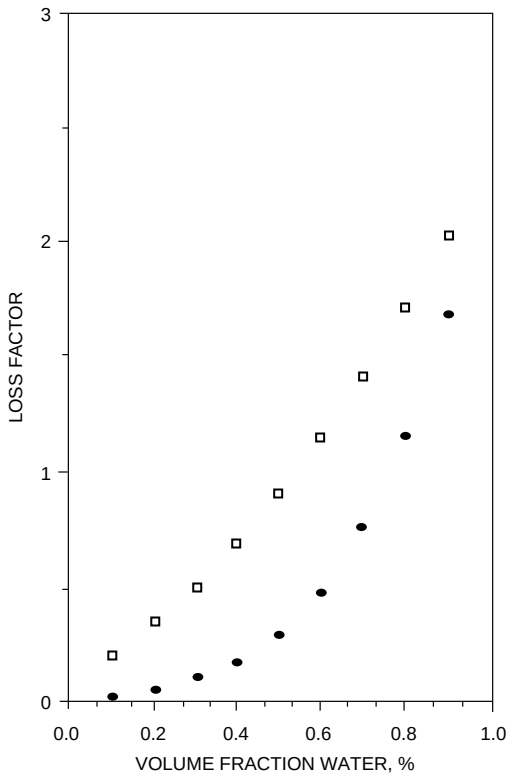

Fig. 2 Computed loss factor values at 23.45 GHz for oil-in-water and water-in-oil emulsions inside Berea sandstone core with a 20% porosity. □, oil in water. ●, water in oil.

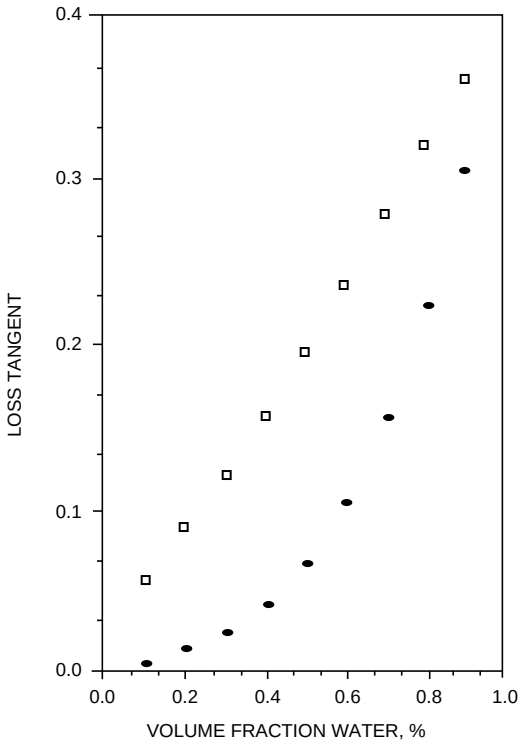

Fig. 3 Computed loss tangent values at 23.45 GHz for oil-in-water and water-in-oil emulsions inside Berea sandstone core with a 20% porosity. □, oil in water. ●, water in oil.

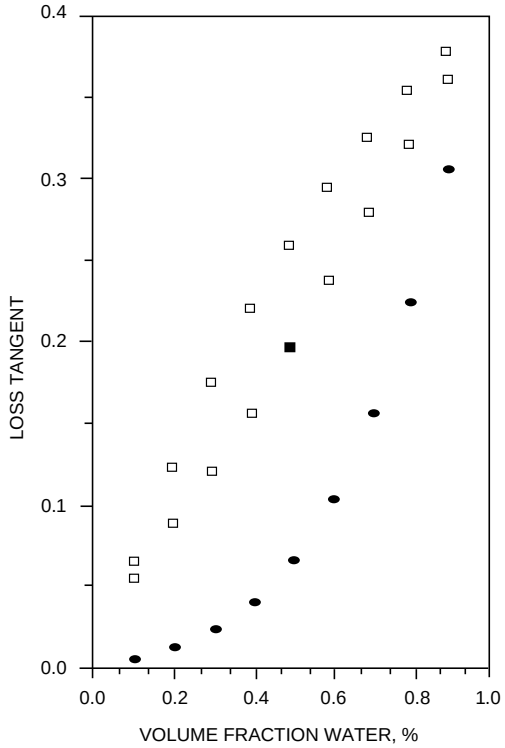

Fig. 4 Computed loss tangent values at 23.45 GHz for emulsified and unemulsified oil and water systems inside Berea sandstone core with a 20% porosity. □, oil in water. ●, water in oil. ■, water.

(PV) of the continuous phase was pumped through to ensure complete saturation. The lowest concentrations of the emulsion were then pumped through the core. The effluent concentrations were monitored by a cavity resonance dielectrometer. A schematic diagram of the experimental setup is shown in Fig. 5.

When the effluent concentrations matched the influent concentrations, steady-state flow conditions were considered to prevail, and the dielectric constant of the emulsions in the porous media was recorded. The next higher concentration of emulsion was pumped through the core, and the procedure was repeated. For W/O emulsions, the Berea sandstone core is first flooded with oil and then 5 PV of oil is pumped through. The oil-filled core was left untouchedfor 1 week. About 5 PV of oil was pumped through before W/O emulsions were introduced.

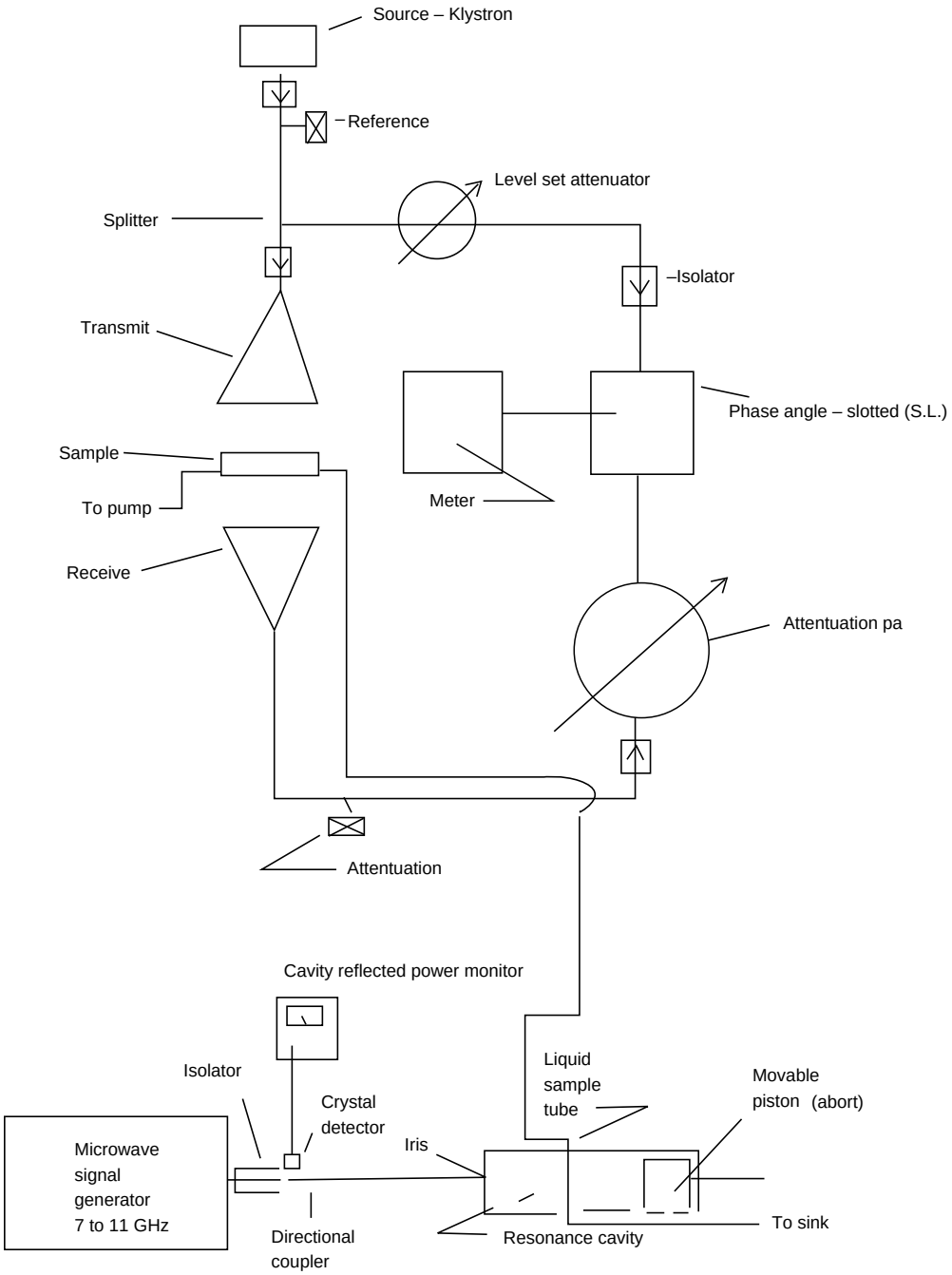

Fig. 5 Schematic of emulsion coreflood experiments with emulsion dielectric behavior inside porous media measured by interference dielectrometer at 23.45 GHz and the effluent concentration monitored by a cavity resonance dielectrometer.

Results

The experimentally measured value of the dielectric loss tangent is shown in Fig. 6. Differences in the dielectric properties of the two emulsion systems are clearly observed. For dispersed phase concentrations of up to 60%, the loss tangent of O/W emulsions in the core is considerably higher than that of W/O emulsions for all concentrations without any overlap.

Analogous to the definition of the dielectric modulus of emulsions outside the porous medium, a dielectric modulus P_{pore} for emulsions inside the porous medium is defined as follows:

$$P_{pore} = \frac{\text{Loss tangent of emulsions}}{\text{Loss tangent of water-saturated core}} \qquad (2)$$

This allows for the comparison of dielectric data obtained at different frequencies for emulsion dielectric data inside porous medium. The computed P_{pore} results are shown in Fig. 7 as a function of volume fraction water. The differences in the dielectric characteristics of the two emulsion types (O/W and W/O) are clearly defined in the plot.

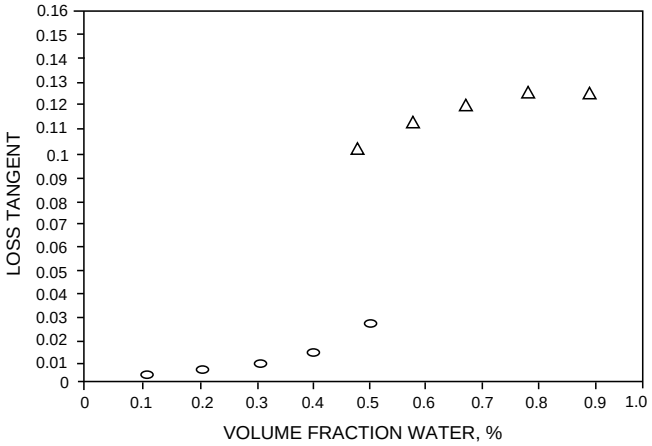

Fig. 6 Experimentally measured loss tangent values at 23.45 GHz for emulsions inside porous media at a 20% rock porosity. ○, water in oil. Δ, oil in water.

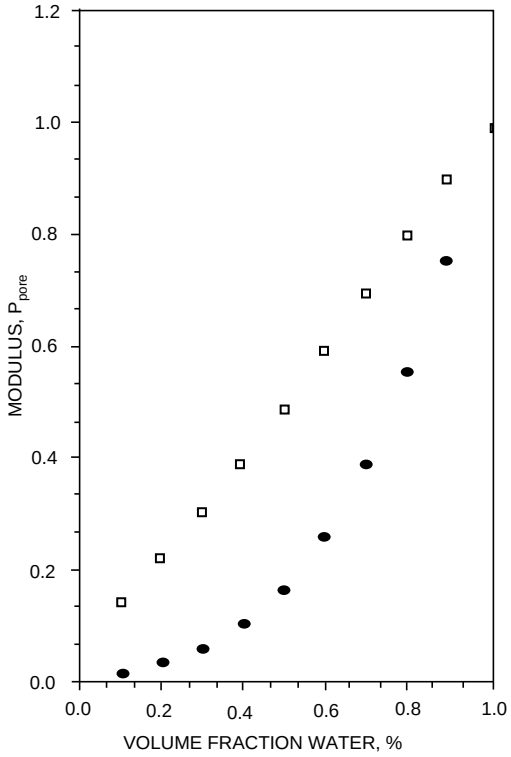

Fig. 7 Computed frequency invariant dielectric modulus P_{pore} for oil-in-water and water-in-oil emulsions inside Berea sandstone core with a 20% porosity. □, oil in water. ●, water in oil.

Both the experimental and theoretical values clearly establish the feasibility of determining emulsion characteristics by dielectric measurements in the microwave region.

References

1. P. N. Sen, C. Scala, and M. H. Cohen, A Self-Similar Model for Sedimentary Rocks with Applications to the Dielectric Constant of Fused Glass Beads, *Geophys.*, 46(5): 781-795 (May 1981).

DEVELOPMENT OF COST-EFFECTIVE SURFACTANT FLOODING TECHNOLOGY

Contract No. DE-AC22-92BC14885

University of Texas
Austin, Tex.

Contract Date: Sept. 30, 1992
Anticipated Completion: Sept. 29, 1995
Government Award: $765,557

Principal Investigators:
Gary A. Pope
Kamy Sepehrnoori

Project Manager:
Jerry Casteel
Bartlesville Project Office

Reporting Period: Oct. 1–Dec. 31, 1994

Objective

The objective of this research is to develop cost-effective surfactant flooding technology by using surfactant simulation studies to evaluate and optimize alternative design strategies, taking into account reservoir characteristics, process chemistry, and process design options such as horizontal wells. Task 1 is the development of an improved numerical method for the simulator so that a wider class of these difficult simulation problems can be solved accurately and affordably. Task 2 is the application of this simulator to the optimization of surfactant flooding to reduce its risk and cost.

Summary of Technical Progress

The goal of Task 1 is to obtain accurate numerical solutions for multidimensional, multicomponent, multiphase chemical flow problems, which are the specific focus of this project. The numerical method used in these simulation studies is a true vertical depth (TVD) flux-limited, high-order finite-difference scheme with a fully implicit formulation. On the basis of this method, a fully implicit, high-resolution compositional chemical flooding simulator is under development. The basic structure, flow equations, and transport property modeling in this simulator were reported previously.[1] The results of tracer flow, water flooding, and polymer flooding in one, two, and three dimensions demonstrate that the simulator gives more-accurate solutions with the use of the high-resolution method than with the use of the conventional numerical methods and is more computationally efficient than IMPES simulators, which require very small time-step sizes for certain problems. The overall increase in accuracy through the use of this new algorithm makes it possible to reduce the overall computational cost by taking larger time-step sizes and fewer nonlinear iterations without sacrificing accuracy or stability compared with the use of conventional methods.

Recent work has focused on code development and extension of the high-resolution implicit method to problems involving more physical–chemical properties. The principal relationships to describe these properties include the phase behavior, viscosity, interfacial tensions, capillary desaturation, adsorption, and permeability reduction as functions of polymer, surfactant, and electrolyte concentrations. The phase-behavior models used in the UTCHEM simulator have been highly successful in simulating chemical flooding processes. So that these models could be applied to the fully implicit simulator, all phase-concentration and phase-behavior equations were formulated in terms of primary variables and derivatives of all phase concentrations were computed with respect to the primary variables. As an example, results of a surfactant flooding simulation are given to demonstrate the agreement between the IMPES simulator (UTCHEM) and the fully implicit simulator and the superior numerical stability of the fully implicit simulator.

Phase equilibrium conditions can be described in terms of a ternary diagram and a binodal curve (Fig. 1). The apexes of the ternary diagram correspond to 100% water, oil, and surfactant concentrations. The boundaries of the various phase regions are determined in part by the binodal curve, and the shape of the binodal curve is affected by salinity. An aqueous–oleic two-phase region exists at very low surfactant concentrations [below the critical micelle concentration (CMC)], and a single microemulsion-phase region exists at high surfactant concentration, above the binodal curve. Below the binodal curve, two phases (the oleic and microemulsion phases or the aqueous and microemulsion phases) or all three phases may exist, depending on the position of the invariant point, which is a fraction of the effective salinity. A uniform grid of 80 gridblocks was used with an injector at one end and a producer at the other. The resident fluid concentrations for oil and water are 0.4 and 0.6, respectively, which gives an initial salinity of 0.65 meq/mL. For aqueous, oleic, and microemulsion phases, the end-point relative permeabilities are 0.14, 0.9, and 0.14, respectively, and the exponents are 2, 2.14, and 2, respectively. The residual saturations are 0.15, 0.4, and 0.15, respectively. The viscosities for oil and water are 2.5 and 0.42 cP, respectively. Lower and upper effective salinity limits are 0.5 and 0.8, and the CMC value is 0.0001. The values of the maximum heights of the binodal curve at zero, optimal, and twice optimal salinities are 0.12, 0.03, and 0.05, respectively. Water containing 0.5% surfactant was injected with the same salinity as that of the resident fluid. The injection rate was 0.02 ft^3/d, and the total injection time was 0.05 d, which gave a total injection of 0.5 pore volume (PV).

The same time-step size of 0.000125 d, corresponding to a Courant number (dimensionless time-step size) of 0.1, was first used for both simulations with the IMPES simulator and the fully implicit simulator. The profiles of microemulsion phase saturation and total oil concentration are shown in Fig. 2. Good agreement between the two results was obtained.

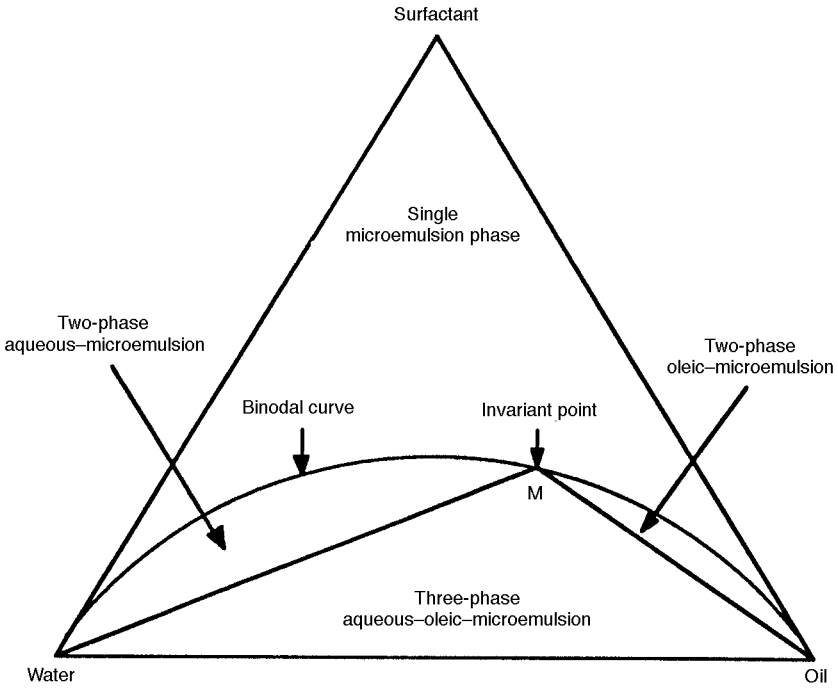

Fig. 1 Schematic representation of binodal curve, invariant point, and different phase regions in a ternary diagram.

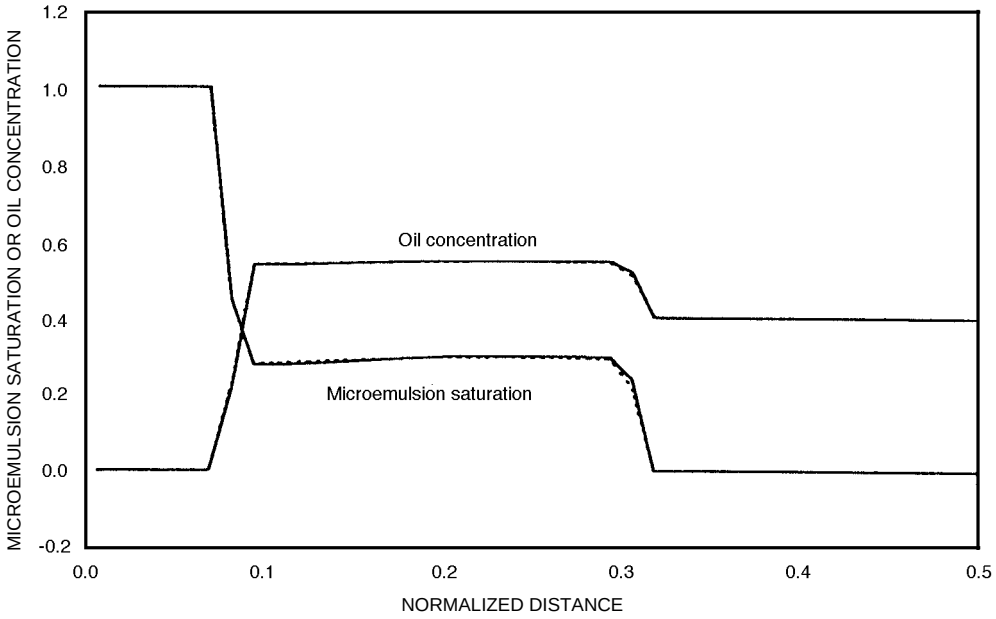

Fig. 2 Simulation of a surfactant flooding problem using the IMPES simulator (—) and the fully implicit simulator (- - - -) at a small time-step size. Number of gridblocks, 80; pore volume injected, 0.5; and Courant number, 0.1.

The time-step size was then increased so that the stability of the two simulators could be compared. Figure 3 gives the results of the fully implicit simulator at a time-step size of 0.001875 d, which corresponds to a Courant number of 1.5 and shows nearly no change in both profiles. The IMPES simulator, however, produced unstable results at a time-step size of 0.0003125 d, which corresponds to a Courant number of 0.25, characterized by severe oscillations in both profiles.

Testing of the implicit simulator is continuing with respect to problems involving more interactions caused by the combinations of various physical–chemical properties. The code is also being optimized to improve the computation efficiency and to make it more user friendly.

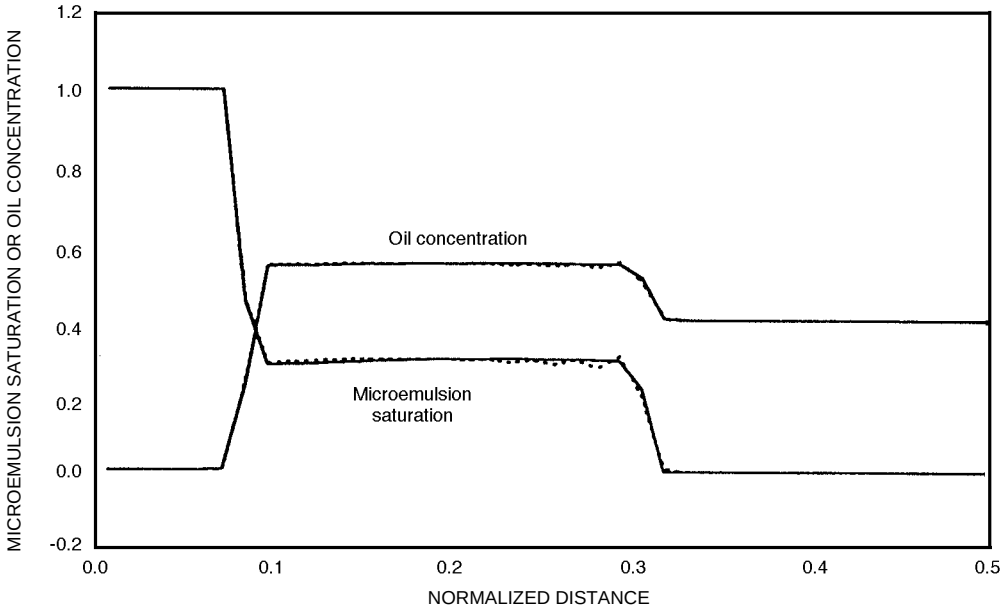

Fig. 3 Simulation of a surfactant flooding problem with the use of the fully implicit simulator at a large time-step size. Number of gridblocks, 80; pore volume injected, 0.5. ——, λ = 0.1. - - - -, λ = 1.5.

References

1. G. A. Pope and K. Sepehrnoori, *Development of Cost-Effective Surfactant Flooding Technology,* Annual Report for the Period September 30, 1992–September 29, 1993, DOE Contract No. DE-AC22-92BC14885, August 1994.
2. N. Saad, *Field Scale Simulation of Chemical Flooding,* Ph.D. dissertation, University of Texas, Austin, Tex., August 1989.

GAS DISPLACEMENT— SUPPORTING RESEARCH

IMPROVED EFFICIENCY OF MISCIBLE CO_2 FLOODS AND ENHANCED PROSPECTS FOR CO_2 FLOODING HETEROGENEOUS RESERVOIRS

Contract No. DE-FG22-94BC14977

New Mexico Institute of Mining and Technology
Petroleum Recovery Research Center
Socorro, N. Mex.

Contract Date: Apr. 14, 1994
Anticipated Completion: Apr. 13, 1997
Government Award: $320,000

Principal Investigators:
Reid B. Grigg
John P. Heller
David S. Schechter

Project Manager:
Jerry Casteel
Bartlesville Project Office

Reporting Period: Oct. 1–Dec. 31, 1994

Objective

The objective of this experimental research is to improve the effectiveness of carbon dioxide (CO_2) flooding in heterogeneous reservoirs. Activities are being conducted in three related areas: (1) further exploration of the applicability of selective mobility reduction (SMR) in the use of foam flooding; (2) possible higher economic viability of floods at slightly reduced CO_2 injection pressures; and (3) taking advantage of gravitational forces during low interfacial tension (IFT), CO_2 flooding in tight, vertically fractured reservoirs.

Summary of Technical Progress

Task 1: SMR Study in CO_2–Foam

The objective of this task is the development of SMR in CO_2–foam flow, enabling field engineers to increase production efficiency in CO_2 flooding of oil reservoirs. This effect, which causes the mobility of CO_2 foam in high-permeability cores to be approximately the same as that in low-permeability cores, is observed with some surfactants. Before field engineers can consider using SMR, it is necessary to demonstrate that the effects observed in the laboratory in individual cores of uniform permeability can be used in

heterogeneous media to reduce the non-uniform flow of displacing CO_2–foam.

New types of experiments need to be performed in which both high- and low-permeability regions are present. These two sections of a flow system, or core, must also be in capillary contact to simulate different portions of a heterogeneous reservoir. The ratio of mobilities between the two sections during the flow of simple fluids and CO_2–foam through these cores will be measured. The experimental need can be met by two types of tests in which well-defined high- and low-permeability regions are arranged differently in the flow system.

One type of experiment satisfying the above criterion involves cores in which high and low permeabilities are in parallel. The core is cut from a rock containing two regions so that the plane separating the two will include the diameter of the core. End-to-end flow through the two sections of the core can then be made to measure the two mobilities. The search for such parallel heterogeneity cores has not yet produced any candidate cores from reservoirs, although two samples of quarried rock that meet this standard have been obtained. One of these is a core cut from a large San Andres outcrop sample (contributed by Texaco), but it exhibits such a large permeability ratio that the experiment would take unduly long. A second choice would come from a block of Berea rock with greater than usual permeability heterogeneities. A core can be cut from this block with a permeability ratio of four or five, which will be more suitable for the proposed tests.

Another experiment of this type is being performed with the two sections coaxial. A 1.5-in.-diameter Berea core has an axially located, 0.5-in. hole filled with fine unconsolidated sand. The pressure drop along the two sections is the same since they are in parallel, and again the mobilities can be measured by observing the flows from the two regions separately. To properly perform this experiment, two back-pressure regulators are used, one each for the output fluids from each section of the core system. A schematic of the overall flow arrangement for this type of parallel experiment used for the coaxial flow described above is shown in Fig. 1.

A second type of experiment involves a core with the different permeability sections in series, so the flow rate will be the same through both sections. In this case, mobility measurements can be made by measuring the two pressure drops across each section. This experiment is similar to the series arrangement of having two separate cores in their own coreholders. In the new arrangement the two sections will be in the same coreholder—either sections of the same rock or separate cores—tightly butted together with a filter membrane for good capillary contact between them. Such an experiment is in progress.

Task 2: Reduction of the Amount of CO_2 Required in CO_2 Flooding

Simulation and Modeling

During this quarter, the focus has been on the implementation of a horizontal well model into MASTER [the Department of Energy's (DOE) pseudo-miscible reservoir simulator]. In the original MASTER code, only the vertical well parallel to the z-axis was considered. Therefore, the first task was to modify the code to allow for flexible well orientation so that wells can also be parallel to the x- or y-axis. The second major modification involved incorporating the well model of Babu et al.[1] into the simulator. The coding of these modifications is near completion.

Two papers related to phase behavior simulation are nearing completion for presentation at the 1995 AIChE Spring National Meeting. One paper outlines an application of an optimization technique for phase equilibrium computations.[2] The other paper provides a method for the calculation of the specific gravity associated with the characterization of the heavier components of crude oil.[3]

A paper that compares the results of phase equilibrium changes during the injection of pure and impure CO_2 into reservoir crude at pressures both below and above the minimum miscibility pressure (MMP) was completed and will be presented at the 1995 SPE International Symposium on Oilfield Chemistry.[4] An abstract of a paper on the effect of pressure on CO_2 oilflood recovery has been submitted for the 1995 Society of Petroleum Engineers Annual Meeting. The paper describes CO_2 corefloods done at Conoco compared with corefloods reported in the literature. The different tests have produced conflicting results on whether production during tests at pressures near miscible conditions would result in significantly lower recovery compared to pressures well into the miscible region. Early indications are that the crude samples and testing procedures significantly affect the results.

Task 3: Low-IFT Processes and Gas Injection in Fractured Reservoirs

Research is continuing in two primary areas: understanding the fundamentals of low-IFT behavior via theory and experiment and modeling low-IFT gravity drainage for application of gas injection in fractured reservoirs. A literature survey of all the reservoir fluid IFT measurements available has been completed. The survey indicated, with strong evidence, that the scaling exponent used in parachor calculations should not be used as an adjustable parameter. Thus, on the basis of fundamental critical scaling and past measurements of density difference and IFT for pure components, parachors of all pure components have been recalculated (if sufficient data were available). Since the parachor is generally a linear function of molecular weight, the equivalent parachor was calculated for the equivalent fractions that are present in crude oil. This method was then compared with other versions of the parachor method found in the literature. It was found that the new method better predicts existing gas–crude oil low-IFT systems. Gas–oil IFT calculations are now understood quite well, although the pendant drop apparatus needs to be used to verify calculation methodology. At that point, crude oil–brine and gas–brine IFTs at reservoir conditions will begin to be researched. This work will lead to a better understanding of the three IFTs that are significant in three-phase flow.

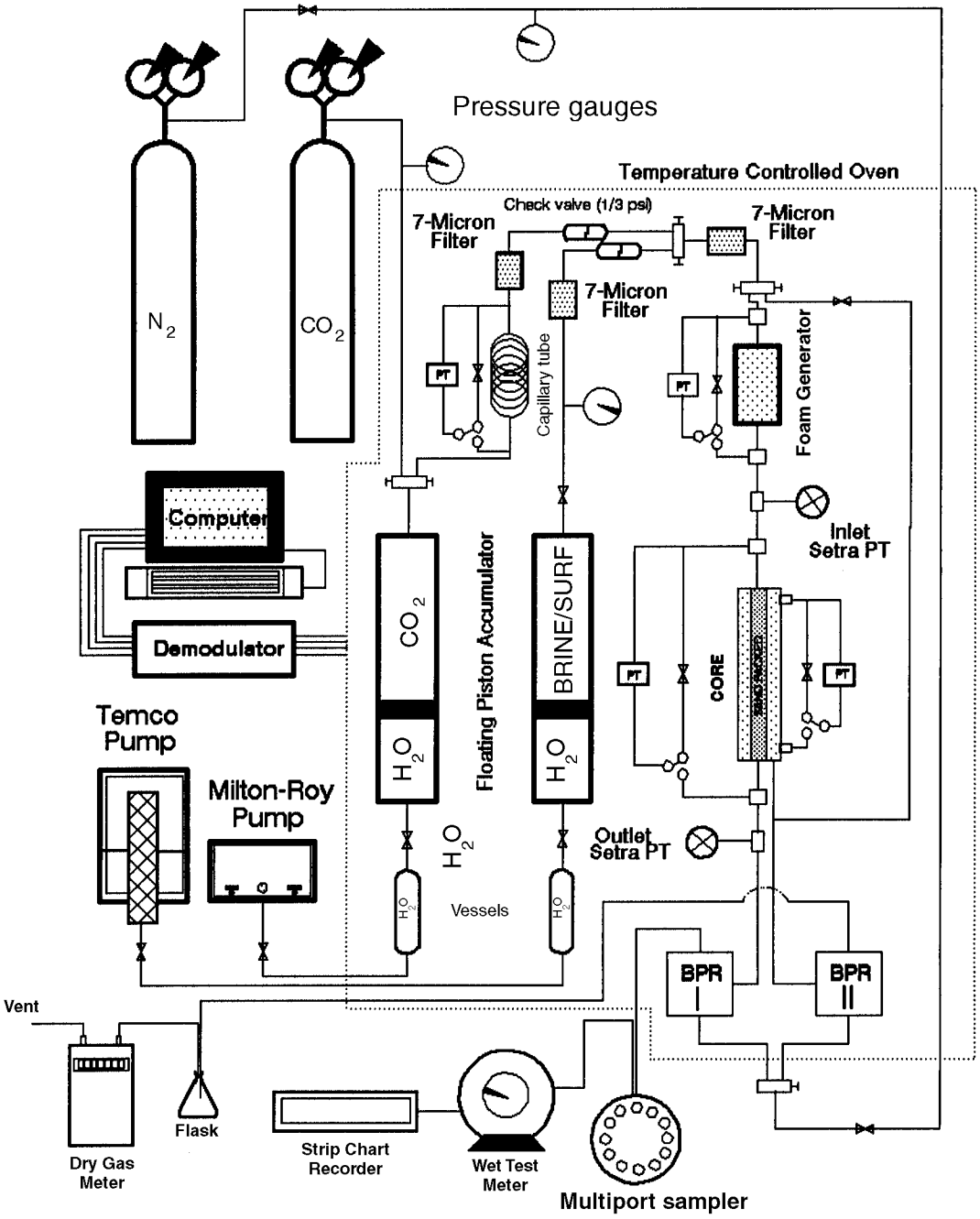

Fig. 1 Schematic diagram of the experimental apparatus.

Status of Pendant Drop Apparatus

The construction of the pendant drop system is complete. Fluids are circulated through the density meter and form drops in a variety of needle bore sizes. There is confidence that ultralow IFT systems will be measurable because the smallest needle bore available has been obtained. Completion of the video imaging facilities involves testing digital cameras, frame grabbers, and imaging software in order to maximize drop resolution and improve IFT measurements.

Low-IFT Gravity Drainage

The system to measure free-fall gravity drainage in long reservoir whole cores at reservoir conditions has been completed. The first test was conducted in Berea sandstone with a permeability of 500 mD. The core was saturated with reservoir brine, flushed with West Texas crude to connate brine, and allowed to age for two weeks. The core was transferred from the Hassler cell (with overburden) into a free-fall gravity drainage cell, which was mounted vertically.

CO_2 was circulated through the cell at near the MMP of the oil. Recovery of oil by gravity drainage was measured as a function of time, as shown in Fig. 2.

The process has also been investigated from a theoretical viewpoint. An analytical model for gravity drainage that better describes existing data has been developed. The data are scarce though, and much more experimental work is necessary to understand the complicated exchange mechanism that occurs in nonequilibrium gravity drainage, such as swelling, vaporization, low-IFT development, and varying capillary pressure as the IFTs are reduced.

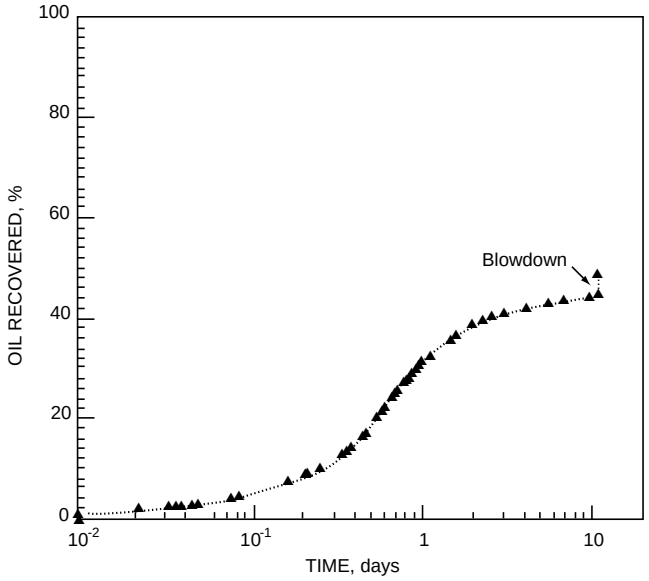

Fig. 2 CO_2 gravity drainage in Berea with Spraberry stock tank oil. Initial water saturation, 0.383.

References

1. D. K. Babu, R. C. McCann, A. S. Odeh, and A. J. Al-Khalifa, The Relation Between Wellblock and Wellbore Pressures in Numerical Simulation of Horizontal Wells, *SPE Reserv. Eng.*, 6(3): 324-328 (August 1991).
2. Paper prepared for presentation at the AIChE Spring National Meeting, Houston, Tex., March 19–23, 1995.
3. Paper prepared for presentation at the AIChE Spring National Meeting, Houston, Tex., March 19–23, 1995.
4. *Dynamic Phase Composition, Density, and Viscosity Measurements During CO_2 Displacement of Reservoir Oil*, paper SPE 28974 prepared for presentation at the Society of Petroleum Engineers International Symposium on Oilfield Chemistry, San Antonio, Tex., Feb. 14–17, 1995.
5. D. Gregory and R. Grigg, *The Effect of Pressure on CO_2 Oilflood Recovery*, paper submitted for presentation at the Society of Petroleum Engineers Annual Technical Conference, Dallas, Tex., Oct. 22–25, 1995.

FIELD VERIFICATION OF CO_2 FOAM

Contract No. DE-FG21-89MC26031

New Mexico Institute of Mining and Technology
Petroleum Recovery Research Center
Socorro, N. Mex.

Contract Date: Sept. 29, 1989
Anticipated Completion: Mar. 28, 1995

Principal Investigators:
F. David Martin
John P. Heller
William W. Weiss

Project Manager:
Royal Watts
Morgantown Energy Technology Center

Reporting Period: Oct. 1–Dec. 31, 1994

Objectives

The objectives of this cooperative industry–university–government project are to transfer promising laboratory research to a field demonstration test, provide research support to design and implement the test, and evaluate the use of foam for mobility control and fluid diversion in a field carbon dioxide (CO_2) flood.

The CO_2–foam field verification pilot test was conducted at the East Vacuum Grayburg–San Andres Unit (EVGSAU), located in Lea Co., N. Mex. This 4-yr project was jointly funded by the EVGSAU Working Interest Owners (WIO), the U.S. Department of Energy (DOE), and the State of New Mexico. The Petroleum Recovery Research Center (PRRC), a division of the New Mexico Institute of Mining and Technology, provided laboratory and research support. Phillips Petroleum Company (PPCo), operator of EVGSAU, acted as project coordinator. On the basis of favorable response from the foam field trial, the DOE granted a 1-yr, no-cost extension of the project to permit the evaluation of a second foam test.

Summary of Technical Progress

Details of response from the foam field tests have been reported in prior progress reports. During this quarter, PPCo converted the offending producing well in the foam pilot area to an injection well. In addition, two new wells were drilled near the pattern boundary. These changes make any further monitoring of the foam pilot area unnecessary. The remaining surfactant will be injected in another pattern (Well No. 3202-013), where a high permeability streak has been identified. Surfactant will be injected at 1000 ppm for several days, and injectivity results from this test will be included in the final report.

PRODUCTIVITY AND INJECTIVITY OF HORIZONTAL WELLS

Contract No. DE-FG22-93BC14862

Stanford University
Stanford, Calif.

Contract Date: March 10, 1993
Anticipated Completion: March 10, 1998
Government Award: $359,000
(Current year)

Principal Investigators:
F. John Fayers
Khalid Aziz
Thomas A. Hewett

Project Manager:
Thomas Reid
Bartlesville Project Office

Reporting Period: Oct. 1–Dec. 31, 1994

Objectives

The objectives of the project include (1) modeling horizontal wells to establish detailed three-dimensional (3-D) methods of calculation that will successfully predict horizontal well performance under a range of reservoir and flow conditions; (2) reservoir characterization studies to investigate reservoir heterogeneity descriptions of interest to applications of horizontal wells; (3) experimental planning and interpretation to critically review technical literature on two-phase flow in pipes and the correlation of results in terms of relevance to horizontal wells; (4) defining methods for determining 3-D coarse grid approximations (e.g., pseudo-functions) for horizontal wells with calculations developed; (5) developing multi-well models interactively coupled to large-scale reservoir simulation; (6) test models with field examples; (7) enhanced oil recovery (EOR) extensions of models to handle compositional effects for miscible displacement, thermal effects for steam processes, and combination processes; and (8) application studies for horizontal wells.

Summary of Technical Progress

The development of models for scaleup and coarse-grid pseudo-functions for horizontal wells in heterogeneous reservoirs continued. The new scaleup method requires positive dissipation for intercell fluxes, which produces a reshaped coarse-grid system with non-negative transmissibilities. The application of the new method successfully reproduced fine-grid pressure distributions for single-phase problems and approximate fine-grid pressure and saturation distributions for two-phase flow examples for a range of mobility ratios. Further testing of the method is under way.

The development of a generalized model for calculating productivity and injectivity indices for a horizontal well in anisotropic reservoirs began. The goal is to calculate productivity of complex well configurations, such as multiple horizontal wells of arbitrary direction emanating from one vertical well.

A study of the completion designs and their impact on production performance of a horizontal well commenced. This study uses a network modeling approach for representing the well completion arrangement that is in communication with the flow in the reservoir. The coupling between the well and the reservoir is facilitated through modular completion software (HOSIM), developed by Norsk-Hydro, and a commercial reservoir simulator (ECLIPSE).

The development of a 3-D Voronoi grid simulator is also progressing. A major facet of this work is the generation and visualization of gridding geometry in 3-D. This aspect of the work is complete and is being tested.

Detailed Well Model for Reservoir Simulation

The objective of this task is to develop a 3-D reservoir simulator on the basis of generalized Voronoi grids that honor horizontal/deviated wells, local flow geometry, faults, major heterogeneities, anisotropy, etc. Difficult geometrical/logical problems associated with automatic generation and visualization of the gridding geometry in 3-D form a significant aspect of this task. The mathematical formulation for the flow simulation should take into account such a complex gridding scheme. Pressure and flow calculations in a wellbore (obtained from a wellbore simulator) will be coupled with similar reservoir variables.

Mathematical Model for Voronoi Grids

Equation 1 represents the application of the conservation law to an arbitrary component $\bar{c}$ in a control volume V with an external area A.

$$-\oint_A \sum_{p=1}^{N_p} \omega_{\bar{c}p} \vec{V}_p \cdot \vec{n} dA = \frac{\partial}{\partial t} \int_V \sum_{p=1}^{N_p} \omega_{\bar{c}p} S_p \phi \, dV \qquad (1)$$

ence approximation of the preceding equation, which results in Eq. 2.

$$\sum_{j=1}^{N_n} \sum_{p=1}^{N_p} (T\omega_{\bar{c}p}\lambda_p)_{ij}(\Phi_{p,j} - \Phi_{p,i}) = \frac{V_{b,i}}{\Delta t}$$

$$\times \sum_{p=1}^{N_p} [(\omega_{\bar{c}p} S_p \phi)^{n+1} - (\omega_{\bar{c}p} S_p \phi)^n]_i + \sum_{p=1}^{N_p} (\omega_{\bar{c}p} q_p)_i^{n+1} \qquad (2)$$

where N_n = number of neighbors of block i
N_p = number of phases in the system
T = transmissibility
$\omega_{\bar{c}p}$ = mass fraction of component $\bar{c}$ in phase p
λ_p = mobility of phase p
$\Phi_{p,j}$ = potential in phase p at node j
$V_{b,i}$ = volume of block i
S_p = saturation of phase p
ϕ = porosity at node i
q_p = source / sink term for node i

For isotropic permeability and an orthogonal grid, a unique transmissibility term can be defined for each surface (of control volume V), which, when multiplied with $(\Phi_j - \Phi_i)$, gives the flux across surface ij. If permeability is an anisotropic tensor and/or grids are nonorthogonal, then the potential difference $(\Phi_j - \Phi_i)$ also affects flow between some of the other surfaces. If the tensor is symmetric, however, then control volume surfaces can be oriented in such a manner that a unique transmissibility can again be found, so potential difference between nodes across surface ij again determines flow only across that surface.[1] Upstream weighting of mobilities can be easily used in such a scheme. The region is assumed to be homogeneous across the surface when such a derivation is made. For small anisotropy, this scheme may work quite well. When significant heterogeneities are considered, however, the effective permeability tensor will have principal axes that vary locally and conflict with the axes of a gridding scheme. The effective permeability tensor is also not necessarily symmetric. Other schemes [control volume finite element (CVFE)] that maintain the flexibility of grids have been proposed, but they have been unable to correctly use upstream weighting of phase mobilities.[2]

Voronoi grids are used in a new approach in the current study. Properties inside the grid are assumed to be homogeneous but may be anisotropic. The flows at the surfaces are constrained so that velocity normal to the surface (i.e., in the direction of the connections) is the same on both sides. Also, in this case (as in the case of CVFE) flow at each connection is not solely dependent on fluid potentials at adjacent points. Because of this, more time [as compared to a generalized perpendicular bisector (PEBI) grid[1]] is needed to assemble the Jacobian matrix, even though the structure of the Jacobian matrix is identical. Because most of the time (normally 80 to 90%) in any simulation is taken by the iterative solver, the computer time of the current scheme will not increase significantly. Upstream evaluation of the mobility at any surface is based on a function that is a linear combination of the potentials affecting flow across that surface. This scheme can be used for asymmetric permeability tensors as well, and it has no restriction on the angles of the tetrahedron generated by a triangulation code other than the requirement that the triangulation be Delaunay. Further features have been added to the code package QHULL[3,4] to generate both two-dimensional (2-D) and 3-D Delaunay triangulations in a way that meets many of the primary reservoir simulation requirements.

Generation of Voronoi Grids

Palagi[5] presented a Voronoi grid generation scheme on a plane. The scheme used to generate the grid in 3-D is presented in this section. The C++ code that implements this scheme is complete and is being tested.

For a set $S = \{p_1, p_2, \ldots, p_n\}$ of n points in Euclidean 3-space, R^3, the associated Voronoi diagram is a sequence $V(p_1), V(p_2), \ldots, V(p_n)$ of convex polyhedra covering 3-space, where $V(p_i)$ consists of all points of 3-space having p_i as the nearest point in the set S.[3] Thus

$$V(p_i) = \{x \in R^d : d(x, p_i) \leq d(x, p_j),\ j = 1, 2, \ldots, n\} \quad (3)$$

where $d(x,p_i)$ denotes the Euclidean distance between points x and p_i.

As a starting point, the Delaunay triangulation of a set of points is constructed with QHULL. The set of tetrahedra thus obtained is used to generate sets of tetra faces, tetra edges, and tetra nodes. These objects contain all the connectivity information (e.g., a tetra edge object contains the number of tetras it is connected to, the ID's of those tetras, the number of tetra faces it is connected to, their ID's and the ID's of the two nodes at the end of the tetra edge).

One Voronoi block is associated with each node. The faces of the block lie on the PEBI planes of each of the edges connected to the node. The intersections of the PEBI plane of an edge, with the PEBI planes of the other edges connected to the node, completely describe the geometry of the face on that edge. In the interior of the domain, these intersections are the circumcenters of the tetrahedron connected to the edge; however, when any of these circumcenters as well as the centers of the tetra faces associated with the edge lie outside the reservoir domain, then the formed Voronoi block faces must be adjusted. This is accomplished by finding the intersection of the PEBI planes with the boundary tetra faces and the boundary tetra edges. Figure 1 shows the generation of Voronoi blocks in 3-D. The figure shows the triangulation, Voronoi grid edges, and faces from three viewpoints.

Figures 2 and 3 show in 2-D the alignment of Voronoi blocks along major reservoir features such as layers, faults, and horizontal/deviated wells. The actual grid in 3-D can have polygonal shapes around the well axis that approximate cylindrical flows (e.g., hexagons). Such grids are shown around the deviated well. Figure 3 shows how the gridding can be efficiently done for dual-lateral wells drilled to drain from two different layers. The Delaunay triangulation of the nodes in Fig. 2 is given in Fig. 4. The nodes were placed in a direction normal to the layer and fault boundaries on both sides and equidistant from the boundaries to generate the Voronoi polygons in Figs. 2 and 3. Thus block boundaries were aligned along layer boundaries, which resulted in better estimates of homogeneous properties inside a block.

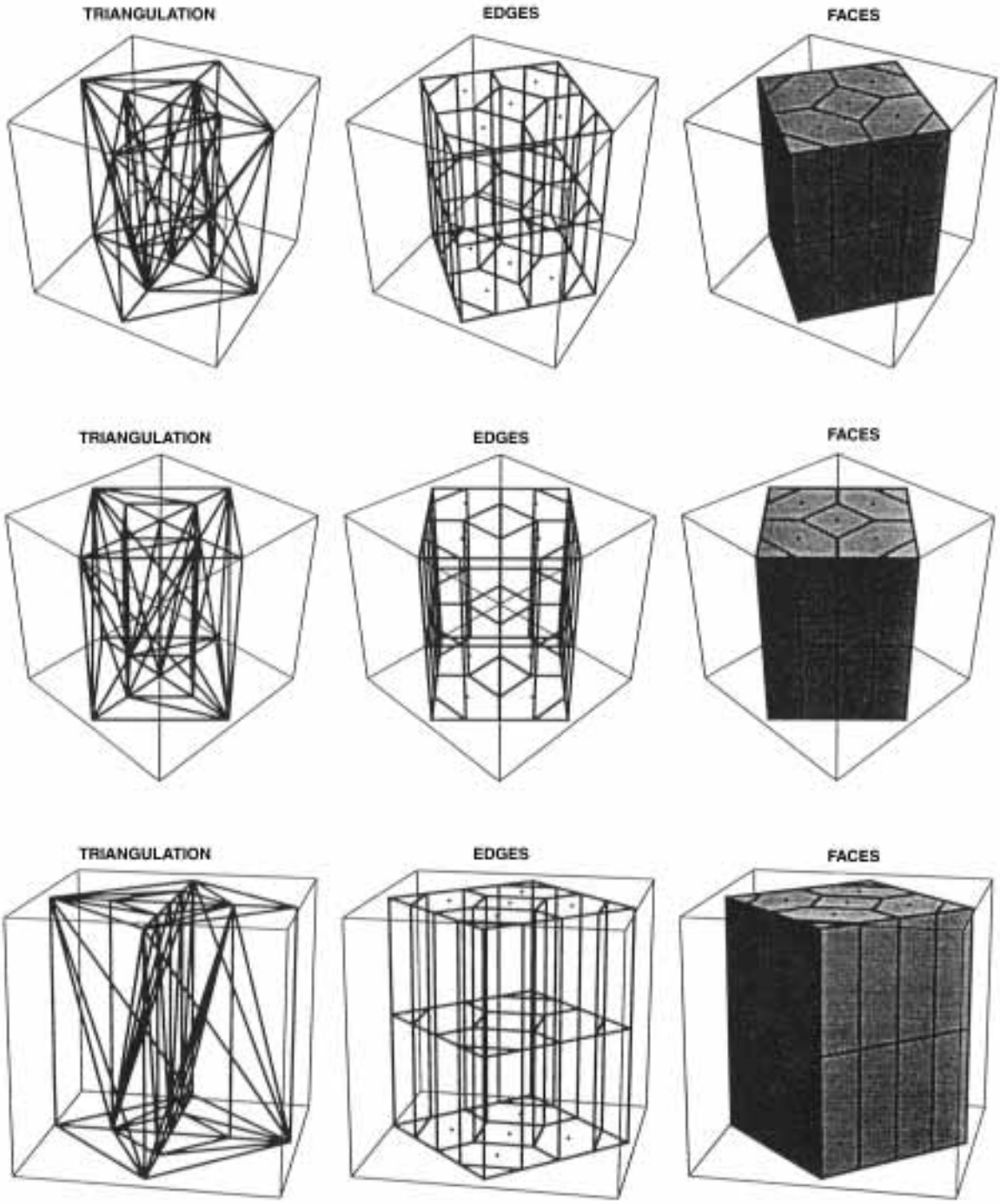

Fig. 1 Triangulation, Voronoi grid edges, and faces in three dimensions (3-D) from three viewpoints.

Algebraic Approximation Scheme

A second algebraic scheme[6] that uses tetrahedra in 3-D or triangles in 2-D as control volumes is described in the following text. Figure 5 shows two such triangles for the 2-D case with a common interface bc. In this face-centered scheme, flux continuity is honored across each face. Φ inside any Δ is a linear interpolant of face pressures. The flux across bc from Δ_1 is given by

$$Q^1_{bc_p} = \lambda_{bc_p} [T^1_{23} (\Phi_2 - \Phi_3) + T^1_{13} (\Phi_1 - \Phi_3)] \quad (4)$$

whereas flux across bc in Δ_2 is

$$Q^2_{bc_p} = \lambda_{bc_p} [T^2_{34} (\Phi_3 - \Phi_4) + T^2_{35} (\Phi_3 - \Phi_5)] \quad (5)$$

The transmissibility term T_{ij} in Eqs. 4 and 5 is a function of the node locations, the permeability tensor, and corners of the

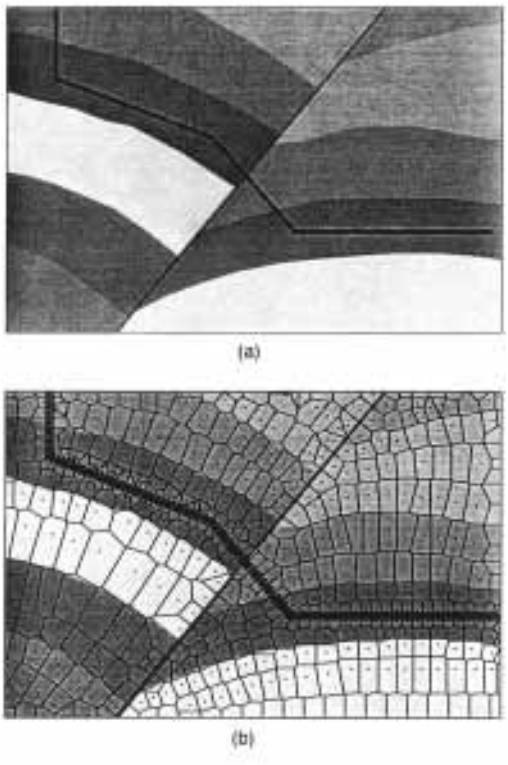

Fig. 2 Voronoi grids for layered reservoir with fault and horizontal well. (a) Schematic of a layered reservoir with fault and well profile. (b) Voronoi grids along deviated well, layer boundaries, and fault.

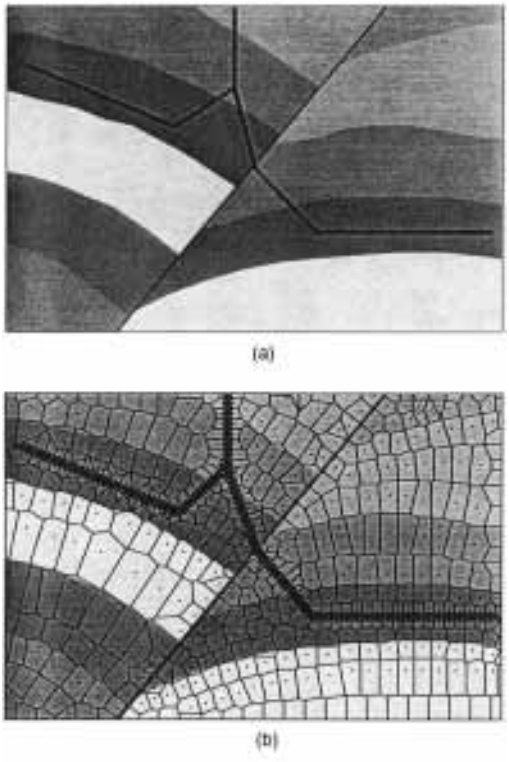

Fig. 3 Voronoi grids for layered reservoir with fault and a dual lateral horizontal well. (a) Schematic of a layered reservoir with fault and well profile. (b) Voronoi grids along dual lateral well, layer boundaries, and fault.

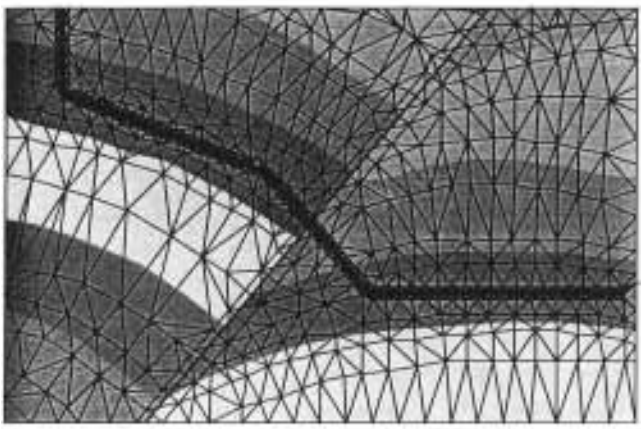

Fig. 4 Delaunay triangulation of nodes for Fig. 2.

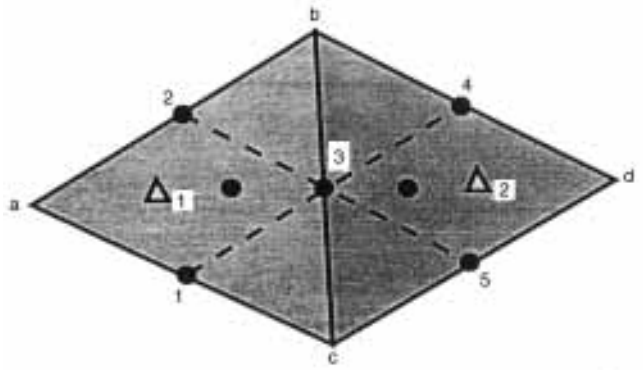

Fig. 5 Description of algebraic approximation formulation.

triangles. It does not vary with time. Flux continuity across the boundary bc leads to

$$\sum_{p=1}^{N_p} Q^1_{bc_p} + \sum_{p=1}^{N_p} Q^2_{bc_p} = 0 \qquad (6)$$

which gives 5-point algebraic approximation involving $\Phi_1, \ldots, \Phi_5$. A material balance equation for each Δ is given by

$$\sum_{i=1}^{3} Q^{n+1}_{p_{ij}} = \frac{V_j}{\Delta t}\left[\left(\frac{\phi S_p}{B_p}\right)^{n+1} - \left(\frac{\phi S_p}{B_p}\right)^{n}\right]_j \qquad (7)$$

where ϕ, S_p, and B_p are taken at barycenter.

Figure 6 shows an example of such a grid. There are 8 triangles and 16 faces. The unknowns in the system are 16 pressures and 8 saturations (two-phase problem). There are 16 flux continuity equations and 8 material balance equations. The flux continuity equations are 5 point in 2-D and 7 point in 3-D. The material balance equations are 9 point in 2-D and 16

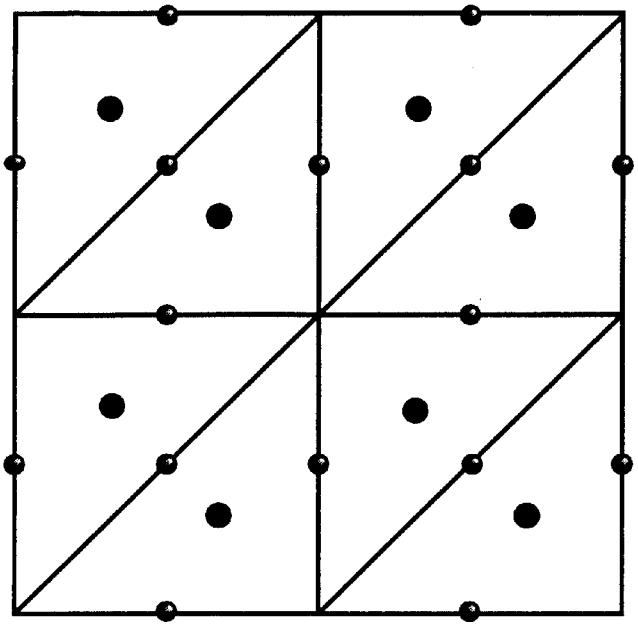

Fig. 6 Algebraic approximation: an example.

point in 3-D. This scheme also handles full and asymmetric permeability tensors. Compared with this scheme, a regular Cartesian scheme will have 9 points in 2-D and 27 points in 3-D. The Cartesian scheme is conceptually much simpler, but it has poor ability to accurately deal with spatially complex reservoir properties and varying well trajectories. The numerical stability of this scheme is still to be tested. Both schemes described are being programmed and will be tested for ability to represent complex geometries, proper representation and simulation of horizontal wells, numerical errors, and central processing unit (CPU) time.

References

1. Z. E. Heinemann, *Advances in Gridding Techniques,* paper presented at the Fifth International Forum on Reservoir Simulation, Muscat, Oman, December 10–14, 1994.
2. L. S. Fung, A. D. Hiebert, and L. Nghiem, *Reservoir Simulation with a Control-Volume Finite-Element Method,* paper SPE 21224 presented at the 11th Society of Petroleum Engineers Symposium on Reservoir Simulation, Anaheim, Calif., February 17–20, 1991.
3. D. Avis and B. K. Bhattacharya, Algorithms for Computing d-Dimensional Voronoi Diagrams and Their Duals, in *Advances in Computing Research,* F. P. Preprate (Ed.), Vol. 1, pp. 159–180, JAI Press, (1983).
4. QHULL, The Geometry Center, University of Minnesota, 1993.
5. C. L. Palagi, *Generation and Application of Voronoi Grids to Model Flow in Heterogeneous Reservoirs,* Ph.D. dissertation, Stanford University, May 1992.
6. M. J. King, BP International, Ltd., Sunbury-on-Thames, United Kingdom, personal communication, 1994.

THERMAL RECOVERY—SUPPORTING RESEARCH

OIL FIELD CHARACTERIZATION AND PROCESS MONITORING USING ELECTROMAGNETIC METHODS

Lawrence Livermore National Laboratory
Livermore, Calif.

Contract Date: Oct. 1, 1984
Anticipated Completion: Oct. 1, 1995
Government Award: $350,000

Principal Investigator:
Mike Wilt

Project Manager:
Thomas Reid
Bartlesville Project Office

Reporting Period: Oct. 1–Dec. 31, 1994

Objective

The objective of this project is to develop practical tools for geophysical characterization of oil strata and monitoring of enhanced oil recovery (EOR) processes in a developed field. Crosshole and surface-to-borehole electromagnetic (EM) methods are being applied to map oil field structure and to provide images of subsurface electrical conductivity changes associated with EOR operations. The goal is to apply surface and borehole EM methods for oil field characterization and monitoring of in situ changes in electrical conductivity during EOR operations.

Summary of Technical Progress

During this quarter an additional set of crosshole EM data was collected at Lost Hills No. 3 and inverted to a two-dimensional (2-D) resistivity model. These data are the third in a series of measurements after the start of steamflooding operations in November 1993. The EM data indicate that significant resistivity decreases continue to occur in the middle and lower Tulare formations at depths greater than 90 m because of the steamflooding. The upper Tulare sands, which are the prime target for the flood, have not changed in resistivity after 10 months of steaming. Temperature logging in one of the EM monitoring holes indicated high temperatures at a depth of 95 m. This is the same depth as the resistivity changes indicated by the EM data.

Development of an inversion code for surface-to-borehole EM data is progressing. One code that uses a scheme similar to the presently used crosshole inversion is under development and will be used initially to invert borehole-to-surface EM data collected at the University of California (UC) Richmond Field Station.

Steamflood Monitoring at Lost Hills No. 3

Mobil Exploration and Production Inc. has operated several EOR projects in central California. Crosshole EM technology is being applied as a pilot test at the Lost Hills No. 3 field. Two fiberglass-cased observation wells (35E and 35W) were drilled along a northeast-southwest profile straddling a steam injector for the combined purposes of crosshole EM surveys and repeated temperature and induction logging. Steam is being injected at depths of 65, 90, and 120 m into upper, middle, and lower members of the Tulare formation, which contains heavy oil. The steam injection is expected to follow the natural northwest-southeast regional strike. The steam plume is expected to develop as an ellipse with the major axis aligned with the natural fractures.

A cross section derived from borehole induction resistivity logs shows that the higher resistivity intervals (10–100 Ω-m) typically represent the oil sands; the lower resistivity units (2–10 Ω-m) are confining silts and shales. The target Tulare oil sands extend from depths of 60 to 120 m in three separate intervals. The upper sand is the thickest and most continuous of the three. It begins at a depth of 60 m, has a thickness of up to 20 m, and dips gently eastward at about 6 degrees. The middle and lower members are thinner and less continuous. The middle member is 3 to 6 m thick and lies at a depth of approximately 90 m. This unit seems to pinch-out near 35W and water-out somewhere between 35E and borehole 4034. The lower unit, which lies at about 110 m, is continuous throughout this portion of the field and dips eastward at about 8 degrees. The water table lies at a depth of 160 m, or just below the base of the cross section.

EM Field Surveys

Crosshole EM data were collected in November 1993, April 1994, and September 1994. The tools were deployed at depths between 30 to 130 m. Receivers were spaced 4 or 8 m apart in borehole 35E, and EM data were collected continuously as the transmitter moved between 130 and 30 m in borehole 35W. EM data were collected at two frequencies, 5 kHz and 20 kHz, although processing is complete only for the 5-kHz results. The error on the crosshole measurements is approximately 2%; this figure is used in estimating data uncertainty during interpretation.

Crosshole EM data were interpreted with the use of a 2-D inversion code developed by the CRADA partner at Schlumberger–Doll Research.[1] A smoothed version of the induction resistivity logs is used in boreholes 35W and 35E as a starting guess for the inversion.

Data Interpretation

The subsurface resistivity distribution between boreholes 35E and 35W before steam injection is shown in Fig. 1a. The darker sections in the images represent higher resistivity zones associated with heavy oil sands; the lighter areas are

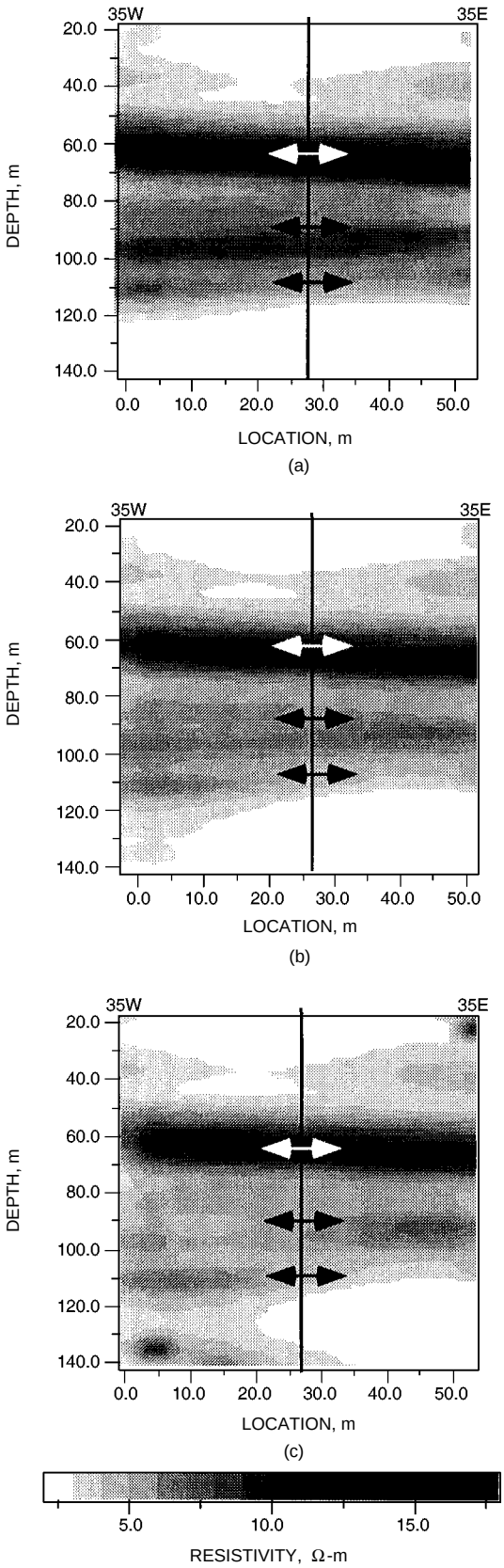

Fig. 1 Cross-well resistivity images before and during steamflooding operations at Lost Hills No. 3. (a) November 1993. (b) April 1994. (c) September 1994.

lower resistivity silts and confining shale beds of 1 to 8 Ω-m, with an average value of 3 Ω-m. The image in Fig. 1a indicates that the upper oil sand is a thick unit dipping gently eastward. The middle and lower sands are thinner and more discontinuous between the wells. The images shown in Figs. 1b and 1c are visibly different only at depths below 70 m. In this portion of the figure, the resistivity has decreased significantly because of the steam injection. In all other parts of the image, the before and after data agree to within a few percent.

Figure 2 shows two different images made by subtracting the baseline image in Fig. 1a from the images in Figs. 1b and 1c. The figure shows that the resistivity has decreased by up to 70% in the region surrounding the injection hole at depths below 80 m. This indicates that a substantial steam chest has formed in the middle and lower sands, and almost none of the steam has gone into the upper oil sand. Because there is considerable steam injection in the upper perforated zone, this implies that there is some connection between the upper and lower oil sands. There may be a connection from the upper to the lower units via natural or man-made fractures. The steam also seems to preferentially flow to the westward in the middle Tulare but eastward in the lower Tulare. The westward movement in the middle oil sand is expected because the producing well to the east of 35E was not completed in the middle oil sand because of high water saturation. The preferential eastward migration in the lower sand is probably attributable to the better eastward stratigraphic continuity in the lower sand, as evidenced by the borehole induction logs and the crosshole EM results.

Recent temperature logs in boreholes 35W and 35E show significant increases in temperature in the middle (35W) and lower (35E) oil sands but no change in the upper oil sands (Fig. 3). The temperature in the hot zones has been progressively increasing since steam injection began. The resistivity decrease corresponding to the temperature increase is expected from field and theoretical results.[2]

From these monitoring results it is clear that the upper Tulare is either losing steam to the middle and lower members, or the steam is propagating out of the section. It is known that the upper unit has a higher oil saturation and historically has more difficulty accepting steam. Whether this unit develops a substantial steam chest over time is not known, but continuing field efforts will be made to track the steam injected into this upper sand.

Development of Inversion Codes for Surface-to-Borehole Data

Surface-to-borehole data sets involve deployment of instruments (either sources or receivers) on the surface to image resistivity distribution at depth. An obvious problem with interpretation of these data is that the surface layer strongly affects the measurements but is not the target of the imaging. A related problem is that a much larger volume of earth must be discretized in order to interpret the results. This results in much larger numerical meshes and slower and more cumbersome software.

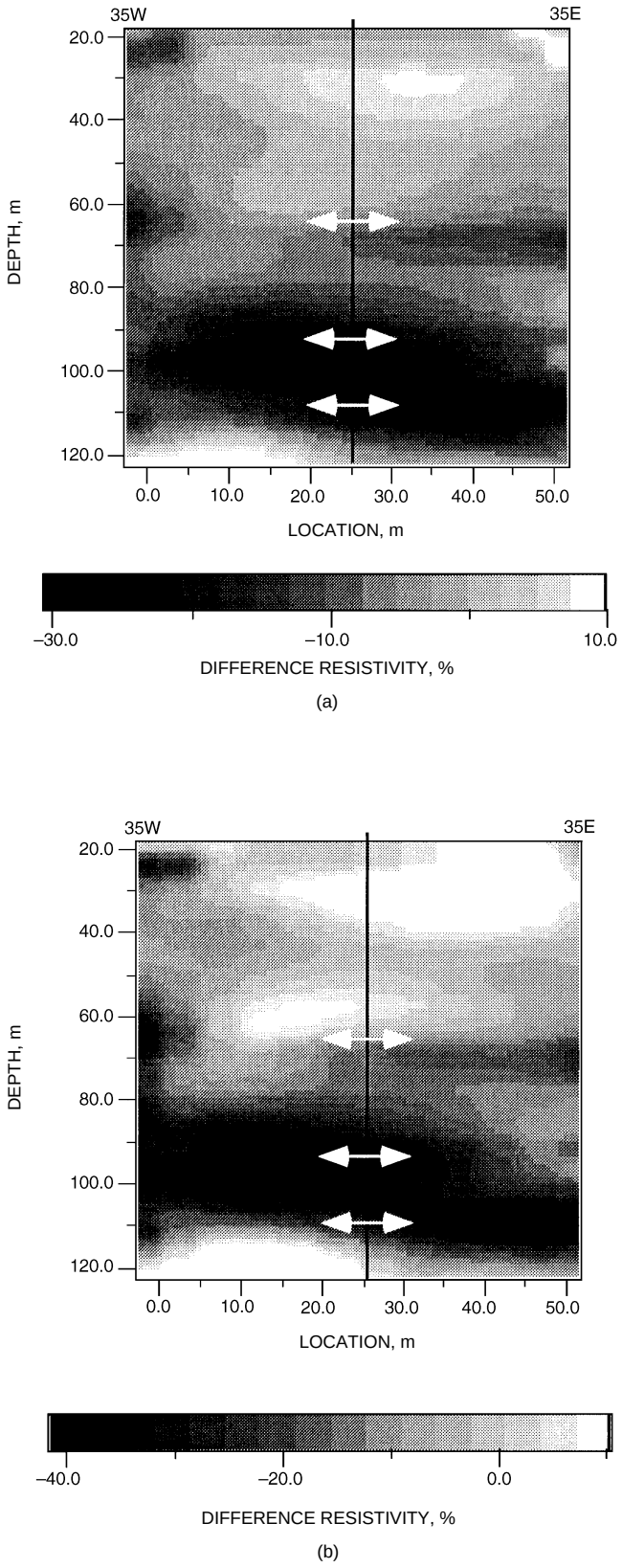

Fig. 2 Percent difference resistivity images during the steamflooding operations. (a) November 1993 to April 1994. (b) November 1993 to October 1994.

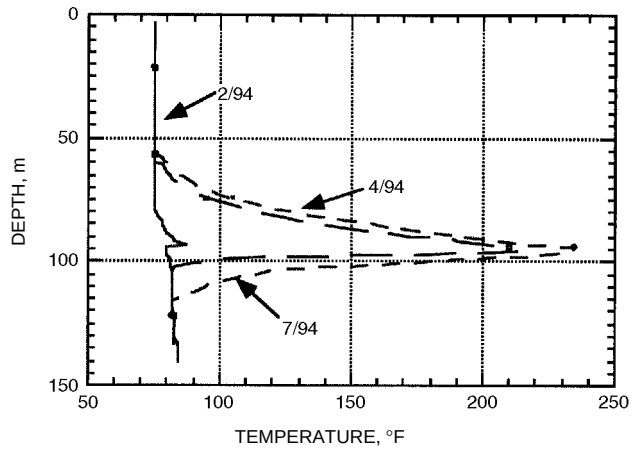

Fig. 3 Temperature logs from wells 35W and 35E during the steam injection process.

The logistical advantages to stock tank barrel (STB) data and recent success at data collection at the Lost Hills field are strong incentives for developing practical inversion algorithms. This task is being approached along several parallel fronts. Initially, a cylindrically symmetric crosshole code will be modified for the surface-to-borehole configuration. This code was initially used in waterflood imaging at UC Richmond Field Station[3] and should be suitable for STB imaging. A second code under development is a three-dimensional algorithm that uses principles outlined in Torres-Verdin and Habashy.[1]

Technology Transfer

An article describing the Lawrence Livermore National Laboratory/Lawrence Berkeley Laboratory (LLNL/LBL) crosshole EM system and applications was submitted for publication to the Society of Exploration Geophysicists during this quarter.[4]

References

1. C. Torres-Verdin and T. Habashy, An Approach to Nonlinear Inversion with Application to Crosswell EM Tomography, *Extended Abstracts, Society of Exploration Geophysicists Annual Meeting*, Washington, D.C., pp. 351-354, 1993.
2. A. J. Mansure, R. F. Meldau, and H. V. Weyland, *Field Examples of Electrical Resistivity Changes During Steamflooding*, paper SPE 20539 presented at the 65th Annual Society of Petroleum Engineers Technical Conference, New Orleans, La., Sept. 23–26, 1990.
3. D. L. Alumbaugh, *Iterative Electromagnetic Born Inversion Applied to Earth Conductivity Imaging*, Ph.D. Dissertation, University of California, Berkeley, 1993.
4. Crosshole Electromagnetic Tomography—a New Technology for Oil Field Characterization, *The Leading Edge of Exploration*, (March 1995).

STUDY OF HYDROCARBON MISCIBLE SOLVENT SLUG INJECTION PROCESS FOR IMPROVED RECOVERY OF HEAVY OIL FROM SCHRADER BLUFF POOL, MILNE POINT UNIT, ALASKA

Contract No. DE-FG22-93BC14864

University of Alaska
Fairbanks, Alaska

Contract Date: Dec. 1, 1992
Anticipated Completion: June 30, 1996

Principal Investigator:
G. D. Sharma

Project Manager:
Thomas Reid
Bartlesville Project Office

Reporting Period: Oct. 1–Dec. 31, 1994

Objectives

The ultimate objective of this 3-yr research project is to evaluate the performance of the hydrocarbon miscible solvent slug process and to assess the feasibility of this process for improving recovery of heavy oil from Schrader Bluff reservoir. This will be accomplished through measurement of pressure–volume–temperature (PVT) and fluid properties of Schrader Bluff oil, determination of phase behavior of Schrader Bluff oil solvent mixtures, asphaltene precipitation tests, slim-tube displacement tests, coreflood experiments, and reservoir simulation studies. The expected results from this project include determination of optimum hydrocarbon solvent composition suitable for hydrocarbon miscible solvent slug displacement process, optimum slug sizes of solvent needed, solvent recovery factor, solvent requirements, extent and timing of solvent recycle, displacement and sweep efficiency to be achieved, and oil recovery.

Summary of Technical Progress

Slim-tube displacement experiments and simulation results were verified and compiled and are summarized in this report. Table 1 provides the summary comparison of recoveries from slim-tube simulation and experiments.

The findings of this study are as follows:

• The pure lean gas from Kuparuk–Schrader Bluff formation is immiscible at reservoir pressure of 1300 psia and temperature of 82 °F, yielding very low recovery in the slim-tube experiment. Thus, if this gas is to be used in field

TABLE 1

Recoveries from Slim-Tube Simulation and Experiments

Solvent	Slim-tube simulation	Slim-tube experiments	% Relative deviation
100% KUPSCH gas	41.85	37.92	9.39
100% PBG	48.46	45.01	7.12
70% PBG/30% NGL	85.56	83.63	2.6
50% PBG/50% NGL	94.55	92.57	2.09
50% PBG/50% NGL	100.0	99.0	1.0
100% CO_2	76.45	71.63	6.31
90% CO_2 /10% NGL	95.25	88.49	7.09
85% CO_2 /15% NGL	100.0	98.01	1.99

Note: KUPSCH, Kuparuk–Schrader Bluff lean gas mixture (90:10). PBG, Prudhoe Bay Gas. NGL, Natural Gas Liquid.

applications, it will be an immiscible water-alternating-gas (WAG)-type process.

• Pure carbon dioxide (CO_2) and Prudhoe Bay Gas (PBG) are also immiscible with Schrader Bluff crude at reservoir conditions. Very high recovery is obtained during pure CO_2 slim-tube experimental runs. This indicates that use of CO_2 may be promising in the field application.

• The enrichment of CO_2 by natural gas liquid (NGL) at 15 mol % NGL resulted in dynamic miscibility at reservoir conditions. This run resulted in 98% oil recovery after injection of 1.2 pore volume (PV). The compositional slim-tube simulation and the equation of state (EOS) predictions also confirmed generation of miscibility. The miscibility was developed primarily by vaporizing gas drive mechanism.

• PBG achieved miscibility after enrichment at 50 mol % of NGL. This slim-tube experimental run resulted in 99% recovery after injection of 1.2 PV of solvent. This compositional simulation predicted 100% recovery after injection of 1.2 PV of solvent, but the multicontact test (MCT) runs conducted on the two-phase EOS simulator did not predict miscibility development for this mixture.

• The lumping of pseudocomponents and determination of EOS parameters appeared to be critical in matching laboratory slim-tube data.

MODIFICATION OF RESERVOIR CHEMICAL AND PHYSICAL FACTORS IN STEAMFLOODS TO INCREASE HEAVY OIL RECOVERY

Contract No. DE-FG22-93BC14899

University of Southern California
Los Angeles, Calif.

Contract Date: Feb. 22, 1993
Anticipated Completion: Feb. 21, 1996
Government Award: $150,000
(Current year)

Principal Investigator:
Yanis C. Yortsos

Project Manager:
Thomas Reid
Bartlesville Project Office

Reporting Period: Oct. 1–Dec. 31, 1994

Objectives

The objectives of this research are to continue previous work and to carry out new fundamental studies in the following areas of interest to thermal recovery: displacement and flow properties of fluids involving phase change (condensation–evaporation) in porous media; flow properties of mobility control fluids (such as foam); and the effect of reservoir heterogeneity on thermal recovery. The specific projects address the need to improve heavy oil recovery from typical reservoirs as well as less conventional fractured reservoirs producing from vertical or horizontal wells.

Thermal methods, and particularly steam injection, are currently recognized as the most promising for the efficient recovery of heavy oil. Despite significant progress, however, important technical issues remain unresolved. Specifically, knowledge of the complex interaction between porous media and the various fluids of thermal recovery (steam, water, heavy oil, gases, and chemicals) is still inadequate. Also, the interplay of heat transfer andfluid flow with pore- and macro-scale heterogeneity is largely unexplored.

Summary of Technical Progress

Vapor–Liquid Flow

During this period work continued on the modeling of vapor–liquid flows in porous media. Work focused on completing the steam displacement pore network simulator and on issues of vapor adsorption–desorption in porous media. The steam displacement simulator is complete and is running efficiently. Effects of injection rate, vapor density, latent heat, and thermal conductivity on the displacement patterns are being investigated. The objective is to quantify similarities and differences in the displacement patterns between isothermal displacements in the absence of phase change and displacements where heat transfer controls phase change and phase behavior. The simulation results will be compared with steam injection experiments in glass micromodels. Work is also under way on the extension to a three-phase system involving oil, water vapor, and water liquid under conditions that simulate steam displacement of oil.

In a different study, vapor adsorption–desorption in tight porous media has been considered, and a pore network model has been developed to describe adsorption–desorption processes.[1] The model includes the possibility of supercritical fluid in tight pores with the use of recent advances from density functional theories, and experimental results from adsorption–desorption experiments were reproduced successfully.[1] In parallel a macroscopic approach is being used to analyze the stability of phase-change fronts in porous media.

Heterogeneity

With the use of optimal control methods, work continued on the optimization of recovery processes in heterogeneous reservoirs. A model problem involving unit mobility ratio in the absence of capillary effects in a heterogeneous reservoir with multiple injection and one production well was used to identify the injection strategy that maximizes the recovery efficiency at breakthrough. The efficiency is maximized by an on–off injection schedule. For example, for the case of two injection wells, the optimal injection strategy consists of injecting from one well only until a critical time is reached and then switching injection to the other well only. The switch time is a function of the well spacing and other geometrical parameters.

The study of the dynamics of invasion fronts in heterogeneous porous media of large aspect ratio at low rates continued. Also, study on the effects of long-range correlations (for example, with the use of fractional Brownian motion statistics) on invasion percolation continued. Preliminary results show that in such cases the resulting invasion features (for example, the capillary pressure curve) are not deterministic but are stochastic. The capillary pressure threshold, the capillary pressure curve, and the relative permeabilities depend on the orientation of the pattern or the invasion direction. The average curves have features that depend smoothly on the degree of correlation, however.[2]

Work also is continuing on the development of rigorous viscous fingering models based on the concept of transverse flow equilibrium (TFE). This approach was extended to miscible displacements in narrow capillaries or Hele–Shaw cells, where the finger width as a function of the mobility ratio was determined. A technical paper on this topic is complete.[3] The results are useful in setting limits on the validity of the approaches currently used for miscible displacements in Hele–Shaw cells and porous media at high rates.

Chemical Additives

Work continued on the behavior of non-Newtonian fluid flow and on foam displacements in porous media. A study was completed for the understanding of the onset of mobilization and flow of foams and of Bingham plastics by devising a new invasion process containing long-time memory[4] based on which the minimum threshold path in a porous medium can be identified. This path was shown to be a self-affine curve of constant tortuosity, from which appropriate estimates on the value of the minimum pressure gradient for flow–mobilization can be developed. The algorithm was also used to study the displacement at low rates of Bingham plastics, the application being on heavy oil recovery as well as on sand production (wormholes).[5] During this quarter a technical paper was completed on the solution of certain mathematical models involving flow and reaction in porous media which was motivated by a problem of foam propagation.[6]

References

1. C. Satik and Y. C. Yortsos, *A Pore Network Model for Adsorption in Porous Media*, paper presented at the 20th Annual Workshop in Geothermal Reservoir Engineering, Stanford, Calif., January 24–26, 1995.
2. C. Du and Y. C. Yortsos, *Invasion Percolation in Correlated Lattices*, in preparation, 1995.
3. Z. Yang and Y. C. Yortsos, *Asymptotic Solutions of Miscible Displacements in Geometries of Large Aspect Ratio*, submitted for publication, 1995.
4. H. Kharabaf and Y. C. Yortsos, *Invasion Percolation with Memory*, submitted for publication, 1995.
5. C. B. Shah, H. Kharabaf, and Y. C. Yortsos, Flow and Displacement of Bingham Plastics in Porous Media, in *Proceedings of the 6th UNITAR International Conference on Heavy Crudes and Tar Sands*, Houston, Tex., February 12–16, 1995.
6. H. Kharabaf and Y. C. Yortsos, A Note on the Solution of Hyperbolic Systems Involving Reactions, *Ind. Eng. Chem. Fundam.* (accepted 1995).

GEOSCIENCE TECHNOLOGY

INTERDISCIPLINARY STUDY OF RESERVOIR COMPARTMENTS

Contract No. DE-AC22-93BC14891

Colorado School of Mines
Golden, Colo.

Contract Date: Sept. 29, 1993
Anticipated Completion: Sept. 30, 1996
Government Award: $753,266

Principal Investigator:
Craig W. Van Kirk

Project Manager:
Robert Lemmon
Bartlesville Project Office

Reporting Period: Oct. 1–Dec. 31, 1994

Objective

The objective of this research project is to document the integrated team approach for solving reservoir engineering problems. A field study integrating the disciplines of geology, geophysics, and petroleum engineering will be the mechanism for documenting the integrated approach. The goal is to provide tools and approaches that can be used to detect reservoir compartments, reach a better reserve estimate, and improve profits early in the life of a field.

Summary of Technical Progress

Reservoir Selection and Data Gathering

During this quarter selected well logs were added to the database. An application was developed to retrieve production history, decline curve analysis information and well completion data, and plot the data and information on a single page for each lease.

Outcrop/Core/Log Analysis and Correlations

A relationship between minipermeameter measurements for permeability and log-derived parameters has been investigated. For the Vern Marshall core–log data, a preliminary relationship between minipermeameter permeability and bulk volume water has been demonstrated. This relationship may be useful in reservoir simulation where core data are not available.

The results of petrography and diagenesis work on the Sussex sandstone indicate that

• Stylolites were commonly found in the study area and may be significant vertical permeability baffles that result in a tortuous reservoir fluid path.

• Most of the porosity in these sandstones appears to be microporosity.

• The origin of the sandstones may be an offshore environment.

• The high carbonate-content cement may indicate the presence of common primary carbonate (sand) grains. A sequence of carbonate-rich and carbonate-poor (silica-cemented) sandstones may be a predictive tool in the framework of sequence stratigraphy. This assumes that the carbonate grains were only available in a certain environment. This hypothesis may explain the common occurrence in the Cretaceous sandstones in this area of interbedded carbonate-cemented and silica-cemented sandstones. Porosity development is better in the carbonate-cemented sandstones.

Seismic Analysis

All work was completed at a three-dimensional (3-D) seismic workstation to ensure that all relevant information was integrated into the 3-D interpretation. The 3-D compressional wave seismic interpretation is complete. One main fault complex trending southwest–northeast has been interpreted. Displacement in the Sussex level was observed. A subtle change in the Sussex reflection trends southeast–northwest and is offset by the main fault. This change in the Sussex reflection character corresponds to the zero-sand line interpreted by the geologic team members. The amplitude variation correlated with the fault pattern and the zero-sand line.

Detailed Reservoir Engineering Evaluation

The reservoir engineering evaluation calculates that, effective October 1993, the cumulative production is 24.8 billion standard cubic feet (BSCF) of gas and 1 million stock tank barrels (MMSTB) of oil in the study area. The study area encompasses approximately 15,360 acres with 62 wells producing from the Sussex formation. The preliminary estimates for remaining oil reserves are 240 thousand stock tank barrels (MSTB) of oil and 5 BSCF of gas. The estimates are based on material balance calculations and decline curve analysis. There is a high degree of uncertainty in the material balance estimates because of the limited amount of pressure data and the difficulty of obtaining good pressure data in a low-permeability reservoir. The decline curve analysis was difficult because of the long flow times necessary to reach pseudo steady-state flow. Linear flow probably exists for up to 10 yr in the lower permeability portions of the reservoir.

The wells in this area have been hydraulically fractured. On the basis of two available well tests, fracture lengths indicate that actual hydraulic fracture lengths are approximately 60 to 80% of the design lengths. The fracture orientation and the geometry of the drainage area are important for optimal well placement in a tight, compartmentalized reservoir. Fracture propagation direction cannot be determined from production data and common well test data.

Permeability Experimental Work

On the basis of permeability experimental work, the following conclusions were reached:

• A correlation of experimental porosity and permeability values with confining stress was developed.

• No general equation was found to transform the relative permeabilities obtained from measurements under lab conditions to the relative permeabilities under reservoir conditions.

• The effects on the relative permeabilities of increasing the net confining stress from 200 to 3500 psig and the temperature from 70 to 140 °F are

1. Relative permeability curves shift slightly to the right while maintaining their shape characteristics.
2. Increased confining stress and temperature have a minor or no effect on endpoints.
3. The shift affects the relative permeability to the oil for the first drainage by progressively increasing its value until a maximum deviation in the upper curvature is reached. Then the deviation decreases as the curves merge and approach the endpoint. The maximum shift to the right is 10%, which can make a significant difference in the relative permeability values in the steepest portion of the curve.
4. The shift affects the relative permeability to the water for the first drainage by progressively reducing its value until a maximum deviation in the lower curvature part is reached. Then the deviation decreases until the curves merge and approach the endpoint. The maximum shift to the right is 10%, which can make a significant difference in the relative permeability values in the steepest portion of the curve.

• The capillary pressure–saturation relationship obtained from the mercury–air experiment and transformed to lab water–oil was found to be comparable with the capillary pressure points obtained from the water–oil displacement experiments.

• The numerical simulation of the lab experiments used the initial core conditions as input. The match of experimental pressure and displaced fluid volume was obtained by changing the relative permeability curves.

Technology Transfer

An abstract of a paper on multidisciplinary team modeling of a complex sandstone reservoir, Colorado, was submitted to the American Association of Petroleum Geologists international conference.[1] The paper includes an example of how the research effort can be incorporated into the classroom.

Reference

1. R. M. Slatt, *Multidisciplinary Team Modeling of a Complex Sandstone Reservoir, Colorado,* paper to be presented at the American Association of Petroleum Geologists International Conference and Exhibition, Nice, France, September 10–13, 1995.

LAWRENCE BERKELEY LABORATORY/ INDUSTRY HETEROGENEOUS RESERVOIR PERFORMANCE DEFINITION PROJECT

Lawrence Berkeley Laboratory
University of California
Berkeley, Calif.

Contract Date: Apr. 1, 1992
Anticipated Completion: September 1995
Government Award: $275,000

Principal Investigators:
J. C. S. Long
E. L. Majer
L. R. Myer

Project Manager:
Robert Lemmon
Bartlesville Project Office

Reporting Period: Oct. 1–Dec. 31, 1994

Objectives

The purpose of this work is to validate geophysical and hydrological techniques for characterizing heterogeneous reservoirs in the most optimal (economic) manner. The overall objective of the project is to develop a methodology that can be used by the petroleum industry in a variety of heterogeneous regimes for characterizing and predicting the performance of petroleum reservoirs. This objective will be accomplished through a cooperative research program between Lawrence Berkeley Laboratory (LBL), British Petroleum, Inc. (BP), and the University of Oklahoma (OU), which is focused on the characterization of heterogeneous reservoirs in a meander-belt porous-medium formation. BP has done characterization and data integration at several test facilities. The present program will continue BP's multiyear efforts at the Gypsy site in northeastern Oklahoma. The resulting research will integrate various geophysical and hydrological methods and apply them at a well-calibrated and characterized site where their use can be assessed. This cooperation will allow techniques developed for waste storage and geothermal energy to be adapted for use in heterogeneous and fractured reservoirs. The work will be coordinated with the cross-well electromagnetic (EM) research and development project and the LBL/Morgantown Energy Technology Center (METC) reservoir performance definition project.

Summary of Technical Progress

Hydrologic-Related Work

The pilot-site well-test analyses that used the iterated function system inversion method (IFSINV) were completed. The final tasks consisted of completing co-inversions of three upper–middle sand channel well tests, which looked for heterogeneity solely in the intervening clay layer; performing a series of co-inversions of the same tests, which sequentially searched for heterogeneity in the clay layer, the middle sand channel, and the upper sand channel; extending the inversions constrained by lithologic information to illustrate a simple energy surface and analyzing the performance of various optimization schemes on it; performing cross-validation studies of upper–middle sand channel inversions; and comparing the IFS method to a traditional geostatistical analysis with single-well tests.

Seismic-Related Work

First arrival times were re-picked for one of the cross-well seismic surveys with care that direct rather than refracted arrivals were picked and inverted to produce a velocity tomogram. Although different constraints were applied to the inversion, it produced results consistent with previous inversions with picks that had been validated. The new inversion does not provide any more information than the previous ones. Although the Gypsy interval is readily apparent as a low-velocity zone, no resolution of features within it is possible with the use of first arrival times alone.

A study on the propagation of guided seismic waves at the Gypsy pilot site was reviewed.[1] An alternate method has been used to look for guided waves through examination of common source gathers. It appears that guided waves may propagate through the lower sand channel, but no such signature has been observed for the upper or middle sand channels.

Integration of Hydrologic and Seismic Work

The pilot-site cross-well seismic surveys conducted by BP were re-examined with the lithology and well-test analysis results in mind, and assessment of the relative value of geologic, hydrologic, and geophysical data was made.

Data Transfer

The first-arrival picks for the cross-well seismic data done at LBL were transmitted to OU, with the suggestion that they be incorporated into the Gypsy data set.

Reference

1. J. O. Parra, B. J. Zook, and H. Collier, *Seismic-Guided Waves for Reservoir Continuity at the Gypsy Test Site, Oklahoma*, paper presented at the Society of Exploration Geophysicists 64th Annual Meeting, Los Angeles, Calif., October 23–28, 1994.

INTEGRATION OF ADVANCED GEOSCIENCE AND ENGINEERING TECHNIQUES TO QUANTIFY INTERWELL HETEROGENEITY

Contract No. DE-AC22-93BC14893

New Mexico Institute of Mining and Technology
Petroleum Recovery Research Center
Socorro, N. Mex.

Contract Date: Sept. 29, 1993
Anticipated Completion: Sept. 30, 1996
Government Award: $250,896

Principal Investigator:
F. David Martin

Project Manager:
Robert Lemmon
Bartlesville Project Office

Reporting Period: Oct. 1–Dec. 31, 1994

Objective

The objective of this project is to integrate advanced geoscience and reservoir engineering concepts with the goal of quantifying the dynamics of fluid–rock and fluid–fluid interactions as they relate to reservoir architecture and lithologic characterization. This interdisciplinary effort will integrate geological and geophysical data with engineering and petrophysical results through reservoir simulation. Subcontractors from Stanford University (SU) and the University of Texas at Austin (UT) are collaborating on the project: SU is supervising the geophysical research and UT is supervising the hydrologic and tracer research. Several members of the Petroleum Recovery Research Center (PRRC) staff are developing improved reservoir description by integrating the field and laboratory data, as well as developing quantitative reservoir models to aid performance predictions.

Summary of Technical Progress

Cross-Well Seismic Test

Field Work

The cross-well seismic field experiment at the Sulimar Queen Unit began on December 18, 1994, and was completed on December 21, 1994. The work site consisted of the well pair No. 1-3 and No. 1-16, shown in Fig. 1. Because tubing, rods, pump, and a packer were to be pulled from the wells, arrangements were made to run a through-pipe gamma-ray, neutron log in Well No. 1-16 where a core analysis was available. The log from Well No. 1-3 is a 1960's style through-pipe gamma-ray, neutron log that was used to identify the interval to be perforated. The initial reservoir description will be dependent on this type of 1960's vintage perforating log.

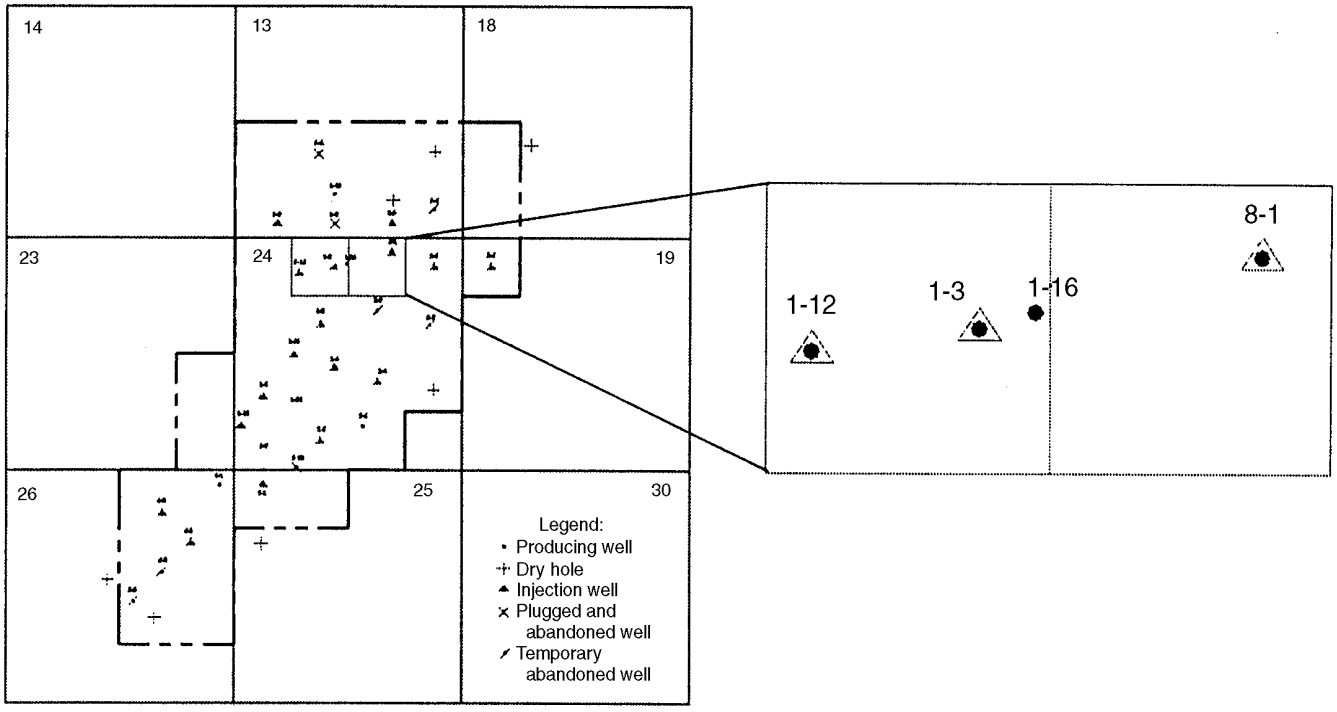

Fig. 1 Field site for cross-well seismic test, Sulimar Queen Unit, Chaves County, N. Mex. (Art reproduced from best available copy.)

Rods, tubing, pump, and packer were removed from the wells in advance of cross-well seismic work. Two workover rigs were left on the wells to facilitate the installation and removal of the seismic sending and receiving equipment.

Seismic field operations commenced December 19, 1994, with the arrival of three TomoSeis staff members, four Computalog wireline operators, a contract field operator from Pecos Petroleum Engineering, three workover rig personnel, and support personnel from SU and the PRRC. Logging continued around the clock with crews working 12-h shifts. Equipment consisted of one TomoSeis recording trailer (which included a computer workstation), one 50-kW generator to power the downhole source, and two wireline trucks (one for the piezoceramic source and the other for the six hydrophones recording string). The sketch in Fig. 2 depicts the sending and receiving equipment.

Depths were calibrated with a gamma-ray tie-in logging run, the receivers were run into Well No. 1-16, and the source lowered into Well No. 1-3. Approximately 9050 traces were collected, with additional traces taken to quantify shooting parameters and noise conditions in the wells. A complete data set (100 × 100) was acquired with no major equipment or acquisition problems. Data quality is good but not as good as expected for the close well spacing. Because of excessive noise in the receiving well, the source and receivers were switched, making Well No. 1-16 (new well) the source well and Well No. 1-3 (old well) the receiving well. The casing cement job in Well No. 1-3 (drilled with a cable tool) is the reason suspected for the excessive noise. Approximately 19,250 traces were collected in this configuration. Noise was prevalent in the data collected in this configuration, but notably quieter than in the initial configuration. The straight lines (tube waves) seen in the unprocessed data (Fig. 3) illustrate the noise problem.

The survey was recorded with 5-ft source and receiver spacing instead of the $3^1/_3$-ft spacing desired. This reduction in sampling was necessitated by the poorer signal-to-noise ratio (SNR) and the fixed budget. Two receiver gathers at 1700 and 1750 ft were collected at 1-ft spacing in order to test the effect of coarser sampling during the data processing. These two gathers might also give a benchmark or reference that can be used for the entire data set. The two gathers collected at 1-ft spacing were chosen at 1700 and 1750 ft to give good angular coverage of the Queen formation. A vertical aperture of 600 ft was recorded, approximately 1.5 times the well spacing. This should provide a good aperture for inversion.

All the field data contained the strong tube waves seen in Fig. 3. Unfortunately, noise obscures most of the signal. A more typical data set (gather) from another survey is provided in Fig. 4. The direct arrival is clearly seen in these data along with some reflections and tube waves. The application of an automatic gain correction (AGC) of the field data given in Fig. 3 reveals the direct arrival of some of the traces, along with evidence of reflected compressional waves, as shown in Fig. 5. The fact that reflections are seen in the raw data is an encouraging sign that the processing will be successful in

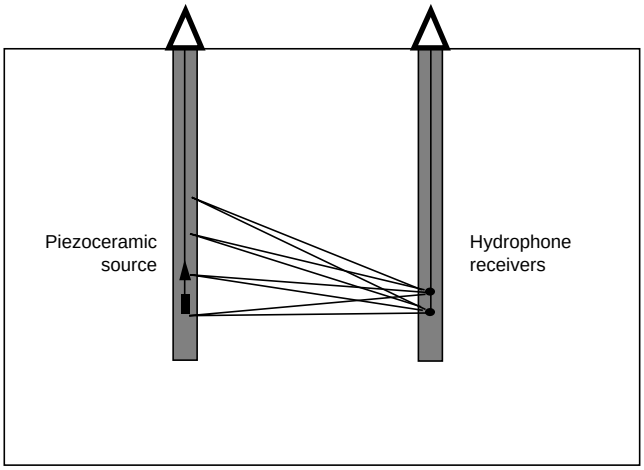

Fig. 2 Sketch of seismic sending and receiving equipment.

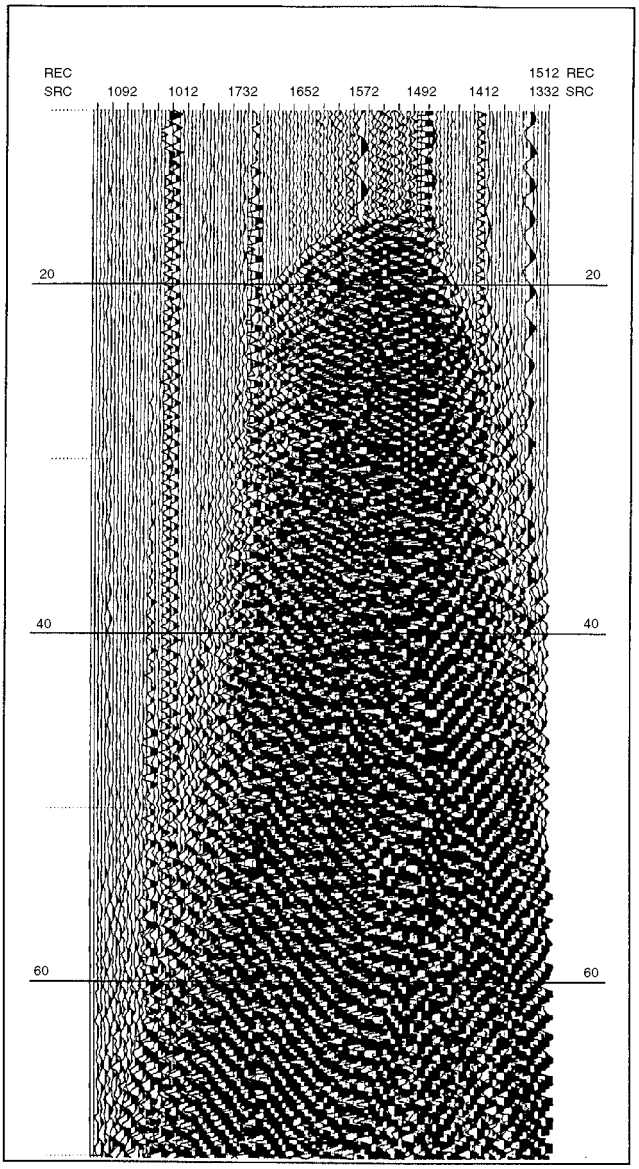

Fig. 3 Display of unprocessed seismic data. (Art reproduced from best available copy.)

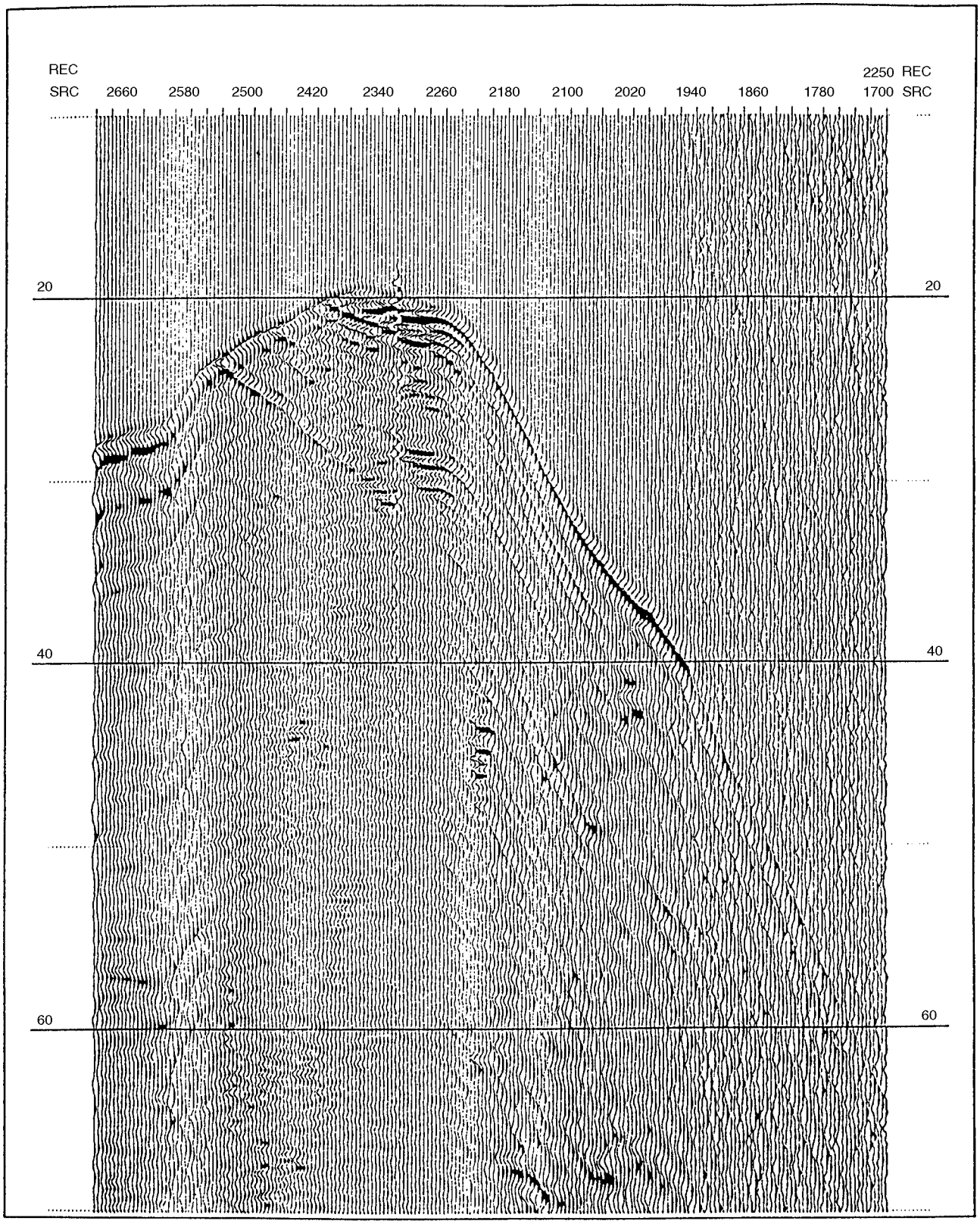

Fig. 4 Typical cross-well seismic survey. (Art reproduced from best available copy.)

extracting more events. Additional filtering techniques will be applied as processing of the seismic data continues.

The through-pipe neutron log run in Well No. 1-16 following the seismic work will be used to develop an interpretation

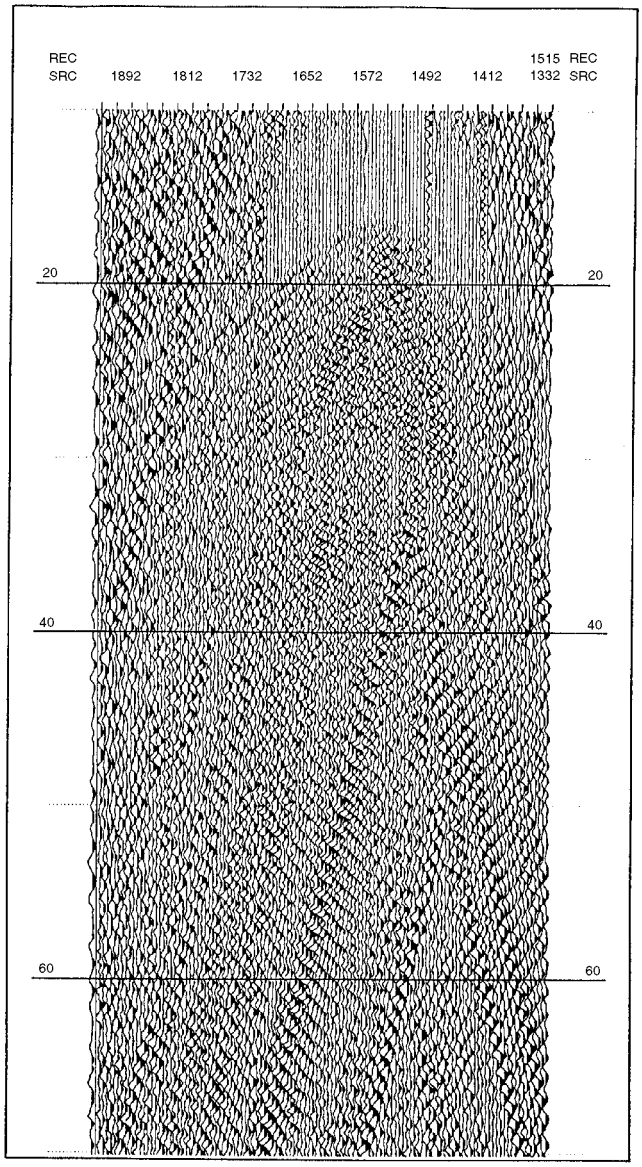

Fig. 5 Modified display of Fig. 3 data. (Art reproduced from best available copy.)

methodology for the old gamma-ray, neutron-perforating logs. A neural network will be trained with the information available from Well No. 1-16 and then used to evaluate the old logs.

Data Management

Computer hardware and software provided by Landmark Graphics Corp. are being used to manage and utilize the data that are accumulated. Among the programs are OpenWorks, the geoinformation and integration frame work; GeoDataWorks, a graphical data query application; StratWorks, an application for well log correlation, cross section creation, fault modeling, and mapping; PetroWorks, a set of tools for petrophysical analysis and well log editing and interpretation; Z-MAP Plus, an advanced system for mapping, interpretive surface and fault modeling, and volumetric calculations; and SeisWorks/2-D and SeisWorks/3-D, packages designed for storage, management, and interpretation of two-dimensional (2-D) and three-dimensional (3-D) seismic data. These programs run on a Sparc10 Workstation also provided by Landmark Graphics.

Landmark has also provided training on the various software packages, and to date, schools on the operation of GeoDataWorks, Z-MAP Plus, StratWorks, and Workflow Management have been attended by the PRRC personnel. Additionally, a presentation, *Reservoir Characterization of Sulimar Queen Field, Chaves County, N. Mex.*, was made for Landmark's Worldwide Technology Forum in December 1994.[1]

Information from the Sulimar Queen field has been entered into the database, including digitized well logs, well locations, well elevations and depths, surface picks, and production data. In addition, 2-D seismic data have been prepared for loading and will be entered and examined.

Reference

1. Martha E. Cather, *Reservoir Characterization of Sulimar Queen Field, Chaves County, N. Mex.*, paper presented at Landmark Worldwide Technology Forum, Houston, Tex., December 1994.

FABRICATION AND DOWNHOLE TESTING OF MOVING THROUGH CASING RESISTIVITY APPARATUS

Contract No. DE-FG22-93BC14966

ParaMagnetic Logging, Inc.
Woodinville, Wash.

Contract Date: March 23, 1993
Anticipated Completion: June 30, 1995
Government Award: $109,000

Principal Investigator:
W. Banning Vail

Project Manager:
Robert Lemmon
Bartlesville Project Office

Reporting Period: Oct. 1–Dec. 31, 1994

Objective

The objective of this project is to validate recently discovered technology dealing with oil well measurement instrumentation that will allow the industry to find missed oil and bypassed gas. This breakthrough technology, already endorsed in principle by the oil and gas industries, will allow identification of missed oil and bypassed gas locations in abandoned fields as well as in existing offshore wells and will also allow increased productivity from low-production wells. There is no other proven technology that can detect such oil behind steel casing, lower the discovery risk, and improve the success rate of recovery of otherwise accessible but undetected oil and gas reserves.

Summary of Technical Progress

It is believed that there may be more potential bypassed oil horizons around existing wells than will be found in the future by wildcat drilling in the continental United States. This new technology could substantially increase the petroleum reserves in the continental United States and obviate the need to drill new wells, particularly in environmentally sensitive areas. This technology initially may be of particular interest to independent oil companies and ultimately will be of great economic value to major oil companies as well. The technology can also be used to monitor enhanced oil recovery (EOR) projects.

This is a continuing research effort into the new field of measuring resistivity of geological formations from within cased wells. Additional data confirming the feasibility of the technology are to be taken in a test well with the existing stop-hold-and-lock apparatus that is called the Through Casing Resistivity Apparatus (TCRA). After these data are obtained, the already existing mechanical apparatus developed in an earlier phase of the project will be modified and new electronic components will be fabricated to test the concept of a moving apparatus called the Moving Through Casing Resistivity Apparatus (Moving TCRA) that is designed to take data at commercially acceptable logging speeds. These steps are considered sufficient for subsequent commercial development by industry. It is important to measure resistivity through casing for at least the following reasons: locating bypassed oil and gas; measuring water breakthrough during waterflooding operations; evaluating reservoirs; measuring through a drill string when the drilling bit is stopped; and environmental monitoring of disposal wells, water wells, etc.

The analysis has begun on the completely successful test results obtained at the MWX-2 well (blind test of the technology). More than 100 figures have been completed to provide a complete record of the data for future theoretical analysis.

A parallel analysis of the theory has been undertaken that shows that ParaMagnetic Logging, Inc.'s calibration constant K can be calculated from first principles. Such first principles calculation gives adequate agreement with the empirically determined calibration constant K used at the MWX-2 well and at prior wells.

RESEARCH PROGRAM ON FRACTURED PETROLEUM RESERVOIRS

Contract No. DE-FG22-93BC14875

Reservoir Engineering Research Institute
Palo Alto, Calif.

Contract Date: Sept. 30, 1993
Anticipated Completion Date: Sept. 29, 1996
Government Award: $443,000

Principal Investigator:
Abbas Firoozabadi

Project Manager:
Robert Lemmon
Bartlesville Project Office

Reporting Period: Oct. 1–Dec. 31, 1994

Objectives

The objectives of this project are to provide experimental data on viscous displacement in fractured porous media for gas–oil displacement processes and analyze the data to examine the nature of displacement improvement from viscous forces. A method that accounts for reinfiltration and capillary continuity not only within the grid cell but also between various grid cells is proposed.

Summary of Technical Progress

Immiscible Gas–Oil Flow in Fractured/Layered Porous Media

Viscous Displacement in Fractured Porous Media

In some fractured reservoirs, a gas pressure gradient of the order of 0.1 psi/ft may be established in the fractures resulting from flow.[1] Such a pressure gradient could allow enhancement of recovery of the matrix oil. Several experiments were conducted to study viscous displacement in fractured porous media, including both gravity drainage with free gas displacement and with forced gas displacement.

The experimental apparatus is depicted in Fig. 1. Two different matrix-fracture configurations (a and b, four experiments each) were used to study viscous displacement in fractured porous media (Fig. 2).

Gravity Drainage

Gravity drainage provides a basis to examine the effect of viscous forces on flow in fractured porous media. In Fig. 3 the

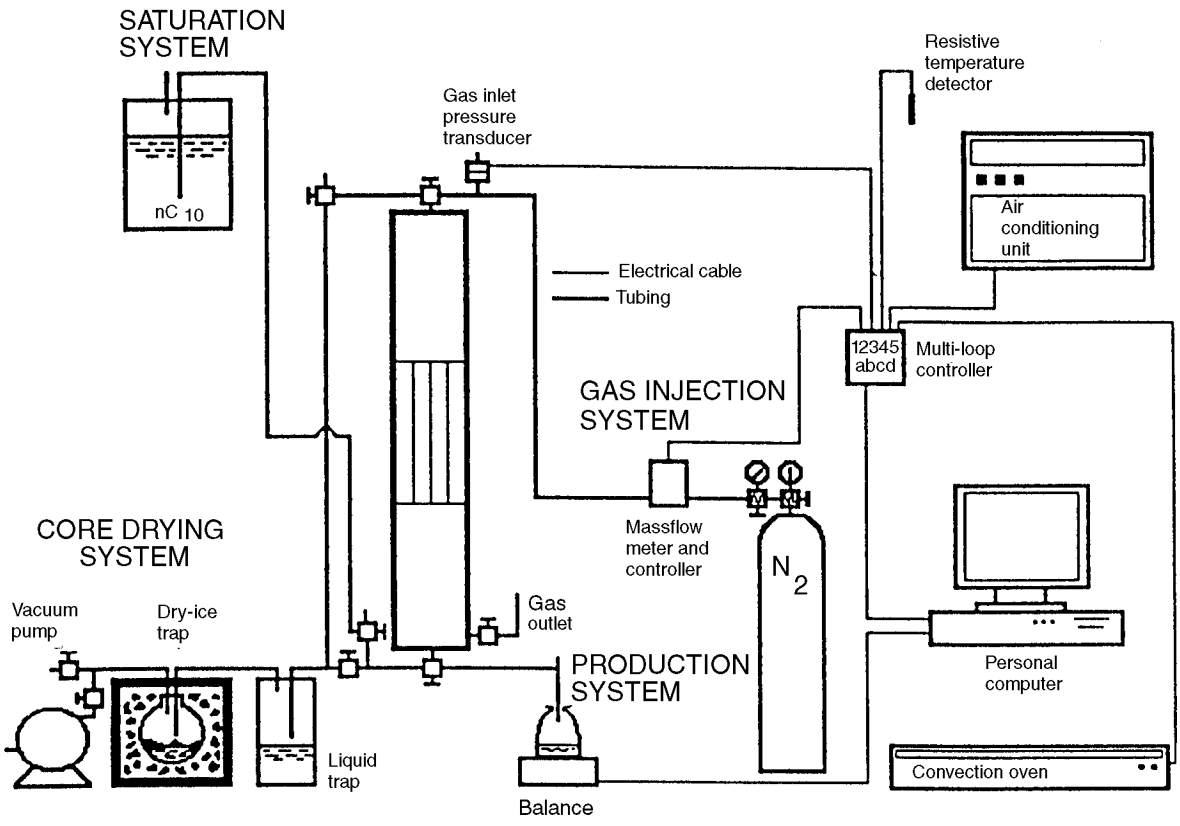

Fig. 1 Viscous displacement experimental setup.

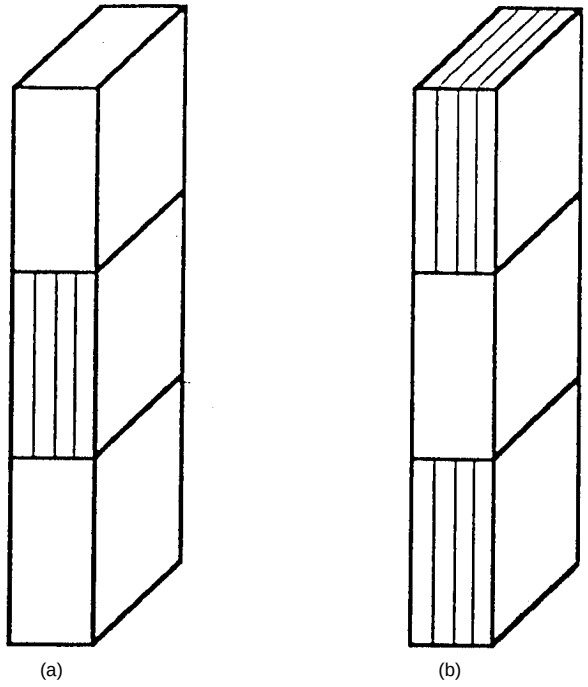

Fig. 2 Matrix-fracture configurations used in the experiments. (a) and (b) represent two different matrix-fracture configurations, four experiments each.

production and rate data for Test 1a (gas–oil gravity drainage), Test 2a (gas injection and gravity drainage), Test 3a (gravity drainage and gas injection), and Test 4a (gas injection at constant psi) are compared. Figure 4 shows the injection pressure data for Tests 2a and 3a. Figure 5 shows the injection rate data for Test 4a. In Fig. 6 the cumulative production and rate data of configuration b experiments are compared. Figure 7 shows injection pressure data for Tests 2b, 3b, and 4b.

Experimental results demonstrate considerable improvement in recovery because of viscous displacement [i.e., matrix oil recovery is improved by 10% of pore volume (PV) in configuration b experiments].

In the simulation of gravity-assisted viscous displacement and pure gravity displacement experiments, an appropriate fracture capillary pressure for laboratory experiments was assumed. Fracture capillary pressure and fracture effective permeability expressions used were taken from Dindoruk and Firoozabadi.[2] The capillary pressures of the configured blocks were calculated from the model of Bentsen and Anli.[3] The effective fracture liquid permeability was approximated by analyzing the flow perpendicular to fracture planes. Because of strong capillarity, small fracture apertures, and rapid desaturation of fractures, fracture-relative permeability becomes relatively unimportant. Numerical results are in good agreement with the experimental data.

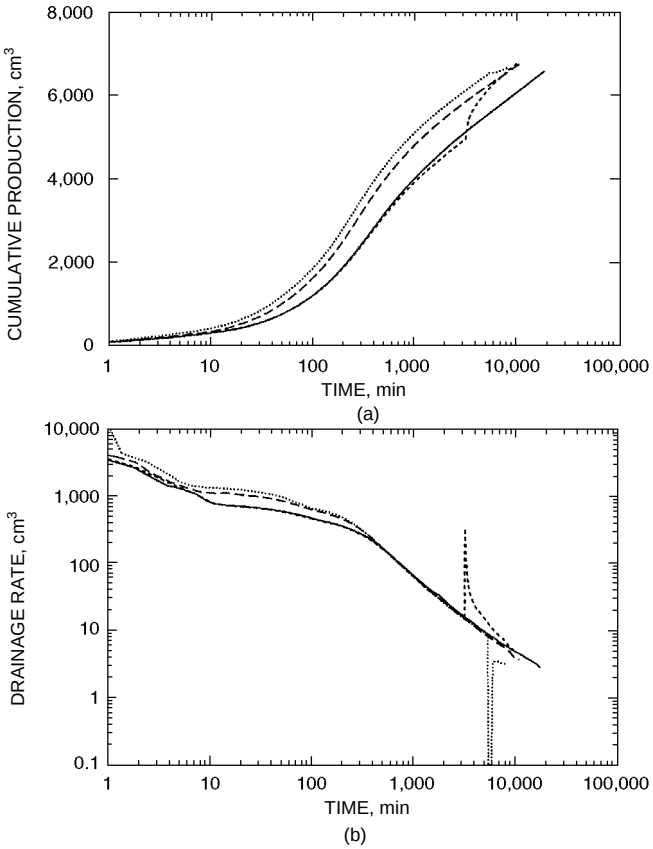

Fig. 3 Comparison of cumulative production (a) and drainage rate (b) data of configuration a. ——, Test 1a, gas–oil gravity drainage. ....., Test 2a, gas injection and gravity drainage. ———, Test 3a, gravity drainage and gas injection. – – –, Test 4a, gas injection at constant psi.

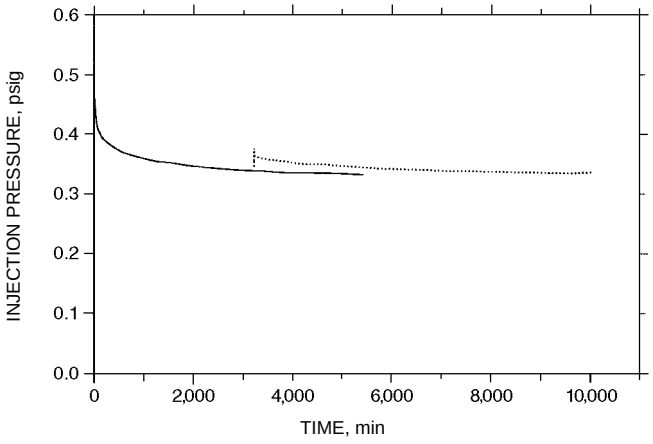

Fig. 4 Injection pressure data for Tests 2a (——) and 3a (.....).

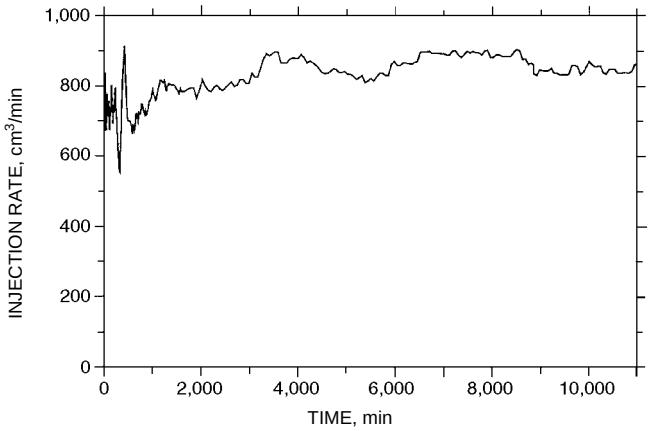

Fig. 5 Injection rate data for Test 4a.

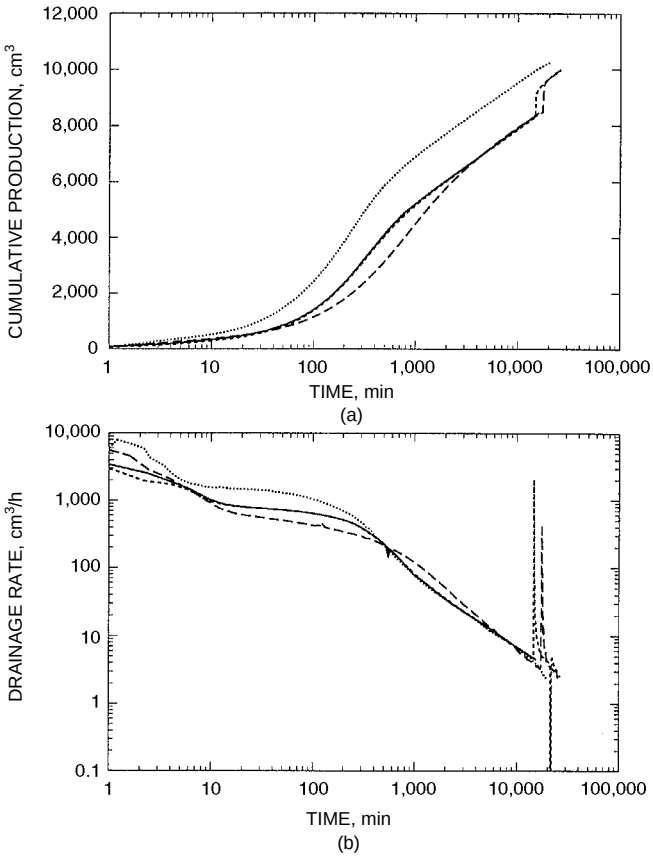

Fig. 6 Comparison of cumulative production (a) and drainage rate (b) data of configuration b. ——, Test 1b, gas–oil gravity drainage. ....., Test 2b, gas injection and gravity drainage. - - - - - -, Test 3b, gravity drainage and gas injection. – – –, Test 4b, gas injection at constant psi.

The simulation analysis has led to the following conclusions:

• Production performance of viscous displacement in a fractured porous medium is influenced mainly by pressure drop across the displacement length; pressure gradient is a measure of fracture aperture and injection rate.

• Effects of viscous forces in a fractured porous medium are very important. Rate and production enhancement after injection of nitrogen indicates the importance of viscous forces.

• Viscous injection can be a viable alternative to accelerate production even for fractured reservoirs close to capillary–gravity equilibrium.

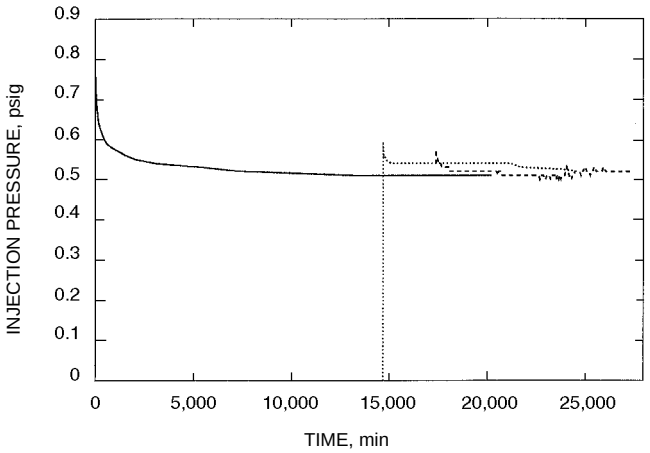

Fig. 7 Injection pressure data for Tests 2b (——), 3b (.....), and 4b (– – –).

Simulation of Fractured Reservoirs

Dual-Porosity Simulation Incorporating Reinfiltration and Capillary Continuity Concepts

Interaction between grid cells. A method is proposed that accounts for reinfiltration and capillary continuity not only within a grid cell but also between various grid cells. The method is based on the observation that the rate of drainage of a matrix block in a stack, when plotted vs. matrix block average saturation, reveals a systematic behavior. In such a plot, the drainage rate of all the matrix blocks can be approximated by two universal curves when only reinfiltration occurs and three universal curves when capillary continuity is accounted for. Therefore fine-grid simulation of a stack of two or three matrix blocks is adequate to calculate the drainage performance of a stack comprised of a large number of matrix blocks.

The procedure for calculation uses a simple material balance.[4,5] A reinfiltration term is added to the dual-porosity model, and the exchange term between the matrix and the fracture is calculated simply.

References

1. A. Firoozabadi and T. Markeset, Fracture Liquid Transmissibility for Gas–Liquid Flow in Fractured Porous Media, *SPE Reserv. Eng.*, 9(3): 201–207 (August 1994).
2. B. Dindoruk and A. Firoozabadi, Computation of Gas–Liquid Drainage in Fractured Porous Media Recognizing Fracture Liquid Flow, *J. Can. Pet. Technol.*, 33(12): (December 1994).
3. R. G. Bentsen and J. Anli, A New Displacement Capillary Pressure Model, *J. Can. Pet. Technol.*, 30(5): 75–79 (September–October 1991).
4. J. Tan and A. Firoozabadi, *Dual-Porosity Simulation Incorporating Reinfiltration and Capillary Continuity Concepts—Part I: Single Gridcell*, Reservoir Engineering Research Institute Report No. 4Q93, February 15, 1994.
5. J. Tan and A. Firoozabadi, *Dual-Porosity Simulation Incorporating Reinfiltration and Capillary Continuity Concepts—PART II: Capillary Continuity in a Computational Gridcell*, Reservoir Engineering Research Institute Report No. 1Q94, May 12, 1994.

GEOSCIENCE/ENGINEERING CHARACTERIZATION OF THE INTERWELL ENVIRONMENT IN CARBONATE RESERVOIRS BASED ON OUTCROP ANALOGS, PERMIAN BASIN, WEST TEXAS AND NEW MEXICO

Contract No. DE-AC22-93BC14895

University of Texas
Bureau of Economic Geology
Austin, Tex.

Contract Date: Sept. 29, 1993
Anticipated Completion: Sept. 28, 1996
Government Award: $354,000

Principal Investigators:
F. J. Lucia
C. Kerans

Project Manager:
Robert Lemmon
Bartlesville Project Office

Reporting Period: Oct. 1–Dec. 31, 1994

Objectives

The primary objective of this project is to investigate styles of reservoir heterogeneity found in low-permeability, pelleted wackestone–packstone facies and mixed carbonate–clastic facies found in Permian Basin reservoirs by studying similar facies exposed in the Guadalupe Mountains. Specific objectives for the outcrop study include construction of a stratigraphic framework, petrophysical quantification of the framework, and testing the outcrop reservoir model for effects of reservoir heterogeneity on production performance. Specific objectives for the subsurface study parallel objectives for the outcrop study.

Summary of Technical Progress

Outcrop Activities

Much of this quarter was occupied preparing data for the October 1994 review meeting in Carlsbad, N. Mex., and preparing reports. Outcrop data continue to be incorporated

into cross sections and maps for improved sequence stratigraphic interpretations and comparison with subsurface data.

Subsurface Activities

Regional cross sections showing facies and sequence stratigraphic boundaries in the Grayburg of the northeastern Central Basin Platform and detailed cross sections of South Cowden field have been prepared and distributed to members of the Reservoir Characterization Research Laboratory. This material was presented at the October 1994 review meeting in Carlsbad, N. Mex.

Characterization of South Cowden field continues. An analysis of available wireline logs from the Moss Unit indicates that only 124 wells have calibrated porosity logs. The rest of the porosity logs are neutron logs scaled in counts-per-second and not suitable for this work. Cased-hole and open-hole neutron logs, acoustic logs, density logs, and combinations of these logs have been calibrated with core data, and the resulting transforms have been used to calculate porosity from 124 wells. A single porosity/permeability transform developed from rock-fabric studies was used to calculate a permeability profile. Original oil saturation has been estimated with the use of a porosity/water-saturation transform developed from capillary pressure data and modified to fit porosity/saturation relationships found in unflooded wells.

Maps showing the distribution of k × kh = permeability × feet (kh), phi × h = porosity × feet (phih), and So × phi × h = oil saturation × porosity × feet (SophiH) have been prepared. The kh maps show good agreement with cumulative production maps. Initial calculations show original oil in place (OOIP) to be approximately 130 million barrels (MMB) of stock tank oil (STO). Total production from the Moss unit is 27 MMBO, resulting in a recovery efficiency of 20%. Therefore, there is about 50 MMB of mobile oil remaining in the Moss Unit.

There are still questions about the gypsum effect on neutron logs in the Emmons Unit. Fifty ft of core from Emmons No. 210 well were sampled every foot and submitted for X-ray diffraction (XRD) analysis for gypsum.

APPLICATION OF ARTIFICIAL INTELLIGENCE TO RESERVOIR CHARACTERIZATION: AN INTERDISCIPLINARY APPROACH

Contract No. DE-AC22-93BC14894

University of Tulsa
Tulsa, Okla.

Contract Date: Oct. 1, 1993
Anticipated Completion: Sept. 30, 1996
Government Award: $240,540

Principal Investigator:
M. Kelkar

Project Manager:
Robert Lemmon
Bartlesville Project Office

Reporting Period: Oct. 1–Dec. 31, 1994

Objectives

The objectives of this research are to use novel techniques from artificial intelligence (AI) and expert systems (ES) to capture, integrate, and articulate key knowledge from geology, geostatistics, and petroleum engineering for the development of accurate descriptions of petroleum reservoirs. The ultimate goal is to design and implement a single powerful ES for use by small producers and independents to exploit reservoirs efficiently.

The main challenge of the research is to automate the generation of detailed reservoir descriptions honoring all the available soft and hard data, which range from qualitative and semiquantitative geological interpretations to numeric data obtained from cores, well tests, well logs, and production statistics. In this sense, the research project is multidisciplinary. It involves a significant amount of information exchange between researchers in geology, geostatistics, and petroleum engineering. Computer science and AI provide the means to effectively acquire, integrate and automate the key areas of expertise in the various disciplines represented in a reservoir characterization ES. Additional challenges are the verification and validation of the ES, because much of the interpretation of the experts is based on extended experience in reservoir characterization.

The overall project plan to design a system to create integrated reservoir descriptions begins with the development of an AI-based methodology to produce large-scale reservoir descriptions generated interactively from geology and well-test data. A parallel second task develops an AI-based methodology that uses facies-based information to generate small-scale descriptions of reservoir properties, such as permeability and porosity. The third task involves consolidation and integration of the large- and small-scale methodologies to produce reservoir descriptions honoring all

the available data. The final task will be technology transfer.

The results of the integration are not merely limited to obtaining better characterizations of individual reservoirs. They have the potential to significantly affect and advance the discipline of reservoir characterization itself.

Summary of Technical Progress

Decomposition of System

The decomposition of the overall system development into smaller component parts has allowed more focus on the expert knowledge required for each component. This decomposition facilitates the implementation of the system and its validation and verification. The three component systems represent how each of the experts in geology, geostatistics, and engineering characterizes the reservoir. Figure 1 describes a model for this breakdown. The concurrent development of these component systems fits into the development of the large- and small-scale aspects of the system. Each component system in the model is depicted as interfacing (through the bi-directional links) with a central repository of reservoir descriptions. Although portions of these descriptions will essentially be passed from component to component as more information is gathered (as shown by the bi-directional links), the model of a central repository is an accurate account of how the components are integrated (i.e., the final descriptions in the repository are consistent with all the information given by the component systems. This system model allows development of the system with the use of an AI technique called blackboard system in which information is centrally located (i.e., on a blackboard), and experts take their turn to update, change, and correct the information on the blackboard.

The prototype system was initially developed in KAPPA-PC to gain an understanding of the representation issues so that each system was provided with the information that it needs, either as raw input or as feedback information from another system. Currently, ES shell is being built in C++ to continue the development of the system. The following sections detail development of each of the component systems.

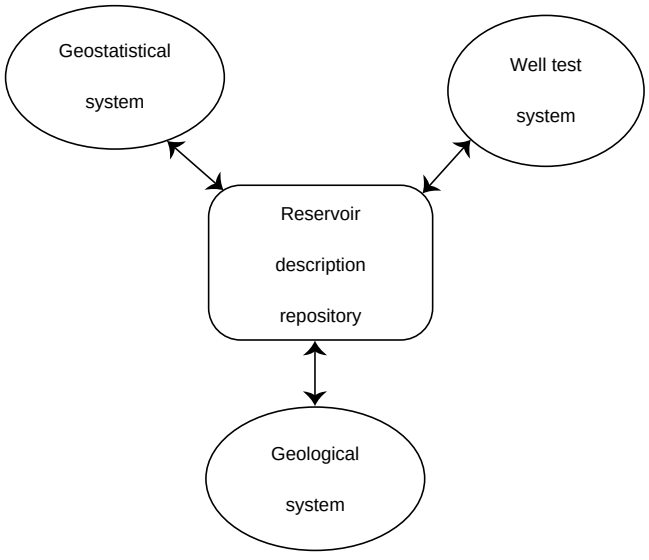

Fig. 1 Expert system decomposition.

Geostatistical System

During this quarter, work concentrated on trying to improve the performance of the simulated annealing (SA) algorithm. The inclusion of flow simulation has a severe impact on the execution time of the algorithm—even when the Laplace transform finite difference (LTFD) methodology is used.[1] Additionally, through analysis of the results obtained, it was concluded that there was an error in the code that had escaped earlier detection (because of its relatively small size). Analysis of the performance of the variogram-based objective function vs. the two-part (variogram and flow simulation) objective function continued.

Analysis of Data Input and Manipulation

Analysis of the behavior of the objective function when the dynamic constraint component is included led to the conclusion that the rate of convergence, which was based on a comparison (which is done in Laplace space) of the observed pressures with the calculated pressures, was too slow and could be accelerated. Additionally, the terminal objective function value being obtained, at about 0.1, was too high to conclude that convergence to a globally optimal solution had occurred. An analysis of the objective function indicated that the Laplace transform of the observed pressure (input) data was not precise enough to adequately represent the true Laplace transform of the real-time pressure values.

The Laplace transform of real-time data involves an integration from zero to infinity

$$L[f(t)] = \int_0^\infty f(t)e^{-ut}\,dt \qquad (1)$$

Normally, rate–pressure–time data have been input at discrete time intervals and only up to a finite time. Thus interpolation and extrapolation of the observed data are necessary to calculate the Laplace transform. Confirmation was made that much more input pressure data than were currently being used were required for interpolation in order to perform a proper transform. At least 10 values per log cycle were recommended. It was further observed that when larger time values—greater than 10 d, for example—were considered, the data density required for interpolation purposes was higher than 10 per log cycle. The method of extrapolation depends on the flow regime characteristics at the time extrapolation is performed [for example, should pseudo steady-state (boundary-dominated) flow exist, then the most appropriate extrapolation method should be a linear extrapolation using the chord slope of the last interval of pressure–time data].[2] Thus some

pre-analysis of the input data is necessary to ensure that the data quality and quantity are adequate and also that the appropriate algorithms are used.

Once this was implemented, convergence was faster and the terminal objective function value reached about one order of magnitude lower, at approximately 0.01. Also, the absolute maximum percentage error between the observed and calculated Laplace space pressure values was reduced to about 0.8%.

Correction of Flow Simulation Code

There were differences between the pressures obtained from ECLIPSE (a commercial simulation package)[3] and the LTFD simulator which, although small, increased with time. Further analysis that compared the results from both simulators with the analytical solution with a homogeneous reservoir case showed that the ECLIPSE results agreed more closely with the analytical results. This confirmed that the error was not caused by truncation or round off in the ECLIPSE time-step values but, in fact, was caused by a faulty subprogram in LTFD. This error has been corrected.

Generation of New Data Sets

In recognition of the direct relationship between the time required for running the simulated annealing algorithm (especially when the flow simulation is included) and the grid resolution, the decision was made to undertake runs with smaller grids (scaled-up grids). The algorithm would then run faster and thus enable speedier analysis of the optimization schemes. New data sets for these runs were generated. The turning bands method,[4] sequential Gaussian simulation (sGs),[5] and simulated annealing (SA)[6] were used in this effort. In addition to generating the data distribution, the variogram models, gray-scale maps, cumulative distribution functions (cdf), and conditioning points that define the data were also required. Complete sets were defined and used for 12×12 (144) and 16×14 (224) grid blocks.

In addition, a code was developed to generate lognormal data, which could then be used to create a training set. Basically, the required mean, variance, and the number of data values needed are input, and the program generates a set of values satisfying those specifications. These data are then used to produce a cdf (and conditioning data if necessary) for use with the SA approach in producing the training set. As expected, it was found that the statistics of the values generated only approximately the required statistics (mean and variance) but that the approximation improved as the number of values generated increased.

With the statistics from the lognormal data obtained, relatively fine-scale heterogeneous permeability grids—81×51 (4131) and 80×70 (5600) two-dimensional (2-D) grid-block systems—were generated with the use of SA with a variogram objective function. Flow simulation was performed with these fine-scale grid systems to obtain pressure–rate–time data. These fine-scale grids were then scaled up by geometric averaging to 27×17 (459) and 16×14 (224) 2-D grid-block systems, respectively, on which the SA algorithm was run with both the one-part (variogram) and the two-part objective functions. The image obtained by this scaling-up technique showed a close resemblance to the true image (apart from being smoother), and also its pressure behavior closely approximated that of the true image on flow simulation.

Code Optimization

A detailed optimization effort of the flow simulation code was undertaken. This required a major overhaul of the existing code to streamline the calculations required for updating the coefficient matrix used in the flow simulation pressure calculations. Although the optimization in an overall sense is complete, testing and further refinements are still in progress. Initial testing has shown that the changes have resulted in some gain in efficiency, but not of the magnitude hoped for. Refinements are still being made, however.

Study of Matrix Perturbation

With each perturbation of the permeability distribution, the coefficient matrix is inverted when solving for the pressure values for the flow simulation part of the SA algorithm. This matrix is only slightly changed—perturbed, in fact—with each perturbation of the permeability of the distribution. Changing the permeability value of one grid block results in 19 changes in the coefficient matrix terms. Specifically, all seven terms in the row corresponding to the block being perturbed are affected along with two terms for each of the six blocks adjacent to the one being perturbed in a three-dimensional (3-D) grid system. If a 2-D grid is being considered, then only 13 changes occur: 5 for the row of the block being perturbed and 2 each for the 4 adjacent blocks.

This implies that, because the matrix is being perturbed, there may be a perturbation approach to updating the matrix inverse instead of having to invert the matrix each time the permeability distribution is perturbed—a computationally expensive process. This approach is being studied.

Observations

Preliminary results indicate that the addition of the dynamic constraint to the objective function of the SA algorithm does improve the match between the training image and the generated image over that obtained when only a variogram objective function is used. From a purely visual examination, gray-scale images of the results from the two-part objective function resemble those of the training image more than those of results with a variogram objective function. Because this type of analysis may be somewhat subjective, an objective measure was applied to determine which image better matches the training image. Analysis of the results with the use of one training image gives the certainty coefficient with the variogram objective function as 0.471, whereas for the two-part objective function,

the coefficient obtained was 0.667, where the certainty coefficient, C, between a simulated variable, V_s, and the true value, V_t, is defined as[6]

$$C = \frac{\sum_{i=1}^{N_s} \left[V_s(\omega_i) - \overline{V}_s\right]\left[V_t(\omega_i) - \overline{V}_t\right]}{\left\{\sum_{i=1}^{N_s} \left[V_s(\omega_i) - \overline{V}_s\right]^2 \sum_{i=1}^{N_s} \left[V_t(\omega_i) - \overline{V}_t\right]^2\right\}^{1/2}} \quad (2)$$

where

$$\overline{V}_s = \frac{1}{N_s} \sum_{i=1}^{N_s} V_s(\omega_i) \quad (3)$$

and

$$\overline{V}_t = \frac{1}{N_s} \sum_{i=1}^{N_s} V_t(\omega_i) \quad (4)$$

A value of C closer to one implies a closer match between the simulated and the true distribution; however, the validity of using the certainty coefficient as a measure of the goodness of match between distributions is still being studied because inconsistent results with this coefficient raise questions about its utility or suitability.

In addition, the simulated distributions were flow-simulated with the use of the ECLIPSE simulator. Comparison of the pressure–time behavior showed a consistently better agreement with the training image by the distribution generated with a two-part objective function over the distribution obtained from a variogram objective function.

Geological System

Log Facies

The approach taken earlier in this project for the recognition of log has not been successful. One reason for the lack of success comes from the great variety of conditions a single log type used in lithologic determination can take on as a result of logging companies, vintages, or hole conditions. Another reason is the inability for this approach to recognize and segment compound or complex log facies patterns. This past approach does work well for solitary occurrences of simple log patterns. Unfortunately, this is not the case for most real-world conditions.

An approach was developed to deal with compound and complex log facies occurrences, and evaluation began early in this quarter. The approach used progressive segmentation of log profiles with values above a given sandstone threshold. Unfortunately, this approach was too computationally intensive to be of practical use.

A new scheme that has been devised will be thoroughly developed and evaluated. This scheme uses techniques from image analysis and will be integrated with a neural network approach so that the wide variety of patterns typical of real log profiles can be learned by the system. The new log facies scheme has the following components: filter, primitive shape classes, comparison routine with objective function, and neural network.

A filter is required to segregate sandstone, mudstone, and marker beds. The filter has the following attributes: value band, depth band, and depth range. The value band is the range of log values that determines whether the value at a given depth is assigned: a scaled sandstone S_x value, where the subscript ranges from 1 to 100; a zero value if it falls within the value band; or a negative value if it falls outside the value band but in the opposite direction of sandstone. The dimensions of the value band may be determined by the user or established by the computer system conducting a spectral evaluation of frequency distribution of log values. For those cases in which log values are excessively noisy, a mid-point moving average will be used over a specified depth band. The profile of log values that fall within the value band is customarily called the shale baseline. The shale baseline may drift over long log transects. A depth range is defined to control the depth over which a given value band and, where necessary, a depth band are valid.

The primitive shape classes are those simple log profile shapes reported earlier (e.g., blocky, funnel, etc.). For a given log segment with assigned values $S_{1\text{-}l00}$, the blocky primitive shape is compared with the log values. For those log values in which the comparison is deemed suitable, the log profile of that shape is assigned. The remaining portion of the log profile is segmented, and other primitive shapes are compared. The thickness of the primitive shapes are first anchored at the S_0 points above and below that given segment. The thickness of successive primitive shapes is determined by the fit of the previous primitive shapes. The result is a log profile that is described by a combination of primitive shape elements with different thicknesses. This approach tends to bias the result by selecting the log profile with $S_{maximum}$ as being a blocky element when most geologists might consider this element to be a part of a thicker bell or funnel shape. Therefore rules must be established to accurately identify certain combinations of elements as being thicker examples of simpler elements. The case of serrated vs. nonserrated log profiles is determined by the variability of log values about the primitive shape.

An objective function is required to determine the best fit of comparisons made between the log values and the primitive shape values. The objective function considers the sum of the differences between the values as a function of the primitive shape class and thickness. The best fit is determined by a minimum threshold in the objective function. When the objective function criteria are achieved, the primitive shape element is assigned to that particular log profile segment.

Annotated Bibliography

The first selection of publications for the annotated bibliography is complete. The 30 papers dealing with the

application of computer and quantitative methods to log facies recognition and correlation have been summarized in about 90-word statements written for non-geologists. This is a highly useful resource for the project as well as others outside the project. This task will continue as new literature is discovered.

Sandstone Geometry Database

The sandstone geometry database for meandering fluvial and fluvial-dominated deltaic systems is being compiled from the literature. The effort is to develop empirical relationships between thickness (available at well locations) and lateral extent along both depositional strike and dip directions. The relationships are extracted directly from the literature, or data are compiled from the literature. This effort is to be used in developing rules for establishing width dimensions for mapping of facies within a genetic interval.

Correlation Program

The structure of the correlation program is diagrammed in Fig. 2. As shown in the figure, the program consists of four main modules: marker bed module, log facies module, intermediate module, and main module.

Marker bed module. The resistivity log is the primary well log used for determining the marker beds. Each well log is identified for potential marker beds, and then the equivalent marker beds along every other well are determined. It is designed so that a pair of marker beds encompass a region of interest. If the bottom marker bed is absent, then only the top marker bed can be given, and the bottom marker bed is assigned a null value. The correlation program is designed to use this form of incomplete information. The output from the marker bed module is a linked list (see Fig. 3). Each node in the list contains information about individual wells: the well name, top marker depth, and bottom marker depth.

Log facies module. The input to the log facies module is a set of well logs. For each well log, the facies occurrences are identified and their shape is determined. The output of the module is a linked list (see Fig. 4). Each node in the linked list contains the name of the well, a pointer to the list of facies occurrences, and a pointer to the next node of the list. Each node in the list of facies occurrences contains the top and bottom depths of the facies occurrence, the shape of the facies occurrence, and the pointer to the next node.

Intermediate module. The role of the intermediate module is to execute both the marker bed and the log facies modules to create the individual data files for every well. The output from the marker bed and the log facies modules will be linked lists containing individual well information. The intermediate module will take each well one at a time from the two lists and associate each subunit with the corresponding stratigraphic interval. Finally, for each well, a data file is created in the format needed by the main module. The pseudocode for the intermediate module is

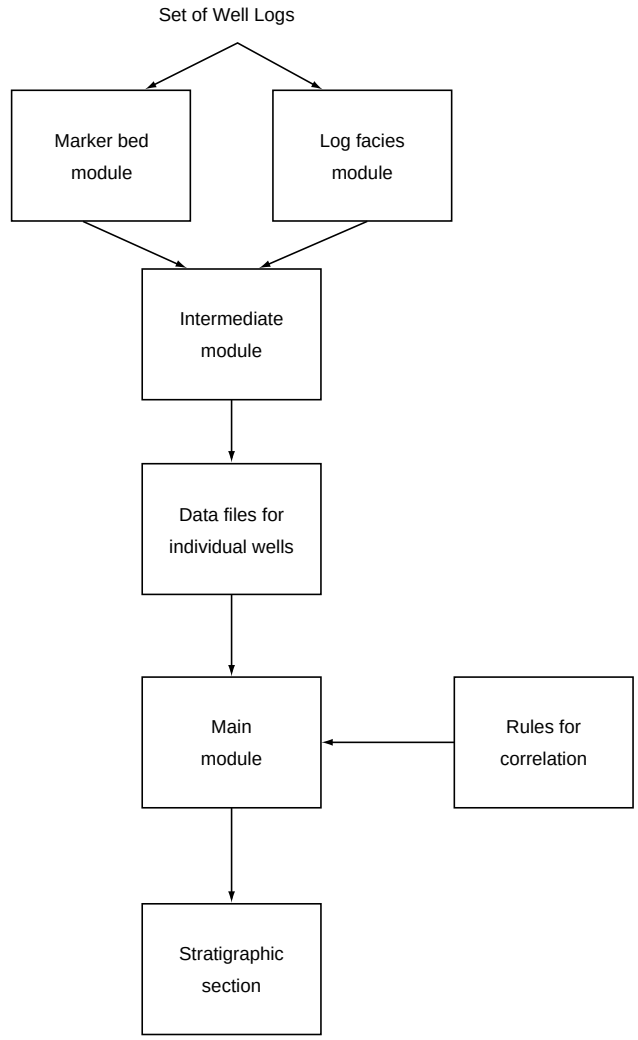

Fig. 2 Structure of correlation program.

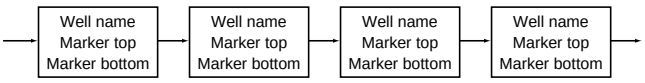

Fig. 3 Marker bed linked list.

```
Do until end of the lists
{
   Create a data file.
   Take two objects, one from each list.
   Write to the file the name of well and well id.
   Write to the file the stratigraphic unit id and the top and
     bottom marker depth.
   For each subunit from the list (obtained from log facies
     program), assign subunit id and write to the file the id,
     top depth, bottom depth and facies shape.
}
```

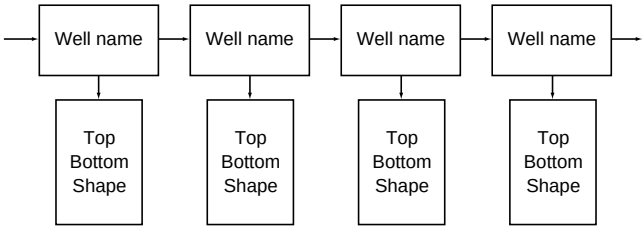

Fig. 4 Log facies linked list.

The form of the data file for each well as output by the intermediate module is shown in Table 1.

The well name, top depth, bottom depth, and the facies information come from the log facies module. The intermediate module will assign the id numbers to the subunits and the stratigraphic units. The top marker depth and the bottom marker depth of each well will come from the marker bed module. The KB and GL elevation will be derived from the log heading of each well. Each of the preceding individual files are read by the main module and the list of well objects is created.

TABLE 1

Data File

Well name	Glen68	character string
Well id	1	integer
Well location(x)	1500 ft	integer
Well location(y)	1600 ft	integer
KB elevation	300 ft	integer
GL elevation	150 ft	integer
Well log depth	7000 ft	integer
Number of stratigraphic units	1	integer
Stratigraphic unit id	1	integer
Number of subunits	2	integer
Top marker depth	1000 ft	integer
Bottom marker depth	2500 ft	integer
Subunit id	1	integer
Top depth	1200 ft	integer
Bottom depth	1400 ft	integer
Facies	?	character string
Subunit id	2	integer
Top depth	1600 ft	integer
Bottom depth	1850 ft	integer
Facies	?	character string

Main module. The input to the main module is the data files for individual wells. This module creates objects consisting of the information from the individual wells and then makes a linked list of these objects. This list is passed as a parameter to the correlation function, which, in turn, creates a list of correlated objects. This list is then passed as a parameter to the display routine, which displays the stratigraphic section of the wells under consideration. The correlated object is a pair of stratigraphic subunits belonging to two wells. The elements of this object are shown in Table 2.

TABLE 2

Correlated Object

Well1 id	integer
Well1 name	character string
Well1 x-co.	integer
Well1 y-co.	integer
Well1 depth	integer
Well2 id	integer
Well2 name	character string
Well2 x-co.	integer
Well2 y-co.	integer
Well2 depth	integer
Stratigraphic unit1 id	integer
Stratigraphic unit2 id	integer
Subunit1 id	integer
Subunit2 id	integer
Top1 depth	integer
Bottom1 depth	integer
Top2 depth	integer
Bottom2 depth	integer
Flag	integer

The integer tags 1 and 2 refer to the two wells under consideration. The display routine takes each correlated object in turn and connects the subunits across the xy plane. Different strata are marked with the top and bottom depths. Furthermore, the strata are colored differently for differentiation purposes. These programs are written using Microsoft Visual C++. The foundation classes are used to support the various objects. Every object that is built is derived from the foundation class object, C-object. Each linked list that is built for a distinct class of objects is derived from the C-oblist of the foundation class.

Well-Test Interpretation

This part of the project uses an ES approach to develop a well test interpretation system that uses data from transient well testing to obtain information about reservoir parameters, such as permeability, reservoir pressure, wellbore conditions, reservoir discontinuity, and other information essential for reservoir studies. On the basis of the information available, the system first identifies the well model. In the interpretation of well tests, especially model identification, two parallel and equally important sources of diagnosis, the pressure transient testing itself and the knowledge of the relevant geological and other engineering information on the well being tested, are widely used by engineers. The former is based on significant shapes displayed on the test signal, which may correspond to features of the tested reservoir. The latter is used to predict the reservoir behavior on the basis of all the available external geological and engineering data. They are complementary to each other. Previous work on the application of AI techniques to this domain has mainly attempted to automate the former diagnostic. The latter case is an expertise that is widely used in practice. The system implemented makes use of data from both the areas to identify the model correctly. The use of data

from both of these areas also helps in the verification of the result, whereby the results of interpretation are checked with the known external data.

Once a model is identified, first estimates of various parameters are required. Initial parameter estimates can be obtained by using the parameter estimation algorithm added to the system. The identified model and the estimated parameters provide a starting point for an automated-type curve-matching analysis.

Previous Work

The model identification part of the system was implemented previously. The system uses the pressure derivative plot to classify wells. The input data are plotted and analyzed to identify the various characteristic segments in the plot. These segments are identified and compared with the existing database of models to pick the correct model. More than one model may fit the description. A symbolic representation approach that creates a simplified representation of the derivative data in terms of predefined symbols is used for model identification. These symbols are then used by the model matching algorithm to match it with the previously stored model information. The matching algorithm can eliminate minor disturbances in the input data.

The system was extended to handle external geological data. Geological data, such as geometry, penetration, porosity, and conductivity, have been used. All the known data can be entered with the use of the user interface. The system allows certain parameters to be left unspecified if they are unknown. With the available information, the system narrows down the list of possible models. A number of rules have been developed to aid this process. The system uses a forward chaining inference mechanism to arrive at the results. This is the first step in the model identification process to be followed by the plot analysis. These procedures together help narrow down the choice as much as possible and pick the model. For inconsistency in the results obtained with the preceding procedures, a message is given to the user to help in the verification of the result.

Further Development/Extensions

For a full automation of the interpretation procedure once a model is proposed, it is necessary to find first estimates for its parameters. Though they are not intended to be the final result of the interpretation, these estimates constitute the starting point for an automated-type curve-matching analysis. The system was thus extended to include a very powerful parameter estimation algorithm. The block diagram in Fig. 5 shows the parameter estimation module in relation to the other modules in the system.

Parameter Estimation

As a step toward complete automation of the well test interpretation system, parameter estimation modules have been added to the system. These modules are used to obtain

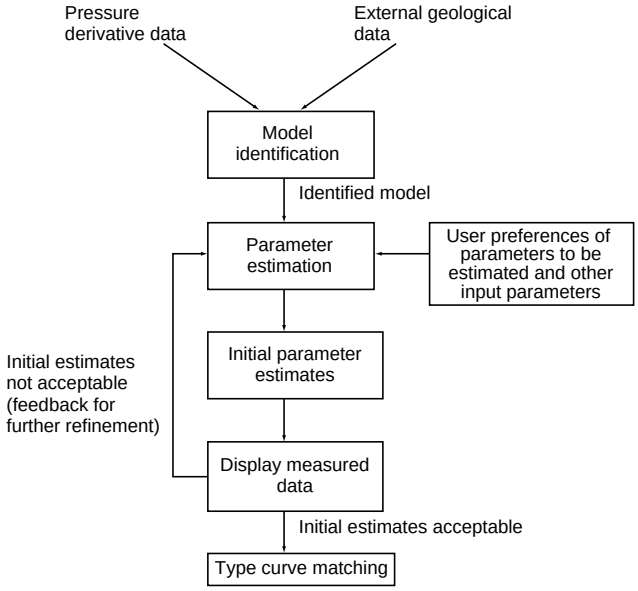

Fig. 5 Parameter estimation module in perspective.

the initial estimates for the well parameters. Parameter estimation is carried out after a model has been selected. Presently, the system carries out the estimation process only after a single model is identified. For multiple models, the user must narrow down the choice to only one model and then select the parameters to be estimated. An interface is provided for this purpose. On the basis of the model identified and the parameters specified, the system builds up an input to the estimation program. The estimation module (presently in FORTRAN) is then executed. The output from this module is obtained in an output file, which gives the values of the required parameters.

The parameter estimation module also produces the calculated pressure and derivative values on the basis of the model and the parameter values. These data are displayed to the user to help in judging the correctness and accuracy of the estimated values. The user may decide to accept these values or may run the estimation procedure again. Refining the estimated values may require changing certain parameters used by the estimation program.

Example

The system has been tested successfully with the available models. The model used here is the finite wellbore radius well. The parameter estimation step is preceded by model identification. Figure 6 shows the model selected by the program. Before parameter estimation, the program determines if the required parameters have been specified. Figure 7 shows the data entry screen for the parameters to be estimated. The user can also specify the objective function to be optimized. The default is regression on pressure derivatives. The user can also specify the minimum and the maximum values of the selected parameters. Work is being done to allow the user to set other variables required by the estimation module, which will give

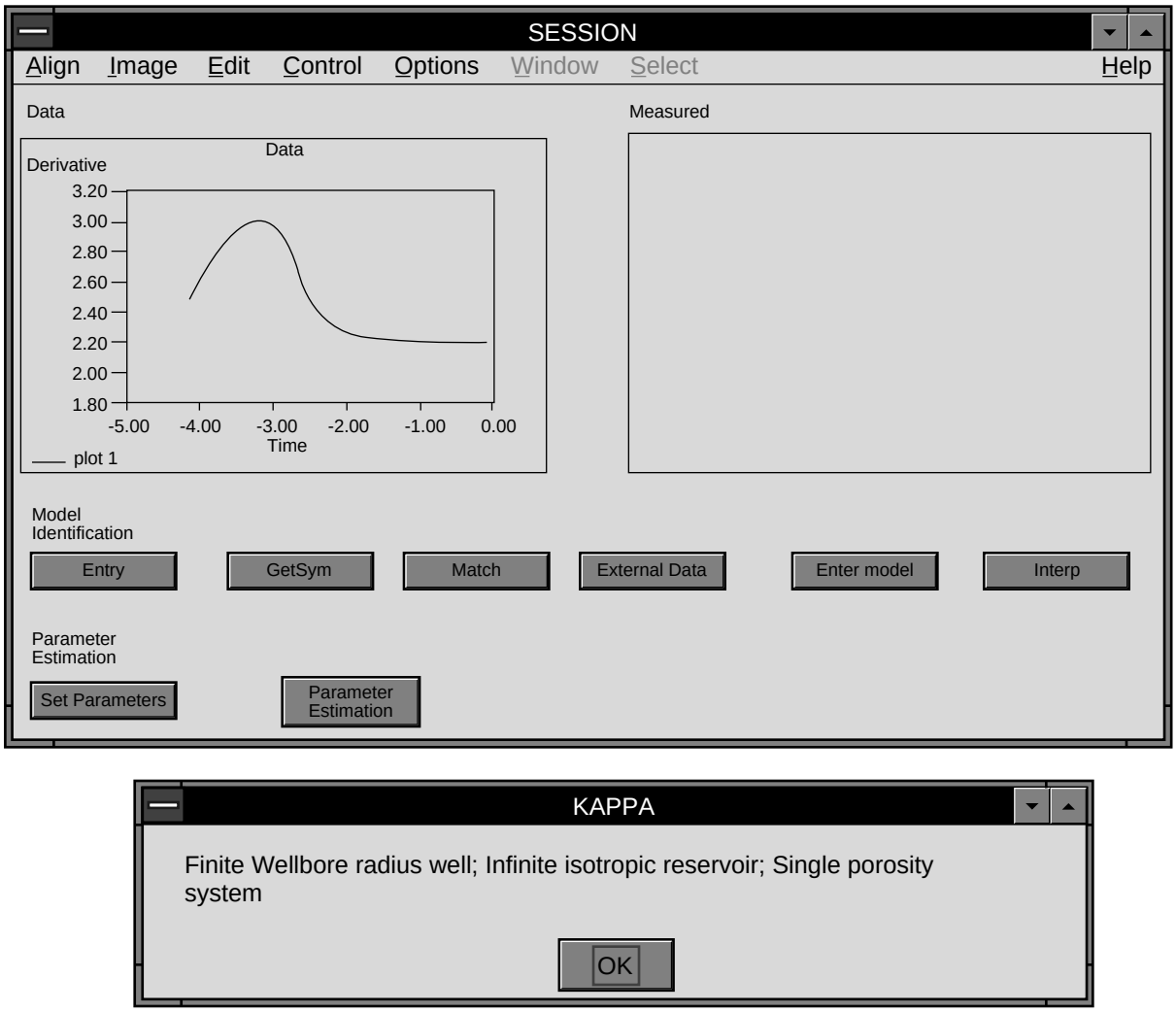

Fig. 6 Model of finite wellbore radius well.

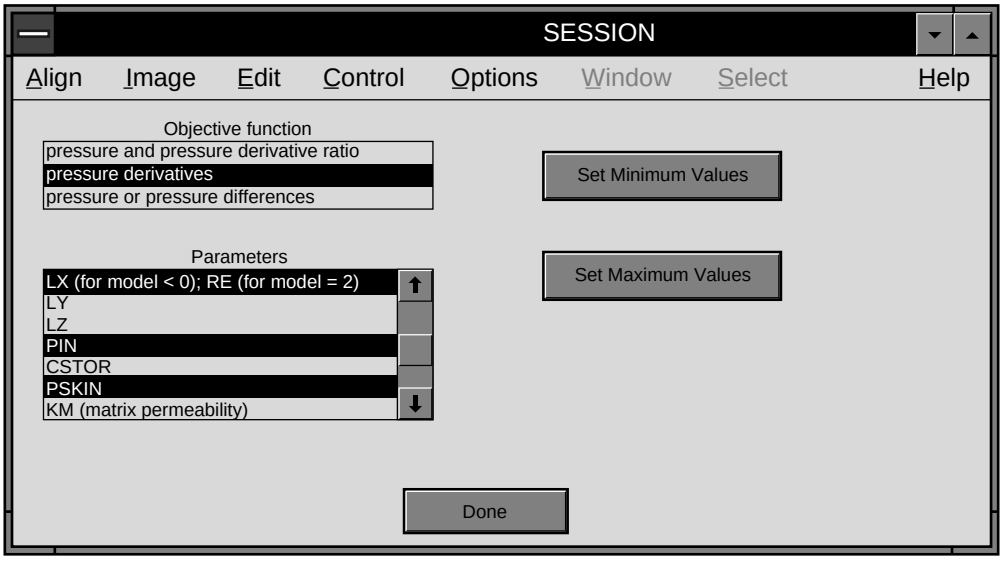

Fig. 7 Data entry screen for parameters to be estimated.

better control of the procedure. Once the parameters have been set, the parameter estimation module is executed. The output from this module is plotted in the measured data window (Fig. 8). This allows the user to compare the result with the input data to check for the accuracy of the estimated parameters. In this case the calculated values match the input data. The initial estimates for the required parameters are written into a data file.

Some reservoir parameters can be specified independently by some external means, which would reduce the number of unknown parameters. The parameter estimation algorithm works better if the number of parameters required to be estimated is small. Apart from type curve matching, the estimated parameters may be used to aid other parts of this project. This information could be used by other groups for checking consistency with the geological information for large-scale reservoir architecture.

Conclusions

The present system contains all the information and modules needed for a completely automated well test interpretation system. Automated module identification has been achieved with pressure derivative data and external geological data. Parameter estimation is carried out to get the first estimates required for type curve matching. With the use of AI techniques, different parts of the system were automated. Though all major sections of the system have been coded, further work and testing are required to make it more robust and accurate.

Changing Development Environments

The KAPPA-PC knowledge base is being used for the implementation of these projects. To be more specific, some of these projects include log facies identification, well-to-well stratigraphic correlation, and marker bed identification. Whereas a rule-based reasoner is available with the inference engine embedded in KAPPA-PC, several limitations have been encountered (for example, programming in the KAPPA language is quite cumbersome). Whereas the KAPPA language is based on C, the syntax is significantly different and limiting (for example, the KAPPA language limits the size of a function to 1400 characters). In addition, the KAPPA language is not so powerful as C or C++. Whereas it is possible to write functions in the C or the C++ language and link them to KAPPA-PC, this process is time consuming. For these reasons, the conclusion has been reached that, by building an inference engine in C++ and porting the code to the C++ language, all additional requirements and extensions made to these projects will be easily implemented. With the access of a more-sophisticated programming language, the new approach and its additional flexibility and power will provide for more efficient and sound results.

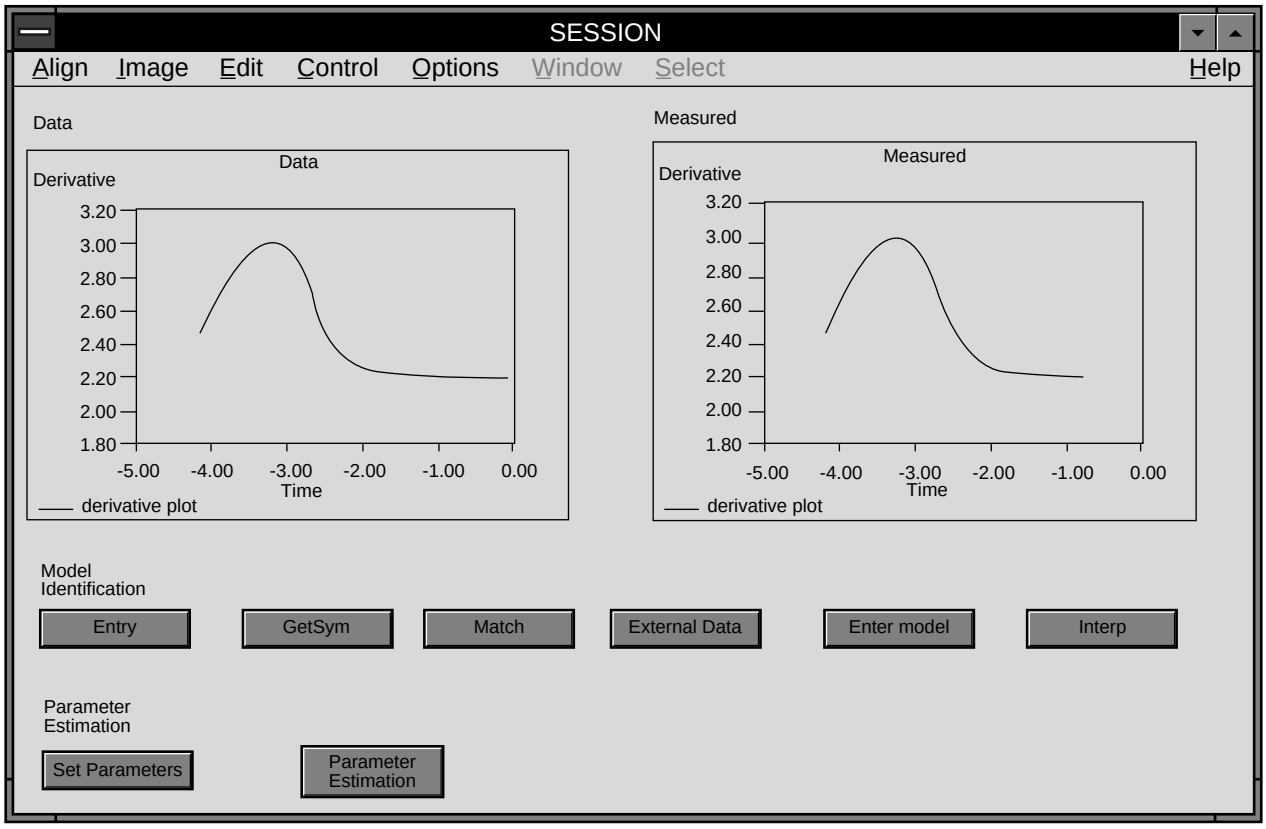

Fig. 8 Measured data window.

Building an Inference Engine

An inference engine is among one of the several components of an ES. It empowers the ES with a reasoning mechanism and search control to solve problems. The most common reasoning method for problem solving in ES is the application of simple logic rules or rule-based reasoning.

Rules have a standard IF–THEN form. The following is an example of a rule:

Given: IF A, THEN B and
IF B, THEN C.

Conclusion: IF A, THEN C.

The IF part contains a set of premises, and the THEN part gives a set of conclusions. The inference engine manipulates the rules through managing the chaining of rules by linking the premises of one rule with the conclusions of another. This reasoning process examines the rules, facts, and relations in the knowledge base during the evaluation. Search control methods are used to minimize the reasoning time.

The goal of this project is to build a special inference engine in C++ in addition to porting code from the KAPPA-PC language to C++. There are numerous advantages to the conversion from KAPPA-PC in building and customizing the ES. The underlying advantage is one of efficiency.

Designing the Inference Engine

The main elements of an inference engine consist of forward chaining, backward chaining, justification, and search strategy. An inference engine can be complicated or simple, depending on the complexity of the rules. With simple rules, forward chaining will suffice. With complicated rules and unstructured logic, backward chaining is more appropriate. The design of this inference engine will be composed of both forms of reasoning mechanisms in addition to the remaining elements mentioned.

Forward chaining steps through the rule list until it finds a rule in which premises match the factor or situation. The rule will then be used or fired to assert a new fact. Once the rule has been used, it will not be used again in the same search; however, the fact concluded as the result of that rule's firing will be added to the knowledge base. The details of the forward-chaining procedure are

1. A fact is asserted.
2. The fact matches the premises of a rule.
3. The system computes the substitution that unifies the fact and the premise.
4. The substitution is applied to the conclusion of the rule.
5. This result is asserted and is available for further forward chaining.
6. Steps 1 through 5 are repeated.

This cycle of finding a matched rule, firing it, and adding the conclusion to the knowledge base is repeated until no more matched rules can be found.

Backward chaining is used when the user makes a query as to whether a certain fact is true and when there is a rule that can determine the query from known information in the knowledge base or from answers given by the user. Backward chaining attempts to prove the hypothesis from facts. Because the current goal is to determine the fact in the conclusion, it is necessary to determine whether the premises match the situation. The details of the backward-chaining procedure are

1. A request is made to achieve a fact (the goal).
2. The goal does not match any known fact.
3. The goal matches the conclusion of a rule.
4. The system computes the substitution that unifies the goal with the conclusion.
5. The substitution is applied to the premise of the rule.
6. The result becomes a new goal of the system.
7. The new goal can do the following:
   - Match a fact in the knowledge base.
   - Match a conclusion of a rule, leading to further backward chaining.
   - Ask the user for the needed information.
   - Fail, in which case the original goal fails.
8. Steps 1 through 7 are repeated.

Justification, the third component of the inference engine, provides the user with a tracing facility. It indicates the history of goal substitution with regard to the last conclusion. Justification gives the name of the rule and the fact used as well as the fact in the rule that has been used.

The final component of the inference engine is the search strategy. Three strategies are available. Depth-first search, breadth-first search, and best-first search. Each uses a slightly different approach to search for a target solution. In a depth-first search, the search moves from top to bottom. In a breadth-first search, movement is performed level by level, and the process examines the nodes on the same level one by one. A best-first search approximates the distance of the target node from the current node and selects the shortest path leading to the target node.

Implementation of the Inference Engine

Implementation of the inference engine involves the development of forward chaining, backward chaining, and justification algorithms as well as the selection and implementation of an appropriate search strategy. In addition, rule structures need to be implemented. With most of the code available for use in book form,[7] the applicable code will be imported through a scanner to Visual C++, a product developed by Microsoft. Once scanned, the code will be debugged and extended. As a result of the availability of the code, a major portion of the process of building the inference engine is simplified. Additional work involves the selection and implemention of a search control strategy, implemention of a justification algorithm, and addressing the issue of prioritizing rules.

References

1. G. J. Moridis, D. A. McVay, D. L. Reddell, and T. A. Blasingame, *The Laplace Transform Finite Difference (LTFD) Numerical Method for Simulation of Compressible Fluid Flow in Reservoirs*, paper SPE 22888 presented at the Society of Petroleum Engineers Annual Technical Conference and Exhibition, Dallas, Tex. October 5–8, 1991.
2. R. de S. Carvalho, *Nonlinear Regression: Application to Well Test Analysis*, Ph.D. dissertation, The University of Tulsa, Tulsa, Okla., 1993.
3. *ECLIPSE 100—Black Oil Simulator*, ECL-Bergeson Petroleum Technologies, Inc., Oxfordshire, England, 1990.
4. A. P. Yang, *Turning Bands Method to Generate 2-D Random Field with Autocorrelation*, University of Texas at Austin, Austin, Tex., April 1987.
5. C. V. Deutsch and A. G. Journel, *GSLIB Geostatistical Software Library and User's Guide*, Oxford University Press Inc., New York, 1992.
6. G. Perez, *Stochastic Conditional Simulation for Description of Reservoir Properties*, Ph.D. dissertation, The University of Tulsa, Tulsa, Okla., 1991.
7. D. Hu, *C/C++ For Expert Systems*, Management Information Source, Inc., 1989.

ANISOTROPY AND SPATIAL VARIATION OF RELATIVE PERMEABILITY AND LITHOLOGIC CHARACTERIZATION OF TENSLEEP SANDSTONE RESERVOIRS IN THE BIGHORN AND WIND RIVER BASINS, WYOMING

Contract No. DE-AC22-93BC14897

University of Wyoming
Laramie, Wyo.

Contract Date: Sept. 15, 1993
Anticipated Completion: Sept. 14, 1996
Government Award: $251,061

Principal Investigator:
Thomas L. Dunn

Project Manager:
Robert Lemmon
Bartlesville Project Office

Reporting Period: Oct. 1–Dec. 31, 1994

Objectives

The objectives of this multidisciplinary study are designed to provide improvements in advanced reservoir characterization techniques. The objectives are to be accomplished through (1) an examination of the spatial variation and anisotropy of relative permeability in the Tensleep sandstone reservoirs of Wyoming; (2) the placement of that variation and anisotropy into paleogeographic, depositional, and diagenetic frameworks; (3) the development of pore-system imagery techniques for the calculation of relative permeability; and (4) reservoir simulations testing the impact of relative-permeability anisotropy and spatial variation on Tensleep sandstone reservoir enhanced oil recovery (EOR).

Concurrent efforts are aimed at understanding the spatial and dynamic alterations in sandstone reservoirs that are caused by rock–fluid interaction during carbon dioxide (CO_2) EOR processes. The work focuses on quantifying the interrelationship of fluid–rock interaction with lithologic characterization in terms of changes in relative permeability, wettability, and pore structure and with fluid characterization in terms of changes in chemical composition and fluid properties. This work will establish new criteria for the susceptibility of Tensleep sandstone reservoirs to formation alteration that results in change in relative permeability and in wellbore-scale damage. This task will be accomplished by flow experiments with the use of core material, examination of regional trends in water chemistry, examination of local water chemistry trends at field scale, and chemical modeling of both the reservoir and experimental systems to scale up the experiments to field scales.

Summary of Technical Progress

The extensive well-log and core analysis database constructed during the first contract year was used to complete the first regional sedimentologic subdivisions of the Upper Tensleep. The initial analysis of the key flow unit and boundary dimensions is also complete. The relative-permeability measurements are on schedule. Anisotropy effects were observed in most sample sets, and some anisotropy calculations were made.

Preparations were made for the reservoir simulation studies and the image analysis. Six Tensleep water samples were collected from the Teapot Dome oil field (NPR-3). These are type B waters (chloride > 10% mol fraction anions).

The second coreflood experiment is proceeding. Also, the water database has been expanded to include waters from adjacent formations to further document lateral and vertical trends in chemical variation.

Regional Frameworks

Work this quarter was concentrated on the subsurface analysis of the Tensleep sandstone as well as on quantifying the dimensions of key flow units. With the use of the extensive well-log database and the Oil and Gas Consultants International Inc. (OGCI) well-log analysis program Production Analyst©, the well-log traces of the Upper Tensleep sandstone were subdivided into a series of sandstone–dolomite packages. These packages represent sea-level controlled, eolian–marine cycles. A few of these cycles can be recognized on a regional scale and have been correlated around the entire Bighorn Basin. Core analysis and description have been

pursued in order to verify well-log interpretations of particular lithofacies. Approximately 25 additional cores have been located for further study, and as many as feasible will be examined and correlated with well logs and added to the regional subsurface analysis.

During the summer of 1994, a series of photomosaics was made of key outcrops along the eastern margin of the Bighorn Basin. Line drawings of the photomosaics have now been made to further delineate and document the systematic hierarchy of bounding surfaces that act as barriers to fluid migration within the Upper Tensleep sandstone. The photomosaics have also been used to calculate the dimensions of particular flow units as exposed in outcrop.

Relative-Permeability Measurements

Relative-permeability laboratory studies are proceeding on schedule. Testing with additional samples is complete. Anisotropy effects identified earlier appear to be confirmed with each additional set of sandstone core plugs. In general, the relative-permeability curves in which flooding is parallel to bedding are much steeper than those in which flooding is perpendicular to bedding. A few exceptions have been found, but the accuracy of these exceptions is being studied carefully. One new consideration that must be evaluated for all samples is the channeling that occurs in some of the sandstones. Occasionally the sandstone cores might contain a very high permeability streak that causes a channel of water to form and subsequently causes nonuniform displacement of oil. This is undesirable because in the theory of deriving relative permeability from displacement data, uniform flooding across the core diameter is assumed. Once a channel forms, the water floods through the channel and no further displacement of oil can occur. The result is a very steep relative-permeability curve. Such problems appear in only a few of the samples. A sufficient number of core samples was obtained that had good displacement results.

Reservoir simulation studies began this quarter with the evaluation of available software at the University of Wyoming. A simple one-dimensional Buckley–Leverett program that will allow a comparison of flooding parallel to bedding vs. flooding perpendicular to bedding is available; however, this approach does not account for crossflow between layers. The use of a black-oil simulator is being considered as an alternative. A copy of a black-oil simulator has been obtained, and work with the simulators will begin during next quarter.

The first set of samples for image analysis work has been selected and submitted for preparation. Calculation of the relative permeability and absolute permeability anisotropy ellipses was delayed.

CO_2 Flood—Formation Alteration and Wellbore Damage

Six water samples from the Tensleep formation and one sample from the Madison formation were collected at the Teapot Dome oil field (NPR-3). This field was chosen because its primary (i.e., original formation water) production is from the Tensleep and Madison formations. Chemical analyses of these samples showed that the waters are rich in both sulfate and chloride and can be classified as type B in terms of the definition for Tensleep formation water chemistry. Chemical modeling for these waters is progressing.

Researchers have compiled 54 and 60 additional water analyses for the Madison and Phosphoria formations, respectively, in the Bighorn Basin from both the Wyoming State Geological Survey and publications. Water chemistries of these two formations were compared with those of the Tensleep formation and were found to be similar, which suggests communication of these formation waters.

The core samples used in the first CO_2 coreflooding experiments have been prepared for analysis. Thin sections of cores (both before and after the experimental run) were completed for microscopic observation. Because the billets for thin sections were taken from the top, middle, and bottom portions of the composite core assemblage, the morphology change of cement minerals along the direction of the solution flow can be observed. The morphology and chemical composition of the cement minerals will be analyzed with scanning electron microscopy (SEM).

The second coreflooding experiment (scheduled for January 1995) will be run under conditions similar to those of the first run but without cores so that chemical contamination from the apparatus can be checked during the run [in particular iron (Fe), because most of the wetted parts of the apparatus are made of stainless steel]. The results of this run will allow exact determination of the elemental flux between cores and solution of the first run.

Project Management and Technology Transfer

Extensive poster and graphics preparation for two papers accepted for presentation at the American Association of Petroleum Geologists Annual Meeting in 1995 was completed this quarter.

GYPSY FIELD PROJECT IN RESERVOIR CHARACTERIZATION

Contract No. DE-FG22-94BC14970

University of Oklahoma
Norman, Okla.

Contract Date: May 19, 1994
Anticipated Completion: May 18, 1995
Government Award: $348,000
(Current year)

Principal Investigator:
Daniel J. O'Meara, Jr.

Project Manager:
Robert E. Lemmon
Bartlesville Project Office

Reporting Period: Oct. 1–Dec. 31, 1994

Objectives

The overall objective of this project is to use the extensive Gypsy field laboratory and data set as a focus for developing and testing reservoir characterization methods that are targeted at improved recovery of conventional oil. The Gypsy field laboratory[1] consists of coupled outcrop and surface sites that have been characterized to a degree of detail not possible in a production operation. Data from these sites entail geological descriptions, core measurements, well logs, vertical seismic surveys, a three-dimensional (3-D) seismic survey, cross-well seismic surveys, and pressure-transient well tests.

The project consists of four interdisciplinary sub-projects: (1) modeling depositional environments, (2) integrated 3-D seismic interpretation, (3) sweep efficiency, and (4) tracer testing.

The first of these aims at improving the ability to model complex depositional environments that trap movable oil. The second is a development geophysics project that proposes to improve the quality of reservoir geological models through better use of 3-D seismic data. The third investigates the usefulness of a new numerical technique for identifying unswept oil through rapid calculation of sweep efficiency in large reservoir models. The fourth explores what can be learned from tracer tests in complex depositional environments, particularly those which are fluvial dominated.

Summary of Technical Progress

During the initial assessment of the data taken at the Gypsy site, several apparent discrepancies in the velocity measurements were observed. Four vertical seismic profiles (VSPs) are available at three of the wells. The travel times determined from the VSP data to the top of the Gypsy interval in each of the wells were in disagreement by as much as 50 ms (Fig. 1). After a review of the sonic logs (Fig. 2) and the VSP data (which were in agreement below 122 m, which was the starting depth for the surveys), near-surface velocity variations were identified as the cause of the large differences. Unfortunately, not all the wells were logged to the surface, and the seismic data were muted so that only a hint of the feature suspected to be responsible for the velocity anomaly could be identified (Fig. 3). A schematic illustration of the feature is shown in Fig. 4.

In addition to the VSP velocity problems, the sonic logs indicated that the velocity of the Gypsy sandstone interval was faster than the surrounding strata, whereas the cross-well seismic measurements indicated that the Gypsy sandstone was much slower than the surrounding strata (Fig. 5). The average velocities from the VSP measurements indicated still another picture of the velocities. The sonic, cross-well, and VSP differences have been explained in

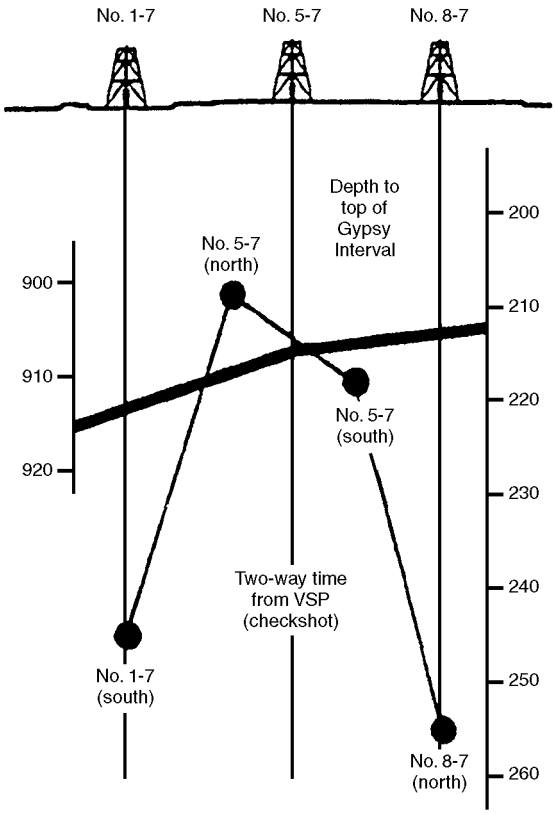

Fig. 1 Schematic illustration of the two-way times (dark circles) to the top of the Gypsy interval as determined from the four vertical seismic profiles (VSPs) at the Gypsy test site. The depth to the top of the Gypsy interval is indicated with a solid line. The sources were approximately 60 m from the surface positions of the wells in the directions indicated. Two surveys were shot in the 5-7 well. All the surveys gave distinct results for the two-way travel time to the top of the Gypsy interval.

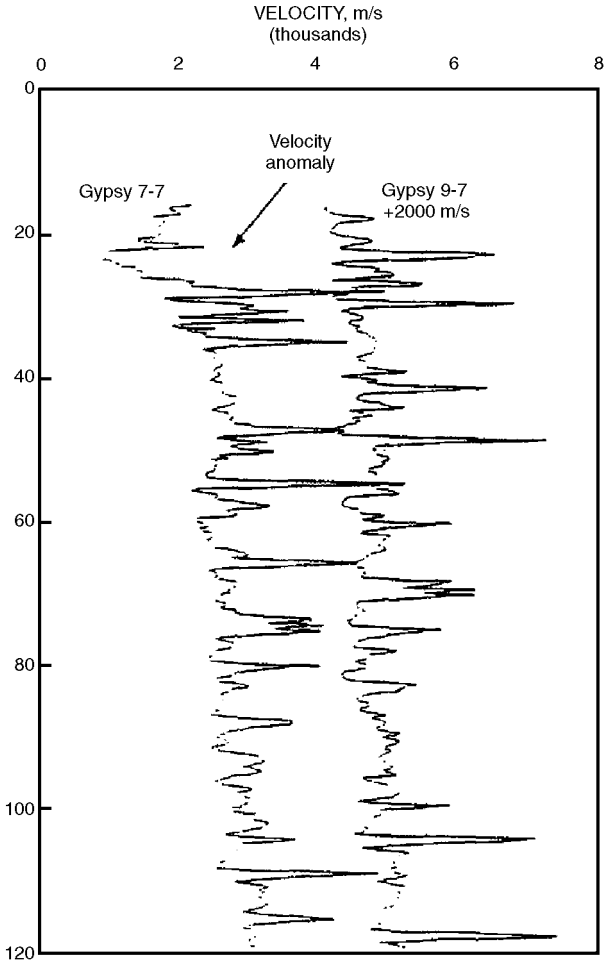

Fig. 2 Comparison of two of the sonic logs at the Gypsy test site that are recorded almost to the surface. As indicated in the figure, a potential near-surface velocity anomaly and some structural changes in the near surface are probably related to near-surface-velocity changes that are responsible for the large differences between the VSPs.

terms of frequency scaling effects caused by attenuation and elastic scattering in layered media.

Figure 6 illustrates why thinly layered media are suspected of having caused the frequency dependence of the measured velocities in the strata surrounding the Gypsy sandstone interval (for example, the marine section above the Gypsy interval consists of layered shales and dolomites). At very high frequencies (e.g., the 10,000-Hz measurements of the sonic logs), the wavelengths are comparable to or shorter than the thickness of the layers. At these frequencies, interval velocities determined by integrating the sonic travel times can be treated as a ray theoretical estimate of the velocity. For lower frequencies, such as the 1000 Hz used for the cross-well measurements, the waves will appear to travel at a slightly slower velocity than that described by ray theory. The reason for the apparent slowing is that scattered energy mixes with the leading wave form. The interference between the direct wave and the scattered signals causes most of the energy to arrive at a later time and thus results in a slower velocity. At the intermediate range of frequencies (1000

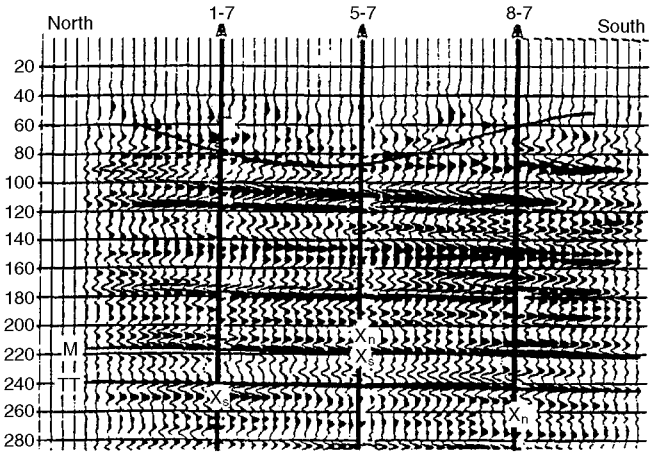

Fig. 3 Three-dimensional seismic traverse through the three wells at the Gypsy test site in which vertical seismic profiles (VSPs) were collected. The "X"s indicate the times to the top of the Gypsy interval for each of the wells. The subscripts "n" and "s" indicate that the source position for the VSP was either north or south of the surface position for the well—a distance of approximately 60 m. The "M" and "TT" represent reflections that approximately mark the top and bottom of the Gypsy sandstone interval. The line at the top indicates the position of a near-surface feature, which appears to be related to the apparent disagreements between the VSPs.

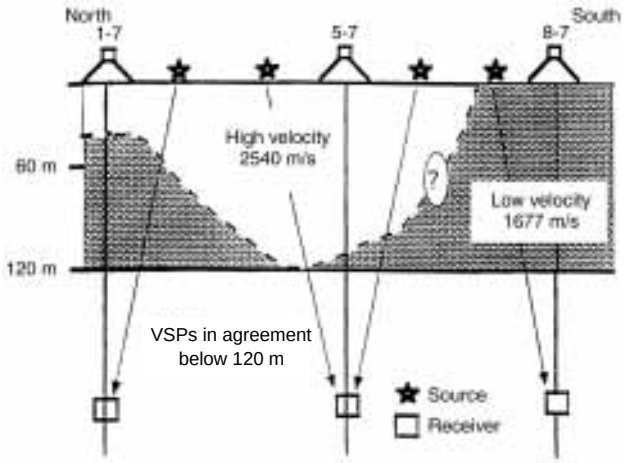

Fig. 4 Illustration of the approximate region of a near-surface velocity anomaly that can be used to reconcile the large differences between the vertical seismic profiles (VSPs) at the Gypsy test site. The dashed line that does not indicate a geological boundary represents the approximate region in which the anomaly is located. The velocities specify the average interval velocities necessary to reconcile the VSP measurements to their starting depth of recording at 122 m.

Hz for the marine section) (i.e., when the wavelengths and bed thicknesses are comparable in size), measurements are frequency dependent. Finally, at very low frequencies (e.g., 30 Hz as assumed for the VSP), the wavelengths are much longer than the layer thicknesses. The velocity reaches its slowest value and becomes independent of frequency at this point.

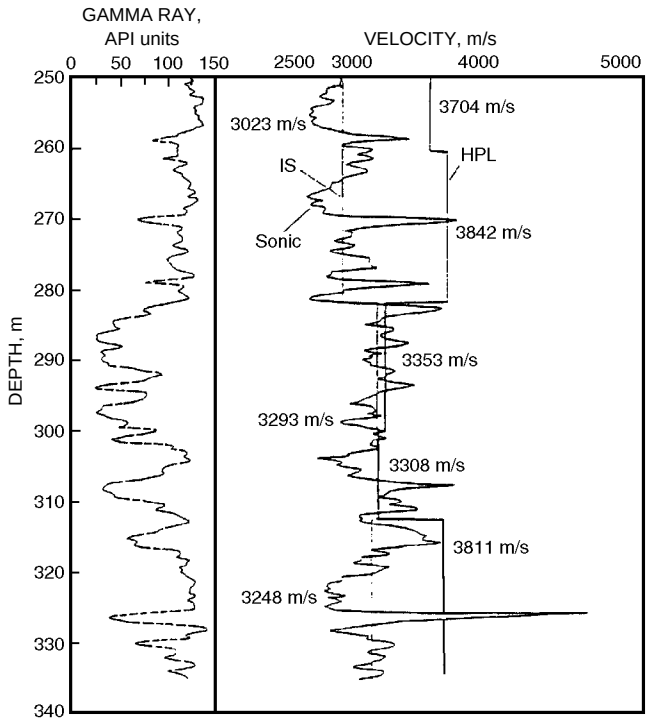

Fig. 5 Gamma ray and velocities from the sonic in the 5-7 well as well as the HPL, a cross-well measurement between the 5-7 and 7-7 wells for the zone including the Gypsy sandstone interval. The velocity values determined from the HPL are plotted on the right side of the plot. The straight lines are used to represent the velocities determined by dividing the distance between wells by the first arrival times. In addition, the velocities obtained by integrating the sonic travel times through selected intervals are drawn through the sonic curves. At face value, the sonic and HPL velocities give contradictory indications of the velocity and impedance profile through the Gypsy sandstone interval.

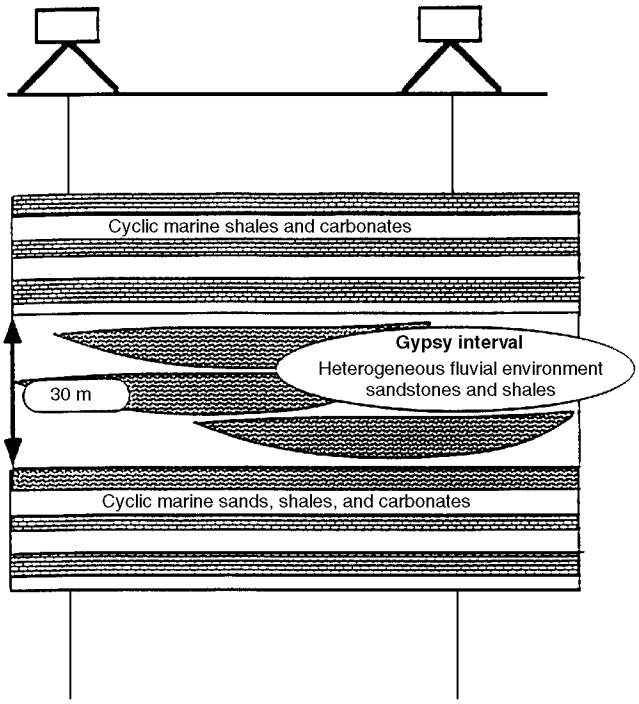

Fig. 6 Schematic of the types of depositional environments, including the Gypsy interval, for the section of the 5-7 well shown in Fig. 5. The strata above and below the Gypsy are cyclic marine sequences, whereas the Gypsy interval is a heterogeneous fluvial environment. The upper marine sequence consists of shales and dolomitic streaks, whereas the lower marine sequence contains sands, shales, and dolomitic streaks.

Backus[2] developed a method of averaging elastic properties for layered media to predict the velocities of a layered medium when the wavelengths are much longer than the thickness of the beds. Following Marion et al.,[3] this velocity will be referred to as the effective medium theoretical velocity (V_{EMT}) and the high-frequency velocity measurements (sonic in this case) as the ray theoretical velocity (V_{RT}). Frequency-dependent velocities between these end limits are defined here as V_{WT}, the wave theoretical velocity.

The integrated sonics have been used to estimate the value of V_{RT} for the upper marine interval. Estimates of the components of the layering in the upper marine section were also made from the sonic and other data so that an estimate of V_{EMT} could be made with software written to use the Backus results. The high-frequency V_{RT} (SONIC) and low-frequency V_{EMT} (VSP) velocity estimates were used to estimate the limits of the effects caused by elastic scattering. With the use of the equations by De et al.,[4] the differences between the effects predicted from scattering and the actual measurements were attributed to attenuation and were modeled. An approximate scaling relation of the type suggested by Marion et al.[3] was used to estimate velocity measurements at 1000 Hz [i.e., wave theoretical velocity (VMT)].

These ideas were used in an interpretation of the frequency-dependent velocity measurements that appeared to be contradictory. The interpretation in terms of elastic-scatttering effects and attenuation is shown in Figs. 7 (vertical propagation) and 8 (horizontal propagation). This new understanding of the velocity measurements at Gypsy represents a critical step in the efforts to match the seismic response at the well control.

The first phase of the project is devoted to the development of one-dimensional (1-D) seismograms at each well to tie the well and seismic data. For this task, the discrepancies in the velocity measurements at different frequencies had to be reconciled. The next step will be to incorporate what has been learned from the well control at the Gypsy test site into the construction of 1-D synthetic seismograms for the wells. This is a critical step toward the two-dimensional (2-D) inversion of selected traverses through the 3-D seismic volume and mapping tasks.

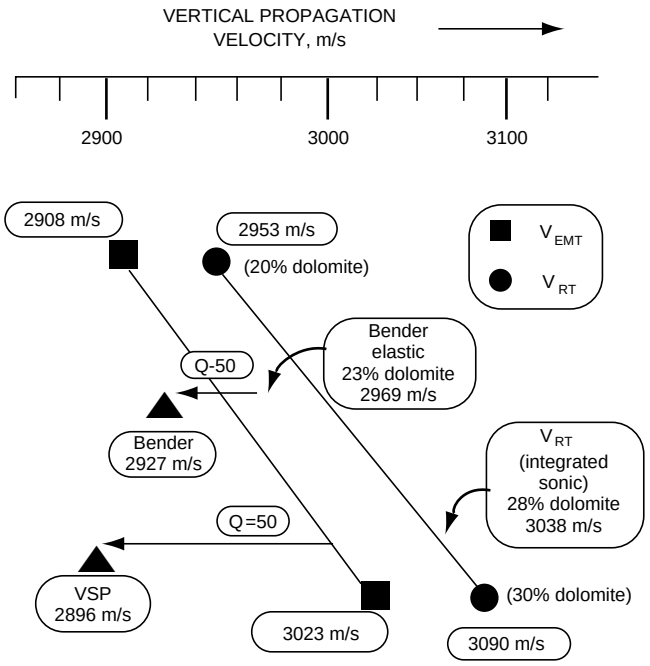

Fig. 7 Illustration of interpretation used for vertical measurements in the upper marine section. The integrated sonic for the interval corresponds approximately to a model with 28% dolomite. The value of V_{RT} of 3038 m/s for 28% dolomite is indicated. The V_{EMT} corresponding to the elastic estimate of the vertical seismic profile (VSP) measurement is 3000 m/s. The attenuation represented by Q = 50 is represented by the arrow from 3000 m/s to the observed value for the VSP (2896 m/s). The VSP and Bender log measurements were made by Burns et al.[5] in a smaller interval than used for this study. The VSP is interpreted as averaging over a slightly larger volume because of the longer wavelengths. The effective percentage of dolomite for the Bender measurements is reduced because of averaging measurements over a restricted subinterval from 250 to 260 m. The model value of the V_{RT} that is equivalent to the interval velocities for this shale-prone interval (based upon integrating the sonic travel times) corresponds to 23% dolomite. The attenuation required (Q = 50) is the same used to explain the VSP measurements.

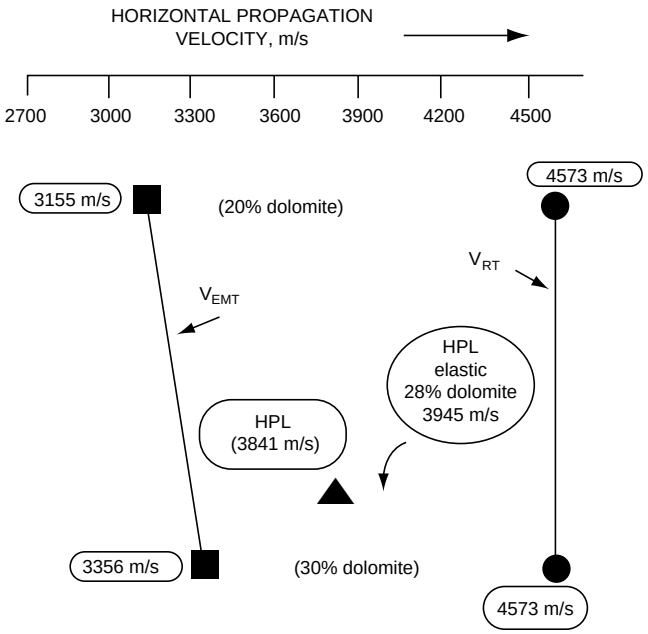

Fig. 8 Interpretation of horizontal velocities in the marine section above the Gypsy sandstone interval. The V_{RT} is the fastest velocity in the layered model corresponding to the dolomite streaks. The V_{EMT} is the effective media results based on the averaging scheme of Backus.[2] The HPL is a cross-well measurement whose velocity estimate is interpreted to best be approximated by wave theory. The value of wave theoretical velocity (V_{WT}) is assumed, for the sake of discussion, to be scaled as indicated to the value indicated (3945 m/s). The actual cross-well velocity measured is 3841 m/s. More detailed wave theoretical modeling is necessary in order to understand the degree of anisotropy expected for the upper marine section.

References

1. J. D. Doyle, D. J. O'Meara, Jr., and E. J. Witterholt, *The Gypsy Field Research Program in Integrated Reservoir Characterization*, paper SPE 24710 presented at the 67th Annual Society of Petroleum Engineers Technical Conference, Washington, D. C., October 4–7, 1992.
2. G. E. Backus, Long-Wave Elastic Anisotropy Produced by Horizontal Layering, *J. Geophys. Res.*, 67: 4427-4440 (1962).
3. D. Marion, T. Mukerji, and G. Mavko, Scale Effects on Velocity Dispersion: From Ray to Effective Medium Theories in Stratified Media, *Geophysics*, 59: 1613-1619 (1994).
4. G. S. De, D. F. Winterstein, and M. A. Meadows, Comparison of P- and S-Wave Velocities and Q's from VSP and Sonic Log Data, *Geophysics*, 59: 1512-1529 (1994).
5. D. R. Burns, E. C. Reiter, X. M. Tang, and J. E. Foley, Elastic Property Scaling Relationships and the Seismic Characterization of Flow Units, unpublished abstract of a presentation to the Gas Research Institute by New England Research, Inc., Quincy, Mass.

RESOURCE ASSESSMENT TECHNOLOGY

ASSIST IN THE RECOVERY OF BYPASSED OIL FROM RESERVOIRS IN THE GULF OF MEXICO

Contract No. DE-AC22-92BC14831

Louisiana State University
Baton Rouge, La.

Contract Date: Feb. 18, 1992
Anticipated Completion: Mar. 18, 1994
Government Award: $2,025,755

Principal Investigator:
Philip A. Schenewerk

Project Manager:
Edith Allison
Bartlesville Project Office

Reporting Period: Oct. 1–Dec. 31, 1994

Objective

The objective of this research is to assist the recovery of noncontacted oil from known reservoirs on the Outer Continental Shelf (OCS) in the Gulf of Mexico. Mature offshore reservoirs, declining oil reserves, declining production, and other natural forces are accelerating the abandonment of offshore oil resources and production platforms. As these offshore wells are plugged and the platforms are abandoned, an enormous volume of remaining oil will be permanently abandoned.

Project research will proceed in three broad phases: data analysis, supporting research, and technology transfer.

Data Analysis. The Tertiary Oil Recovery Information System (TORIS)-level data will be collected on the major fields located in the piercement salt dome province of the Gulf of Mexico OCS. Representative reservoirs will be studied in detail to evaluate undeveloped and attic oil reserve potential. These detailed investigations will be used to calibrate the TORIS-level predictive models and to assess the recovery potential of advanced secondary and enhanced oil recovery (EOR) processes and the exploitation of undeveloped and attic oil zones for salt dome reservoirs in the Gulf of Mexico.

Supporting Research. Supporting research will focus on the modification of public domain reservoir simulation models to simulate accurately the conditions encountered in the piercement salt dome province of the Gulf of Mexico. Laboratory research will focus on the development of fluid relationships to be used in the simulation of miscible and immiscible processes in the project area.

Technology Transfer. A significant effort is planned to transfer the results of this project to potential users of the technology.

Summary of Technical Progress

TORIS Predictive Modeling

Progress continues in reducing the TORIS data to fit a simplified model and redescribing the resource to accommodate known production behavior and certain geologic assumptions.

Critical Process Parameter Laboratory Experiments

In the experiments (done as part of thesis work),[1] it was determined that attic oil recovery, upstructure oil recovery by down-structure gas injection, is a feasible and economical process. Three types of experimental models were used: a micromodel, a prototype sandpack, and a large-scale sandpack. The micromodel glass apparatus was used to visually observe the gas migration process. The prototype sandpack was used to explore the design parameters for a large-scale sandpack. The large-scale apparatus was used to investigate oil recovery mechanisms. In all experiments, the core was vertical. The water-saturated sandpack was oilflooded to irreducible water saturation. Water was then injected from the bottom port, which produced oil from the center and left a high oil saturation in the upper portion of the core. Gas was injected from the center port, and the core was shut in to soak in order to allow time for gas migration. Numerical simulations were performed to investigate the effects of soak time, slug size, dip angle, and injection scheme. Results demonstrated that the gas injection process was capable of recovering a substantial quantity of attic oil and that gas utilization factors were favorable.

Reference

1. A. D. Manne, *Attic Oil Recovery by Gas Injection,* Master's Thesis, Louisiana State University, Baton Rouge, La., 1994.

CONTINUED SUPPORT OF THE NATURAL RESOURCES INFORMATION SYSTEM FOR THE STATE OF OKLAHOMA

Contract No. DE-FG22-94BC14853

Oklahoma Geological Survey
University of Oklahoma
Norman, Okla.

Contract Date: Sept. 19, 1994
Anticipated Completion: Sept. 18, 1995
Government Award: $300,000
(Current year)

Principal Investigators:
Charles J. Mankin
Mary K. Banken

Project Manager:
R. Michael Ray
Bartlesville Project Office

Reporting Period: Oct. 1–Dec. 31, 1994

Objective

The objective of this research program is to continue developing, editing, maintaining, using, and making publicly available the Oil and Gas Well History File portion of the Natural Resources Information System (NRIS) for the state of Oklahoma. This contract funds the development work as a continuation of earlier contract numbers DE-FG19-88BC14233, DE-FG22-89BC14483, and DE-FG22-92BC14853.The Oklahoma Geological Survey (OGS), working with Geological Information Systems (GIS) at the University of Oklahoma (OU) Sarkeys Energy Center, has undertaken the construction of this information system in response to the need for a computerized, centrally located library containing accurate, detailed information on the state's natural resources. Particular emphasis during this phase of NRIS development is placed on oil and gas data for Osage County, which is under the authority of the Osage Tribal Council (OTC).

Summary of Technical Progress

The NRIS Well History File contains historical and recent completion records for oil and gas wells reported to the Oklahoma Corporation Commission (OCC) on Form 1002-A and reported to the OTC on the Osage County completion form. At the start of this quarter, the Well History File contained 378,243 records, providing geographical coverage for all of Oklahoma except the eastern portion of Osage County. Data elements on this file include American Petroleum Institute (API) well number, lease name and well number, location information, elevations, dates of significant activities for the well, and formation items (e.g., formation names, completion and test data, depths, and perforations). In addition to the standard Well History File processing, special projects are undertaken to add supplemental data to the file from well logs, scout tickets, and core and sample documentation.

Processing of OCC's oil and gas well completion reports (Form 1002-A and the Osage County form) is proceeding smoothly. Well records are being photocopied, prescanned, keyed, and edited for Osage County and for all new (or

previously missing) records obtained from the OCC. Approximately 4500 well records were keyed and added to the file this quarter; about 3000 more records were keyed but have not been added to the file because processing was suspended to prepare for the January data release. Thus, as of December 1994, the database contained 382,807 records. The Well History File progress by NRIS Regional Division in is shown in Table 1. The current record counts by county are displayed in Fig. 1.

TABLE 1

Well History File Progress by Regional Division

Area of coverage	Start of contract	Current	Net increase
Southeast region	67,883	68,127	244
Southwest region	72,955	73,284	329
Northeast region	140,766	144,339	3,573
Northwest region	34,103	34,365	262
North-central region	62,536	62,692	156
Total	378,243	382,807	4,564

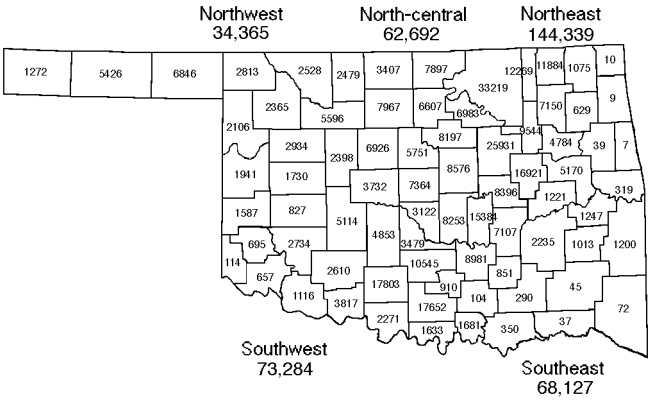

Fig. 1 Status of well history database project as of Dec. 31, 1994. Total well records, 382,807.

Both general and specialized edit procedures were continued on the well data. Search strategies are used to research well records with incorrect location data and well records that should be cross-referenced. Oklahoma Tax Commission lease numbers are being assigned to well records through a combined machine and manual matching process between the Lease and Well Files. Field names and codes are also added to well records based on a matching process that matches field location data. During this quarter new edit routines were implemented for the new data elements that were added for Osage County records and for new directional drilling data on the 1002-A forms.

Although the geographical coverage for most of Oklahoma is considered complete, it is also recognized that across the state there are areas from which well completion reports are missing. Special efforts are under way to identify these areas and obtain data on the missing wells (for example, the Lease File/Well File matching efforts continue as a means of identifying areas with missing 1002-A forms). Identified wells that are not on the Well History File are sent to Sooner Well Log Service, and any missing 1002-A forms available through their collection are obtained and added to the File.

Efforts to standardize the formation names on the Well History File are continuing. A personal computer (PC)-based program being used has a conversion table to standardize spellings and allows the user to build interactively new entries for the conversion table as new spelling variations are encountered. More than 95% of the reported names in the state have been standardized through these efforts. This formations-editing process is further enhanced by the addition of a table to determine the standard Franklinized abbreviation for each reported name following the convention with which industry users are familiar.

One goal of the NRIS system involves efforts to assign leases and wells to fields on the basis of the official field outlines as designated by the Midcontinent Oil and Gas Association's Oklahoma Nomenclature Committee (ONC). Some areas exist in which significant field extension drilling has taken place, but the ONC has had insufficient resources to update the field boundaries accordingly. Information packages are produced from the NRIS system for selected areas to assist the ONC in updating their field outlines. These packages include well data listings and well spot maps. On the basis of this input, the ONC began by updating several gas-field boundaries; emphasis has now shifted to oil-field boundaries as work proceeds on a separate U.S. Department of Energy (DOE) project involving the identification and evaluation of Oklahoma's fluvial-dominated deltaic reservoirs. Overall, unassigned gas production comprises 9% of the annual average production, and unassigned oil production comprises 15%.

Significant efforts were undertaken during this quarter to prepare for the January 1995 data release because this would be the first release of nearly 100 new data elements for the 1002-A forms and the Osage County records. New release formats were designed, and new format programs were written to accommodate these changes.

Public Data Release

Since early 1991 efforts have been made to disseminate NRIS information through meetings, workshops, OGS annual reports, and mass mailings to numerous individuals, companies, and organizations. As a result, a dramatic response to the release of NRIS data began during the summer of 1991 and has continued. Feedback from the public reflects an enthusiasm about this new resource for the oil and gas industry in Oklahoma. Data and analyses have been provided that would not have been feasible before construction of the NRIS system.

Two commercial firms subscribe to the Well History File, and several inquiries are received each quarter from small

companies and independents who typically acquire NRIS subsets for particular project areas. NRIS well data have been made available through the Oklahoma City Geological Society Library with very positive results. The high level of interest by library members has led to the acquisition of thousands of records by several members each quarter as well as constructive feedback on user-detected data anomalies. The Library is cataloging its extensive well-log collection and tying each log to the corresponding NRIS well record, which enhances efforts to locate missing well records.

The OGS is establishing a computing facility to promote user access to the NRIS data, initially by OGS staff and eventually by the public. Visual Basic user interfaces, along with a PC-level relational database management system (Oracle), are being used to develop menu-driven retrieval systems customized to NRIS data. A new Novell network system is being installed to allow multi-user access to the databases. A large digitizer, large plotter, and desktop scanning equipment enhance the capabilities available through GeoGraphix and Radian CPS/PC contour mapping software as well as through ARC/INFO, a GIS spatial analysis tool. Additionally, Platte River Associates has agreed to donate their land-grid and associated cultural data for use in the facility.

The NRIS data are significant in several other in-house projects (for example, the computing facility will become the central location for NRIS data access and distribution in the OGS' forthcoming role as Regional Lead Organization for the Southern Midcontinent under the Petroleum Technology Transfer Council program). Another project funded by DOE involving the study of Oklahoma's fluvial-dominated deltaic oil reservoirs also includes technology transfer as an underlying goal.

MICROBIAL TECHNOLOGY

THE USE OF INDIGENOUS MICROBES TO SELECTIVELY PLUG THE MORE POROUS ZONES TO INCREASE OIL RECOVERY DURING WATERFLOODING

Contract No. DE-FC22-94BC14962

Hughes Eastern Corporation
Jackson, Miss.

Contract Date: Jan. 1, 1994
Anticipated Completion: June 30, 1999
Government Award: $508,835
(Current year)

Principal Investigators:
Lewis R. Brown
Alex A. Vadie

Project Manager:
Rhonda Lindsey
Bartlesville Project Office

Reporting Period: Oct. 1–Dec. 31, 1994

Objective

The objective of this work is to demonstrate the use of indigenous microbes as a method of profile control in waterfloods. It is expected that, as the microbial population is induced to increase, the expanded biomass will selectively block the more-permeable zones of the reservoir and thereby force injection water to flow through the less-permeable zones, which will result in improved sweep efficiency.

This increase in microbial population will be accomplished by the injection of a nutrient solution into four injectors. Four other injectors will act as control wells. During Phase I, two wells will be cored through the zone of interest. Special core analyses will be performed to arrive at the optimum nutrient formulation. During Phase II, nutrient injection will begin, the results will be monitored, and adjustments to the nutrient composition will be made, if necessary. This phase also will include the drilling of three wells for postmortem core analysis. Phase III will focus on technology transfer of the results. One outcome expected of this new technology will be a prolongation of economical waterflooding operations (i.e., economical oil recovery should continue for much longer periods in producing wells subjected to this selective plugging technique).

Summary of Technical Progress

Phase I. Planning and Analysis

The work for Phase I of the project was divided into seven tasks. The first five tasks, The Drilling of Two New Injection Wells for the Acquisition of Cores and Other Data, On-Site Handling of Cores, Core Analysis To Determine Microbial Enhanced Oil Recovery (MEOR) Requirements, Microbial Analyses of Cores, and Laboratory Waterflooding Test of Live Cores, are complete. The sixth task, Acquisition of Baseline Production and Injection Data, is continuing through chemical and microbiological analyses of injection water and production fluid. The seventh task, Analysis of Baseline Data, has begun and will continue through the next quarter.

Phase II. Implementation

This phase involves initiation of nutrient injection and the analysis of results. Construction of the first nutrient injection skid is complete. The skid was designed for mixing the dry nutrients into a solution made with field waterflood water and with the capability of pumping 100 to 300 gal/d of solution.

The results of laboratory experiments on live cores were scaled into field operation. Nutrient solutions were prepared and injected into the first test pattern injection well beginning November 21, 1994, on the basis of a feeding regime established from laboratory data. After favorable mechanical performance of the first skid, construction of three additional skids began in December 1994.

The test injector well is Well 2-14 No. 1. The test pilot producer wells are Wells 2-13 No. 1, 2-15 No. 1, 11-3 No. 1, and 2-11 No. 1. The control injector well is Well 2-4 No. 1. The control producer wells are Wells 35-13 No. 1, 35-14 No. 1, 3-1 No. 1, 2-3 No. 1, and 2-5 No. 1.

FIELD DEMONSTRATIONS

GREEN RIVER FORMATION WATERFLOOD DEMONSTRATION PROJECT, UINTA BASIN, UTAH

Contract No. DE-FC22-93BC14958

Lomax Exploration Company
Salt Lake City, Utah

Contract Date: Oct. 21, 1992
Anticipated Completion: Oct. 20, 1995
Government Award: $1,304,000

Principal Investigators:
John D. Lomax
Dennis L. Nielson
Milind D. Deo

Project Manager:
Edith Allison
Bartlesville Project Office

Reporting Period: Oct. 1–Dec. 31, 1994

Objective

The objective of this project is to evaluate the successful Monument Butte Unit waterflood and transfer the technology to other parts of the Unit and to the Travis and Boundary Units.

The project is designed to increase recoverable petroleum reserves in the United States. In 1987, Lomax Exploration Co. started a waterflood in the Monument Butte Unit that targeted the Green River formation. This was a low-energy, geologically heterogeneous reservoir that produced a waxy crude oil. Primary production yielded about 5% of the original oil in place (OOIP). As a result of the waterflood project, it is estimated that the total production from the unit will exceed 20% of OOIP.

Summary of Technical Progress

Field Drilling and Production Results

Monument Butte Unit

The Monument Butte Unit No. 7-34 was spudded on Nov. 7, 1994, and put on production Dec. 24, 1994. The No. 7-34 produced 1436 bbl of oil [an average of 179 bbl of oil per day (BOPD)] and 403 Mcf of gas for the 8 days of production.

As of Dec. 31, 1994, the Monument Butte Unit No. 10-34 (project well), put on production the last quarter of 1992, had produced 13,164 bbl of oil and 18,106 Mcf of gas, and the Monument Butte No. 9-34 (project well), drilled and completed in December 1993, had produced a total of 14,362 bbl of oil and 10,930 Mcf of gas. As of Dec. 31, 1994, the total Monument Butte Unit production from the inception of the project (October 1992) had increased from 781,095 bbl of oil to a total of 994,110 bbl of oil, or a 213,015 (27%) increase, and the total gas production had increased from

2,052,978 Mcf of gas to 2,172,303 Mcf of gas, or a 119,325 Mcf (6%) increase. As of Dec. 31, 1994, approximately 2,910,276 bbl of water had been injected. Approximately 33,000 bbl of water is being injected on a monthly basis.

Travis Unit

The Travis Unit No. 5-33 (project well) was spudded on Oct. 25, 1994, and put on production Dec. 12, 1994. The well produced 1181 bbl of oil (an average of 62 BOPD) and 1426 Mcf of gas in 19 days of production.

As of Dec. 31, 1994, the cumulative water injection in the Travis Unit was 616,075 bbl; the total Travis Unit production from the inception of the project (October 1992) had increased from 257,242 bbl of oil to a total of 285,995 bbl of oil, or a 28,753 bbl (11%) increase; and the total gas production had increased from 1,195,570 Mcf of gas to 1,339,305 Mcf of gas, or a 143,735 Mcf (12%) increase. Approximately 10,000 bbl of water is being injected on a monthly basis.

Boundary Unit

The Boundary Unit No.12-21 (project well) was spudded on Nov. 11, 1994, and put on production in January 1995. Approval to drill and case three additional development wells in the Boundary Unit to validate the geologic extent of the Green River formation sands has not been received; however, the first well is planned for March 1995.

The regional maps show that the Duchense fault zone passes through the Boundary Unit; thus it can be inferred that a strong east-west fracture trend will be present in all the sandstone units. Work on these fractures suggests that they will develop in the sandstone but will not pass through the bounding shale beds. Thus, unless an offset in stratigraphy indicating a fault is documented, these fractures will not result in vertical permeability between overlying and underlying sandstone beds. These fractures will create an east-west fracture permeability. Hydrofracturing may enhance this east-west permeability and could result in short-circuiting. The induced fracture envelope will probably be ellipsoidal with the major axis oriented east-west.

D sandstone. The greatest thickness of D sandstone is located in the No. 7-20 well. The upper unit (D_1) contains about 23 ft of gross sand, but it has no apparent continuity with sands in nearby wells. From work in the Monument Butte Unit, the D_1 sand is interpreted as a deltaic deposit. It is likely that a better quality D_1 reservoir will be present in the northwest quarter of Section 20.

In contrast, the D_2 zone has a fluvial origin. In the Boundary Unit wells, the D_2 zone has two separate sands separated by shales of variable thickness. D_2 is a channel-sand system oriented north to northwest. Permeability anisotropy resulting from depositional processes may be oriented parallel to these trends.

C sandstone. C sandstone is present in wells No. 7-20 and No. 11-21. Exploration in the eastern portion of Section 11-21 may discover additional C reservoirs.

A sandstone. Well No. 7-20 contains the thickest accumulation of A; however, the upper- and lower-A sands in No. 7-20 do not have equivalent units in adjacent wells. An isopach of A in the Boundary Unit reveals an ancient fluvial system. The No. 13-21 well was not drilled deep enough to penetrate the entire section where A sands were likely to be found.

Lower Douglas Creek (LDC) sandstone. The only viable LDC sands are in well No. 15-20. Well Nos. 7-20 and 9-20 have a siltstone section in the LDC interval. It is believed that the western half of Section 20, particularly the southwestern half, is prospect for LDC sandstones.

Castle Peak sandstones. The upper Castle Peak sandstone is present in well Nos. 9-20 and 5-21. Well Nos. 13-21 and 11-21 were not drilled deep enough to verify the presence or absence of this reservoir. In well No. 5-21, this sand is present as two beds with net sands of 2 ft (upper) and 8 ft. In well No. 9-20, the sand has three components; 5 ft (upper), 8 ft, and 6 ft net. The beds are at the same stratigraphic horizon in both wells.

Reservoir Analysis: Near-Wellbore Effects–Wax Precipitation Models

Wellbore heat-transfer calculations indicated a strong possibility of wax precipitation in the near-wellbore region. Therefore wax precipitation models that would predict onset of precipitation were explored. Weingarten and Euchner[1] developed a simple solubility model to calculate the solubility of paraffin component in liquid oil:

$$\ln x_{ps} = \frac{-\Delta H_f}{R}\left(\frac{1}{T} - \frac{1}{T_f}\right) \qquad (1)$$

With this simple representation, the solubility of the paraffin fraction in the oil at any given temperature can be calculated with the use of the heat of fusion and the melting point of the pseudo-component. If the solubility of the fraction in oil exceeds the initial concentration of the paraffin component in oil, then all the paraffin will remain in solution. Paraffin precipitation will occur when the solubility is lower than the initial concentration of paraffin in oil. Weingarten and Euchner[1] extended the concept to the prediction of wax appearance points of live oils at high pressures. Ring and Wattenbarger[2] adopted the concept in simulating oil production from paraffinic reservoirs susceptible to paraffin precipitation. This approach does not consider detailed oil composition data.

Won[3-5] developed a series of models for predicting solid–liquid and solid–liquid–vapor equilibria through a framework that used detailed oil compositions in solid–liquid equilibria predictions. Rigorous expression for the solid–liquid K-values, K_{iSL}, was shown to be

$$K_{iSL} = \frac{s_i}{x_i} = \frac{\gamma_i^L}{\gamma_i^S} \exp\left\{\left[\frac{\Delta H_f}{RT}\left(1 - \frac{T}{T_f}\right)\right]\right.$$

$$\left. + \frac{\Delta C_p}{R}\left(1 - \frac{T_f}{T} + \ln\frac{T_f}{T}\right) + \int_o^P \frac{\Delta V}{RT}\, dP\right\} \qquad (2)$$

Won neglected the last two terms within the exponential. In his earlier paper, Won[3] assumed the ratio of activity coefficients, γ_i^L / γ_i^s to be equal to 1.0, whereas in a later paper on solid–liquid–vapor equilibria[4] he calculated the ratio with the regular solution theory. Pure-component solubility parameters were required with this approach for solid–liquid equilibria calculations. Later, Won[5] used a more sophisticated irregular solution theory for the calculation of activity coefficients. Hansen et al.[6] contended that the wax appearance points calculated by Won's models for about 17 crude oils were considerably higher than the experimental values, and they proposed an alternate model for the calculation of activity coefficients. The model appeared to perform better than Won's model, even though activity coefficients predicted by the model were of the order of 10^{-10}. Pedersen et al.[7] concluded that Hansen's model did not provide a phenomenological advantage over Won's models and proceeded to use Won's model with modified expressions for heats of fusion, solubility parameters, and the Δc_p term in the K-value expression. Won[4] proposed the following expressions for solubility parameters with the regular solution theory:

$$\delta_{iL} = \left(\frac{\Delta H_v - RT}{v} \right)^{1/2}_{1,L} \tag{3}$$

$$\delta_{iS} = \left(\frac{\Delta H_v + \Delta H_f - RT}{v} \right)^{1/2}_{i,S} \tag{4}$$

Won[4] listed the values of solubility parameters that were obtained but did not discuss computation of heats of vaporization. The following methodology can be used for the calculation of heat of vaporization. Heat of vaporization at normal boiling is given by Reid et al.[8]

$$\Delta H_{vb} = RT_c T_{br} \left[\frac{3.978 T_{br} - 3.95\gamma + 1.555 \ln k}{1.07 - T_{br}} \right] \tag{5}$$

Heat of vaporization at 25 °C, used for the calculation of the solubility parameters, is determined with the following expression[8]:

$$\Delta H_v = \Delta H_{vb} \left(\frac{1 - T_{r25\,^\circ C}}{1 - T_{br}} \right)^n \tag{6}$$

where n is given by

$$n = \left[\left(0.00264 \frac{\Delta H_{vb}}{RT_b} \right) + 0.8794 \right]^{10} \tag{7}$$

The boiling point T_b is calculated with standard correlations.

The heats of vaporization for normal paraffins calculated by the above-mentioned approach were verified with experimental values.[9] The solubility parameters calculated with the method described are different from those listed by Won[4] for components up to C_{45}. Pedersen et al.[7] developed independent correlations for solubility parameters. They also modified the expression for heat of fusion used by Won to reflect the presence of nonparaffins in the oil and considered the effect of heat capacity differences in the solid and liquid phases. This modified Won's method has been the most successful model for the prediction of wax appearance points and wax amounts for 17 North Sea crude oils. The wax appearance points for Hansen's oil numbers 1 and 2 and for a paraffinic crude from Green River formation, Utah, were calculated by

1. Assuming the activity coefficients were equal to 1.
2. Using the solubility parameters listed by Won.[4]
3. Using the solubility parameters obtained via correlations presented herein.
4. Using the solubility parameters listed by Pedersen et al.[7]
5. Using the solubility parameters listed by Pedersen et al., and modifying the expression for heat of fusion, also proposed by Pedersen et al.[7]

Results of these calculations are shown in Table 1.

Wax appearance points calculated by neglecting the effect of activity coefficients and by using the solubility parameters

TABLE 1

Comparison of Wax Appearance Points (K) Calculated by Different Methods

Oil*	Method 1	Method 2	Method 3	Method 4	Experimental†
Oil 1	339	340	349	326	304
Oil 2	332	333	339	321	312
Oil 10	316	317	328	301	314
Oil 12	324	325	333	311	305
Utah oil	349	350	–	340	322

*Oils 1, 2, 10, and 12 are North Sea crudes. Compositional data on these oils have been provided by Hansen et al.[6] Utah oil is from the Green River formation in the Monument Butte field.

†Experimental values for the North Sea crudes were reported by Pedersen et al.[7]

listed by Won[4] are almost identical. When solubility parameters determined by established correlations are used, the predictions are worse. A simple adjustment of solubility parameters does not improve the predictions significantly. The adjustment of heats of fusion brings the predicted values closer to experimental values, but there is considerable deviation between experimental and calculated wax appearance points even after further modifications proposed by Pedersen et al.[7] are made.

A brief review of solid–liquid equilibria calculations for the prediction of wax precipitation and calculations performed as part of this study underscores the fact that tuning models to predict wax appearance points or wax amounts may not yield adequate models. If phase compositions are considered, model predictions will improve. In this regard, data on phase compositions are necessary, particularly for oils that contain substantial fractions of heavy components. The calculations shown in Table 1 indicate that, even after a 10 to 30 K adjustment (for the presence of gas, pressure, etc.) at temperatures predicted by the wellbore model, paraffin precipitation is certain in reservoirs containing the Green River crude.

Technology Transfer

J. D. Lomax and M. D. Deo made presentations for the National Research Council Panel that reviewed the U.S. Department of Energy's reservoir class projects.

Nomenclature

K_{iSL} = solid–liquid equilibrium coefficient, dimensionless
R = universal gas constant, J/mol-K
s_i = mole fraction of component i in solid phase, dimensionless
T_b = temperature at normal boiling point, dimensionless
T_{br} = reduced temperature at normal boiling point, dimensionless
T_c = critical temperature, K
T_f = fusion temperature, K
x_i = mole fraction of component i in liquid phase, dimensionless
x_{ps} = solubility of solid paraffin (that can be dissolved) in oil, dimensionless
Δc_p = heat capacity change of fusion, cal/mol-K
ΔH_f = latent heat of fusion, cal/mol
ΔH_v = latent heat of vaporization, cal/mol
ΔH_v = latent heat of vaporization at normal boiling
ΔV = volume change on fusion, cm^3
δ_{iL} = solubility parameter of component i in liquid phase, $(cal/cm^3)^{0.5}$
δ_{iS} = solubility parameter of component i in solid phase, $(cal/cm^3)^{0.5}$
γ_i^L = activity coefficient of component i in liquid phase, dimensionless
γ_i^S = activity coefficient of component i in solid phase, dimensionless

References

1. J. S. Weingarten and J. A. Euchner, Methods for Predicting Wax Precipitation and Deposition, *SPE Product. Eng.*, 3(1): 121-126 (February 1988).
2. J. N. Ring and R. A. Wattenbarger, *Simulation of Paraffin Deposition in Reservoirs,* paper SPE 24069 presented at the Western Regional Meeting of the Society of Petroleum Engineers, Bakersfield, Calif., March 30–April 1, 1992.
3. K. W. Won, *Continuous Thermodynamics for Solid–Liquid Equilibria: Wax Formation from Heavy Hydrocarbon Mixtures,* paper presented at the AIChE National Spring Meeting, Houston, Tex., March 1985.
4. K. W. Won, Thermodynamics for Solid Solution–Liquid–Vapor Equilibria: Wax Phase Formation from Heavy Hydrocarbon Mixtures, *Fluid Phase Equilibria,* 30: 265-279 (1986).
5. K. W. Won, Thermodynamic Calculation of Cloud Point Temperatures and Wax Phase Compositions of Refined Hydrocarbon Mixtures, *Fluid Phase Equilibria,* 53: 377-396 (1989).
6. J. H. Hansen, A. Fredenslund, K. S. Pedersen, and H. P. Ronningsen, A Thermodynamic Model for Predicting Wax Formation in Crude Oils, *A.I.Ch.E.J.*, 34(12): 1937-1942 (1988).
7. K. S. Pedersen, P. Skovborg, and H. P. Ronningsen, Wax Precipitation from North Sea Crude Oils. 4. Thermodynamic Modeling, *Energy and Fuels,* 5: 924-932 (1991).
8. R. C. Reid, J. M. Prausnitz, and B. E. Poling, *The Properties of Gases and Liquids,* 4th ed., McGraw-Hill, Inc., New York, 1987.
9. R. H. Perry and C. H. Chilton, *Chemical Engineers' Handbook,* Fifth ed., pp. 3-118, McGraw-Hill Book Company, Inc., New York, 1973.

IMPROVED RECOVERY DEMONSTRATION FOR WILLISTON BASIN CARBONATES

Contract No. DE-FC22-94BC14984

Luff Exploration Company
Denver, Colo.

Contract Date: June 10, 1994
Anticipated Completion: June 9, 1997
Government Award: $483,284

Principal Investigator:
Larry A. Carrell

Project Manager:
Chandra Nautiyal
Bartlesville Project Office

Reporting Period: Oct. 1–Dec. 31, 1994

Objectives

The objectives of this project are to demonstrate targeted infill and extension drilling opportunities, better determinations of oil in place, methods for improved completion efficiency, and the suitability of waterflooding in certain shallow-shelf carbonate reservoirs in the Williston Basin in Montana, North Dakota, and South Dakota.

Summary of Technical Progress

Reservoir Analysis and Characterization

Three-Component Seismic Evaluation and Acquisition

Original plans in the North Sioux Pass (Ratcliffe) T. 26 N., R. 57–58 E., Richland County, Montana, study area included possible acquisition of a dipole sonic log or a multioffset vertical seismic profile (VSP) to test viability and parameter design for shear-wave acquisition in the area. Cost proposals from Schlumberger and Halliburton for a VSP ranged from $95,000 to $100,000 and do not include the electric wireline truck and well preparation. Cost for a dipole log was estimated at $28,000 by Halliburton and does not include well preparations for pulling and rerunning tubing and rods. Although a VSP and dipole sonic log could provide very valuable data for design of a three-component program, the costs are high and the availability of suitable wells is a problem. A decision was made to shoot and record a test line on the basis of parameters from synthetic modeling. The test line would provide direct field tests of surface-to-surface three-component data over a productive Ratcliffe area with postulated fracturing. Cost estimates for a 3-mile two-dimensional (2-D) test line are in the range of $40,000, about equal to the total cost estimated for acquiring a dipole log and one-third the cost of a single-well VSP survey.

Three-Component Seismic Modeling

In preparation for the design and acquisition of three-component seismic data to evaluate fracture trend detection in the Richland County, Montana, study area, some detailed modeling was undertaken. The purposes of the modeling were to determine the viability of using a shear source, to evaluate recording converted shear waves generated from a P-wave source, and to develop appropriate acquisition parameters.

A detailed velocity model was constructed for the proposed three-component test site. Up-hole times and refractor velocities derived from proximal conventional 2-D seismic data provided near-surface velocities for the first three model layers. The remaining 145 layers, which extended from 1500 ft to 12,760 ft, were derived from blocked sonic and density log data from the Superior Oil No. 2A Vanderhoof well in sec. 13, T. 25 N., R. 58 E., Richland County, Montana (Fig. 1). Shear-wave velocities were calculated for the upper layers and were based on a carbonate relationship for deeper layers. Western Geophysical used a proprietary modeling package to generate synthetic records for surface P-wave, in-line S-wave, and cross-line S-wave sources as well as P-wave sources buried at depths of 98 and 200 ft. Western Geophysical is unable to provide a written report because of the proprietary license agreement for the modeling/synthetic software package.

The S-source synthetic models did not indicate useful P-wave conversion and had significant levels of surface noise. The surface P-wave source did not give viable S-wave data. Both buried P-source synthetics showed good in-line S-wave conversion. The deeper-source synthetic model exhibited significantly less surface-wave noise, primarily because the source was below the uppermost layer.

As a result of the modeling effort, Western Geophysical recommended that the test line be acquired with a buried explosive source at more than 110 ft with an 88-ft group interval, potted or bunched phones laid out in line, and a record length of 4 s. A 3-mile line has been designed to cross the Cattails field area at approximately 45° to postulated fracture trends and should optimize assessment of converted shear-wave recording for the area. On the basis of significant source-generated noise from modeling, a decision was made to not use the shear-vibrator sources for the test line. In addition, verbal communication with ARCO research personnel indicated that excellent converted-wave data were obtained in a similar, nearby setting in North Dakota.

Three-Mile Test Line

A 3-mile 2-D test line for shear-wave acquisition is scheduled for the Ratcliffe study area in Richland County, Montana, in March 1995. Bids for this acquisition are being evaluated. The evaluation of shear-wave recording and detection with a dipole log or VSP survey is not viable both for economic reasons and availability of suitable wellbores. The cost of a VSP survey was found to exceed the shooting of a 2-D three-component test line. A test line has been selected to cross a Ratcliffe field within the field-activity outline. The Cattails field (T. 25–26 N., R. 58–59 E., Richland County, Montana) is oil-productive from the Ratcliffe without structural closure (Fig. 1). The test line will evaluate fracturing across an excellent Ratcliffe field analogy for the study area. The 2-D three-component test line (Figs. 1 and 2) will be used to determine if shear data can be recorded and whether shear data (indicating fracturing) correlate to producing areas in the Ratcliffe.

Seismic Interpretation, Bowman County, North Dakota

The interpretation of 1970s-vintage 2-D seismic data has been enhanced by the reprocessing of data sets across Red River producing areas at SW Amor, Stateline, Cold Turkey Creek, and Grand River School (Fig. 3). Reprocessing methods include the application of refraction statics and radon stacking, which provide significant noise reduction. Resulting sections provide good resolution and higher frequency, which allow detailed interpretation of subtle faulting.

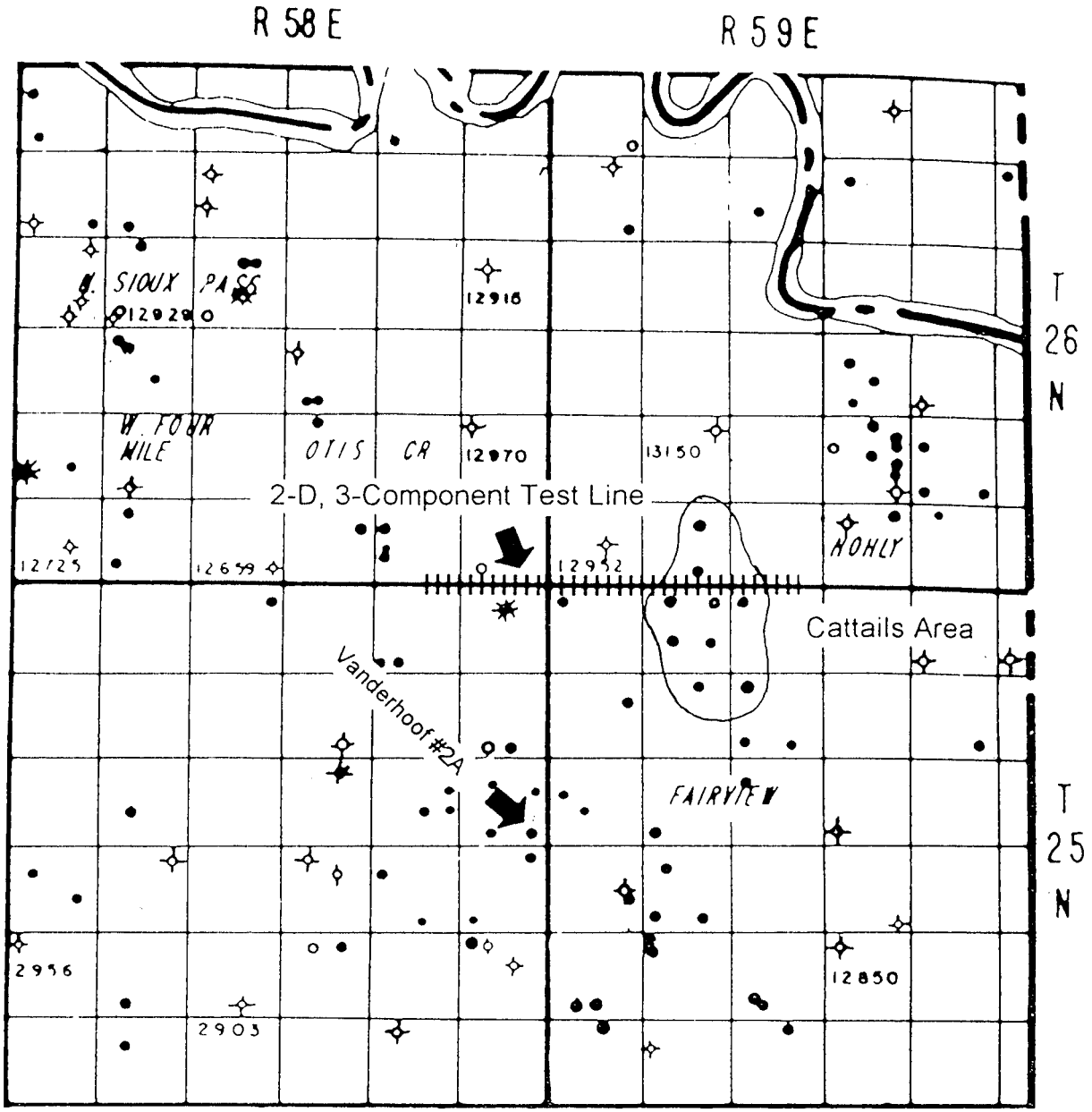

Fig. 1 Location of 2-D, three-component test line and Vanderhoof No. 2A well. The test line will cross the Cattails (Ratcliffe) field and evaluate postulated fracture trends. Well logs from the Vanderhoof No. 2A well were used to develop an earth model for shear wave analysis. (Art reproduced from best available copy.)

Figures 4 and 5 depict examples from east-west seismic line CA9-4 crossing the center of the SW Amor area. Figure 4 shows the original data as processed in 1972. These dynamite data were acquired at 440-ft group intervals and are sixfold. The original processing was performed on 4-ms resampled data and was standard technology for that era. The reprocessed data shown in Fig. 5 exhibit frequencies of 65 Hz at Red River time compared with approximately 40 Hz from the original processing. Seismic cross sections are displayed at the same scale for comparison.

Reprocessed 2-D seismic data from four areas indicate small faults with 40 to 50 ft of vertical offset at Ordovician Winnipeg time (about 300 ft below the Red River). Throw dies upward and is not detectable by Duperow time. Major faulting in the SW Amor area consists of a single down-to-the-northeast fault trending north-northwest to south-southeast (Fig. 3). Maximum throw at the Winnipeg is 45 to 50 ft. The fault dips at approximately 45°. Several smaller faults in the area approximately parallel this main fault, which bounds the SW Amor feature on the northeastern flank.

Faulting at the Grand River School area (Fig. 3) trends west-northwest to east-southeast with vertical offsets similar to those found in the Cold Turkey Creek area of 40 to 50 ft at Winnipeg time. There is no displacement at Duperow time shown on the 2-D cross section for line HA6-7 (Fig. 6).

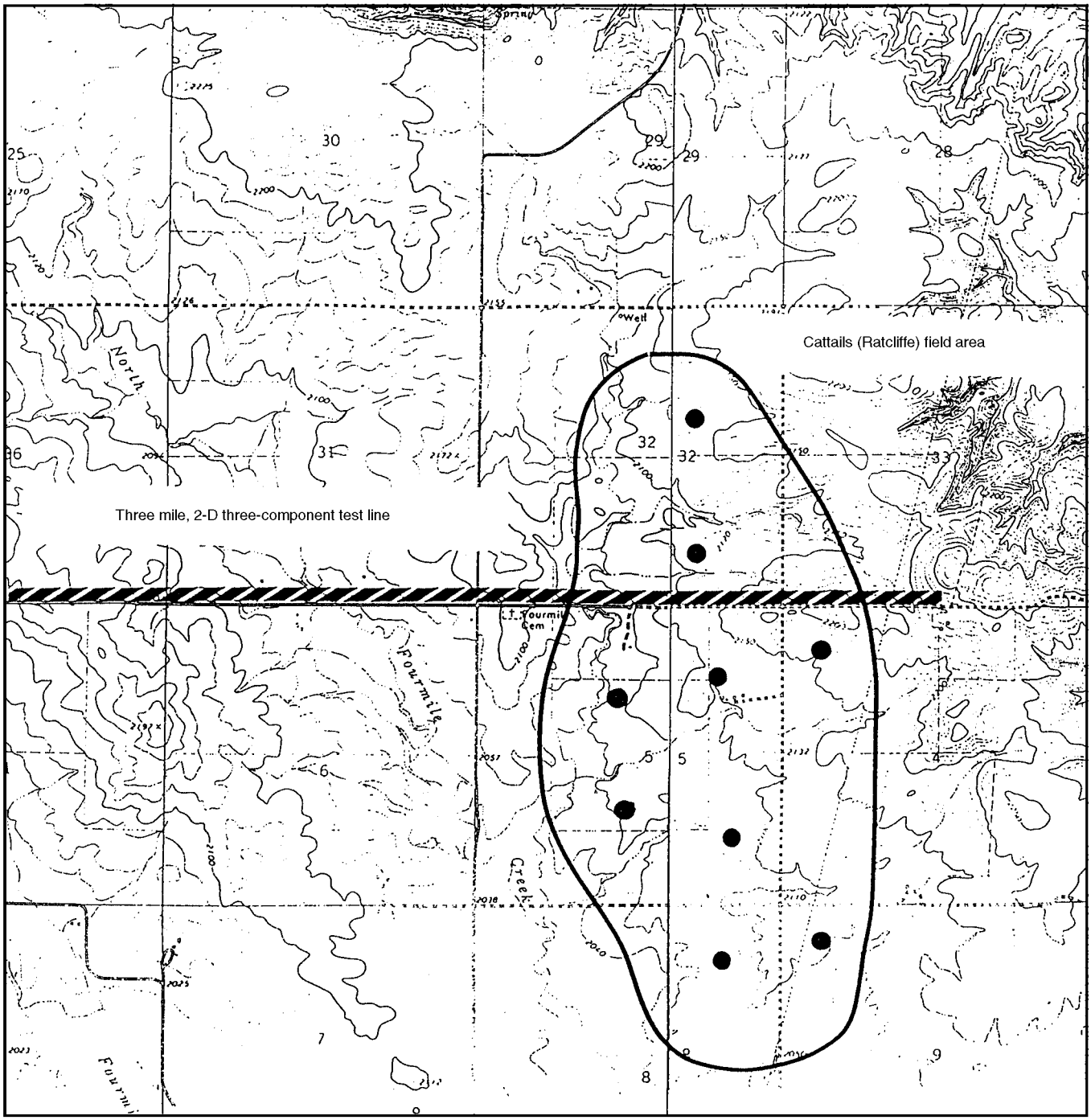

Fig. 2 Topographical map of the 2-D three-component test line area (Dore and Fairview, NW quadrangles). The location of the test line will be along county road right-of-way. (Art reproduced from best available copy.)

These faults bound a series of small horst and graben blocks in the Grand River area. The faults turn northwest to southeast in direction as they extend west across the Cold Turkey Creek area. The faulting at Cold Turkey Creek is typified by 2-D line CTC-27 and is shown in Fig. 7. Minor small-displacement faults parallel the major trend. The major down-to-the-northeast fault in the Cold Turkey Creek and Grand River School areas appears to dip at approximately 30°, which suggests a component of horizontal stress at the time of faulting.

Geophysical Interpretation—SW Amor, Bowman County, North Dakota

The new seismic line LECDOE 94-1 is about 2.6 miles in length and covers portions of secs. 29, 30, and 31 in T. 130 N., R. 103 W. and portions of sec. 36 in T. 130 N., R. 104 W.

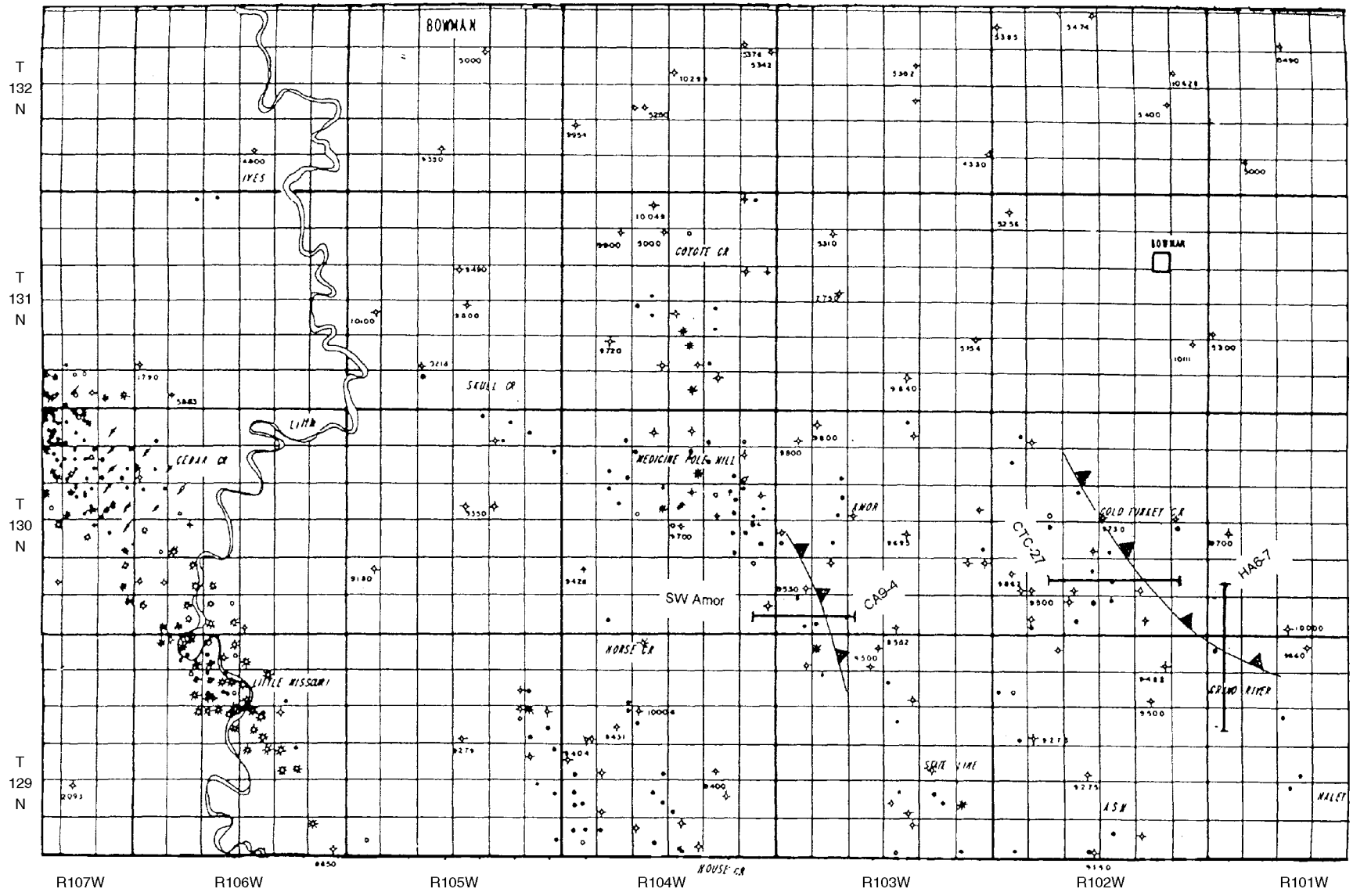

Fig. 3 Location of Red River areas in Bowman County, North Dakota, where reprocessed 2-D seismic data have allowed better definition of faulting components of growth history. (Art reproduced from best available copy.)

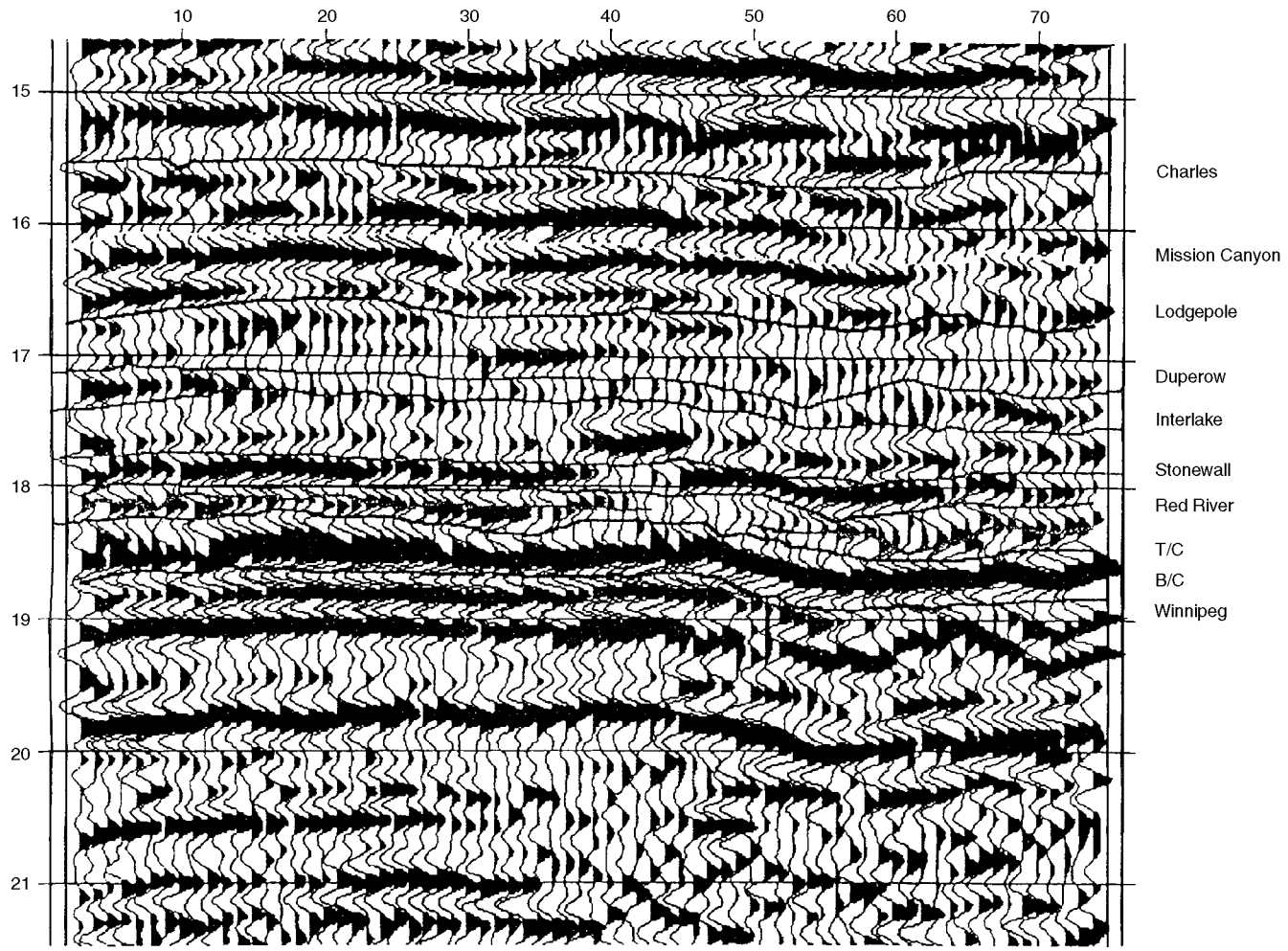

Fig. 4 2-D seismic section CA9-4 from the SW Amor area, Bowman County, North Dakota, before modern processing.

Primary objectives of the line were to provide additional control to the $SW^1/_4$ sec. 30 and $NW^1/_4$ sec. 31, T. 130 N., R. 103 W. and to provide sharper imaging of faulting. The recording parameters were 10 lb of dynamite at 60 ft, 110-ft group intervals [55-ft common depth point (CDP) intervals] and produced 20-fold coverage and usable frequency at the Red River of about 70 Hz. Previously recorded data had parameters of 25 lb of dynamite at 110 ft, 440-group intervals (220-ft CDP intervals) and produced sixfold coverage and usable frequency at the Red River of about 45 Hz.

The new data do not appreciably change previous interpretations of the reservoir or reservoir limits. Faulting is observed at Winnipeg time at trace locations 56 and 110 on line LECDOE 94-1. These normal faults may cut the Red River but die out by Interlake time and have displacements of 9 and 3 ms at the Winnipeg for traces 56 and 110, respectively. The fault at trace 56 can be correlated to faulting observed on the other east-west lines covering the reservoir area. Maximum displacement of this fault is 11 ms (about 55 ft) at Winnipeg time at trace location 50 on line CA9-4. This fault can be confidently used to define the east-side reservoir limits of the SW Amor Red River reservoir. Other faulting is minor and does not correlate between seismic lines; however, it is evident that there is a grain of potential Red River faulting that is parallel to the east-side fault and north-south structural axis.

Time structure and isochron maps of 12 horizons from Greenhorn to Winnipeg time were evaluated, and it was concluded that the Interlake–Winnipeg isochron map correlates best with log, drill stem testing, and production data. Time-structure maps at all horizons fail to demonstrate closure. Time-structure and isochron maps of Winnipeg, Red River, and Interlake horizons indicate a separate growth history of the north area (Nygaard No. 2-31 and No. 44-30 wells) from the south area (Nygaard No. 1-5, No. 2-31, and No. 2-32 wells). This suggests the potential for reservoir segregation between these areas.

Three-Dimensional Survey at Cold Turkey Creek

Screening has been completed and a final area selected for the first Bowman–Harding area three-dimensional (3-D) seismic survey. The Cold Turkey Creek (Red River) area

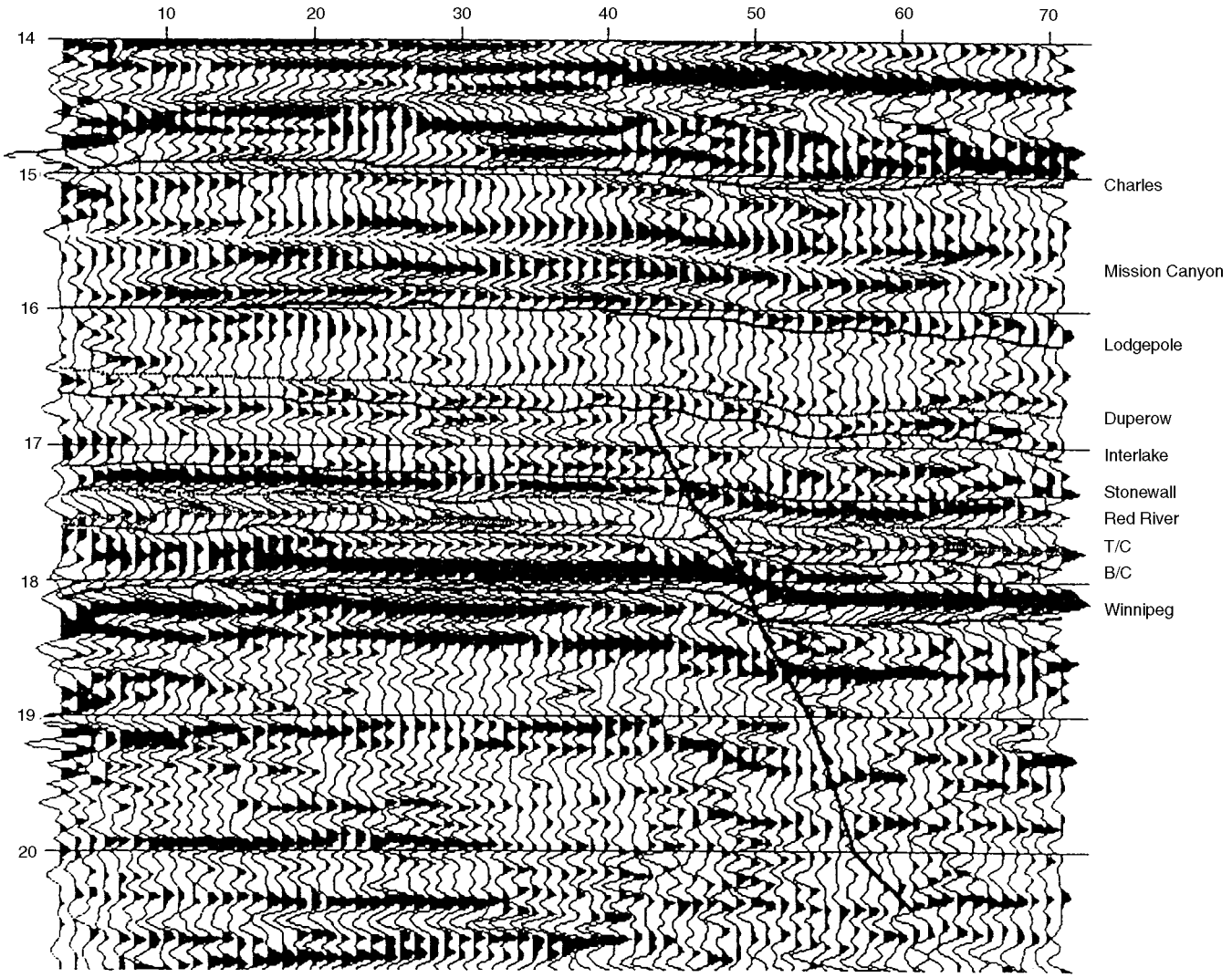

Fig. 5 2-D seismic section CA9-4 after modern processing. The higher frequency content shows greater detail, which allows subtle fault interpretation. The fault is down to northeast trending north-northwest. The maximum throw is 45 to 50 ft at Winnipeg time.

(T. 130 N., R. 102 W., Bowman County, North Dakota) was selected. A receiver area of 4.35 square miles (Fig. 8) was determined to optimize project objectives at minimal cost. Bids were obtained, and Reliable Exploration Inc. was selected as the acquisition contractor on the basis of technical capability, experience in the area, availability, and cost. The contractor is currently permitting and anticipates recording the survey by March 1, 1995, if there are no weather delays. Final staggered-brick acquisition design includes 378 10-lb dynamite charges buried at 60 ft in a 1760-ft source pattern perpendicular to receiver-line spacing. A total of 720 receivers will be deployed in eight parallel lines of 60 channels each with 880-ft line spacing. The recording patch will include 480 live geophone groups. Subsurface bin size will be 110 by 110 ft. At least 64% of the survey area (2.78 square miles) will have a minimum of 12-fold.

A total of three 3-D seismic surveys have been recorded by various companies not involved in this project in Bowman County, North Dakota, during 1994. These surveys were recorded with the use of Vibroseis sources with 165 by 165 ft (or greater) bin sizes. These surveys have been used for basic structural interpretation in exploration plays. No drilling has yet resulted from these surveys. The design selected for the Cold Turkey Creek will use a finer bin size for greater subsurface resolution and dynamite sources to obtain higher frequency than possible with Vibroseis by 15 to 20 Hz. The higher frequency and finer bin design will offer greater stratigraphic interpretation of the Red River interval.

Petrographical Studies

Petrographical studies of the Red River and Ratcliffe formations have begun. Approximately 10 cores from the upper and lower Red River intervals will be selected for detailed analysis and descriptions. Approximately four cores from the Ratcliffe study area will be analyzed. The analyses will include photo record of slabbed core on slides and video; thin-section analysis

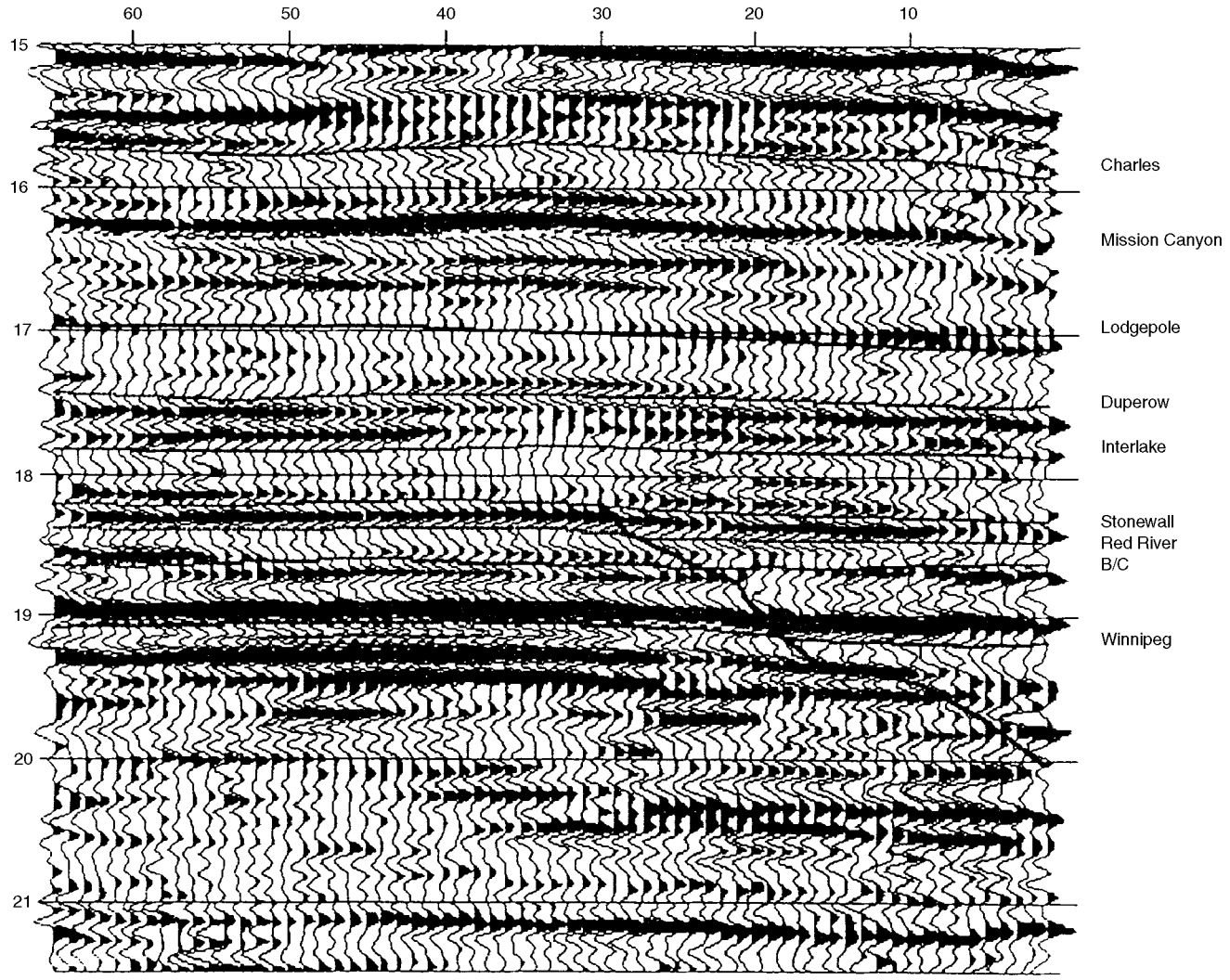

Fig. 6 Reprocessed 2-D seismic section HA6-7 from the Grand River School area with fault interpretation. The shallow fault angle at Grand River School and Cold Turkey Creek suggests a component of horizontal stress at the time of faulting.

with photographic record; correlation of rock type and description with conventional porosity, permeability, and fluid saturation records; correlation of rock type with electric log evaluation; depositional and digenetic processes; and porosity–permeability development relating to sediment material, water depth, post-depositional alteration, or fracturing.

Producibility Problem Characterization and Analysis

Extended-time pressure buildup tests were performed at two wells. One is a Ratcliffe completion in the Richland County study area and the other is a Red River completion in the Bowman–Harding study area. These pressure buildup data were acquired by acoustic surface-recording equipment. The pressure data are being evaluated and will be used as baseline data for comparison after reworking the completed intervals with the jetting-lance technology.

Recovery Technology Evaluations

Horizontal jetting-lance operations were attempted unsuccessfully in the Luff Travers No. 1-6 well (sec. 6, T. 22 N., R. 3 E., Harding County, South Dakota) during December 1994. Two attempts to drill horizontal holes were made during the period Dec. 5–10, 1994. On the last attempt, the casing was penetrated and 2 ft were drilled into the formation before pressure was lost through the lance. Attempts to retract and release the drilling tool were unsuccessful. From Dec. 12 to Dec. 20, 1994, fishing operations were conducted. The Red River Upper and Middle zones are still accessible in the wellbore for future attempts.

The effort to use the 50-ft horizontal jetting-lance tool as designed shows that the tool is in a developmental stage and not yet implementable. Because of this conclusion, Luff Exploration Co. management decided not to bill for charges related to this work. During the next several months,

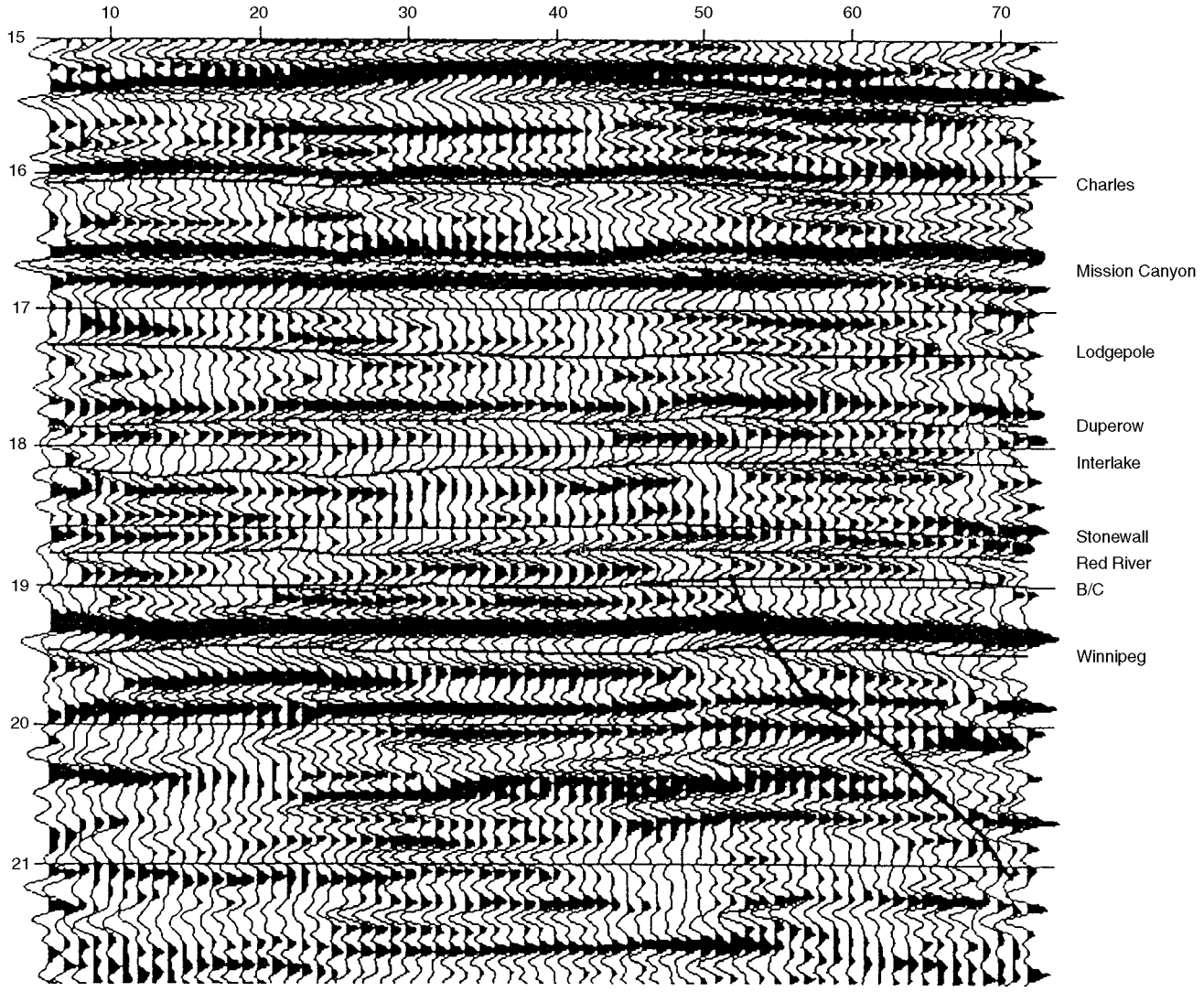

Fig. 7 Reprocessed 2-D seismic section CTC-27 from Cold Turkey Creek showing fault interpretation. The fault is down to northeast at 30 degrees from vertical. Maximum displacement is 40 to 50 ft at Winnipeg time.

improvements in the design of the 50-ft tool will be tested in a less-expensive environment. If this leads to the conclusion that the tool is beyond the developmental stage, the 50-ft jetting-lance tool will be returned to the Luff Travers well.

As an alternative to the 50-ft jetting-lance tool, another service company has been contacted to perform jetting operations with a tool that has an extension of 10 ft. This tool design has been successfully used at depths necessary for project activities. Cost and procedures are being prepared for four wells within project field-activity areas.

Activities Required for Project Continuation

A meeting was held in December 1994 with working interest owners of the SW Amor (Red River) field (T. 129–130 N., R. 103 W.), Bowman County, North Dakota, to review geological, geophysical, and engineering interpretations toward possible unitization in a waterflood project or injection pilot. Further meetings will be held after jetting-lance completions in the Red River are successfully performed with a water injectivity test.

Environmental Compliance

The seismic acquisition activities in Richland County, Montana, and Bowman County, North Dakota, are in nonsensitive areas. The 2-D three-component test line in Richland County, Montana, is shown in Fig. 7. The 2-D line will be located in the road right-of-way shown on the Dore and Fairview, NW quadrangles. The 3-D seismic acquisition at Cold Turkey Creek is shown in Fig. 8. This figure shows a 3-D area overlain on the Bowman, SW quadrangle. The topographical and associated floodplain maps relevant to these seismic activities have been submitted.

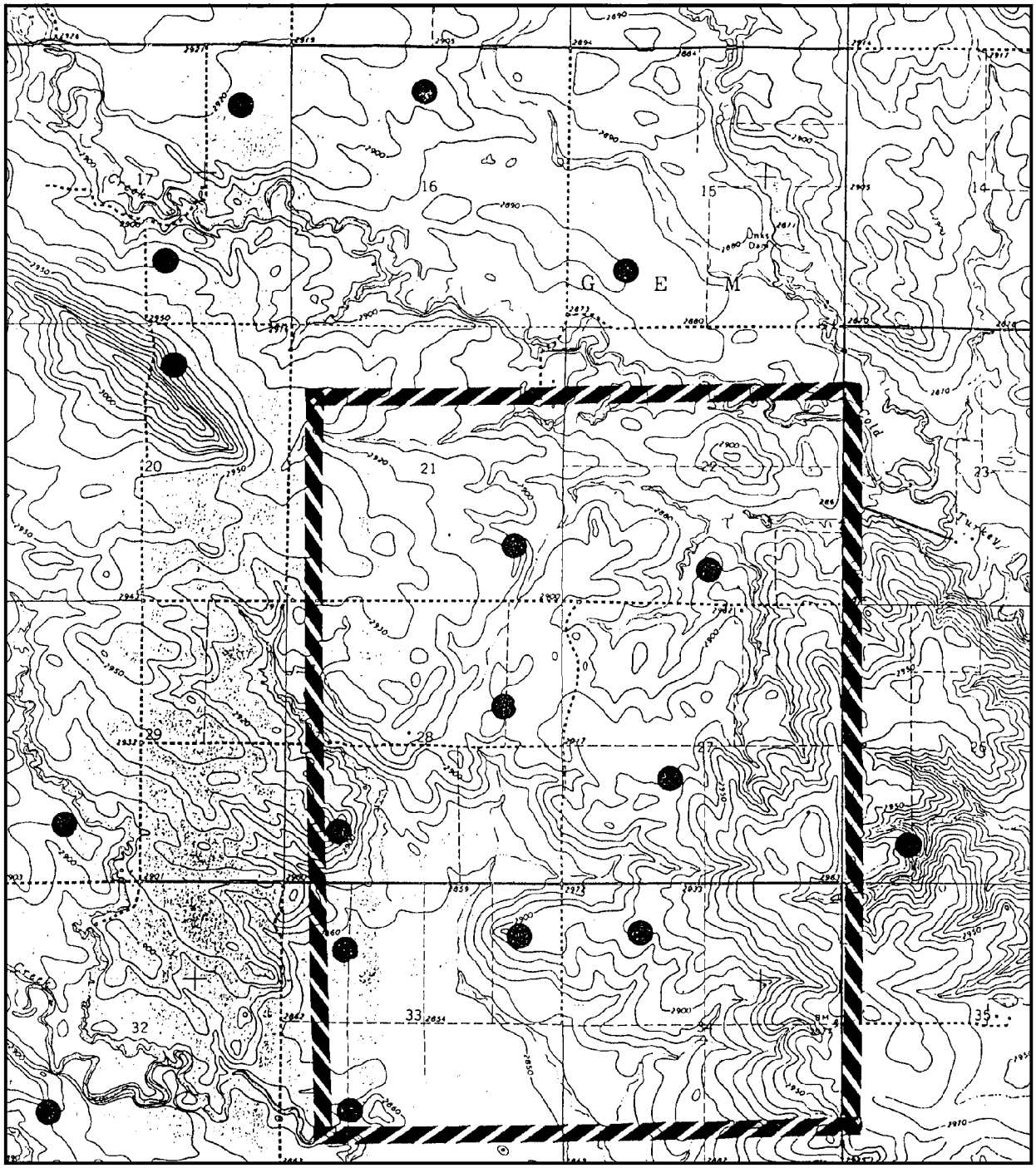

Fig. 8 Topographical map of the Cold Turkey Creek 3-D seismic area (Bowman, SW quadrangle). The 3-D survey is located on agricultural land used for cattle grazing and wheat.

VISUAL DISPLAY OF RESERVOIR PARAMETERS AFFECTING ENHANCED OIL RECOVERY

Contract No. DE-AC22-93BC14892

Michigan Technological University
Houghton, Mich.

Contract Date: Sept. 29, 1993
Anticipated Completion: Sept. 30, 1996
Government Award: $272,827

Principal Investigator:
James R. Wood

Project Manager:
Robert Lemmon
Bartlesville Project Office

Reporting Period: Oct. 1–Dec. 31, 1994

Objectives

The principal objective of this project is to provide the operators of small- to medium-sized oil fields with the tools necessary to undertake an enhanced oil recovery (EOR) reservoir characterization and evaluation of quality and sophistication similar to those performed by large oil companies. The techniques will be demonstrated in a field trial on Pioneer Anticline in the southern San Joaquin Valley. The study will include collection, visualization, and manipulation of well-log and borehole-sample data. Physical and chemical property data gathered from laboratory measurements of conventional core and cuttings will be used to develop algorithms relating geological and engineering parameters to log responses. Digitized logs calibrated in this fashion will be used to characterize the reservoirs in fields on the Pioneer Anticline. Core, well-log, and production data will be assembled in a commercial personal computer (PC)-based database manager. The database manager will be used to provide data input to commercial visualization software to produce two-dimensional (2-D) and three-dimensional (3-D) representations of reservoir geometry, facies and subfacies stratigraphy, and distribution of remaining oil in place as well as spatial displays of measured and calculated reservoir parameters. These database and visualization tools will be used to evaluate the reservoirs for EOR. In addition, rock alteration caused by interaction with hot fluids will be modeled quantitatively and used to predict reservoir response to thermal EOR. Many of these tasks are being performed on expensive computer workstations by major oil companies. A primary objective of this project is to transfer this workstation technology to PCs, where programs can be run for a tenth of the cost by small independent operators.

Summary of Technical Progress

Spatial Database Manager

Microsoft (MS) Access is being used as the project database manager. Data tables for geochemical, petrographic and geophysical well logs, well header information, and well production data are complete. Log data and well header information for 15 project wells and X-ray-diffraction (XRD) and Fourier transform infrared spectroscopy (FTIR) data traces for about 30 samples have been stored in the database. Data reporting forms and graphing macros are being prepared. Individual databases established in Excel, Lotus, and QuattroPro spreadsheets were uploaded to the Access database.

Data Collection

Digitization of the more than 45 wells that will be used to construct maps and 3-D visualizations of the Miocene reservoirs on Pioneer Anticline is complete. All the well logs that will be used in this project are digitized, corrected, plotted on uniform scales, and hung on the same datum. Preliminary correlations have been made, and a network for structural and stratigraphic cross sections has been laid out through the study area. Five cross sections are under construction with more to follow.

The QuattroPro spreadsheet being used to document, display, and inventory the log data set was expanded to include all 242 wells for which data or well files have been obtained. More than 45 wells that have the best log coverage or are in the most critical locations will be used in the main study, which will be confined to a 12-section area in T. 11 N., R. 22 E. Although the main study area will be confined to the eastern end (nose) of the Pioneer Anticline, these additional wells will be available to provide regional perspective.

Data Analysis and Measurement

Data preparation and log calibration were completed on the three wells that have both conventional core and modern log suites: the McKittrick Front No. 415 and No. 418 wells in Cymric field and the Tenneco No. 62x-30 well in Pioneer field (Figs. 1 and 2). Because log calibration is time consuming and the McKittrick Front No. 418 well contains over 700 ft of conventional core with thousands of petrophysical analyses, the completion of calibration for these three wells represents a significant step forward in project development.

The log core petrophysical calibrations for the three best wells are essentially complete. Additional refinement of the calibrations will be performed as the results of XRD, rock chemistry, and FTIR analyses of core materials become available, but for now there is a working calibration equal to that used in most reservoir studies. Analysis and modeling of the other 45+ wells with log suites, but no core, can now begin.

The FTIR subtask has concentrated on development of analytical technique and acquisition and utilization of standards. Mathematical inversion techniques have been

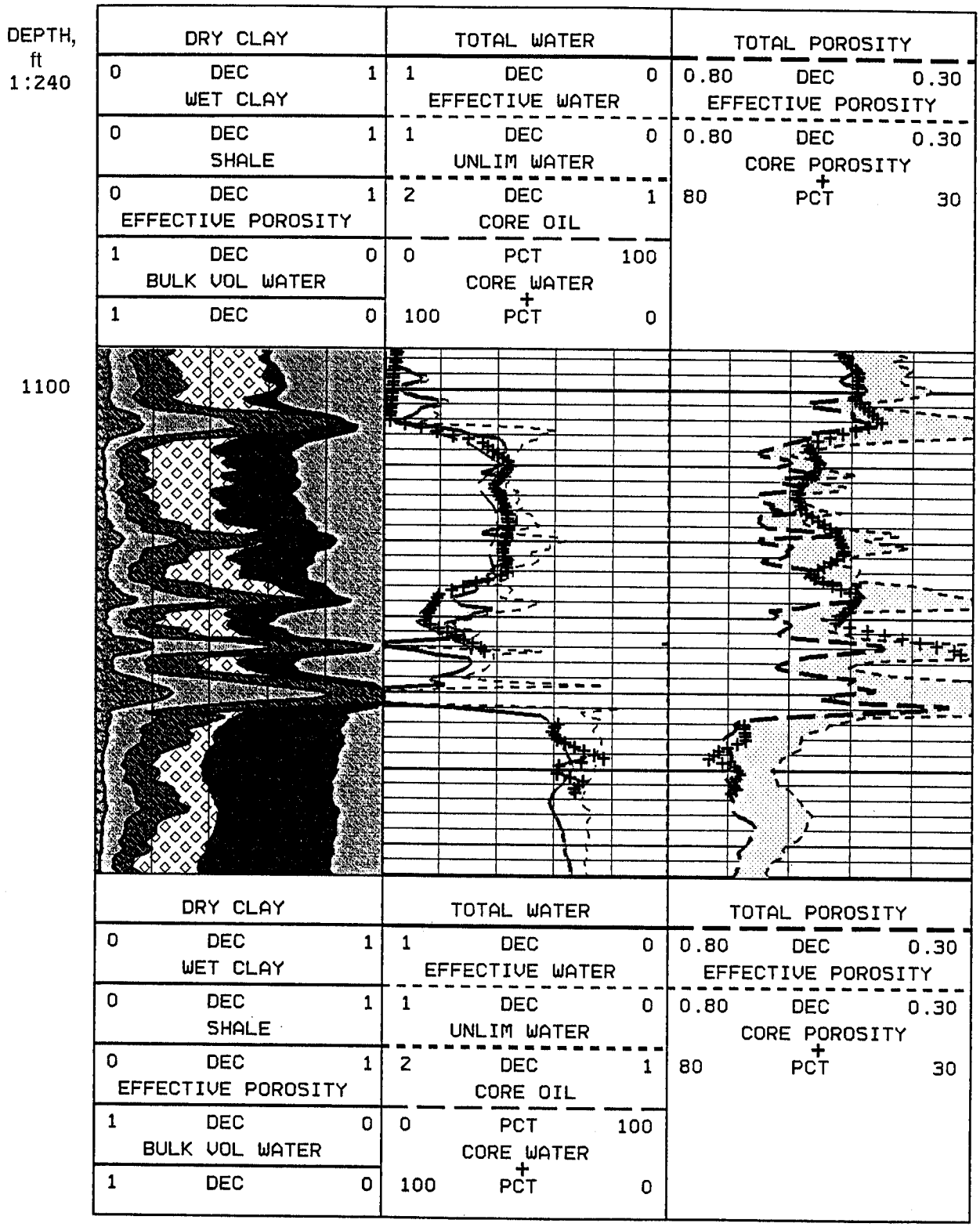

Fig. 1 Analyzed results log calibrated to core in the Unocal McKittrick Front No. 418 well, Cymric field. Interval includes the Tulare formation–Monterey formation contact. Note large increase in porosity across contact and very high porosity in Monterey Opal-A facies diatomite beneath the contact. This interval represents just a small portion of the 700 ft of core that was calibrated to the log suite in this well.

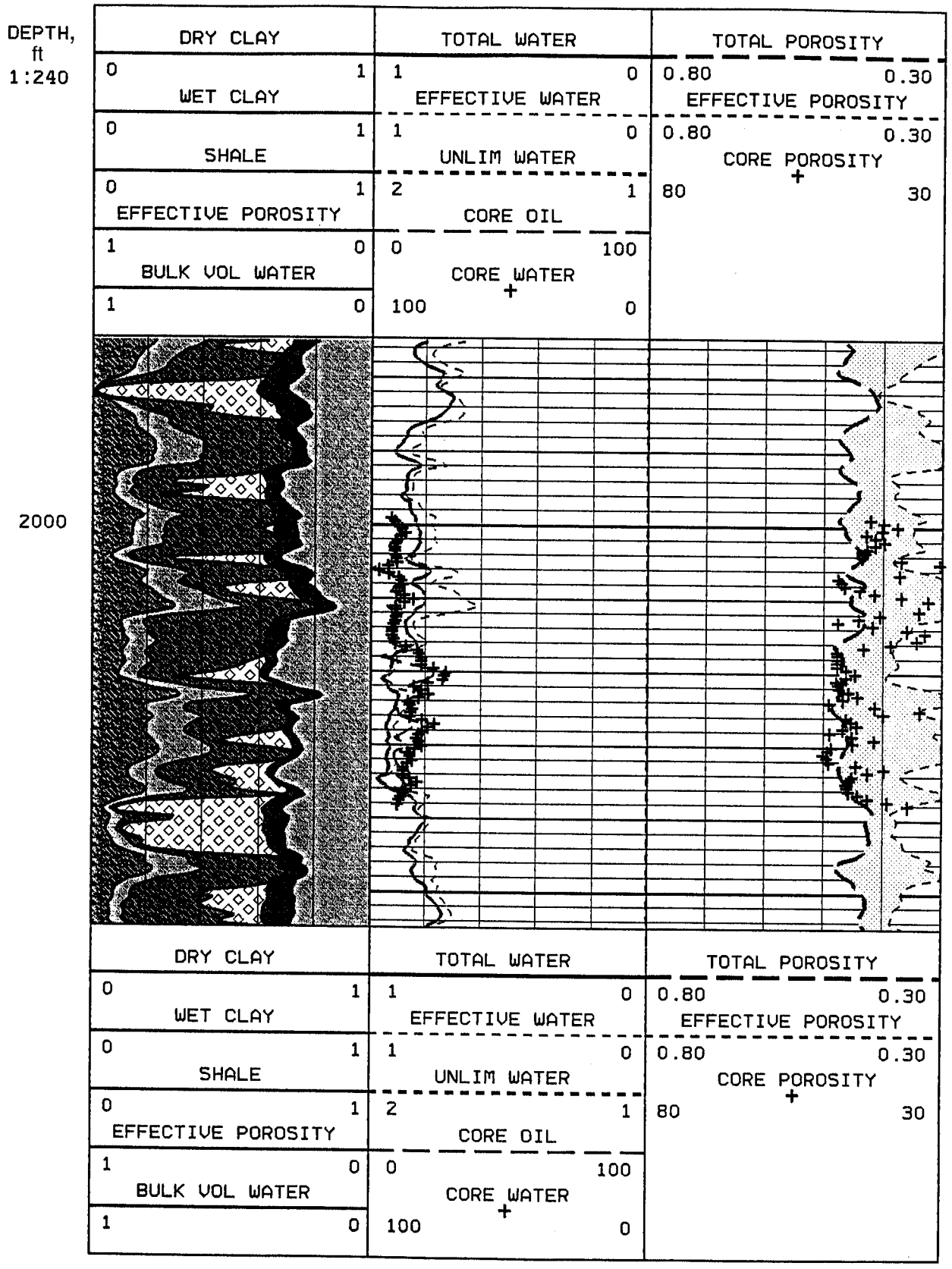

Fig. 2 Analyzed results log calibrated to core in the Tenneco No. 62x-30 well, Pioneer field. Note the much lower porosity in the Opal-CT facies encountered in this well.

developed, and work will shift to analysis of cuttings from the Pioneer field with emphasis on quantitative mineralogy of the silica facies in the Monterey formation. Reliable analytical techniques for sample preparation are in hand, and a suite of mineral standards suitable for analysis of Monterey samples has been accumulated.

Material from the McKittrick Front calibration wells is being analyzed with the use of scanning electron microscopy (SEM) petrographic image analysis (PIA). The fine-grained nature of the Monterey reservoir facies makes the material difficult to characterize petrographically with standard thin-section microscopy. An attempt will be made to control the SEM results through constraints provided by bulk chemical analyses (standard wet chemistry) and the FTIR results.

Modeling

The geochemical modeling program CHILLER will be used to model fluid–rock interaction. The stable isotope modeling program ISOTOPIA will model the stable isotopic evolution of the fluid and the minerals. In preparation for modeling of steamflooding, the mass transfer and stable isotope modeling programs have been tested by modeling the interaction of an arkosic sandstone assemblage with sea water. The results indicate that both programs produce sound results.

Technology Transfer

Development of the multimedia program was switched from Macintosh MacroMind Director to the Windows environment. The hardware and software necessary for writing to CD-ROM are available for use in another department at Michigan Technological University.

RECOVERY OF BYPASSED OIL IN THE DUNDEE FORMATION USING HORIZONTAL DRILLING

Contract No. DE-FC22-94BC14983

Michigan Technological University
Houghton, Mich.

Contract Date: Apr. 28, 1994
Anticipated Completion: Apr. 27, 1997
Government Award: $800,000

Principal Investigator:
James R. Wood

Project Manager:
Chandra Nautiyal
Bartlesville Project Office

Reporting Period: Oct. 1–Dec. 31, 1994

Objective

The objective of this project is to provide the operators of the small- to medium-size oil field with the tools necessary for an enhanced oil recovery (EOR) evaluation of the same quality and sophistication that only large international oil companies have been able to afford to date.

Summary of Technical Progress

Project Management

Although project members are located at four sites (Tampa, Fla.; Houghton, Mich.; Kalamazoo, Mich.; and Los Angeles, Calif.), project coordination has been successful. Trips are made to work on project tasks with other project members, and the computer network and server at Michigan Technological University (MTU) comprise a critical link in the communications network.

Reservoir Characterization

Geologic, geophysical, hydrologic, and engineering techniques are being used to quantify reservoir heterogeneities and controls on producibility. The Crystal field is the focus of the characterization effort, but up to 30 other Dundee fields are being studied as well. Well and log data sets and production data sets for all 30 fields are complete.

Well Log Acquisition, Digitization, and Analysis

Well data, including drillers' logs, wireline logs, and seismic data from the Crystal and other Dundee formation hydrocarbon fields in the Michigan Basin (Fig. 1), were acquired. Digitized logs of 342 wells that currently produce or have produced from the Dundee formation in the seven-county study area were purchased from Maness Petroleum Co. Multiple logs exist for each well and include gamma-ray, caliper, lithodensity, neutron-porosity, various types of resistivity, and some sonic logs. The logs total about 3 million linear feet of digitized data. All deep wells in the area are included in the log suite. The data-gathering phase of the well log program is complete, and activity has advanced to the construction of maps and cross sections from well data.

During this quarter production data were added to the well-file database; the data provide the capability for mapping production as well as geology. Well location maps were constructed for all 30 fields. Contour maps were constructed for several fields on the top of the Dundee formation (Fig. 2), the top of the Dundee formation porosity zone (which is well below the top of the Dundee and varies in stratigraphic position throughout most fields) (Fig. 3), and initial production (Fig. 4). Simple computer-generated cross sections were constructed for the same fields (Fig. 5). Construction of contour maps and cross sections for the remaining fields will

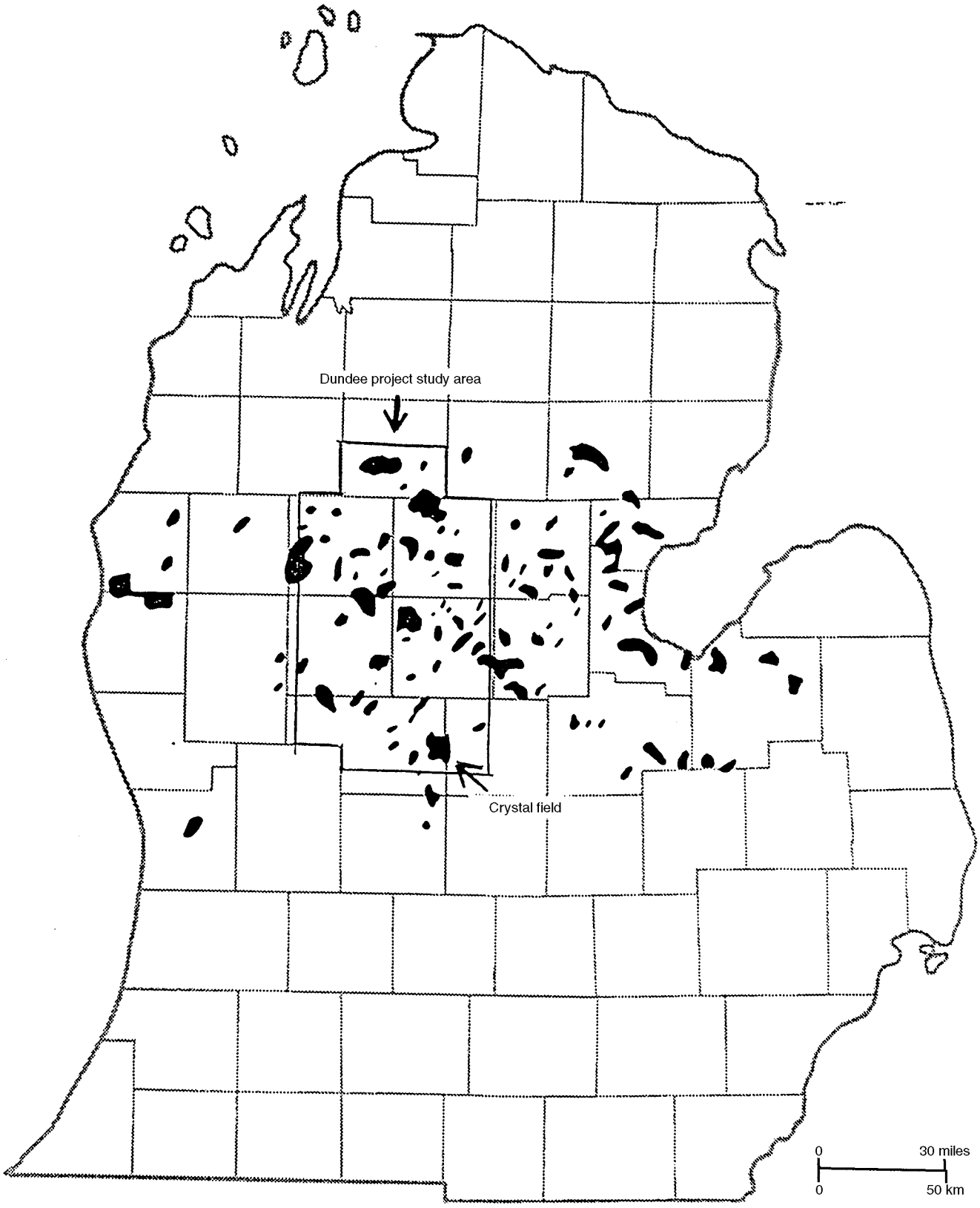

Fig. 1 Dundee formation oil and gas fields.

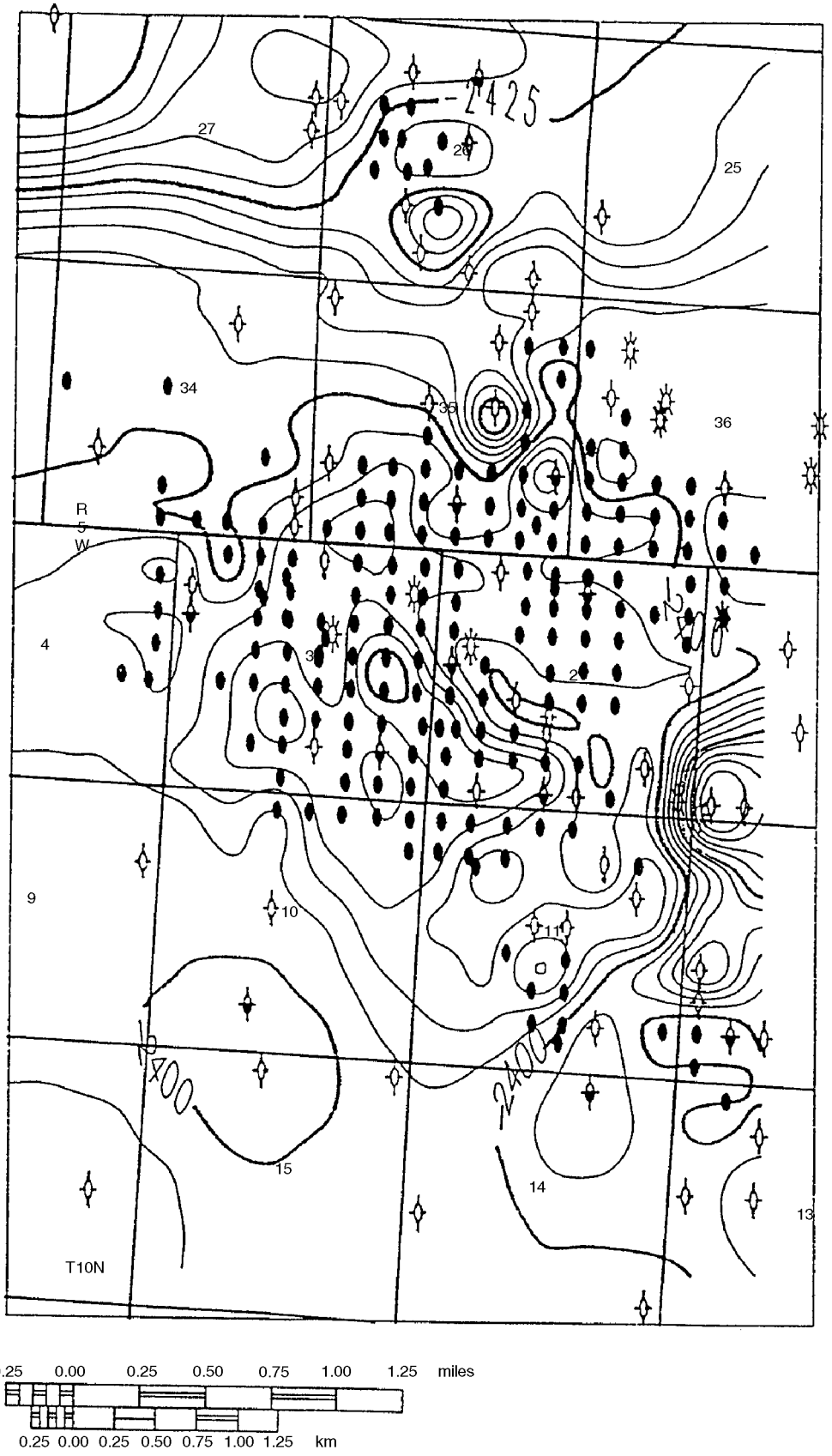

Fig. 2 Structure contour map on top of subsea zone, Dundee formation, Crystal field. Contour interval, 5 ft.

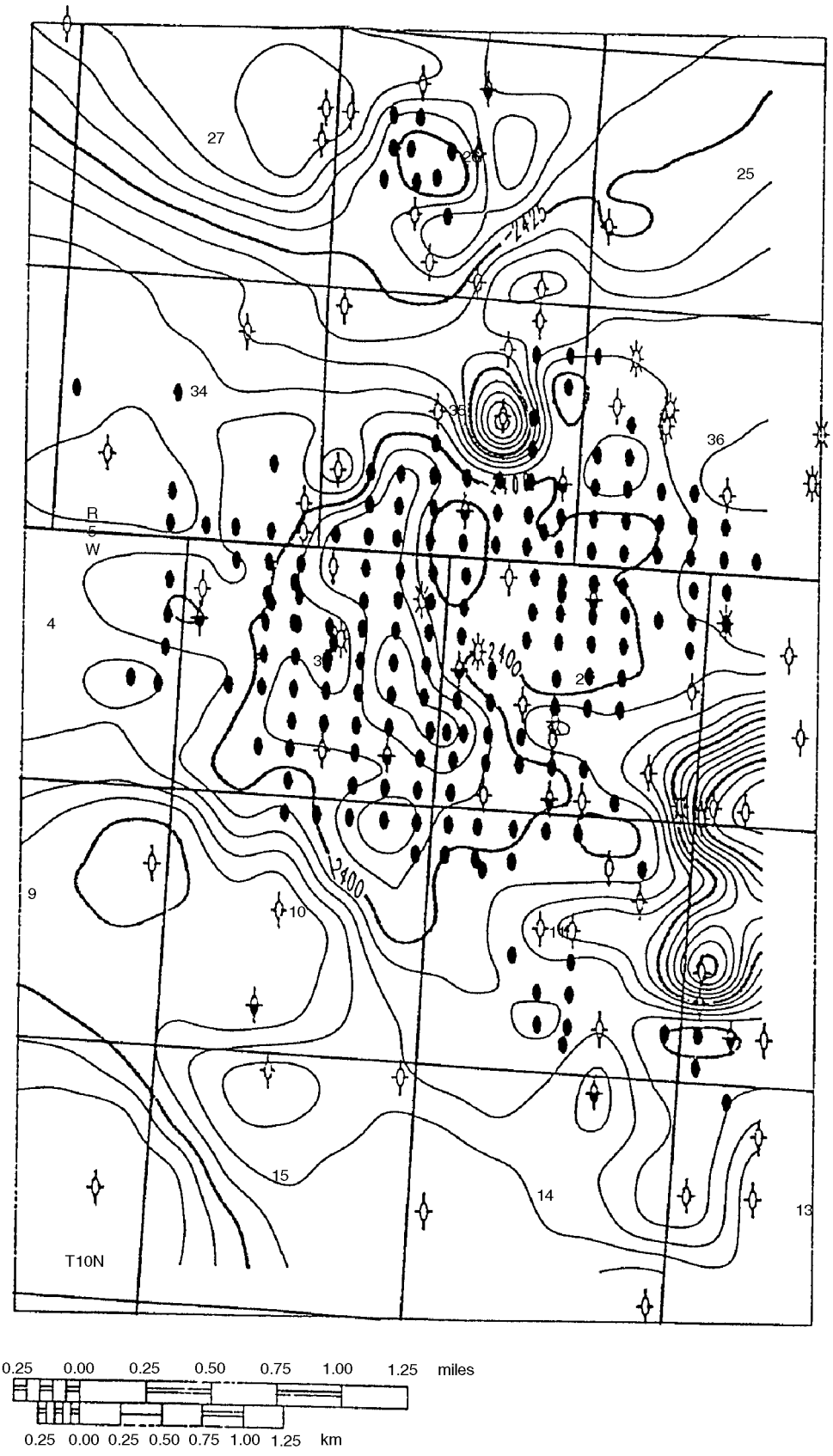

Fig. 3 Structure contour map on top of porosity subsea zone, Dundee formation, Crystal field. Contour interval, 5 ft.

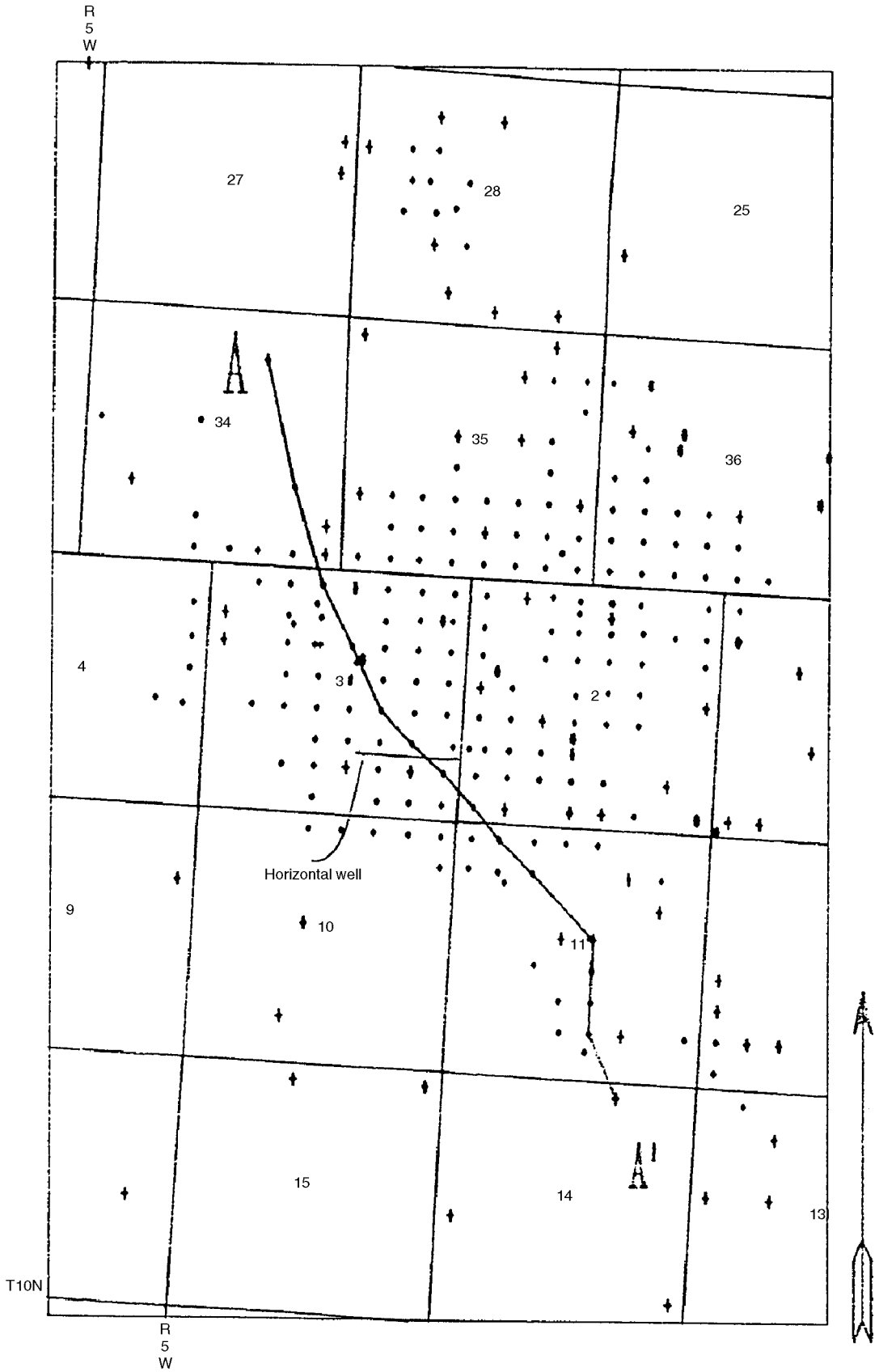

Fig. 4 Cross section of initial production fields, Crystal field.

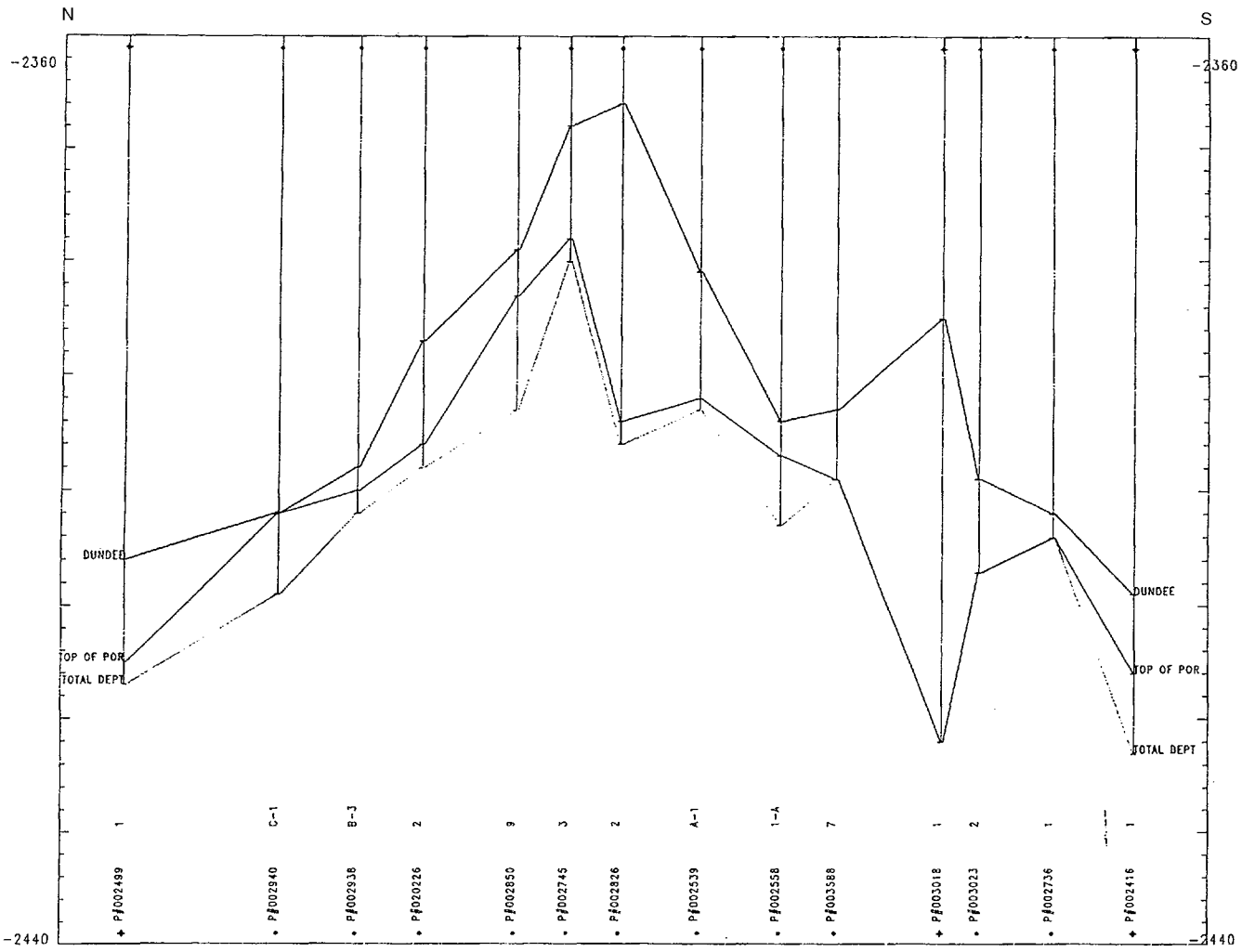

Fig. 5 Structural cross section, Crystal field.

continue. With production data for all the fields in the database, cumulative production maps can be constructed. Interval isopach maps of top Dundee to top Dundee porosity zone will also be constructed.

Winterfield Field

A Master's thesis is being written on Winterfield field (Fig. 6), which possesses more modern log data than most other Dundee formation fields. In addition, several Winterfield wells penetrate the entire Dundee porosity zone, which allows a more thorough evaluation of the reservoir than can be done elsewhere. The Winterfield study will delineate possible economic zones of bypassed oil in the Dundee formation by characterizing the structural, stratigraphic, and lithological components of the formation with the use of well data, petrophysical log data, and production data.

Porous dolomite above the oil–water contact, capped by either the Bell shale or tight Dundee limestone, is the producing lithology within the Dundee formation. The producing zones can be discerned readily from a suite of geophysical logs (Fig. 7). These logs can be further enhanced to determine corrected porosity values in the producing interval. Corrected porosity values were calculated for all wells with the use of the KOBRA:XPLOT algorithm of TerraSciences TerraStation software, which is based on Schlumberger cross-plots. Water and oil saturation values were calculated and plotted as a contour map. Potential areas for further exploration can be delineated by comparing leases that appear to be underachievers relative to structural position, initial production tests, and relative production with surrounding similar wells that produce from similar lithologies.

Core Acquisition and Analysis

Twenty to thirty cores of the Dundee formation from throughout the state of Michigan are available. Cuttings samples are also available from 60 to 100 Michigan wells. There are no cores in Crystal field, the site of the field trial. The closest Dundee core is in an output well 8 to 10 miles away

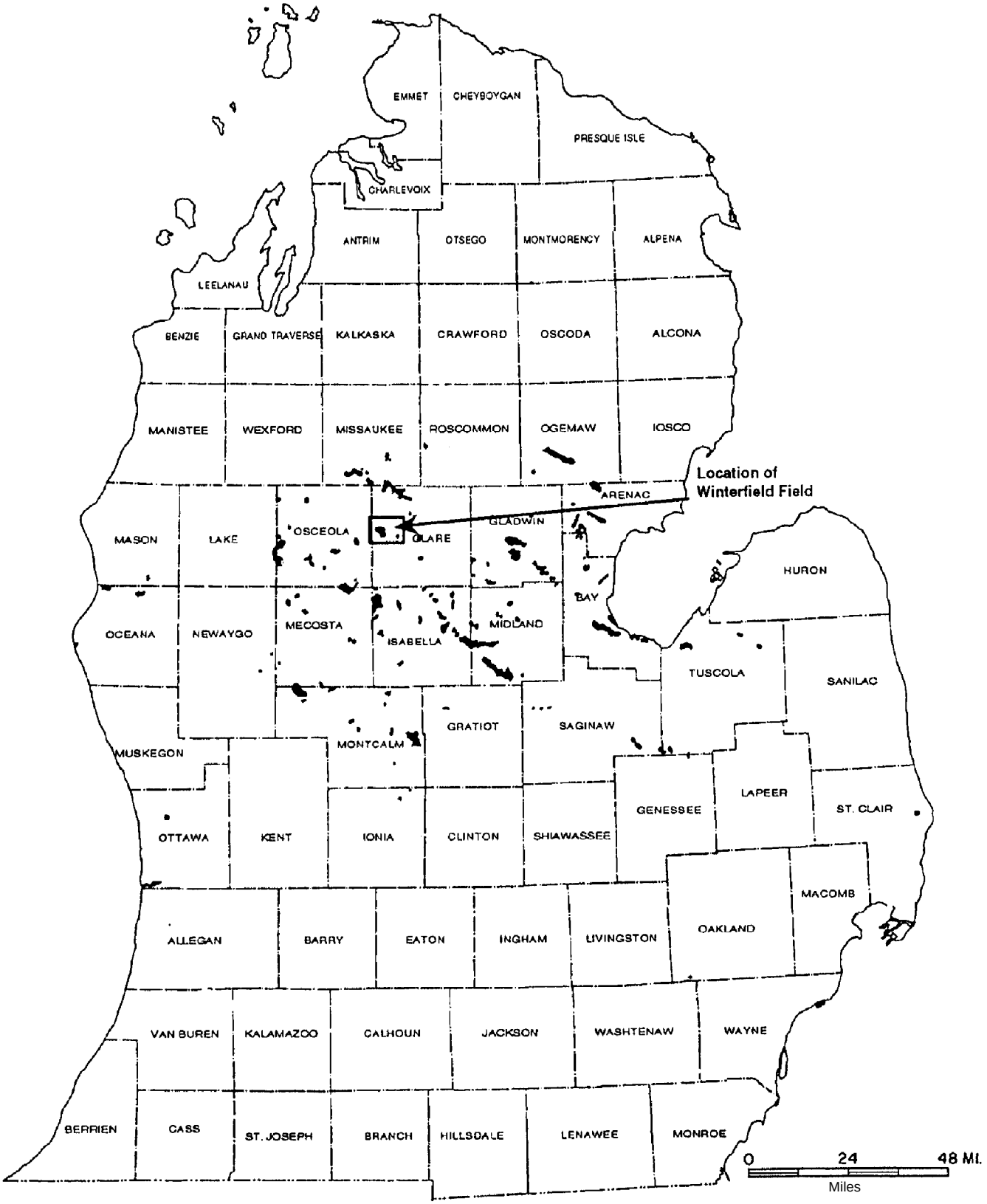

Fig. 6 Map of Dundee oil fields in Michigan. Note NW-SE lineations of fields.

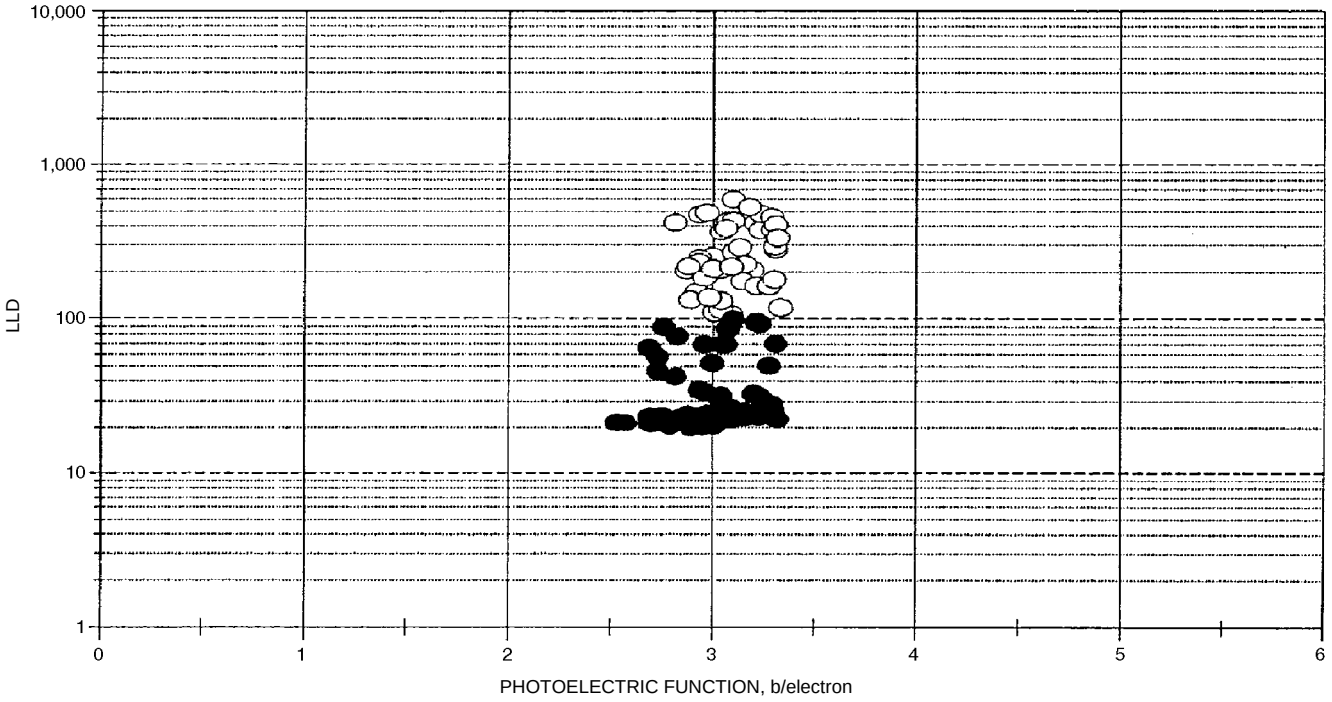

Fig. 7 Photoelectric function–LLD cross-plot (Dart Oil and Gas, Austin 3-31). ○, oil saturated. ●, water saturated.

from Crystal field. Thus a good vertical core through the Dundee formation in Crystal field is an essential element of the reservoir characterization study.

Scanning electron microscope (SEM) analyses of a few selected samples were made at Western Michigan University (WMU), and Fourier transform infrared (FTIR) radiation spectroscopy analyses have begun at MTU. Techniques for performing quantitative analyses of rock samples with FTIR are being developed as part of another Master's thesis. Hydrocarbon and produced-water samples from the Crystal field have yet to be collected and analyzed.

Database Management

Thirty Dundee formation fields are being studied. Well data (driller's logs and scout tickets), log data, and production data sets for all 30 fields are complete. The data are stored in TerraSciences TerraStation database at WMU.

Drilling Program

Drilling of the horizontal well at Crystal field was delayed pending completion of an environmental survey (Fig. 8). A vertical well at an appropriate location in the project area has been designed and permitted. The well will be cored through the producing interval of the Dundee formation, and the cores will be analyzed for porosity, permeability, and fluid saturations. A full set of well logs will be run. These data will be incorporated into the existing database for the project area and used to calibrate the measurement while drilling logs which will be run during the drilling of a horizontal leg and which will be drilled as a sidetrack from the vertical test well.

Technology Transfer

A prototype multimedia-based shell using MacroMind Director was designed and developed as a technology transfer mechanism. All data and information associated with the project will be stored on a hard disk and will be accessible via the interactive multimedia shell program. At the end of the project, all data, graphics, tutorials, manuals, etc., will be stored on CD-ROM for distribution to the U.S. Department of Energy and the target audience within the petroleum industry.

The project managers have contracted to present an exhibition booth at the American Association of Petroleum Geologists (AAPG) annual meeting to be held in Houston, Tex., March 5–8, 1995. The booth will include a poster display describing project goals and progress to date.

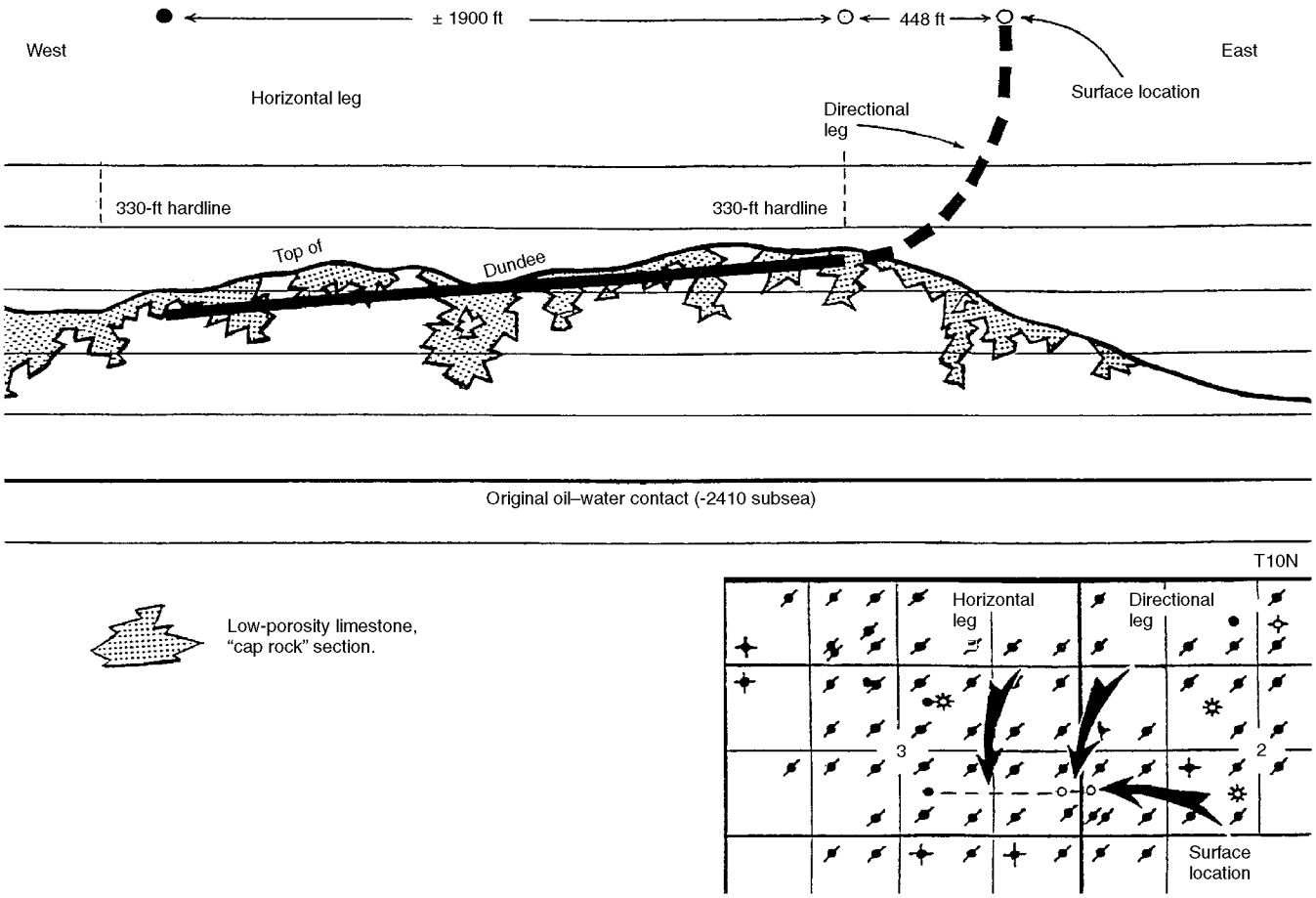

Fig. 8 Geologic cross section of proposed horizontal well location at Crystal field.

APPLICATION OF RESERVOIR CHARACTERIZATION AND ADVANCED TECHNOLOGY TO IMPROVE RECOVERY AND ECONOMICS IN A LOWER QUALITY SHALLOW SHELF CARBONATE RESERVOIR

Contract No. DE-FC22-94BC14990

Oxy USA, Inc.
Midland, Tex.

Contract Date: Aug. 3, 1994
Anticipated Completion: June 14, 1996
Government Award: $1,922,000

Principal Investigator:
Archie Taylor

Project Manager:
Chandra Nautiyal
Bartlesville Project Office

Reporting Period: Oct. 1–Dec. 31, 1994

Objectives

The objective of the project is to show that the use of advanced technology can improve the economics of carbon dioxide (CO_2) projects in low-permeability reservoirs. The approach involves the use of tomography and pore throat measurements to enhance reservoir characterization. Cyclic CO_2 stimulations and fracture treatments will be used to increase and facilitate oil recovery to improve project economics. Reservoir description and simulation will be used along with cyclic CO_2 stimulations and fracture treatments to arrive at an optimum operating plan to be instituted during the second budget period. Work in the area of cyclic CO_2 stimulation and reservoir characterization took place prior to the official start date (Aug. 3, 1994) under pre-award approval.

Work accomplished during this quarter included detailed petrophysical description of cores from the observation wells, integration of the petrophysical data into a geologic model, acquisition of the tomography surveys, initial processing of tomographic data, completion of enhanced interpretation of three-dimensional (3-D) seismic volume in the U.S. Department of Energy (DOE) demonstration area, development of relationship between seismic attributes and well log parameters, and completion of cyclic CO_2 stimulation treatments.

Six tomography surveys are yet to be conducted. Processing of the tomographic data has been slow, but it will accelerate with upgraded computing power. The initial CO_2 injection into one of the cyclic wells is incomplete.

Summary of Technical Progress

Reservoir Characterization

Updating Existing Characterization

The petrophysical analysis on the two observation well cores is complete. The analysis included thin-section descriptions on 85 samples, scanning electron microscopy (SEM) analysis on 60 samples, determination of rock fabric, and correlation of rock fabrics to log response. In addition, rock fabrics are being related to depositional environments and sequences.

A collaborative analysis of the two observation well cores to determine depositional environment and sequence stratigraphy was performed. The description and analysis of eight additional West Welch Unit (WWU) cores within the DOE project area are complete. Fifty-three thin sections taken from the WWU No. 3211 were described and photographed. An existing thin-section analysis was available on WWU No. 4849. The abundance of these section data allowed construction of a revised rock fabric classification for the WWU. Rock fabric classes increased from eight to nine. The new system was used to classify the core analysis from WWU No. 3211. The revised and expanded petrophysical data are being input into the geological database.

Observation Wells

The second observation well was drilled and completed in October 1994.

Tomography Survey

Nine additional wells were deepened and directional surveys run, which brings the total number of wells prepared for tomography acquisition to 15. Only one well, WWU No. 48-28, remains to be deepened and surveyed. Seven of the wells were plugged back and placed in service.

The data-acquisition phase of the tomography survey began Oct. 13, 1994, with testing to determine the best possible parameters to obtain frequency content, number of shots, and number of air guns required for best energy levels. It was determined that optimum results can be obtained with one air gun and four to eight shots per profile over most of the project. Activation of the source at 12 to 15 levels for each tomogram will achieve 5-ft spacing across the zone of interest and create a signal around 1500 Hz. All data are being acquired with the digital (rather than analog) receivers. Two air guns are required on the longer distance receiver to source profiles to achieve an adequate energy level.

Production began on Oct. 21, 1994, on the North pattern, which consists of source well No. 7916 and receiver wells No. 32-6, No. 79-1, No. 32-3, No. 4832, No. 48-24, No. 7914, and No. 48-27. Data acquisition was complete by Dec. 1, 1994. Production on the South pattern was complete by Dec. 18, 1994. The South pattern consists of source well No. 4852 and receiver wells No. 4841, No. 48-22, No. 48-27, No. 48-9, No. 48-28, No. 4843, and No. 48-8. A tie between the two patterns was established by sourcing in well No. 48-25 and receiving in well No. 48-27 (Fig. 1). The first phase of the survey was completed Dec. 21, 1994, with a total of 10 tomograms being acquired; 6 tomograms are yet to be surveyed. The field data quality ranged from good to excellent.

Data processing occurs in two stages. The first stage sorts, picks, and stacks both the compression and shear wave data. The second stage quality checks the stack and performs inversions to produce the final tomogram for each data set. The first stage processing is complete on receiver wells No. 32-6, No. 7914, and No. 48-25 in the North pattern. The second stage processing to date has produced a preliminary tomogram on well No. 32-6. Once the first tomogram is processed as final state, the processing sequence will be set to allow the remaining tomograms to be produced more quickly.

3-D Seismic Data

Seismic inversion processing was undertaken in the WWU project area to enhance the stratigraphic interpretability of the seismic data for the San Andres pay zones. A post-stack F-X deconvolution was applied to the seismic volume to improve the signal-to-noise ratio. A spectral shaping filter was applied to match the reflectivity of the seismic trace to that found in well log data. A phase correction of 90° was necessary to balance the energy between the seismic amplitude series and the log reflectivity data. Calibration of seismic amplitude to average sonic reflectivity was completed on a sample-by-sample basis to calculate velocities. A low-frequency component (less than 8 Hz) was created with the use of the structural interpretations for seven horizons across the seismic volume with the sonic log data. A 3-D velocity model was derived to combine with the inverted seismic data for the final output file.

A data-driven methodology described by Shultz et al.[1–2] has been developed to integrate seismic attribute data with well log data. The geological workstation software, Stack Curves System (SCPC), has been updated to emulate this data integration technique. The method has been successfully applied with SCPC to another field. The pore volume of a Queen sandstone reservoir across a 3-D seismic volume has been described with the relative amplitude, the instantaneous frequency, the instantaneous phase, and the two-way time thickness all measured across the reservoir interval.

Saturation Distributions

Although the petrophysical analysis resulted in the identification of nine different rock fabrics, it has been concluded that only four rock types (three productive and one

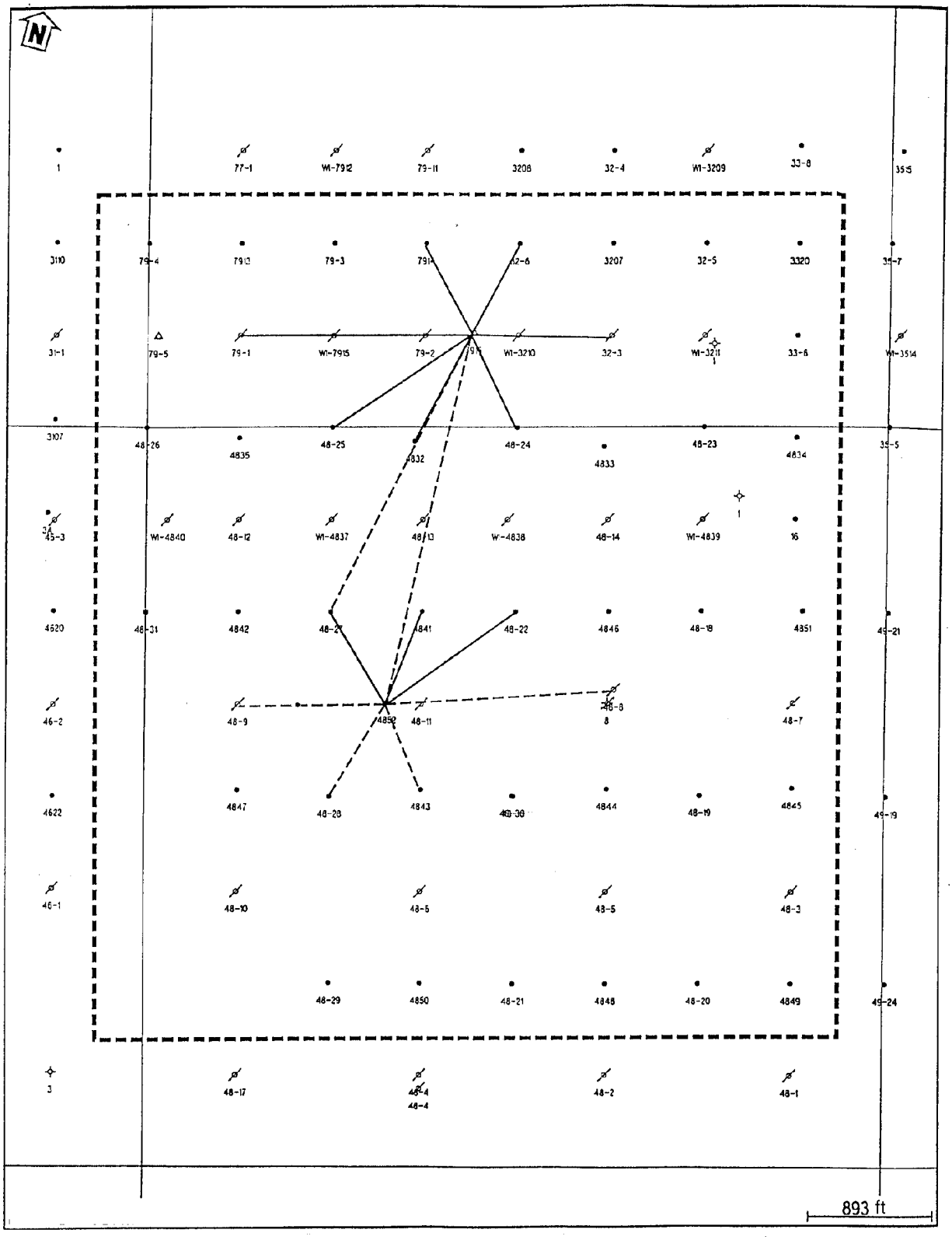

Fig. 1 Plat of West Welch Unit wells.

nonproductive facies) are significant in the development of the reservoir simulator. A preliminary geologic model that consists of 19 layers was built into the reservoir simulator for a limited area (60 acres) in the eastern portion of the WWU. The geological facies correlation was used to construct the 19-layer model on the basis of well control, which resulted in

the pinchout of some layers between wells. The preliminary production and injection history match was much better than that obtained with simpler geologic models that do not project zone pinchout. This was done prior to startup of the DOE project.

Laboratory Testing Requirements

Descriptions of the proposed test procedures for the special core analysis were submitted to various laboratories for cost estimates. The main purpose of the analysis is to obtain water–oil relative permeability and miscible CO_2 performance data.

Cyclic CO_2 Stimulation Evaluation

The initial CO_2 stimulation treatment in WWU No. 4835 and WWU No. 4851 was reported previously. After approximately 16-d soaking periods, the wells were flowed back in early October 1994. Both wells have since been placed on pump. The average production for WWU No. 4835 before the treatment was 15 bbl of oil per day (BOPD). The maximum oil rate recovered after treatment is 21 BOPD. A question exists as to the average pretreatment producing rate on WWU No. 4851. A portable tester used in July 1994 indicated 30 BOPD, but the lease satellite tester in September 1994 indicated only 20 BOPD. The well has recorded a maximum producing rate of 48 BOPD after treatment.

WWU No. 3205 was stimulated with 5 million cubic feet (MMCF) of CO_2 and allowed to soak 18 d before flowback started on Nov. 5, 1994. Pretreatment production was 4 BOPD. The well flowed only gas for 25 d. Placed on pump on Dec. 3, 1994, the well has averaged only 3 BOPD on pump and exhibits symptoms of interference.

WWU No. 4847 was stimulated with 5 MMCF of CO_2 and allowed to soak 21 d until flowback began in mid-November 1994. Prior production was 9 BOPD. Since the well was placed on pump, it has averaged 8 BOPD.

Figures 2 to 13 contain performance data on the four wells that have been stimulated.

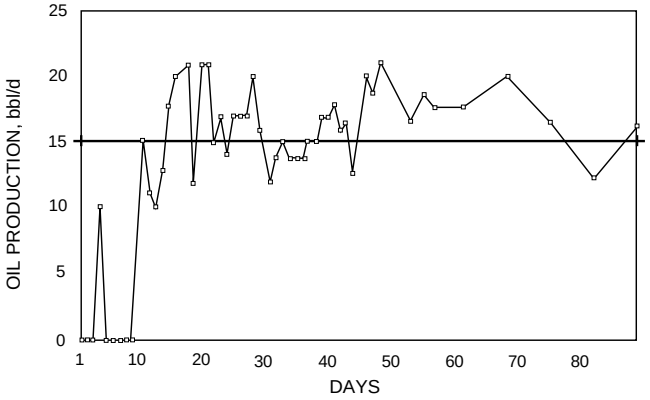

Fig. 2 West Welch Unit No. 4835 cyclic CO_2 treatment. Oil production: +, before treatment. —□—, after treatment.

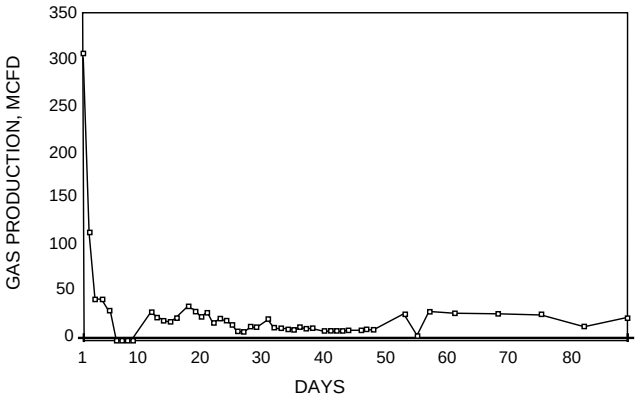

Fig. 3 West Welch Unit No. 4835 cyclic CO_2 treatment. Gas production: +, before treatment. —□—, after treatment.

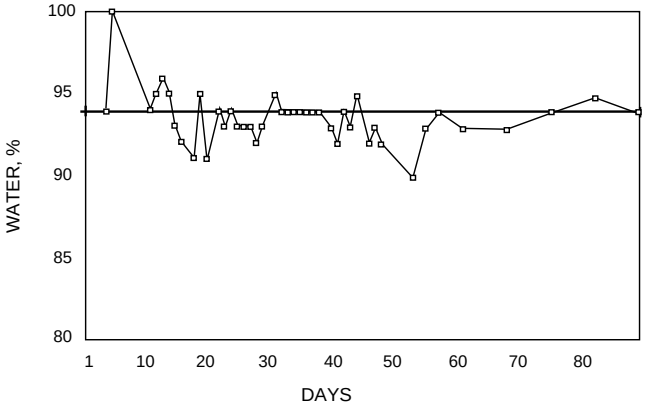

Fig. 4 West Welch Unit No. 4835 cyclic CO_2 treatment. Water cut: +, before treatment. —□—, after treatment.

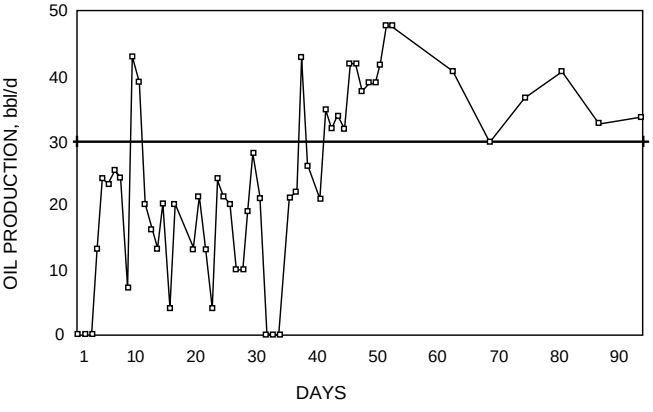

Fig. 5 West Welch Unit No. 4851 cyclic CO_2 treatment. Oil production: +, before treatment. —□—, after treatment.

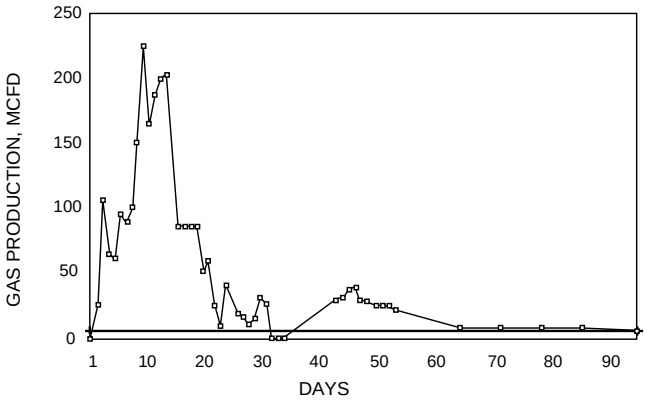

Fig. 6 West Welch Unit No. 4851 cyclic CO_2 treatment. Gas production: +, before treatment. —□—, after treatment.

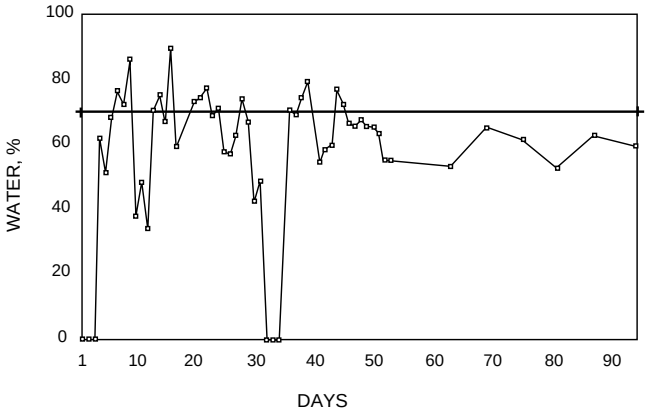

Fig. 7 West Welch Unit No. 4851 cyclic CO_2 treatment. Water cut: +, before treatment. —□—, after treatment.

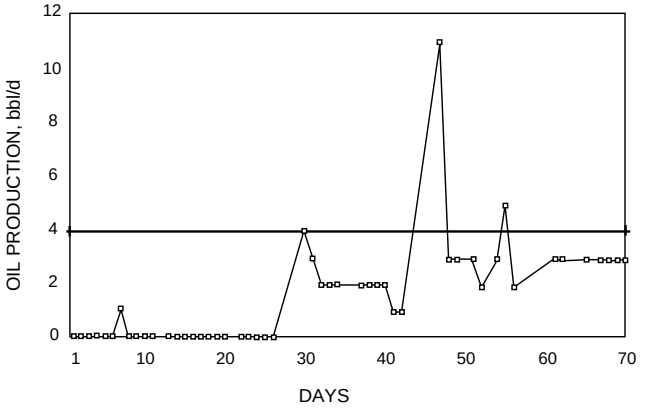

Fig. 8 West Welch Unit No. 3205 cyclic CO_2 treatment. Oil production: +, before treatment. —□—, after treatment.

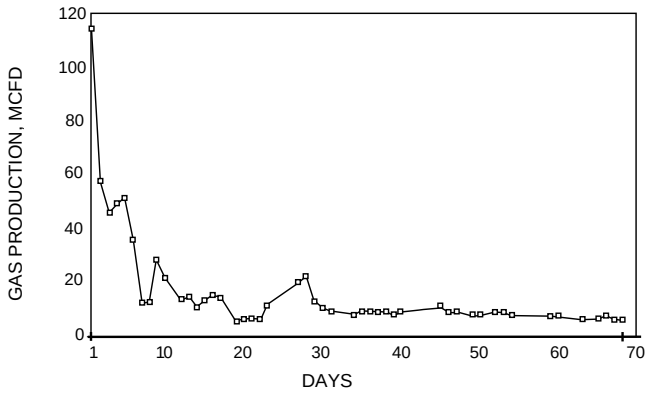

Fig. 9 West Welch Unit No. 3205 cyclic CO_2 treatment. Gas production: +, before treatment. —□—, after treatment.

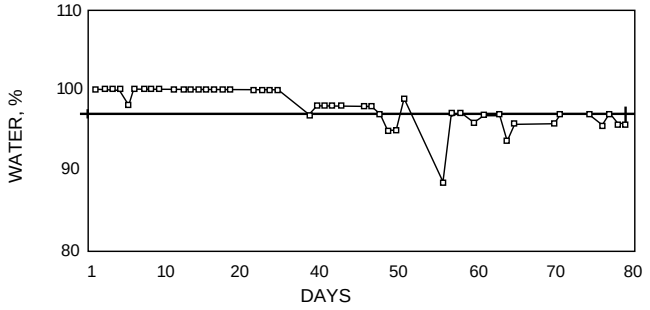

Fig. 10 West Welch Unit No. 3205 cyclic CO_2 treatment. Water cut: +, before treatment. —□—, after treatment.

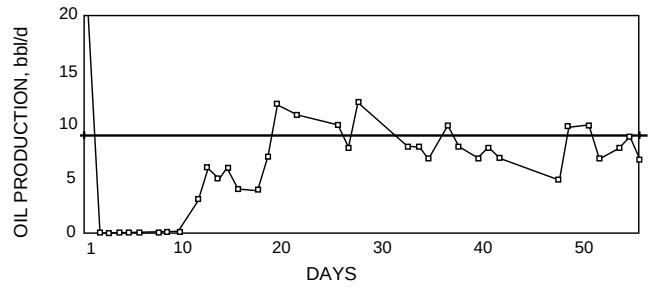

Fig. 11 West Welch Unit No. 4847 cyclic CO_2 treatment. Oil production: +, before treatment. —□—, after treatment.

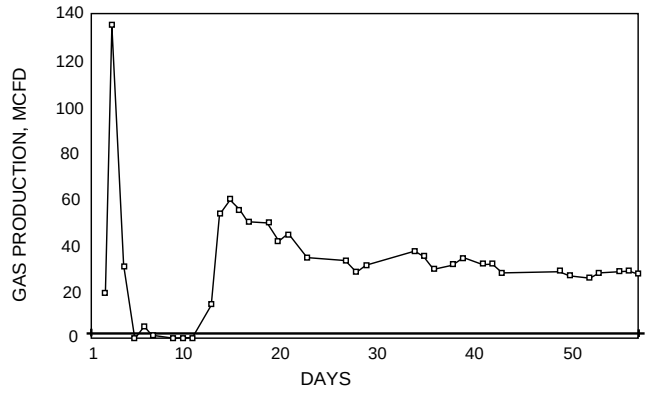

Fig. 12 West Welch Unit No. 4847 cyclic CO_2 treatment. Gas production: +, before treatment. —□—, after treatment.

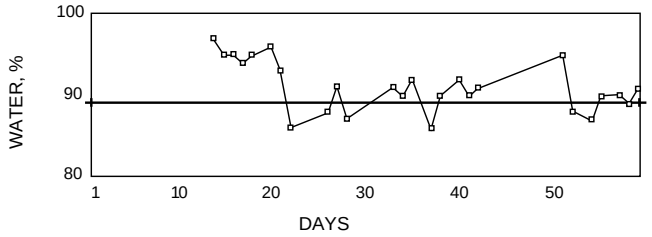

Fig. 13 West Welch Unit 4847 cyclic CO_2 treatment. Water cut: +, before treatment. —□—, after treatment.

References

1. P. S. Schultz, S. Ronen, M. Hattori, and C. Corbett, Seismic-Guided Estimation of Log Properties: Part 1: A Data-Driven Interpretation Methodology, *Leading Edge*, 13(5): 305-310, 315 (May 1994).
2. R. S. Ronen, P. S. Schultz, M. Hattori, and C. Corbett, Seismic-Guided Estimation of Log Properties: Part 2: Using Artificial Neural Networks for Nonlinear Attribute Calibration, *Leading Edge*, 13(6): 674-678 (June 1994).

CO_2 HUFF 'N' PUFF PROCESS IN A LIGHT OIL SHALLOW SHELF CARBONATE RESERVOIR

Contract No. DE-FC22-94BC14986

Texaco Exploration and Production Inc.
Midland, Tex.

Contract Date: Feb. 10, 1994
Anticipated Completion: Dec. 31, 1997
Government Award: $474,870
(Current year)

Principal Investigator:
Scott C. Wehner

Project Manager:
Jerry Casteel
Bartlesville Project Office

Reporting Period: Oct. 1–Dec. 31, 1994

Objectives

The principal objective of the Central Vacuum Unit (CVU) carbon dioxide (CO_2) Huff 'n' Puff (HnP) project is to determine the feasibility and practicality of the technology in a waterflooded shallow shelf carbonate (SSC) environment. The results of parametric simulation of the CO_2 HnP process coupled with the CVU reservoir characterization components will determine if this process is technically and economically feasible for field implementation. The technology transfer objective of the project is to disseminate the knowledge gained through an innovative plan in support of the U.S. Department of Energy's (DOE) objective of increasing domestic oil production and deferring the abandonment of SSC reservoirs.

Summary of Technical Progress

Texaco Exploration and Production Inc's. (TEPI) long-term plans are to implement a full-scale miscible CO_2 project in the CVU. The current market precludes acceleration of such a capital-intensive project, however. This is a common finding throughout the Permian Basin SSC reservoirs. It is believed that the immiscible CO_2 HnP process might bridge this longer term miscible project with near-term results. A successful implementation would result in near-term production, or revenue, to help offset cash outlays. The DOE partnership provides some relief from the associated research and development risks, which allows TEPI to evaluate a proven Gulf Coast sandstone technology in a waterflooded carbonate environment. Numerous sites exist for widespread replication of this technology following a successful field demonstration.

Cross Sections

Cross sections through all study area wells within the producing horizons of Texaco-operated acreage are complete. These cross sections were stratigraphically hung on the Grayburg Marker. Formation tops shown on the cross sections include the Grayburg Dolomite, Grayburg Sandstone, Upper San Andres, Lovington Sandstone, and the Lower San Andres. These tops represent the macro-zonation, which is based on a deterministic approach. The cross sections were developed with the commercial software, Geographix Evaluation System.

Initial Water Saturation Distribution and Oil–Water Contact

One of the more important milestones associated with the reservoir characterization component of the project is determination of original oil in place (OOIP); therefore an evaluation of fluid saturations was warranted. Capillary pressure data were used to define the initial saturations above an oil–water contact (OWC) or zero capillary pressure level [water saturation (S_w) = 100%)]. A study of electric logs defined the OWC to be at –1000 ft from sea-level datum. The average initial water saturation (S_{wi}) of the main pay zone was then established at 20% with the use of the capillary pressure data.

The culmination of this exercise was the selection of a pseudo-OWC surface, or an economically attractive OWC within the transition zone (TZ), which would be used in the calculation of OOIP. The data were reviewed and considered, and it was decided that it was more important that the OOIP

be calculated to represent the hydrocarbon section available for application of the proposed technology. A detailed study of past and current completions identified a fairly constant surface at –700 ft subsea to be the average bottom of the producing horizon. This artificial horizon will be used in subsequent evaluations of OOIP. A Leverett J (S_w) function was developed from capillary pressure measurements. This defined saturation profile will be applied to the massive database described in the geostatistics section of this report for initial simulation model conditions. Material balance will allow the estimation of current saturations by injection pattern for waterflood efficiency review.

Geostatistical Realizations

Geostatistics are being used to distribute wellbore data to interwell locations (cells). A more realistic distribution of the data than the typical algorithm used in mapping software is expected. Normalized porosity and permeability data from 455 wells in the project area were available for use, but this figure has been reduced to 322 wells because statistical variations were introduced by sonic logs which do not account for secondary porosity. Markers within the pay were taken from the project database. Variograms suggest an east-west bias to the porosity distributions. This trend follows the strike of the basin margin.

At 752,400 cells, the geostatistical software is handling a large volume of data for the study. The three-dimensional (3-D) gridding consists of 150 layers within the San Andres formation with an aerial distribution of 76 rows by 66 columns. The layers are 4 ft thick. Each cell is 250 ft × 250 ft on a side. This work is being performed on a personal computer with a geostatistical software package developed by Texaco called GRIDSTAT. In this project, the model area had to be broken into sections because of its size. After working with several grid generations, it became obvious that the software was not properly using the data from wells in adjacent sections, which resulted in banding. The software code was subsequently refined, and the banding problems were eliminated. An acceptable porosity grid for the project area has been defined for the San Andres formation. Final tasks will involve the generation of geostatistical grids within the overlying producing horizons of the Grayburg formation.

Originally, it was anticipated that the variograms developed from the porosity data would be used in construction of the permeability grids, but the redistribution of permeability data, which were defined on the basis of their relative position in the reservoir, was a concern. This approach was abandoned in favor of the direct application of the neural network permeability relationships corresponding to the geostatistically distributed porosity. Efforts are under way to apply the neural network to this massive porosity grid.

The 250 ft × 250 ft aerial grids are being used to determine saturations throughout the field study area. Work is under way to define the grid requirements for the site-specific simulation model. The coarser grid of the field will not allow the detail needed for the compositional simulation model. Further, the detailed grid is prohibitively large for the field review requirements. The intent is to avoid any averaging of kriged data within the simulation model. Grid-size optimization is proceeding with input from compositional simulation experts, so the end product will better support the simulation process.

Conditional simulations will be performed on the site-specific model area in conjunction with the parametric simulation tasks. An evaluation will be made to determine if the porosity variograms constructed from the field-wide data are applicable to the site-specific model area before the conditional simulations.

Waterflood Review

A review of waterflood efficiencies has been initiated to allow proper selection of the eight sites for the field demonstration of the proposed technology. The results of the parametric simulation studies will be coupled with the waterflood review information so that a sufficient variation in reservoir conditions/character can be selected to support the parametric studies' findings. Guidelines will be developed to assist operators in selecting candidate sites on the basis of this information and actual field trials.

The study is currently limited to evaluation of effects not related to OOIP because the final figures will not be available until completion of the geostatistical exercises. Review of various relationships is progressing, however; no abnormalities are suggested in these initial studies.

On the basis of the cursory review of currently available data, a site-specific model area has been selected. It is located in the northern area of sec. 6, T. 18 S., R. 35 E., Lea County, New Mex. This model area represents average reservoir conditions known to exist within the study area. It will cover four existing 40-acre, five-spot injection patterns. The size of the model will allow for the potential to analyze results from more than one field demonstration. This was done as a safety precaution should the initial site mechanically fail. The model area is to be drilled on a higher density well spacing, which will provide modern logging suites. These data will help refine the model and provide a measure to the geostatistical efforts. The drilling is not part of the cost-share DOE project.

Parametric Simulation

Western Atlas' DESKTOP-PVT program has been used to develop an equation of state (EOS) that will be incorporated in the compositional simulations for the CVU HnP process. Previous development efforts had focused on the three-parameter Peng–Robinson EOS. A completely satisfactory match of the liquid volume fraction at high mol% CO_2 mixtures could not be found with this EOS.

Development efforts were shifted to the Zudkevitch–Joffe–Redlich–Kwong (ZJRK) EOS. A much better match of the liquid volume fraction at high mol% CO_2 mixtures was found with the ZJRK equation. This type of data is typically the most

difficult to match. The general procedure for matching laboratory data with an EOS was previously discussed. An additional procedure has been instituted that involves simultaneously matching pure CO_2 densities with the laboratory CO_2–oil phase behavior data. It was found that an EOS does not typically predict pure CO_2 density sufficiently well when it is matched only to the laboratory CO_2–oil phase behavior data. When pure CO_2 density was also included in the matching process, the prediction of pure CO_2 density was much improved without significant degradation of the liquid volume fraction matches. Proper matching of CO_2 density is important when determining the amount of CO_2 used in a process.

Slim-tube experiments previously performed to determine the CVU crude system's minimum miscibility pressure (MMP) were successfully simulated with the newly developed ZJRK EOS. Representative gas–oil relative permeability curves were used. The ability to match these tests with representative relative permeability curves gives added credibility to the EOS. Good matches were obtained for the oil recovery as a function of the volume of CO_2 injected for several pressures. Included were pressures below the MMP, such as 1100 psia, as well as pressures above the MMP, such as 3000 psia. This is significant because tests at pressures below the MMP are not often simulated. Experimentally, at the 1100-psia pressure, the injected CO_2 did not displace an equal volume of oil from the slim tube even at the start of the test; rather, a portion of the CO_2 dissolved in the oil. The newly developed EOS was able to match this behavior. The ability of the EOS to predict proper behavior below the MMP is important because the HnP tests will initially operate below the MMP in the near-wellbore vicinity.

Future work will involve the actual parametric simulations of the HnP process. A finely gridded radial model will be used so that accurate pressure profiles near the wellbore can be determined. The parameters investigated will include both reservoir characteristics and operating strategies.

IMPROVED OIL RECOVERY IN MISSISSIPPIAN CARBONATE RESERVOIRS OF KANSAS—NEAR TERM—CLASS 2

Contract No. DE-FC22-93BC14987

University of Kansas
Lawrence, Kans.

Contract Date: Sept. 18, 1994
Anticipated Completion: Sept. 18, 1998
Government Award: $3,169,252

Principal Investigators:
Tim Carr
Don W. Green
G. Paul Willhite

Project Manager:
Chandra Nautiyal
Bartlesville Project Office

Reporting Period: Oct. 1–Dec. 31, 1994

Objective

The objective of this project is to examine incremental reserves from Osagian and Meramecian (Mississippian) dolomite reservoirs in western Kansas by reservoir characterization to identify areas of unrecovered mobile oil. The project addresses producibility problems in two fields; specific reservoirs target the Schaben Field in Ness County, Kansas, and the Bindley field in Hodgeman County, Kansas. The problems of inadequate reservoir characterization, drilling and completion design, and non-optimum recovery efficiency will be addressed. The results of this project will be disseminated through various technology transfer activities.

At the Schaben demonstration site, the Kansas team will conduct a field project to demonstrate better approaches to identify bypassed oil within and between reservoir units. The approach will include

- Advanced integrated reservoir description and characterization, which includes integration of existing data and drilling, logging, coring, and testing three new wells through the reservoir intervals. Advanced reservoir techniques will include high-resolution core description, petrophysical analysis of pore system attributes, and geostatistical analysis and three-dimensional (3-D) visualization of interwell heterogeneity.
- Computer applications that will be used to manage, map, and describe the reservoir. Computer simulations will be used to design better recovery processes and to identify potential incremental reserves.
- Comparison of the reservoir geology and field performance of the Schaben field with the slightly younger Bindley field in adjacent Hodgeman County, Kansas.
- Drilling of new wells between older wells (infill drilling) to contact missed zones.
- Demonstration of improved reservoir management techniques and of incremental recovery through potential deepening and recompletion of existing wells and targeted infill drilling.

The project is an effort to make Kansas producers more aware of potentially useful technologies and to demonstrate in actual oil field operations how to apply them. A major emphasis of the Kansas project will be collaboration of University scientists and engineers with

the independent producers and service companies operating in the state. An extensive technology transfer effort will be made to inform other operators of the results of the project. In addition to traditional technology transfer methods (e.g., reports; trade, professional, and technical publications; workshops; and seminars), a public domain relational database and computerized display package will be made available through the Internet and other means of electronic access.

Summary of Technical Progress

Acquisition and Consolidation of Available Data

All wells in and surrounding Schaben field that contain production, log, and/or core information have been identified from computer databases and paper records. All digital well locations were checked and corrected if necessary. Unique well identifications (API numbers) were checked and assigned if necessary. Digital cultural data were downloaded and checked (e.g., political boundaries and townships and sections). This forms the geographic and well database into which all geologic, engineering, and production data will be loaded. The data will be stored under an Openworks-compatible database. ORACLE, the primary relational database management system, was obtained and loaded.

Cores were described at the macroscopic level, and samples were selected for further analysis. Samples for petrographic analysis were sent for thin sections.

Logs from approximately 200 wells are either in the process of being digitized or have been digitized. The digital log data are being loaded into Landmark's Stratworks and TerraSciences' TerraStation for geologic analysis.

Reservoir Characterization

Preliminary petrophysical and core analyses are complete and indicate that the reservoir is highly vertically stratified, of variable lithology (limestone, dolomite, and chert), and has high bulk water volume. The complexity of the reservoir and the diverse nature of extant logs (i.e., various vintages, quality, and type) make the gathering of additional high-quality logs tied to core data important to an adequate reservoir description.

Technology Transfer

The technology available to be transferred is limited at this time; however, for related work on a Kansas interactive oil and gas field map, production data from Schaben field and Ness County were used as a prototype. The production data for the state, county, and individual fields are available online through the Internet. The data can be accessed through the Petroleum Research Section's home page (http://crude1.kgs.ukans.edu/). Even though the site is not publicized, the number of users, which includes a number of independent oil companies, has increased. Information will continue to be posted on the Internet.

REVITALIZING A MATURE OIL PLAY: STRATEGIES FOR FINDING AND PRODUCING UNRECOVERED OIL IN FRIO FLUVIAL–DELTAIC RESERVOIRS OF SOUTH TEXAS

Contract No. DE-FC22-93BC14959

University of Texas
Bureau of Economic Geology
Austin, Tex.

Contract Date: Oct. 21, 1992
Anticipated Completion: Dec. 31, 1994
Government Award: $817,911

Principal Investigator:
Noel Tyler

Project Manager:
Edith Allison
Bartlesville Project Office

Reporting Period: Oct. 1–Dec. 31, 1994

Objectives

Project objectives are divided into three major phases. The first phase, reservoir selection and initial framework characterization, consisted of the initial tasks of screening fields within the play to select representative reservoirs that have a large remaining oil resource and are in danger of premature abandonment and performing initial characterization studies on selected reservoirs to identify the potential in untapped, incompletely drained, and new pool reservoirs. The second phase will involve advanced characterization of selected reservoirs to delineate incremental resource opportunities. Subtasks include the volumetric assessments of untapped and incompletely drained oil and an analysis of specific targets for recompletion and strategic infill drilling. The third phase of the project will consist of a series of tasks associated with technology transfer and the extrapolation of specific results from reservoirs in this study to other heterogeneous fluvial–deltaic reservoirs within and beyond the Frio play in South Texas.

Summary of Technical Progress

Project work during the present quarter consisted of the completion of second-phase tasks associated with the

delineation of incremental recovery opportunities in the representative Frio fluvial–deltaic Sandstone reservoirs in Rincon and Tijerina–Canales–Blucher (TCB) fields selected for detailed studies. Documentation of interim results was completed to fulfill Annual reporting requirements and to provide adequate material for technology transfer at upcoming professional meetings scheduled in 1995.

Strategies for Incremental Recovery in Selected Frio Reservoirs

The potential for infield resource additions is a function of the original oil volume in place, the present level of development, and the degree of internal geologic complexity of the reservoir being produced. Studies on selected Frio reservoirs in both Rincon and TCB fields have identified the current level of development in individual reservoir units and documented that reservoir geometry within each stratigraphic reservoir interval is variable and provides important controls on the level of flow communication within a single reservoir unit. Stratigraphic heterogeneity and variability in reservoir quality exhibited within these reservoirs are directly re sponsible for the distribution of original oil in place (OOIP) and have also been primary controls on present recovery efficiencies.

Rincon Field Reservoir Studies

In Rincon field, documentation of stratigraphic heterogeneity and identification of the presence of flow barriers within and between individual Frio D reservoir units are the primary goals of continuing studies to understand styles of reservoir compartmentalization and to delineate the location of incompletely drained and undeveloped reservoir compartments. Frio D reservoir sandstones have more complex facies patterns and a greater degree of stratigraphic variability, and, as a result, the composite reservoir zone has a significantly lower recovery efficiency than E series reservoirs. The relatively poor recovery efficiency of the Frio D reservoir zone is an artifact of current well spacing that is greater than the size of reservoir compartments that collectively make up the total storage space of the mobile oil resource in the Frio D reservoir zone.

Net sandstone isopach maps and log facies maps of eight individual reservoir subunits in the productive Frio D-E interval were combined with production data to document completion density present within each subunit. Completion maps prepared for each reservoir subunit also identify locations of wells with completions in vertically adjacent subunits so that possible areas where vertical communication between zones may have influenced production may be identified. Reservoir areas were calculated for each of the eight mapped subunits, and volumetric calculations were computed for each reservoir area. These volumetric calculations will form the basis for more-accurate OOIP estimates for each of the reservoir subunits.

Results from calculations of reservoir areas and volumes for each reservoir subunit in the productive Frio D-E interval in Rincon field are being combined with results from petrophysical modeling of water saturations to generate more-accurate OOIP calculations for each of the reservoir units. The development of petrophysical models to calculate porosity, permeability, and water saturation in Rincon reservoirs was completed first in wells with core data and will ultimately incorporate results from special core analyses and petrographic examination. Different porosity–permeability relationships for reservoir units that exhibit channel and bar geometries have been identified and will be incorporated into petrophysical porosity modeling. When petrophysical studies of target reservoir intervals in each field area are complete, volumes will be calculated and known production subtracted to determine the remaining volume of reserves. Through this process, untapped and incompletely drained compartments will be identified, and those interpreted to contain the largest volumes of remaining oil will represent the best targets for near-term incremental recovery by recompletions and strategic infill drilling.

TCB Field Reservoir Studies

In the TCB field, representative reservoir zones from each of the three architectural styles identified in productive TCB reservoirs are the focus of detailed stratigraphic mapping to identify untapped compartments containing significant volumes of mobile oil. Architectural styles include the vertically stacked, laterally isolated style of the sand-rich middle Frio Scott reservoir; the vertically and laterally isolated style of the sand-poor middle Frio Whitehill Unit; and the vertically isolated and structurally complicated style exemplified in the lower 21-B zone, which includes the Mary and Marie sandstones and various other stratigraphic equivalents. In vertically and laterally isolated reservoirs like the Scott, compartments are more easily identified because their boundaries are clearly limited by channel and splay margins. This style of reservoir may also contain the potential for stratigraphically trapped accumulations located off the crest of the structure because of the presence of narrow sinuous channel sandstones that form arcuate concave-updip sandstones. The identification of untapped compartments is more complicated in vertically stacked, laterally isolated reservoir bodies because of the variable nature of bed boundaries in which low-permeability mudclast-rich layers at the base of channels may create complete or only partial seals between channel sandstones. The Scott has produced less than 5% of the OOIP, as calculated from operator-supplied maps and petrophysical parameters, and these low recoveries indicate extensive unrecognized reservoir compartmentalization.

The 21-B zone represents the laterally isolated, structurally complicated reservoir architecture style that is common throughout the lower Frio section. A series of faults perpendicular to dip-oriented distributary channel sandstones isolates these reservoirs into short, narrow segments and creates

compartments of limited extent. This zone is by far the most prolific reservoir in the greater TCB field area and contains the highest potential for incremental oil recovery.

Contacts that represent boundaries between various facies within a fifth-order unit and boundaries between individual sandstone bodies were used to measure and map net sandstone thickness for subunits within the Scott, Whitehill, and 21-B reservoir zones. Available routine core analysis data from wireline cores and porosity data from geophysical logs are used to determine the petrophysical nature of facies and intrafacies boundaries to more fully evaluate the competency of these surfaces to act as barriers or baffles to fluid migration. Available engineering data are also being evaluated to assess intercompartmental communication.

Characterization of Heterogeneity Style and Permeability Structure in a Sequence Stratigraphic Framework in Fluvial–Deltaic Reservoirs

Industry has generally recognized opportunities for infill drilling and recompletion, but not to the extent that these approaches can be fully used to increase near-term oil recovery in all depositional systems. This is especially true in complex compartmentalized reservoirs. Past infill drilling has not targeted specific incompletely drained or untapped compartments, in part because of the lack of integration of geology and engineering in seeking advanced development opportunities in mature fields. Only a limited number of geological studies have investigated the nature of flow barriers and flow baffles in fluvial–deltaic reservoirs. Further, work on outcrops has only recently begun to assist in geostatistical characterization of fluvial–deltaic reservoir heterogeneities, to address the question of scale-up of reservoir properties, and to demonstrate the significant need for integration of geologic detail in reservoir simulation.

An industrial associates program at the Bureau of Economic Geology was formed in 1992 to address these problems and to develop an understanding of sandstone architecture and permeability structure in a spectrum of fluvial–deltaic reservoirs deposited in high- to low-accommodation settings and to translate this understanding into more realistic, geologically constrained reservoir models. This fluvial–deltaic sandstone heterogeneity investigation research program in fluvial–deltaic sandstones is funded by 14 companies (Amoco Production Co., BP Exploration Operating Co. Ltd., Chevron Oil Field Research Co., Conoco, Inc., Exxon Production Research Co., Intevep S.A., Japan National Oil Co., Kerr-McGee Corp., The Louisiana Land and Exploration Co., Mobil Research and Development Corp., Occidental International Exploration and Production, Inc. and OXY USA, Inc., Oryx Energy Co., Statoil, and Union Oil Co. of California) who are the source of the 50% co-funding for the Bureau's Class I Oil Project. The approach is to quantify the interrelationships among sequence stratigraphy, depositional architecture, diagenetic history, and permeability structure through detailed outcrop characterization. Sand-body geometry and permeability data collected from outcrop form the basis for the construction of reservoir models and the conduction of flow simulation. This work is adding significantly to overall knowledge applicable to the subsurface reservoir discontinuities encountered in the Frio of South Texas.

Technology Transfer Activities

In addition to specific project tasks, the second-year annual contract report was completed and submitted to the U.S. Department of Energy (DOE) for review. Presentations were prepared and given to the project manager in November 1994 and to a National Research Council review panel that convened in mid-December to evaluate progress on selected projects in the DOE Class I and Class ll reservoir program.

Three abstracts highlighting project results from play-wide reservoir assessment[1] and from initial reservoir characterization studies in each field area[2,3] were accepted for presentation at the American Association of Petroleum Geologists annual meeting in March of 1995. In addition to these abstracts, a Bureau of Economic Geology Report of Investigations on play-wide resource assessment and identification of remaining oil potential in the Frio fluvial–deltaic sandstone play is in final stages of preparation for publication.[4] Two papers discussing aspects of the Rincon and TCB field studies were also prepared for submittal to the 1995 Gulf Coast Association of Geological Societies Meeting in October 1995.[5,6]

References

1. M. H. Holtz and L. E. McRae, *Modeling Reservoir Attributes and Estimating Additional Hydrocarbon Potential for Redevelopment in Fluvial–Deltaic Reservoirs: An Example from the Frio Fluvial–Deltaic Sandstone Play in South Texas,* paper to be presented at the American Association of Petroleum Geologists Annual Meeting, Houston, Tex., March 5–8, 1995.
2. L. E. McRae and M. H. Holtz, *Reservoir Architecture and Permeability Characteristics of Fluvial–Deltaic Sandstone Reservoirs in the Frio Formation, Rincon Field, South Texas,* paper to be presented at the American Association of Petroleum Geologists Annual Meeting, Houston, Tex., March 5–8, 1995.
3. P. R. Knox and L. E. McRae, *High Resolution Sequence Stratigraphy: The Key to Identifying Compartment Styles in Frio Formation Fluvial–Deltaic Reservoirs, TCB Field, South Texas,* paper to be presented at the American Association of Petroleum Geologists Annual Meeting, Houston, Tex., March 5–8, 1995.
4. M. H. Holtz and L. E. McRae, *Modeling Reservoir Attributes and Estimating Additional Hydrocarbon Potential for Redevelopment in Fluvial–Deltaic Reservoirs: An Example from the Frio Fluvial–Sandstone Play in South Texas,* Bureau of Economic Geology Report of Investigations, in press.
5. L. E. McRae and M. H. Holtz, Strategies for Optimizing Incremental Recovery from Mature Reservoirs in Oligocene Frio Fluvial-Deltaic Sandstones, Rincon Field, South Texas, *Trans., Gulf Coast Assoc. Geol. Soc.,* 4: 423-434 (October 1995).
6. P. R. Knox and L. E. McRae, Application of Sequence Stratigraphy to the Prioritization of Incremental Growth Opportunities in Mature Fields: An Example from Frio Fluvial-Deltaic Sandstones, TCB field, South Texas, *Trans., Gulf Coast Assoc. Geol. Soc.,* 4: 341-359 (October 1995).

INCREASED OIL PRODUCTION AND RESERVES FROM IMPROVED COMPLETION TECHNIQUES IN THE BLUEBELL FIELD, UINTA BASIN, UTAH

Contract No. DE-FC22-92BC14953

Utah Geological Survey
Salt Lake City, Utah

Contract Date: Sept. 30, 1993
Anticipated Completion: Sept. 29, 1998
Government Award: $412,890

Principal Investigator:
M. Lee Allison

Project Manager:
Edith Allison
Bartlesville Project Office

Reporting Period: Oct. 1–Dec. 31, 1994

Objective

The objective of this project is to increase the oil production and reserves in the Uinta Basin by demonstration of improved completion techniques. Low productivity is attributed to gross production intervals of several thousand feet that contain perforated thief zones, water-bearing zones, and unperforated oil-bearing intervals. Geologic and engineering characterization and computer simulation of the Green River and Wasatch formations in the Bluebell field will determine reservoir heterogeneities related to fractures and depositional trends. This will be followed by drilling and recompletion of several wells to demonstrate improved completion techniques on the basis of the reservoir characterization. Technology transfer of the project results will be an ongoing component of the project.

Summary of Technical Progress

Subsurface Studies

Two stratigraphic cross sections in the Roosevelt Unit area of the Bluebell field (vertical scale approximately 150 ft/in.) are complete. Cross section A-A′ incorporates 10 wells and trends approximately west–east along depositional strike (Fig. 1). Cross section B-B′ trends roughly north–south and shows a total of five wells, including the two proposed demonstration wells: the Michelle Ute (sec. 7, T. 1 S., R. 1 E.) and Malnar Pike (sec. 17, T. 1 S., R. 1 E. Uinta Baseline)

Studies of lithology, sedimentary structure, fossil content, and fracture descriptions are complete for 10 cores. Samples were prepared for thin-section and X-ray-diffraction analyses. Graphical representation of the core descriptions will be produced with software for recording and displaying stratigraphic data.

Core samples were selected from various lithofacies for completion—fluid sensitivity studies. All the samples are from perforated intervals. The samples are a carbonate from the upper Wasatch transition/lower Green River formation, a sandstone from the Wasatch formation, and a sandstone and a carbonate from the deeper lower Wasatch transition (Flagstaff equivalent?) interval.

Subsurface fracture analysis is being done with borehole imaging logs and data from oriented cores. These data will be combined with the surface-fracture data to determine fracture orientation and distribution on a field-wide scale. The Bluebell field fracture study will be combined with another surface/subsurface fracture study being conducted by the Utah Geological Survey of the Duchesne field, southwest of the Bluebell field, to develop a basin-wide model.

The digitization of geophysical well logs in and around the Bluebell field is complete. The database consists of 240 logs from 80 wells. Preliminary correlation of the digital logs of field-wide markers is complete. This data set will be used to generate major structure and interval thickness maps. The digital data will also be used for detailed porosity, clay content, and fluid-saturation calculations.

Engineering Studies

In the Michelle Ute well, 69 zones are perforated, whereas in the Malnar Pike well, 50 zones are perforated. A comprehensive model of the Michelle Ute well was described previously. Features of the Malnar Pike model are

Area	40 acres (16 ha)
Reservoir depth	9,582 to 14,360 ft (2,920 to 4,376 m)
Grid	$8 \times 8 \times 49$
Grid size (x and y)	165 ft (50 m)
Grid size (z)	Varied
Porosity	0.0 to 0.32%
Pressure gradient	0.5 psi/ft (11.3 KPa/m)
Oil gravity	35 °API
Gas gravity	0.75
Initial gas/oil ratio	1,100 scf/stock tank barrel
Initial bubble point pressure	3,800 psi (26,200 KPa)
Initial oil saturation	0.7 (constant)
Bottomhole pressure	
first year	3,000 psi (20,690 KPa)
subsequent years	2,000 psi (13,790 KPa)

Several assumptions were made about the reservoir properties so that the simulated production would match the historical production. A constant pressure gradient of

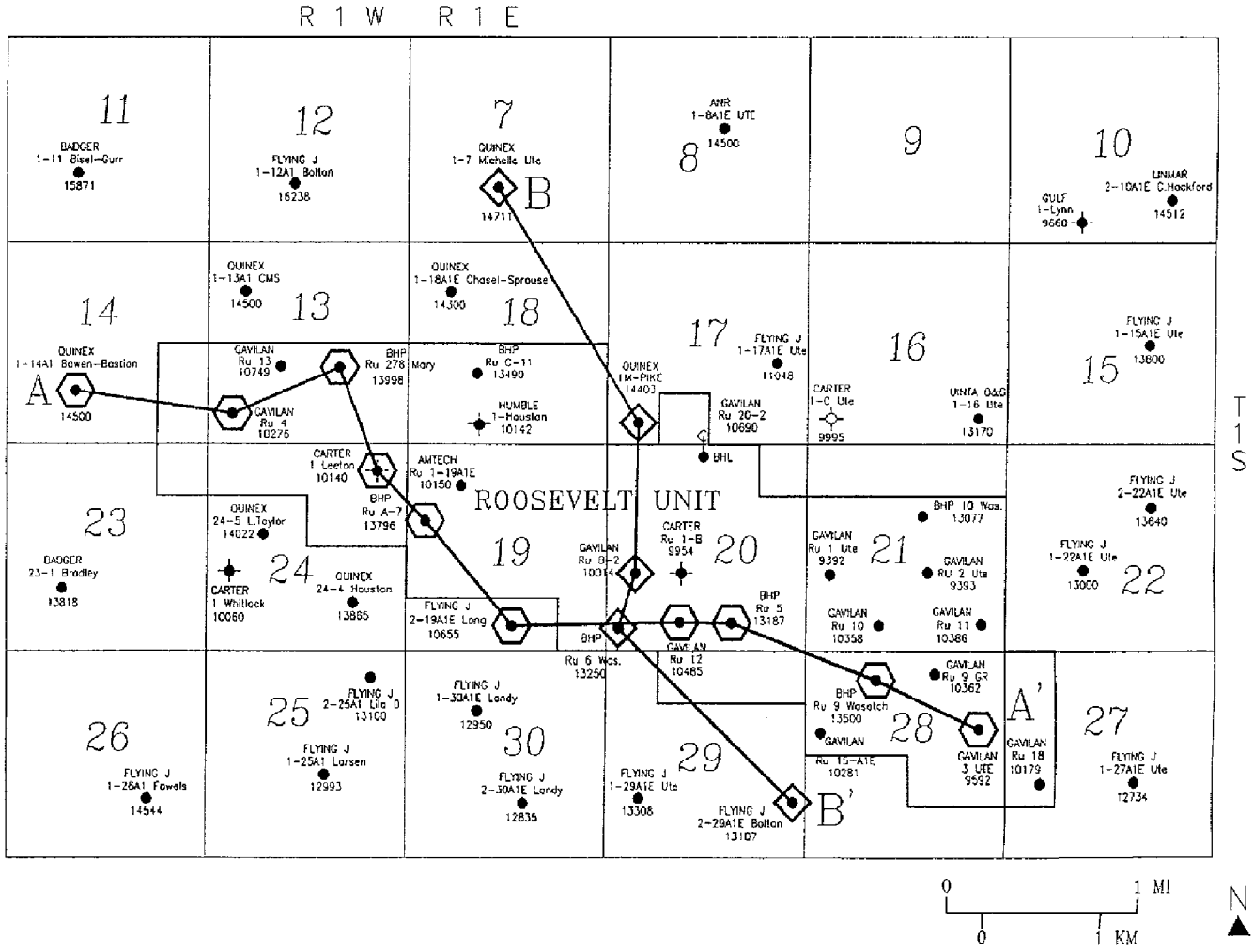

Fig. 1 Index map of the Roosevelt Unit area showing wells used for the stratigraphic cross sections A-A′ and B-B′. ●, oil well. ✦, abandoned oil well. ✧, gas well. –●–, deviated well.

0.5 psi/ft (11.3 KPa/m) was used. The field production operations were essentially duplicated by opening perforations at appropriate times to represent the addition of new perforations over the history of the well. In contrast to the Michelle Ute model, a constant permeability of 0.31 mD was used in these simulations. The challenge in the Malnar Pike simulations was to match the large water production. This was accomplished by making adjustments to the water relative permeabilities at low water saturations. The actual oil, gas, and water productions are compared with the simulation results in Figs. 2 to 4, respectively. The oil and gas productions are fairly well matched by the model. Even though the total water production is well matched by the simulations, the initial water production is significantly lower than the simulated production. This suggests that the latter set of perforations may have penetrated an aquifer.

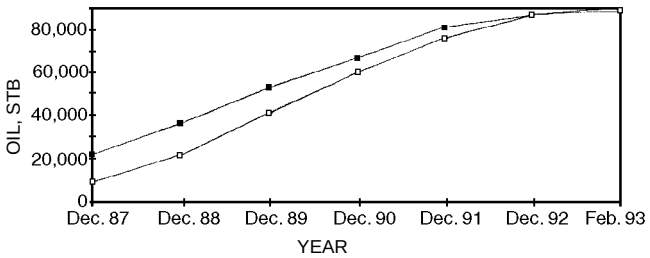

Fig. 2 Actual vs. simulated yearly oil production, Malnar Pike well (sec. 17, T. 1 S., R. 1 E.). –■–, field data. –□–, simulated result.

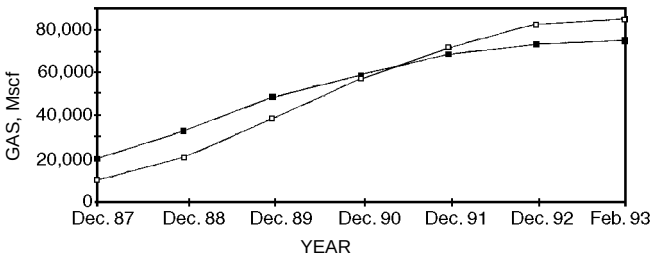

Fig. 3 Actual vs. simulated yearly gas production, Malnar Pike well (sec. 17, T. 1 S., R. 1 E.). –■–, field data. –□–, simulated result.

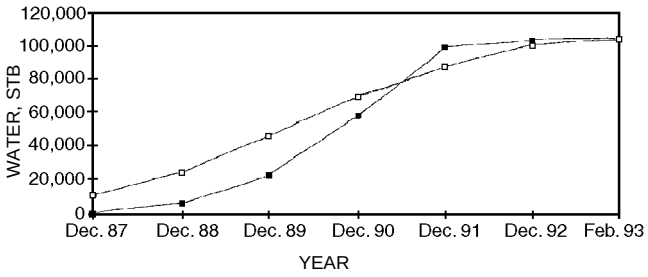

Fig. 4 Actual vs. simulated yearly water production, Malnar Pike well (sec. 17, T. 1 S., R. 1 E.). –■–, field data. –□–, simulated result.

Technology Transfer

One technical presentation was made during the quarter as part of the Bluebell field project technology transfer activities.[1]

Reference

1. A. Garner and T. H. Morris, *Reservoir Characterization Through Facies Analysis of the Lower Green River Formation for Hydrocarbon Production Enhancement in the Altamont–Bluebell Field, Uinta Basin, Utah,* paper presented at Geological Society of America Annual Meeting, Seattle, Wash., October 24–27, 1994.

GEOLOGICAL AND PETROPHYSICAL CHARACTERIZATION OF THE FERRON SANDSTONE FOR THREE-DIMENSIONAL SIMULATION OF A FLUVIAL–DELTAIC RESERVOIR

Contract No. DE-AC22-93BC14896

Utah Geological Survey
Salt Lake City, Utah

Contract Date: Sept. 29, 1993
Anticipated Completion: Sept. 29, 1996
Government Award: $1,225,482

Principal Investigator:
M. Lee Allison

Project Manager:
Robert Lemmon
Bartlesville Project Office

Reporting Period: Oct. 1–Dec. 31, 1994

Objective

The objective of this project is to develop a comprehensive, interdisciplinary, and quantitative characterization of a fluvial–deltaic reservoir that will allow realistic interwell and reservoir-scale modeling to be used for improved oil-field development in similar reservoirs worldwide. The geological and petrophysical properties of the Cretaceous Ferron sandstone in east-central Utah (Fig. 1) will be quantitatively determined. Both new and existing data will be integrated into a three-dimensional (3-D) representation of spatial variations in porosity, storativity, and tensorial rock permeability at a scale appropriate for interwell to regional-scale reservoir simulation. Results could improve reservoir management through proper infill and extension drilling strategies, reduce economic risks, increase recovery from existing oil fields, and provide more-reliable reserve calculations. Transfer of the project results to the petroleum industry is an integral component of the project.

Summary of Technical Progress

The technical progress is divided into several sections corresponding to the Regional Stratigraphy and Case Studies tasks of the project. The primary objective of the Regional Stratigraphy task is to provide a more-detailed description and interpretation of the stratigraphy of the Ferron sandstone outcrop belt from Last Chance Creek to Ferron Creek (Fig. 1). Photomosaics and a database of existing surface and subsurface data are being used to determine the extent and depositional environment of each parasequence and the nature of the contacts with adjacent rocks or flow units.

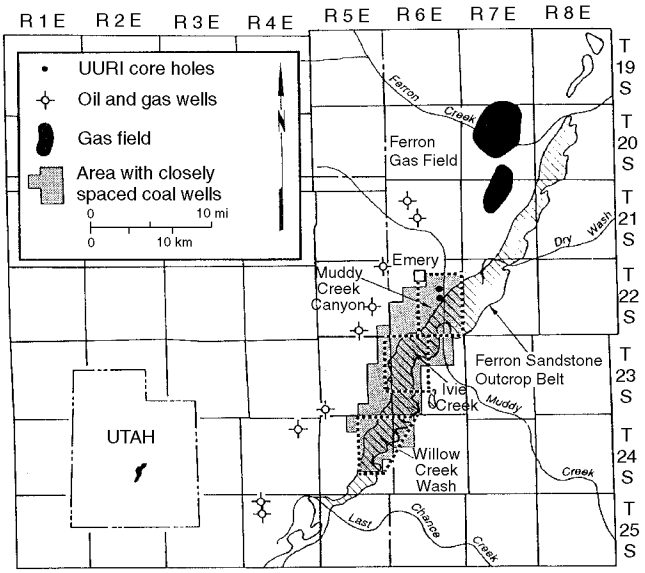

Fig. 1 Location map of the Ferron sandstone study area (cross-hatched) showing detailed case-study sites (outlined by heavy dashed lines). UURI, University of Utah Research Institute.

The primary objective of the Case Studies task is to develop a detailed geological and petrophysical characterization, at well-sweep scale or smaller, of the primary reservoir lithofacies typically found in a fluvial-dominated deltaic reservoir. Interpretations of lithofacies, bounding surfaces, and other geologic information are being combined with permeability measurements from closely spaced traverses and from drill-hole cores to develop a 3-D view of the reservoirs within three case-study areas (locations shown in Fig. 1).

Regional Stratigraphy

Surface Mapping/lnterpretation of the Outcrop Belt

The Utah Geological Survey (UGS) continues to combine digitized land-based and aerial photographs of the Ferron sandstone outcrop belt into reproducible photomosaics with the use of image-editing software. A total of 1823 photos depict 80 miles (130 km) of Ferron sandstone outcrop. Interpretations of parasequence boundaries, lithofacies, and various field data (such as measured section and gamma-ray transect locations) are being plotted on the photomosaics as part of both the regional and case-study analyses. These interpretations will be confirmed later in the field.

Collection and Interpretation of Existing Surface and Subsurface Data

The UGS has completed collection and compilation of available published and unpublished maps, measured sections, well logs, core descriptions, reports, and other data. There are 486 wells in the study area, of which 413 were cored. By Dec. 31, 1994, the UGS had acquired 138 geophysical logs and 1800 ft (550 m) of core or core descriptions from these wells (Table 1). Information from 232 wells has been entered into ASCII files; 456 of the 486 total wells were also entered into the UGS-developed INTEGRAL database being used for the Ferron project (Table 1). Interpretations (thickness, type of lithology, and geologic description) are complete for 473 wells.

All base maps have been digitized for the seven 7½ quadrangles within the study area. Drill-hole locations (petroleum exploratory and development wells and coal core holes), measured sections, coal outcrops, coal mined-out areas, drainages, and the top and base of the Ferron sandstone are also digitized on these base maps.

Case Studies

Core Holes

Four core holes were drilled in the Ivie Creek case-study site: the Ivie Creek Nos. 3, 5a, 9, and 9a (Fig. 2). These core holes were designed to evaluate the lithofacies and reservoir characteristics of the Ferron sandstone Nos. 1 and 2 sandstone parasequence sets. The total depths of the core holes are 443, 320, 200, and 310 ft (135, 98, 61, and 95 m, respectively). The core holes are located downdip 200 to 1200 ft (60 to 365 m) from the Ferron outcrop. The pattern of the core holes was designed to capture the various reservoir changes in the No. l and No. 2 parasequence sets over an area analogous in size to a small oil field. A total of 430 ft (131 m) of core was recovered from Nos. 1 and 2 sandstone parasequence sets. This core is stored at the UGS Sample Library and is available for study by interested parties.

Geophysical logs run in the Ivie Creek Nos. 3, 5a, and 9a core holes include the formation density, caliper, and gamma-ray logs (Fig. 3). Sonic and dipmeter logs were recorded in the Ivie Creek No. 3, the only core hole that was able to hold water. The Ivie Creek No. 9 core hole was abandoned because of

TABLE 1

Summary of Well, Geophysical Log, and Core Data Collected for the Ferron Sandstone Study Area

Source of wells	No. of wells with geophysical logs	No. of logs obtained by the UGS*	No. of wells cored/ footage cored	Core obtained by the UGS,* ft	No. of wells recorded in ASCII files*	No. of wells recorded in INTEGRAL*
Oil and Gas						
University of Utah Research Institute	2	2	2/800	800	0	2
ARCO Oil and Gas Company	7	7	7/3527	Descriptions only	0	7
British Petroleum	5	5	5/1000	1000	0	0
Other	59	41	0	0	0	46
Coal						
CONSOL Inc.	357	62	356/unknown	Descriptions only	232	339
U.S. Geological Survey	37	15	29/1402	Descriptions only	0	36
Bureau of Land Management	0	0	6/1156	Descriptions only	0	7
Western States Mineral Corporation	12	0	0	0	0	12
Hidden Valley Coal Company	7	6	7/463	Descriptions only	0	7
Total	486	138	412/8348	1800	232	456

*Obtained by Utah Geological Survey (UGS) as of Dec. 31, 1994.

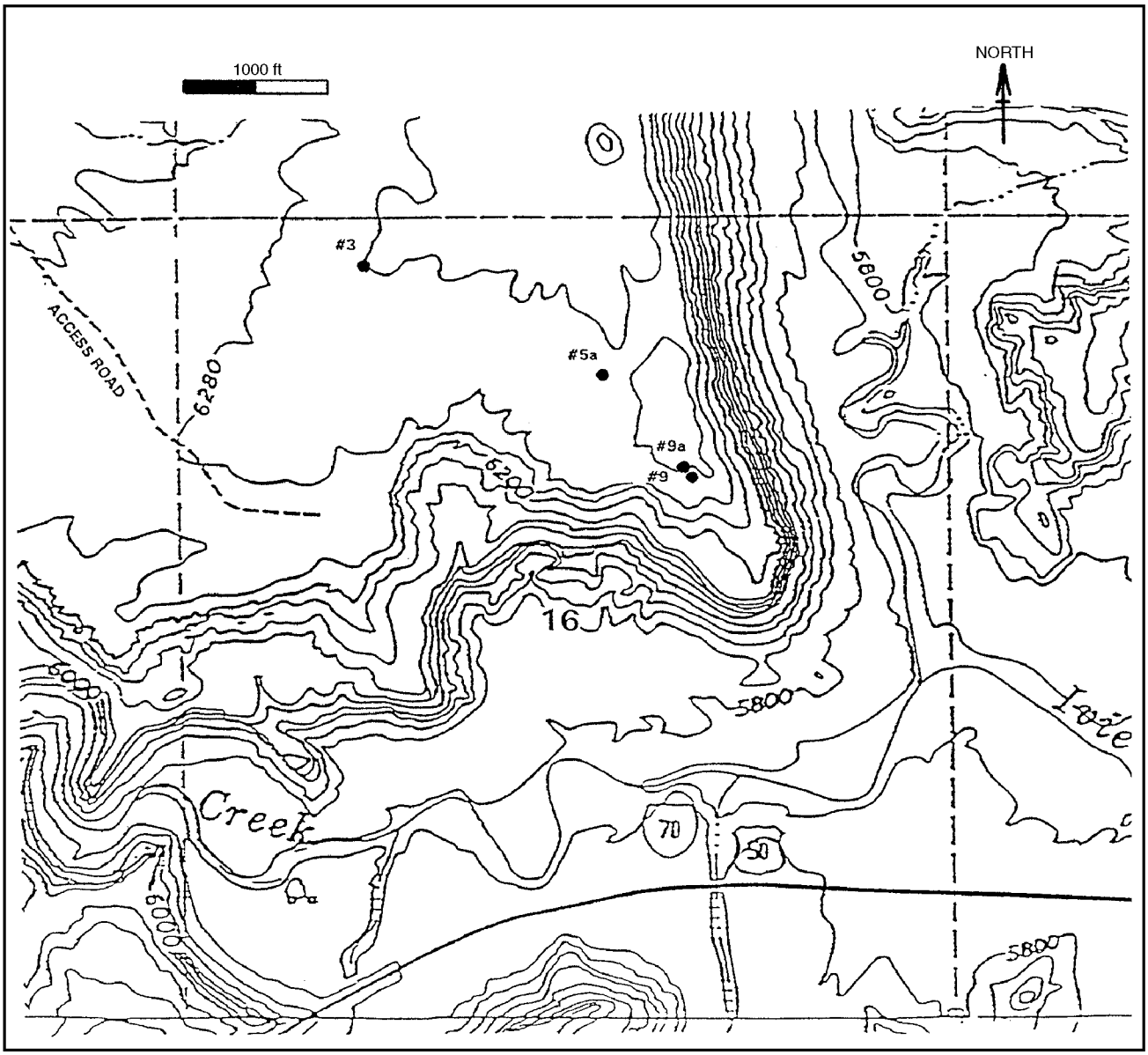

Fig. 2 Location of four core holes (Ivie Creek Nos. 3, 5a, 9, and 9a) drilled in the Ivie Creek case-study area, sec. 16, T. 23 S., R. 6 E., Salt Lake Base Line, Emery County, Utah. Three of the holes cored the Nos. 1 and 2 sandstones. Base map modified from U.S. Geological Survey Mesa Butte and Walker Flat $7^1/_2$-ft topographic maps; contour interval is 40 ft (12 m).

problems before coring and logging operations could be completed. Continuous logging of the core recovered from the Ivie Creek Nos. 3, 5a, and 9a core holes was conducted with a computer-interfaced multisensor track that simultaneously recorded natural gamma, density (via gamma-ray attenuation), and magnetic susceptibility. These data are being used to determine porosity and clay content, which are the dominant controls on fluid flow (permeability) in the Ferron sandstone and most other oil-producing fluvial–deltaic reservoirs.

The No. 1 sandstone parasequence set represents a river-dominated delta deposit that changes from proximal to distal (where the sandstone pinches out) from east to west across the Ivie Creek area. The No. 2 sandstone parasequence set contains more and cleaner sand, which indicates a more wave-influenced environment of deposition.

Mini-Permeameter Measurements

Seven permeability transects, four vertical and three subhorizontal (parallel to bedding) were made on the outcrop at the Ivie Creek case-study site during the 1994 field season (Fig. 4). The transects as a group sample the proximal, middle, and distal portions of the delta-front rocks of the No. l sandstone. Transect locations were designed to encompass most of the lithofacies present in the delta-front sequence. Data from these transects will be used to determine the

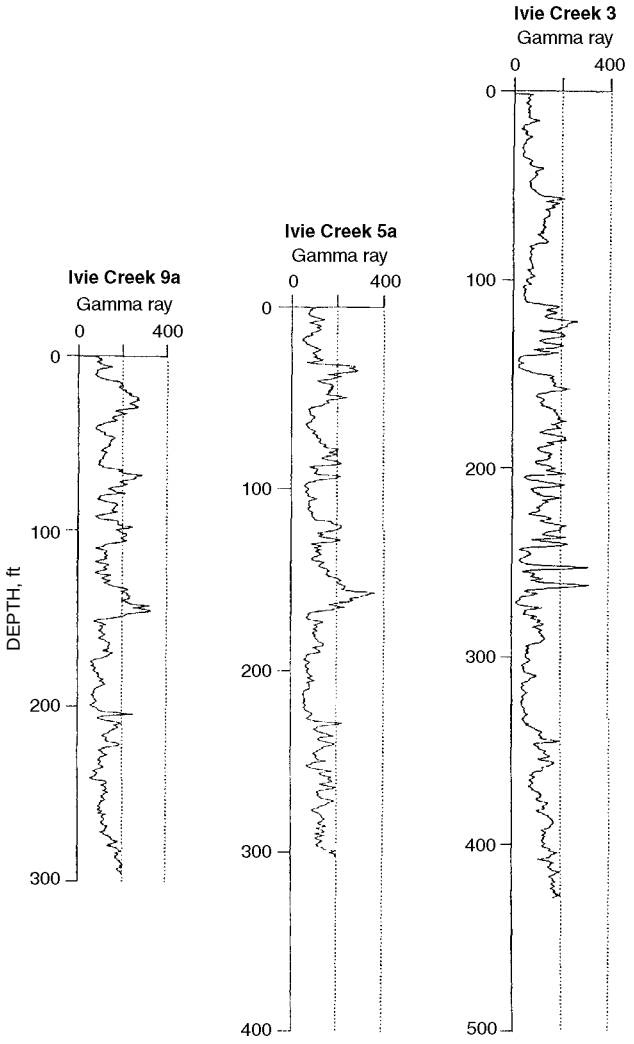

Fig. 3 Gamma-ray logs, in API units, from the Ivie Creek Nos. 9a, 5a, and 3 core holes (locations shown in Fig. 2).

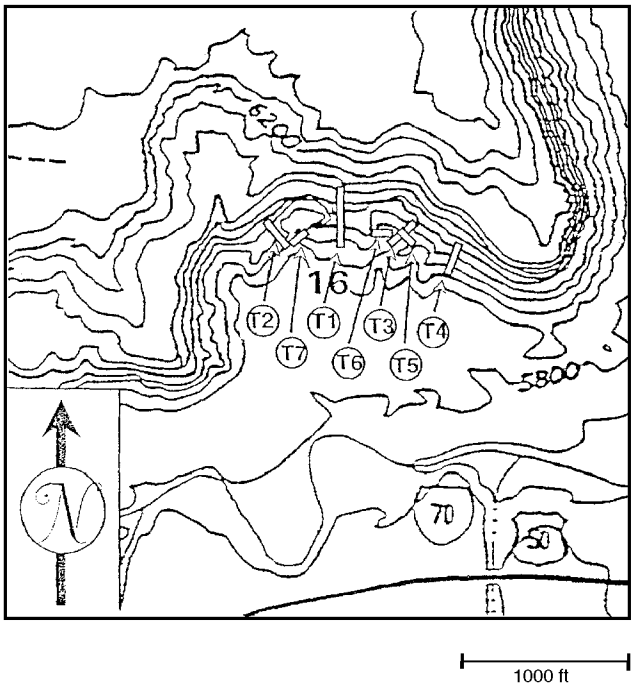

Fig. 4 Location of seven permeability transects (vertical and parallel to bedding) in the Ivie Creek case-study area, sec. 16, T. 23 S., R. 6 E., Emery County, Utah. Base map modified from U.S. Geological Survey Mesa Butte and Walker Flat 7⅜-ft topographic maps; contour interval is 40 ft (12 m).

statistical structure of the spatially variable permeability field within the delta front, to investigate how geological processes control the spatial distribution of permeability, and to evaluate permeability measurement techniques.

Mini-permeameter testing in the laboratory is complete for transects Tl, T2, T3, T4, T5, T6, and T7 (Fig. 4). Core plugs obtained from the No. 2 sandstone in the field and core from the Ivie Creek 5a and 9a core holes were also tested. These permeability data and related information are being entered into spreadsheets for subsequent analysis and transfer to the INTEGRAL database. Several additional core plugs were obtained in the field from the most proximal locations of the No. 1 sandstone, east of the mini-permeameter transects at the Ivie Creek site. These samples will also be tested for comparison to the other portions of the delta-front rocks.

The results of mini-permeameter tests performed on core plugs collected from the No. 1 sandstone along vertical (T1, T2, T3, and T4) and horizontal (T5, T6, and T7) outcrop transects are shown in Figs. 5 and 6, respectively, and the results from Nos. 1 and 2 sandstones along transect T1 are shown in Fig. 7. A large percentage of the rock tested apparently has a permeability lower than the resolution of the mini-permeameter (approximately 2 mD). Overall, permeabilities in the No. l sandstone are relatively low, less than about 50 mD. In the No. 2 sandstone (Fig. 7), permeabilities are locally much higher, in excess of 80 mD. A clear increase in permeability within distinct bedforms of the No. l sandstone exists from distal to proximal transects (T2 to Tl to T3 to T4). Although permeability values are below instrument resolution in horizontal transects T6 and T7 (Fig. 6), results obtained from T5 suggest that there is a definite permeability structure that may correspond to mappable variations in lithology and grain size.

During field and laboratory testing, sufficient information was collected to compare the results of in situ testing (k-hole) with laboratory tests performed on core (k-plugs) collected from the holes tested in the field (Fig. 8). The in situ tests generally produce larger permeability values. This effect might result from differences in surface preparation; the core plugs are trimmed with a saw, whereas testing surfaces in the in situ holes are chipped to a roughly flat surface. Because in situ testing requires a large field commitment (in time and personnel) and appears to provide overestimates of rock permeability, the collection and laboratory testing of core plugs will continue to be emphasized.

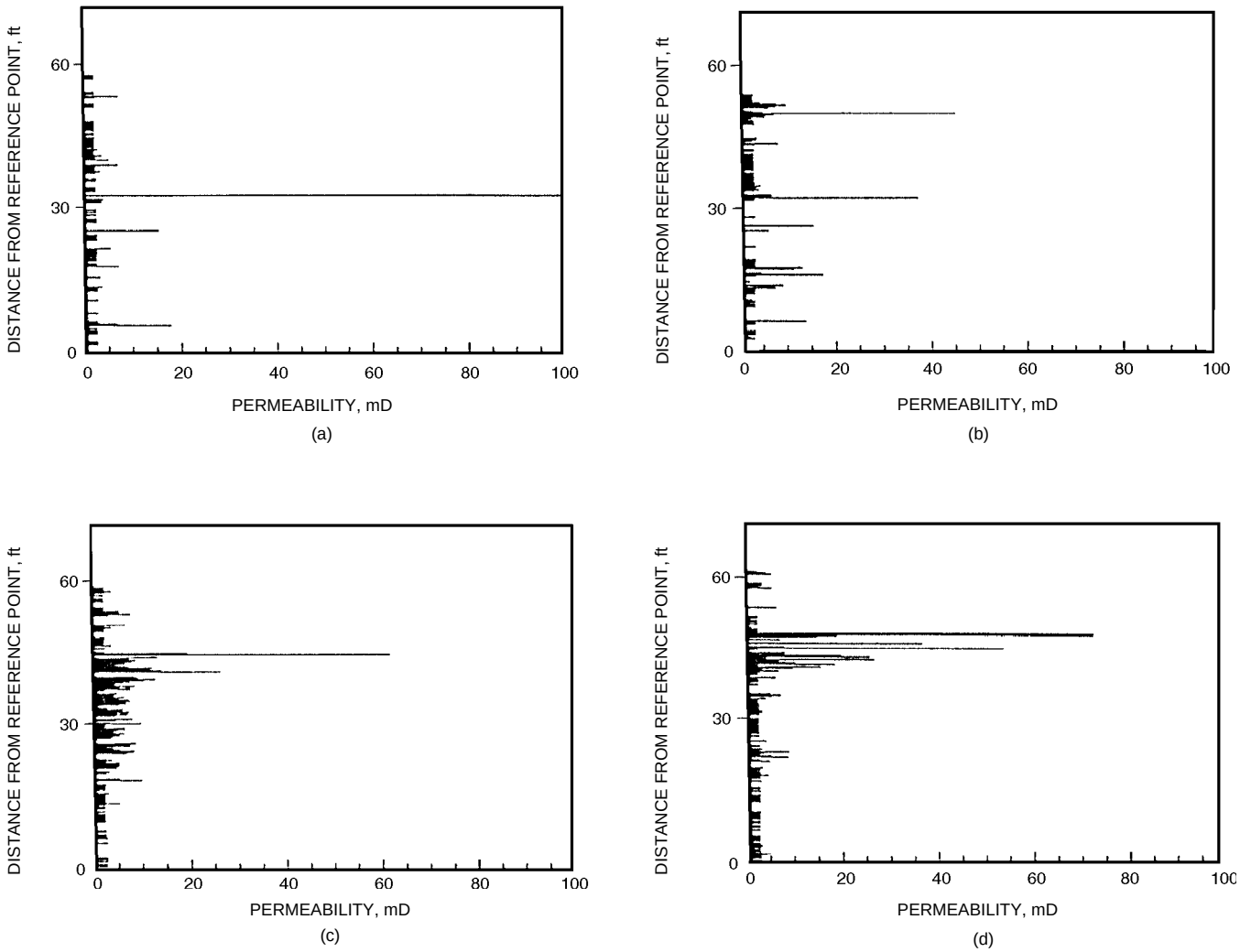

Fig. 5 Results of mini-permeameter tests on core plugs collected from the No. 1 sandstone along vertical transects T1(a), T2(b), T3(c), and T4(d) (locations shown in Fig. 4). Reference points do not necessarily coincide with a common geological feature.

Outcrop core-plug samples of both the Nos. 1 and 2 sandstones in the Ivie Creek case-study site were collected during the 1994 field season to characterize the vertical and lateral variations of petrophysical properties, such as density, velocity, mineralogy, and porosity. These samples were also tested for permeability (Fig. 9). Figure 9 shows that at least 14% porosity is required to obtain measurable permeabilities with the mini-permeameter. Data shown in part a of Fig. 9 are grouped to illustrate that grain-size variations appear not to influence the relationship between permeability and porosity. Similarly, data shown in part b of Fig. 9 indicate that permeability–porosity relationships are comparable for both the Nos. l and 2 sandstones.

Detailed mini-permeameter testing is being performed with Mobil Oil Corp.'s stage-mounted automated mini-permeameter. Permeability data are being collected at 0.05-ft (1.5-cm) intervals along the core recovered from the Ivie Creek drilling operations. Figure 10 illustrates low permeabilities obtained from two core segments from the Ivie Creek 5a (No. 2 sandstone) and 9a (No. l sandstone) core holes. Overall, the results are similar to those obtained from outcrop-derived core plugs.

Reservoir Modeling

Software designed to transfer line drawings of reservoir architectural elements was acquired. Digital images from photographs, used as base maps for creating digital lithofacies maps, are being loaded into the computer. Trace maps have been digitized and analysis has begun. Data from previous studies of the Ferron sandstone are being used for two-dimensional (2-D) reservoir simulations and the coding of the 3-D version. All procedures are being documented, and final testing of the 2-D code is under way.

Technology Transfer

Two technical presentations were made during the quarter as part of the Ferron Sandstone project technology transfer activities.[1-2]

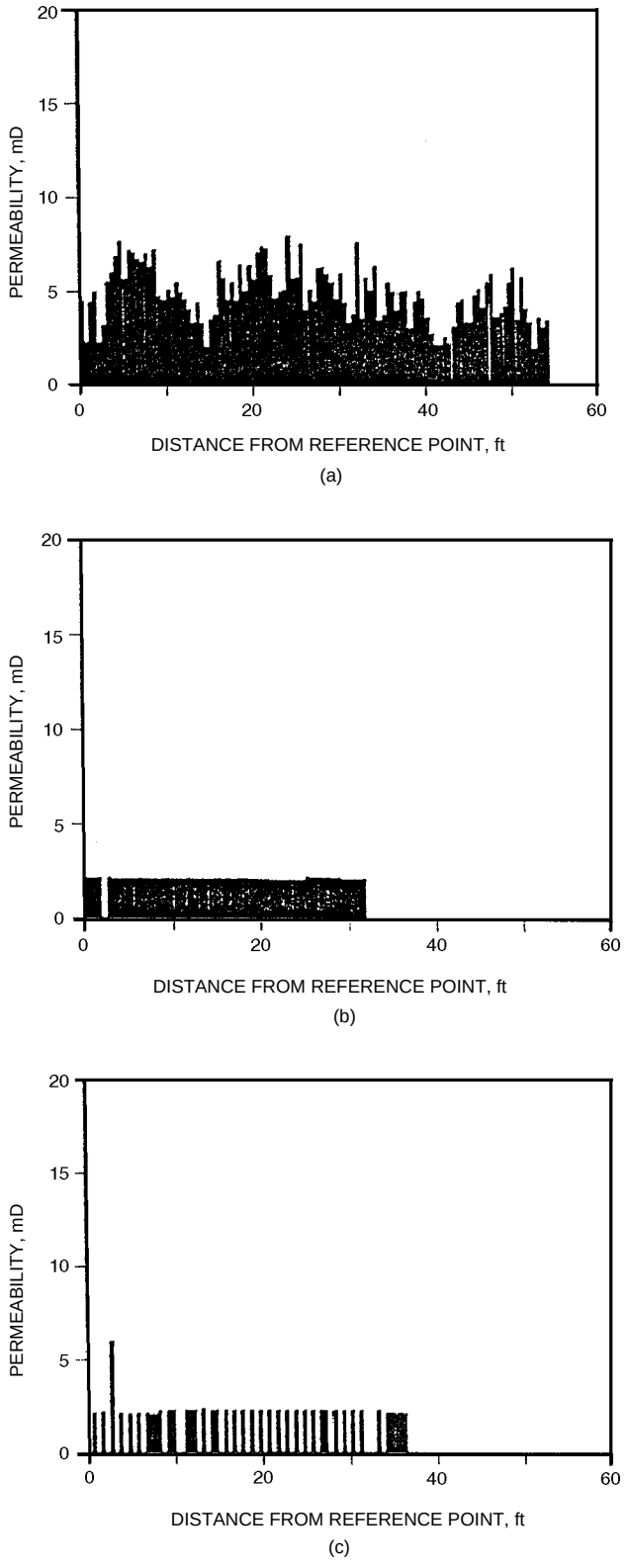

Fig. 6 Results of mini-permeameter tests on core plugs collected from the No. 1 sandstone along horizontal transects T5(a), T6(b), and T7(c) (locations shown in Fig. 4).

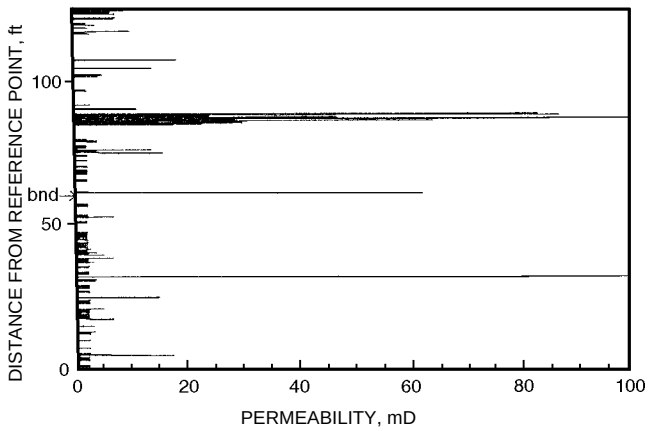

Fig. 7 Results of mini-permeameter tests on core plugs collected from the Nos. 1 and 2 sandstones along vertical transect T1 (locations shown in Fig. 4). bnd, boundary between the Nos. 1 and 2 sandstones.

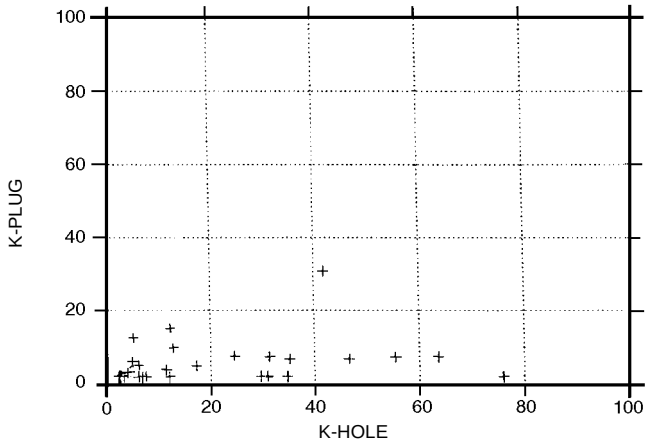

Fig. 8 Comparison of results (in millidarcys) of mini-permeameter tests on core plugs (k-plug) collected from holes where in situ tests (k-hole) were also conducted.

References

1. R. D. Adams and F. W. Stapor, *Response of Delta Morphology and Progradational Style to Changes in Accommodation, Sedimentation, and Basin Topography: Ferron Sandstone, East-Central Utah,* paper presented at Geological Society of America annual meeting, Seattle, Wash., October 24–27, 1994.
2. R. D. Adams, *Influence of Tectonics, Sea Level, and Basin Topography on the Geometry of a Deltaic System: Ferron Sandstone, East-Central Utah,* paper presented in Distinguished Lecture Series, University of Utah Department of Geology and Geophysics, November 1994.

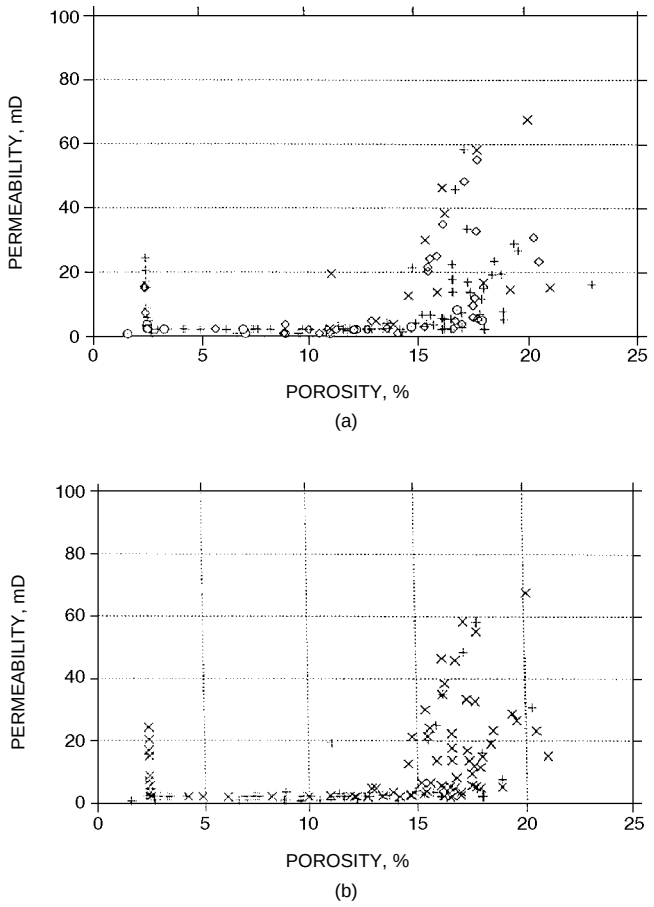

Fig. 9 Comparison of permeability and porosity values obtained for core plugs collected from outcrop: (a) samples grouped by grain size (+, fine grained; o, silty/shaley; ◇, medium grained; x, coarse grained) and (b) samples grouped by parasequence set [the sampled Nos. 1(+) and 2(x) sandstones].

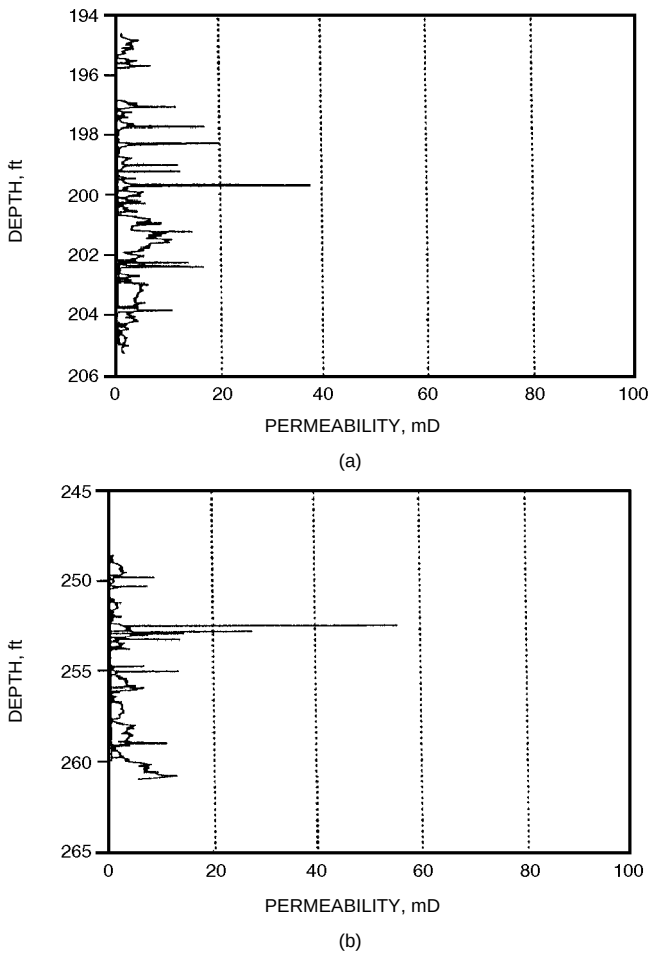

Fig. 10 Results of detailed mini-permeameter tests (0.05-ft spacing) on slabbed core obtained from the Ivie Creek 5a(a) and 9a(b) core holes.

DYNAMIC ENHANCED RECOVERY TECHNOLOGIES

Contract No. DE-FC22-93BC14961

Columbia University
New York, N.Y.

Contract Date: July 5, 1993
Anticipated Completion: Oct. 30, 1995
Government Award: $7,742,000

Principal Investigator:
Roger N. Anderson

Project Manager:
Edith Allison
Bartlesville Project Office

Reporting Period: Oct. 1–Dec. 31, 1994

Objective

The objective of this project is to test the concept that the growth faults in a Gulf of Mexico field are conduits through which the producing reservoirs are charged and the proposal that enhanced production can be developed by producing from the fault zone. The field demonstration will be accomplished by drilling and production testing of growth fault systems associated with the Eugene Island Block 330 (EI 330) operated by Pennzoil in federal waters off Louisiana.

Summary of Technical Progress

Database Management

Fluid-Flow Monitoring Using Industry Multiple Three-Dimensional (3-D) Seismic Data Sets

The 1992 Shell/Exxon data set (received December 1994) is being reformatted and integrated with the two 3-D seismic

surveys, the Texaco/Chevron data set and the Pennzoil et al., data set. The preliminary normalization of the Shell data set is complete (Fig. 1). Five new Advanced Visual Systems, Inc. (AVS) modules have been coded that perform interesting morphological operations on 3-D seismic data, such as skeletonization, histogram equalization, histogram matching, and construction of project description files.

Geological Analyses of Industry 3-D Seismic Surveys

Landmark has completed its task of comparing the traditional interpretation of the horizons and faults and the reinterpreted reflector horizons and faults.

The development of the computer software for correlating well logs from EI is in its final phase. This phase involves invoking statistical methodology for rating all possible correlations between any two time series, which at present are simulated well logs. Once the testing is complete, a composite well log of the EI field, which has already been assembled from all available well logs in the basin, will be correlated to a composite oxygen isotope curve dating back through the Pliocene. Correlations obtained will be used to constrain stratigraphic ages, sedimentation rates, and hopefully fault displacement rates throughout the basin.

Real-Time Visualization Database

A new addition to the on-line database is World Wide Web, which is on line now. Anyone on the Internet can browse through the database provided that he or she has an HTML document browser. The link is named http://www.Ideo.columbia.edu/GBRN/GBRN_Brochure.

Field Demonstration Experiment

Interpretation of Results of Well Experiments

An article was published in the December 1994 issue of *Petroleum Engineer International* summarizing an overview

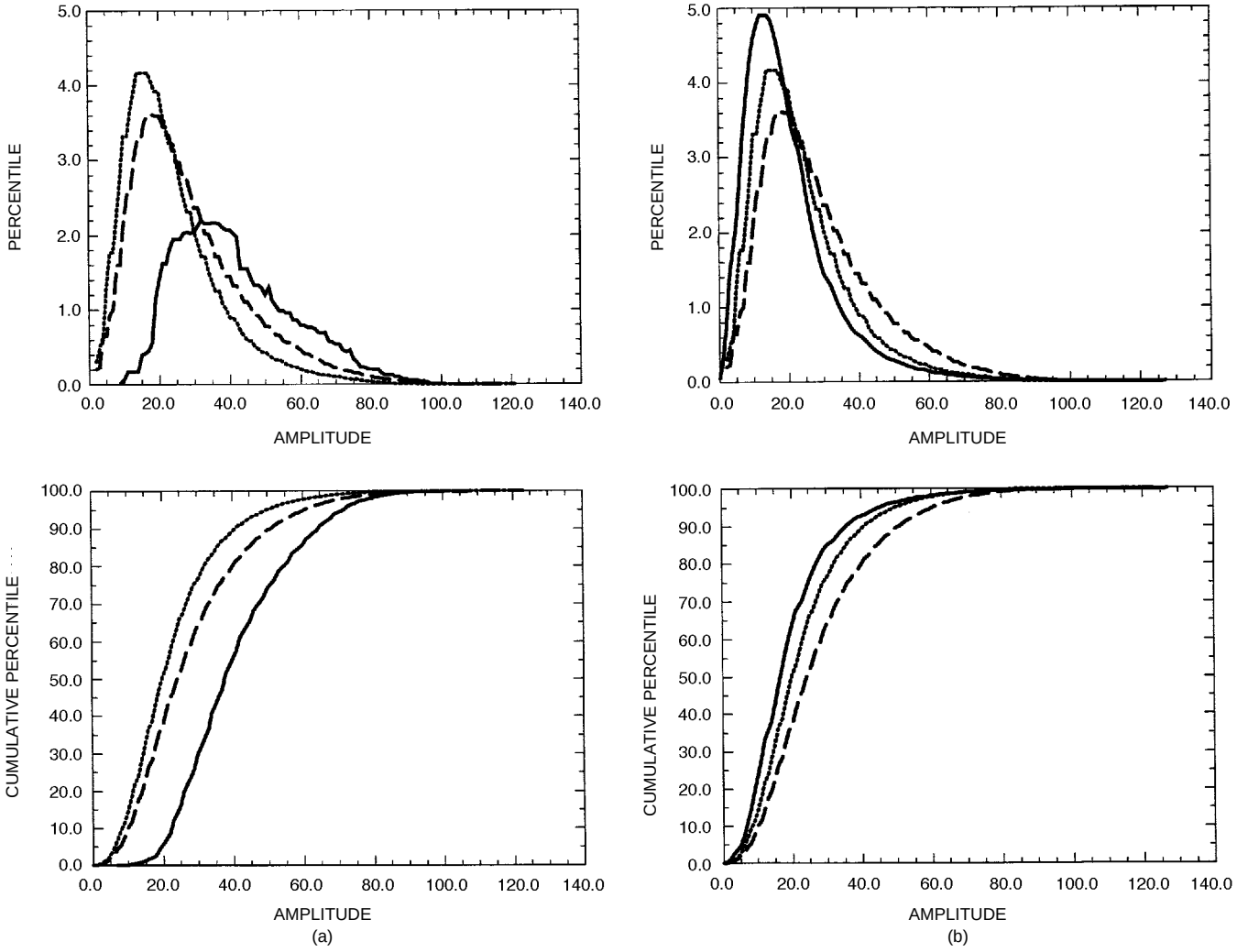

Fig. 1 Normalization of the Shell data set before (a) and after (b) scaling. —, Shell. ...., Texaco. — —, Pennzoil.

of the Global Basins Research Network (GBRN) project a year after the field demonstration experiment.[1]

Reservoir Characterization

Acquisition of A-12 Core

Pennsylvania State University (PSU) has received permission from Pennzoil to obtain all the core data associated with the A-12 well (EI Block 316), including color Formation Micro-Imager paper log, thin-bed analysis, and core photos as well as the whole core itself. This core will be housed in the PSU Core Repository.

Structure Maps

Work has continued on assessing the phase and polarity of the 3-D seismic surveys so that wireline picks can be confidently tied to seismic reflectors.

Temperature Mapping

Work on the two-dimensional (2-D) temperature model for conduction and advection to monitor the combined influence of fluids flowing in the fault system and of the salt is in process. This is the last step before conceiving a 3-D model for conduction and advection of heat that should allow the best understanding of the thermal regime in this area and in active fault systems in general.

Amplitude Mapping Analysis

The patent application for four-dimensional (4-D) seismic amplitude imaging [titled "4-D Seismic Interpretation and Imaging Utilizing Amorphous Diffuse Intra- and Inter-Period (ADIP) Projectors"] is still in process. Significant methodologies to generalize it into a techniques patent that will be more useful to disparate data sets are in process.

Modeling

The Akcess.Basin modeling system was simplified in a major way during this quarter by modifying it so that grid changes caused by compaction, salt diapirism, or faulting are specified accurately during the pre-processing step. The grid movement in Akcess.Basin is specified by external files. These changes, together with some additions to the preprocessor, allow fault movements to be included in 2D and 3D. The fault modeling task, which had been problematic, is 100% complete.

Geochemistry

Inorganic Geochemistry

In general, work has focused on finishing analyses of Pathfinder well samples and expanding the investigation to reservoir sands. The earlier work on this latter objective, in which about 150 thin sections from Pennzoil were examined, was limited by the lack of additional rock from which isotope samples could be obtained. Thus additional sidewall cores were obtained from Pennzoil.

Petrography

Twenty-five thin sections of sidewall cores from the HB sand were examined for diagenetic minerals. These samples are from traverses perpendicular to the main growth fault in Block 330. Albitization of plagioclase appears to be common in several of the samples (well No. B16, 6120 and 6126 ft; well No. B3ST, 6852 and 6797 ft; well No. A7ST, 6537 ft; and well No. C15ST, 5204 and 5300 ft) in which fresh plagioclase is scarce. If confirmed by microprobe, this occurrence of albitization is anomalously shallow and may represent unusual fluids from a chemical or thermal point of view. Calcite cement is common in some samples, comprising up to 70% of the sample in some cases (well No. B16, 6140 and 6144 ft) and averaging 2 to 10% in most samples. The cement exists as extremely fine-grained aggregates in pores and as ragged overgrowths on larger detrital grains. Rare, bright yellow–orange luminescent poikilotopic cement is present in at least one sample (well No. C15ST, 5274 ft). Sampling is being conducted for stable and strontium isotope analysis on selected samples.

Organic Geochemistry

An experiment on hydrous pyrolysis of an oil-soaked core sample from a Pathfinder core is in process to determine if good kinetic and yield data can be obtained on cracking of EI 330 oil to gas within a reservoir rock typical of the area.

The Pathfinder CD-ROM entitled "Results of the Pathfinder Drilling Program into a Major Growth Fault" is expected to be released early in 1995. The conclusions reached from the CD-ROM are that analyses of Pathfinder well samples show no evidence of recent migration–fractionation either along the A fault or within the cored section. Analyses are still in progress to look for fractionations associated with smaller scale oil and gas movement along more minor faults in Pathfinder cores. The relatively sulfur-rich EI 330 oils, including those from the Pathfinder well, belong to a single chemical family, probably derived from a marine, carbonate-rich Jurassic or Lower Cretaceous source rock.

Maturities of all EI 330 oils, including the Pathfinder well samples, are about calculated reflectance values (Rc) = 0.8% at the beginning of the oil window; however, gas maturities for non-Pathfinder gases are about 1.3 to 1.5% at the end of the oil or at the beginning of the wet gas windows.

An hypothesis for how oil and gas migration might be occurring into EI 330 reservoirs was proposed. Oil contained within deep reservoir rocks is periodically pressurized with sufficient gas to break through the overpressure and drive gas and oil upward through the red fault system into Pleistocene reservoirs. This process accounts for the bright seismic reflections that appear to mark the migration paths from deep source zones below hard geopressure up along the faults into the overlying reservoirs. It also accounts for the kerogen

maturation anomalies adjacent to the fault zone as well as for the apparent changes in oil and gas compositions over time and the persistent overproduction in the EI 330 field.

Technology Transfer

In October 1994 the Weiss Energy Hall was opened at the Houston Natural History Museum. The GBRN participated in the design of the geology and geophysics rooms of the Energy Hall, and Engineering Animation, Inc., in collaboration with a GBRN storyboard, provided the showcases entry-way video wall depicting the formation of oil and gas from the Big Bang to burial. The GBRN video "Field of Streams" about the EI 330 field and the U.S. Department of Energy Field Demonstration Experiments is continuously showing in the geology room as a permanent display.

Reference

1. L. B. Billeaud, R. N. Anderson, P. B. Flemings, and J. Austin, Active Gas and Oil Migration Sought in a Growth Fault Zone, *Pet. Eng. Int.*, 66(12): 17-18, 20-22 (December 1994).

IDENTIFICATION AND EVALUATION OF FLUVIAL-DOMINATED DELTAIC (CLASS I OIL) RESERVOIRS IN OKLAHOMA

Contract No. DE-FC22-93BC14956

Oklahoma Geological Survey
University of Oklahoma
Norman, Okla.

Contract Date: Jan. 15, 1993
Anticipated Completion: Dec. 31, 1997
Government Award: $1,390,752
(Current year)

Principal Investigators:
Charles J. Mankin
Mary K. Banken

Project Manager:
Rhonda Lindsey
Bartlesville Project Office

Reporting Period: Oct. 1–Dec. 31, 1994

Objectives

The Oklahoma Geological Survey (OGS), the Geological Information Systems (GIS) Department, and the School of Petroleum and Geological Engineering at the University of Oklahoma are engaging in a program to identify and address Oklahoma's oil recovery opportunities in fluvial-dominated deltaic (FDD) reservoirs. This program includes the systematic and comprehensive collection and evaluation of information on all of Oklahoma's FDD reservoirs and the recovery technologies that have been (or could be) applied to those reservoirs with commercial success. This data collection and evaluation effort will be the foundation for an aggressive, multifaceted technology transfer program that is designed to support all of Oklahoma's oil industry, with particular emphasis on smaller companies and independent operators in their attempts to maximize the economic producibility of FDD reservoirs.

Specifically, this project will identify all FDD oil reservoirs in the State; group those reservoirs into plays that have similar depositional and subsequent geologic histories; collect, organize, and analyze all available data; conduct characterization and simulation studies on selected reservoirs in each play; and implement a technology transfer program targeted to the operators of FDD reservoirs to sustain the life expectancy of existing wells with the ultimate objective of increasing oil recovery.

The elements of the technology transfer program include developing and publishing play portfolios, holding workshops to release play analyses and identify opportunities in each of the plays, and establishing a computer laboratory that is available for industry users. The laboratory will contain all the play data files, as well as other oil and gas data files, together with the necessary hardware and software to analyze the information. Technical support staff will be available to assist interested operators in the evaluation of their producing properties, and professional geological and engineering outreach staff will be available to assist operators in determining appropriate recovery technologies for those properties.

Summary of Technical Progress

The execution of this project is being approached in three phases. Phase 1, Planning and Analysis, includes system design, play definition, and database development activities. Data from the Natural Resources Information System (NRIS), an Oklahoma data system, that has been developed through the support of the U.S. Department of Energy's (DOE) Bartlesville Project Office, have provided the foundation for this data collection effort. Phases 2 and 3 include many ongoing activities from Phase 1 but emphasize project implementation and technology transfer activities in which the collected information is organized and made available to the industry through the various methods.

This quarter was a transitional period between the phases; phase 1 activities continued while revised subtasks and schedules were finalized for phases 2 and 3.

Phase 1: Planning and Analysis

Design/Develop Database Systems

Work this quarter focused on the development of user-friendly interfaces to the NRIS and FDD data. When these are fully developed, users will be able to easily access all the data collected through this project. Database management software was purchased to be used for supporting the very large multiuser databases that will be available through the user-lab computer network.

Work was initiated to convert the operator database to the personal computer (PC) network. This database will be used to track program participation by operators from the various plays. The FDD reservoir and bibliography database systems that were developed will continue to be used for the foreseeable future because the new database management software development will concentrate on reformatting the NRIS well, lease, and field mainframe databases for access at the PC level. Eventually, the final two FDD databases will be converted, and the documentation for those databases will be completed after that conversion.

For phases 2 and 3, the ongoing activities of this task will be continued and reported under Task 1, Database and Applications Development.

Data Research

Primary efforts for this quarter were devoted to data research activities. Project staff provided four new data packages to the Oklahoma Nomenclature Committee (ONC). These packages contained maps and print listings of fields, leases, and wells for areas with large volumes of oil production from unassigned leases (i.e., leases outside field boundaries). The packages assist the committee as they delineate the official oil-field boundaries in which FDD reservoirs occur. Packages from this quarter included a six-township area in Hughes county with high unassigned Booch production; a nine-township area in the western part of the Oklahoma panhandle with unassigned Morrow production; a six-township Morrow production area in the eastern part of the Oklahoma panhandle; and another six-township Booch area in Hughes, Seminole, and Okfuskee counties. As the ONC defines new field boundaries, the NRIS field files are updated to reflect the changes.

Public domain data research continued as a primary emphasis during this quarter as project staff continued to collect data on FDD reservoirs from literature and theses. Research during this quarter concentrated on reservoirs scheduled for presentation during the first three play workshops. This included the Morrow, the Layton and Osage–Layton, and the Booch reservoirs. The data captured in these searches are being entered into the databases and are being used to develop trend maps and other illustrations of the FDD plays.

The reservoir characterization and simulation efforts were continued this quarter for the Booch sand in the Greasy Creek field. After the well logs were analyzed, maps were created to show the development of three principal layers that define a Booch channel. The log data were further used to produce isopach and structure maps for input to the reservoir simulation software. Within the Morrow play, the Rice Northeast field has been identified as the target candidate. Research continues to identify an appropriate field for the Layton and Osage–Layton play.

For phases 2 and 3, the ongoing activities of this task will be continued as part of the data analysis and preparation for each play publication and workshop.

Play ID/Folio Plans

Routine meetings of play leaders have continued, at which various aspects of the play definitions are discussed and plans are developed for the ongoing work. During this quarter plans were discussed for producing the play folio publications and conducting the workshops. The content and format of a typical workshop publication were outlined. The maps, or plates, to be included with each publication will share one of two possible bases for the state of Oklahoma. One base will be for western ranges of the state and will include the panhandle. The other base will include the main body of the state minus the panhandle. These two base areas were decided on to allow all maps to be produced at a scale of 1:500,000. By dividing the state in this way, each play area can be mapped at a scale that will allow adequate detail and yet not be too large for use. Both of these bases will include county boundaries, township–range grids, and selected city locations.

Also this quarter the number of potential workshop attendees and potential workshop locations were addressed. Lists of operators with recent production in various FDD plays were generated from the NRIS database. On the basis of the addresses of the operators, along with the number of operators in each FDD reservoir, potential sites were suggested for workshop presentations. Efforts are under way to investigate the sites for adequate presentation facilities.

For phases 2 and 3, the ongoing activities of this task will be continued as part of the preparation for each play publication and workshop.

Computer Applications

User-lab development activities include both the acquisition of hardware and software and the development of user interfaces for the data and applications that will be available through the user lab.

Work this quarter focused on development of a Visual Basic language interface, which will allow easy access to the NRIS and FDD data. The Windows-based application uses mouse point-and-click technology for selecting wells according to various selection criteria. The interface was tested by play geologists using subsets of the NRIS well data. Their comments and suggestions were used to make modifications to the system. When these are fully developed, users will be able to easily access all the data collected through this project.

Oracle database management software was purchased to support the very large multiuser databases that will be available through the user-lab computer network. Oracle will be installed next quarter after the current network software is upgraded to Novell Netware 3.12. The databases created in the current database management system will continue to be operated for now but will eventually be converted to Oracle. The new Oracle system will work with the Visual Basic interface and will allow access to various Windows-based applications.

User-lab activities also include the development of plans for the business management and operation of the lab facility. During this quarter various issues related to the operation of the lab were identified. These issues include operating hours, staffing plans, training, security, and fees. The approaches used by other similar facilities are being investigated.

For phases 2 and 3, the ongoing activities of this task will be continued and reported under Database and Applications Development.

Management/Reporting

Some progress was made this quarter on the completion of management reporting requirements. An annual report was completed that incorporated much of the information originally designated for topical reports.

A project review meeting was held with representatives from the DOE Bartlesville Project Office. Project efforts were reviewed, and refinements in the phase 2 and 3 schedules were identified.

Phases 2 and 3

Database and Applications Development

Database, applications, and user-lab development efforts were continued during this quarter.

Play Analyses, Publications, and Workshops

Analysis and preparation for the first scheduled Morrow play workshop were the primary focuses during this quarter with the workshop planned for June 1995. Analysis of Morrow data along with the preparation of text and illustrations proceeded. Initial data analysis efforts were also under way for the Booch play (scheduled for August 1995) and the Layton and Osage–Layton play (scheduled for November 1995).

Professional Outreach

Most of the professional outreach activities are scheduled to begin after the workshops have been initiated in 1995. The exception to this schedule is with the reservoir characterization and simulation efforts, which require ongoing interactions with industry participants. These efforts continued this quarter for the Booch play in the Greasy Creek field and for the Morrow play in the Rice Northeast field.

Management and Reporting

The first quarterly technical progress report of this task was submitted.

UNITED STATES DEPARTMENT OF ENERGY
BARTLESVILLE PROJECT OFFICE
P.O. BOX 1398
BARTLESVILLE, OKLAHOMA 74005

OFFICIAL BUSINESS
PENALTY FOR PRIVATE USE, $300

Return this sheet to above address, if you
do NOT wish to receive this material ☐,
or if change of address is needed ☐
(indicate change, including ZIP code).